

**NATURAL ANTIBODY RECOGNITION, SIGNALING AND SURVEILLANCE
IN v-Ha-ras- AND PKC- β 1-OVEREXPRESSING 10T $\frac{1}{2}$ FIBROBLASTS**

by

HONGSHENG WANG

A Thesis

Submitted to the Faculty of Graduate Studies

in Partial Fulfillment of the Requirements

for the Degree of

Doctor of Philosophy

Department of Immunology

University of Manitoba

Winnipeg, Manitoba

May, 1998



National Library
of Canada

Acquisitions and
Bibliographic Services

395 Wellington Street
Ottawa ON K1A 0N4
Canada

Bibliothèque nationale
du Canada

Acquisitions et
services bibliographiques

395, rue Wellington
Ottawa ON K1A 0N4
Canada

Your file Votre référence

Our file Notre référence

The author has granted a non-exclusive licence allowing the National Library of Canada to reproduce, loan, distribute or sell copies of this thesis in microform, paper or electronic formats.

The author retains ownership of the copyright in this thesis. Neither the thesis nor substantial extracts from it may be printed or otherwise reproduced without the author's permission.

L'auteur a accordé une licence non exclusive permettant à la Bibliothèque nationale du Canada de reproduire, prêter, distribuer ou vendre des copies de cette thèse sous la forme de microfiche/film, de reproduction sur papier ou sur format électronique.

L'auteur conserve la propriété du droit d'auteur qui protège cette thèse. Ni la thèse ni des extraits substantiels de celle-ci ne doivent être imprimés ou autrement reproduits sans son autorisation.

0-612-32033-2

**THE UNIVERSITY OF MANITOBA
FACULTY OF GRADUATE STUDIES

COPYRIGHT PERMISSION PAGE**

**NATURAL ANTIBODY RECOGNITION, SIGNALING AND SURVEILLANCE
IN v-Ha-ras- AND PKC- β 1-OVEREXPRESSING 10T $\frac{1}{2}$ FIBROBLASTS**

by

HONGSHENG WANG

**A Thesis/Practicum submitted to the Faculty of Graduate Studies of The University
of Manitoba in partial fulfillment of the requirements of the degree**

of

DOCTOR OF PHILOSOPHY

Hongsheng Wang ©1998

**Permission has been granted to the Library of The University of Manitoba to lend or sell
copies of this thesis/practicum, to the National Library of Canada to microfilm this thesis
and to lend or sell copies of the film, and to Dissertations Abstracts International to publish
an abstract of this thesis/practicum.**

**The author reserves other publication rights, and neither this thesis/practicum nor
extensive extracts from it may be printed or otherwise reproduced without the author's
written permission.**

TABLE OF CONTENTS

	page
DEDICATION	vi
ACKNOWLEDGMENTS	vii
LIST OF TABLES	viii
LIST OF FIGURES	x
LIST OF ABBREVIATIONS	xii
ABSTRACT	xv
CHAPTER 1. INTRODUCTION	1
PART I. LITERATURE REVIEW	2
(A) Natural Antibodies, an Overview	2
1. Multireactivity, autoreactivity and high connectivity nature of NAb	2
2. Production of NAb	4
3. Binding properties	6
4. Biological functions	9
(1) Physiological role	9
(2) Anti-infection activity	10
(3) NAb in immunoregulation	11
(4) Anti-tumor activity	13
(B) Protein Kinase C	17
1. Isoforms and structure	17
2. Activation and downregulation	19
3. Substrates	22
(1) MARCKS	23
(2) Cytoskeletal proteins	24
(3) Cell surface molecules	25
(4) Intracellular signaling transducers	26
4. Involvement of PKC in tumorigenesis	27
(1) PKC isoform overexpression and tumor induction	27
(2) PKC activity and specific isoform expression in tumors	28
(3) Role of PKC in transformation by oncogenes	29

	page
(C) Ras Oncogene and Signal Transduction	31
1. Mammalian ras family	31
2. Activating mutation and tumorigenesis	31
3. The ras signaling network	32
PART II. OBJECTIVES	35
CHAPTER 2. PROTEIN KINASE C EXPRESSION IN 10T½ CELLS ASSOCIATED INCREASED NATURAL ANTIBODY ACQUISITION WITH SURVEILLANCE OF PRENEOPLASIA AND HOMEOSTASIS OF THE ORGANISM	38
ABSTRACT	39
INTRODUCTION	40
MATERIALS AND METHODS	42
Mice and sera	42
Cells	42
In vitro drug treatment	42
Fluorescence-detected NAb binding	43
Preparation of cell membrane and cytosolic fractions	44
Sodium dodecyl sulfate-polyacrylamide gel electrophoresis (SDS-PAGE)	45
Western Blotting analysis	45
Ras infection of PKC-4 vs 10T½ and colony formation	46
Tumorigenicity assays	47
[¹³¹ I]deoxyuridine ([¹³¹ I]dUrd) labeling and in vivo natural resistance assay	47
Statistical analysis	48
RESULTS	48
NAb binding and PKC expression of PKC-4, I3T2.1 and 10T½	48
Colony formation, tumorigenicity and ras-infection of PKC-4, I3T2.1 and 10T½ cells	54
Sensitivity of PKC-4 to natural resistance in vivo	60
NAb binding of H7 treated cells	60
NAb binding of E-64d treated cells	60
NAb binding and PKC expression by TPA treated cells	63
DISCUSSION	65

	page
CHAPTER 3. NATURAL ANTIBODY BINDING-INDUCED INTRACELLULAR SIGNALING EVENTS IN C3H 10T$\frac{1}{2}$ FIBROBLASTS	71
ABSTRACT	72
INTRODUCTION	73
MATERIALS AND METHODS	76
Cell culture	76
Fluorescence-detected NAb binding	76
Purification of IgG and IgM from normal C3H mice serum	77
NAb and TPA treatment for Western blotting analysis	79
Preparation of membrane and cytosolic fractions	80
SDS-PAGE	80
Western blotting analysis	80
Shedding of RPTP α	81
Cell cycle analysis by flow cytometry	81
Statistical analysis	82
RESULTS	82
NAb binding to cells at 4°C versus 37°C and 4°C shifted to 37°C	82
PKC expression in cells treated with NAb at 4°C versus 37°C and 4°C shifted to 37°C	86
Detection of protein tyrosine phosphorylation in PKC-4 cells treated with NAb at 4°C versus 4°C shifted to 37°C	94
PKC expression and NAb binding to cells treated with TPA	94
Detection of RPTP α in supernatants from cells preincubated with NAb followed by a raise in the temperature from 4°C to 37°C	98
Cell cycle analysis following NAb treatment	103
DISCUSSION	108
CHAPTER 4. NATURAL ANTIBODY INTERACTION WITH CELL SURFACE MOLECULES EXPRESSED ON v-Ha-ras- AND PKC-β1- OVEREXPRESSING 10T$\frac{1}{2}$ FIBROBLASTS AND L5178Y-F9 LYMPHOMAS	120
ABSTRACT	121
INTRODUCTION	122

	page
MATERIALS AND METHODS	124
Mice and sera	124
Cell culture	125
In vivo selection	125
Retroviral myc oncogene infection	125
Neuraminidase treatment	126
Fluorescence-detected NAb binding	126
Fluorescence-detected CD44 expression	126
Preparation of cell membrane-specific NAb	127
Purification of IgG and IgM NAb from normal C3H and DBA/2 serum	127
Preparation of cell membrane antigens	127
Preparation of released cell surface antigens from the supernatant of cells incubated at 4°C with and without NAb and raised to 37°C	128
Immunoprecipitation	129
SDS-PAGE	130
Immunoblotting	130
Gelatin zymography	131
Statistical analysis	132
RESULTS	132
SDS-PAGE fractionation and immunoblotting analysis of membrane molecules	132
Shedding of cell surface structures	136
NAb immunoblotting of molecules in cell supernatant	139
Anti-mouse Ig precipitation of molecules from supernatant of NAb-coated cells raised to 37°C	139
Analysis of RPTP α expression and NAb immunoblotting	142
Analysis of CD44 expression and NAb immunoblotting	147
CD44 in the L5178Y-F9 lymphoma system	147
CD44 expression	147
CD44 expression and NAb binding of tumors grown in vivo	150
Binding of anti-CD44 MAb and NAb to neuraminidase treated cells	150
CD44 in the fibroblast system	152
CD44 expression in 10T $\frac{1}{2}$ and variants	152
CD44 expression and NAb binding in ras-transformed cells after myc oncogene introduction	152
Binding of CD44 MAb and NAb to Neuraminidase treated cells	152
CD44 expression and NAb binding of tumors grown in vivo	156
Immunoblotting analysis of CD44 with NAb	156
Analysis of gelatinase expression	156

	page
DISCUSSION	163
CHAPTER 5. REDUCED TUMORIGENICITY AND METASTASIS OF SYNGENEIC TUMOR INOCULA IN XID-BEARING CBA/N AND B CELL NORMAL C3H AND DBA/2 MICE TREATED WITH NATURAL ANTIBODIES	174
ABSTRACT	175
INTRODUCTION	176
MATERIALS AND METHODS	178
Mice	178
Natural antibodies	179
Tumor cells	179
^[131] I]-dUrd elimination assay	180
Metastasis assay	180
Tumorigenicity assay	181
Statistical analysis	181
RESULTS	182
s.c. tumorigenicity of RI-28 in CBA/N mice given purified natural IgG and IgM i.v.	182
s.c. tumorigenicity of LYNAb ⁺ in DBA/2 mice and I3T2.1 in C3H mice given whole syngeneic serum NAb i.v.	185
i.v. RI-28 elimination in CBA/N mice given syngeneic serum NAb i.v.	185
Ras overexpressing I3T2.1 i.v. metastasis in C3H mice given whole serum NAb i.v.	188
DISCUSSION	188
CHAPTER 6. DISCUSSION	195
REFERENCES	208

To my grandfather

ACKNOWLEDGMENTS

First of all, I would like to express my deep sense of gratitude to my supervisor, Dr. Donna Chow, for providing me the opportunity to study tumor immunology, my favorite subject in medicine, which has attracted me for years. I will always be grateful for her valuable suggestions, enthusiastic encouragement, teaching and support.

My special thanks go to my wife, Xiaowei Wang, and my whole family for their love and understanding.

Many thanks to all of the people in the lab, and in particular Xiumei Feng, Ziyuan Zhang and Ken Hughes for their help and friendship.

I would also like to express my appreciation to the many staff and students at the Bannatyne Campus who have provided me with advice and assistance, and in particular Dr. Edward Rector for operating the flow cytometer.

Finally, I would like to acknowledge the Faculty of Graduate Studies of the University of Manitoba for awarding a graduate fellowship.

LIST OF TABLES

CHAPTER 2

page

Table 2.1.	NAb binding to I3T2.1, PKC-4 and parental 10T½ cells	49
Table 2.2.	NAb binding of subconfluent vs confluent 10T½ variants	51
Table 2.3.	PKC- α and PKC- β 1 expression in membrane and cytosolic fractions of 10T½ variants	52
Table 2.4.	Colony formation by 10T½ vs PKC-4 cells with and without ras infection	55
Table 2.5.	Tumorigenicity of 10T½, PKC-4 and ras-infected variants	57
Table 2.6.	Elimination of ¹³¹ I-dUrd-labelled PKC-4 vs 10T½ cells in vivo	61
Table 2.7.	NAb binding of cells treated with PKC inhibitors or TPA for 2 days	62

CHAPTER 3

Table 3.1.	NAb binding at 4°C vs 37°C	84
Table 3.2.	NAb binding at 4°C vs 4°C shifted to 37°C with and without H7 treatment	85
Table 3.3.	Membrane PKC- α and PKC- β 1 expression in PKC-4 cells treated with purified NAb, pre-absorbed NAb or anti-H2 ^k MAbs HB20	89
Table 3.4.	p60 tyrosine dephosphorylation in PKC-4 cells treated with purified NAb	97
Table 3.5.	NAb binding of cells after short-term TPA treatment	100
Table 3.6.	NAb binding of PKC-4 cells treated briefly with TPA in the presence of H7, H1004 or E-64d	101
Table 3.7.	NAb inhibition of cell growth in low serum culture	104
Table 3.8.	Influence of FBS and NAb on growth of I3T2.1 cells	106

Table 3.9.	Influence of FBS and NAb on cell cycling of I3T2.1 cells	107
------------	--	-----

CHAPTER 4

Table 4.1.	RPTP α expression in cellular compartments of subconfluent and confluent cells	144
Table 4.2.	RPTP α immunoprecipitation from confluent cells	146
Table 4.3.	CD44 expression in L5178Y-F9 variants	148
Table 4.4.	Anti-CD44 MAb binding in L5178Y-F9 and LYNAb ⁺ cells treated with neuraminidase	151
Table 4.5.	CD44 expression in 10T $\frac{1}{2}$ variants	154
Table 4.6.	CD44 expression in parental and the v-myc/neo ^r -infected I3T2.1 cells	155
Table 4.7.	Anti-CD44 MAb binding to I3T2.1 cells treated with neuraminidase	157
Table 4.8.	NAb and anti-CD44 MAb binding to I3T2.1 and in vivo selected variants	158

CHAPTER 5

Table 5.1.	RI-28 binding of natural IgG and IgM antibodies purified from CBA/J serum	183
Table 5.2.	Elimination of ¹³¹ I-dUrd-labeled RI-28 in CBA/N mice pre-treated with NAb versus saline	189
Table 5.3.	Metastasis of I3T2.1 cells in C3H mice pre-treated with serum NAb	190

LIST OF FIGURES

page

CHAPTER 2

- | | | |
|----------|---|----|
| Fig 2.1. | PKC- α expression in membrane fractions of subconfluent 10T $\frac{1}{2}$ variants | 53 |
| Fig 2.2. | PKC- α expression in 10T $\frac{1}{2}$ variants treated with TPA | 64 |
| Fig 2.3. | PKC- β 1 expression in PKC-4 cells treated with TPA | 66 |

CHAPTER 3

- | | | |
|----------|---|-----|
| Fig 3.1. | Expression of PKC- α in membrane fractions of PKC-4 cells treated with purified NAb | 87 |
| Fig 3.2. | Expression of PKC- β 1 in membrane fractions of PKC-4 cells treated with purified NAb | 88 |
| Fig 3.3. | Expression of PKC- α in membrane fractions of PKC-4 cells treated with purified NAb, pre-absorbed NAb and NAb-depleted syngeneic serum | 90 |
| Fig 3.4. | Expression of PKC- α in membrane fractions of 10T $\frac{1}{2}$ cells treated with purified NAb | 92 |
| Fig 3.5. | Expression of PKC- α in membrane fractions of I3T2.1 cells treated with purified NAb | 93 |
| Fig 3.6. | p60 tyrosine dephosphorylation in PKC-4 cells treated with purified NAb | 95 |
| Fig 3.7. | p60 tyrosine dephosphorylation in PKC-4 cells treated with purified NAb and pre-absorbed NAb | 96 |
| Fig 3.8. | PKC expression in response to TPA treatment | 99 |
| Fig 3.9. | Shedding of RPTP- α induced by NAb | 102 |

CHAPTER 4

- | | |
|----------|---|
| Fig 4.1. | Immunoblotting of cell surface molecules from 10T $\frac{1}{2}$ |
|----------|---|

	variants with eluted NAb	134
Fig 4.2.	Immunoblotting of purified biotinylated membrane molecules with purified NAb	135
Fig 4.3.	Immunoblotting of the membrane proteins with purified IgM or IgG NAb	137
Fig 4.4.	Shedding of cell surface structures	138
Fig 4.5.	Immunoblotting of released cell surface molecules with purified NAb	140
Fig 4.6.	Immunoprecipitation and immunoblotting of a 90-KDa molecule with purified NAb	141
Fig 4.7.	RPTP α expression in 10T $\frac{1}{2}$ variants	143
Fig 4.8	Immunoprecipitation of RPTP α from 10T $\frac{1}{2}$ variants	145
Fig 4.9.	Immunoprecipitation of CD44 from I3T2.1 and L5178Y-F9 variants	149
Fig 4.10.	Immunoprecipitation of CD44 from 10T $\frac{1}{2}$ variants	153
Fig 4.11.	Gelatin zymography of membrane fractions from 10T $\frac{1}{2}$ variants	160
Fig 4.12.	Gelatin zymography of membrane fractions from PKC-4	161
Fig 4.13.	Immunoblotting of the 90-KDa molecule with purified NAb	162
CHAPTER 5		
Fig 5.1.	Cumulative tumor frequency of RI-28 in CBA/N mice pre-treated 3 times with purified CBA/J NAb	184
Fig 5.2.	Cumulative tumor frequency of LYNAb ⁺ in DBA/2 mice pre-treated 5 times with syngeneic serum NAb	186
Fig 5.3.	Cumulative tumor frequency of I3T2.1 in C3H mice pre-treated 5 times with syngeneic serum NAb	187

LIST OF ABBREVIATIONS

ADCC	antibody-dependent cell-mediated cytotoxicity
Anti-Gal	anti- α -galactosyl
BCS	bovine calf serum
BSA	bovine serum albumin
DAG	diacylglycerol
DMSO	dimethyl sulfoxide
ECL	enhanced chemiluminescence
EGF	epidermal growth factor
ELISA	enzyme-linked immunosorbent assay
FACS	fluorescence-activated cell-sorting
FBS	fetal bovine serum
FITC	fluorescein isothiocyanate-conjugated
G418	geneticin
GAP	GTPase activating protein
GDP	guanosine diphosphate
GM-CSF	granular macrophage-colony stimulating factor
GTP	guanosine triphosphate
HBSS	Hanks' balanced salt solution
HRP	horseradish peroxidase
ICAM-1	intercellular adhesion molecule-1

IFN	interferon
IL-2	interleukin 2
IP3	inositol 1,4,5-triphosphate
IVIg	intravenous immunoglobulin
i. v.	Intravenous
[¹³¹I]dUrd	[¹³¹I]deoxyuridine
LPS	Lipopolysaccharide
M-CSF	macrophage-colony stimulating factor
MAb	monoclonal antibody
MAP(ERK)	mitogen-activated protein kinase
MARCKS	myristoylated alanine-rich C kinase substrate
MCF	mean channel fluorescence
MEK	mitogen-activated protein kinase kinase
MHC	major histocompatibility
MOI	multiplicity of infection
NAb	natural antibody
neo^r	neomycin resistance
NK	natural killer cell
PAF	platelet activating factor
PAGE	polyacrylamide gel electrophoresis
PBS	Phosphate buffered saline
PDGF	platelet-derived growth factor

PE	phycoerythrin
PI-PLC	phosphoinositide-specific phospholipase C
PIP2	phosphatidylinositol 4,5-bisphosphate
PI3 kinase	phosphatidylinositol 3 kinase
PKA	protein kinase A
PKC	protein kinase C
PKM	protein kinase M
PS	phosphatidylserine
PTK	protein tyrosine kinase
PTP	protein tyrosine phosphatase
RBC	red blood cell
RPTP α	receptor-like protein tyrosine phosphatase α
RTK	receptor tyrosine kinase
s.c.	subcutaneous
SDS	sodium dodecyl sulfate
TCR	T cell receptor
t_d	t -dependent Student t test
t_i	t -independent Student t test
TNF	tumor necrosis factor
TPA	12-O-tetradecanoylphorbol-13-acetate
xid	X-linked immunodeficiency

ABSTRACT

Extensive evidence supports a role for polyclonal serum natural antibody (NAb) acting as a mediator of natural resistance against tumors in mice. However, little is known about its mechanisms of action or about the phenotype of susceptible cells. C3H 10T $\frac{1}{2}$ fibroblasts overexpressing an activated ras oncogene or a PKC- β 1 gene increased their NAb binding capacities, identifying PKC, an integral signaling molecule of normal cellular activation, as a key regulator of NAb binding structures. This, coupled with corresponding decreases in expression of membrane PKC- α and NAb binding in resting confluent 10T $\frac{1}{2}$ cells raised the possibility that, in general, cells activated through PKC are NAb sensitive. In addition, NAb interaction with 10T $\frac{1}{2}$ variants initiated a signal transduction mechanism including activation of PKC, shedding of cell surface molecules and bound NAb, a reduction in phosphotyrosine levels of a membrane-associated 60 KDa molecule, and, over time, the inhibition of DNA synthesis. Together with the increased in vivo elimination of the high NAb binding PKC- β 1-overexpressing cells and the beneficial effect of passive syngeneic NAb in the rejection of syngeneic tumors injected s.c. and i.v. in both xid-bearing B cell deficient and B cell normal mouse models, the data argued that NAb not only participates in tumor surveillance of preneoplasia and neoplasia but contributes to homeostasis of the organism.

CHAPTER 1

INTRODUCTION

PART I. LITERATURE REVIEW

(A) Natural antibodies, an overview

1. Multireactivity, autoreactivity and high connectivity nature of NAb

In 1900, Landsteiner and his group first reported that normal humans, who had never undergone experimental immunization, had antibodies that were able to react with heterologous and isologous red blood cells causing agglutination and lysis of the cells (reviewed in Landsteiner, 1900). Later, these normal antibodies were defined as natural antibodies (NAbs), which refer to those immunoglobulins existing in the serum of physiologically healthy individuals that have not been intentionally immunized (Boyden, 1965). NAbs have been detected in normal sera from humans, rabbits, mice, rats and even fish (reviewed in Dighiero, 1997). NAbs are mostly of the IgM and IgG class in mice (Avrameas, 1991; Berneman et al., 1992), and belong to the IgM, IgG and IgA isotypes in humans (Yadin et al., 1989).

Studies with monoclonal NAbs obtained by fusions of human or mouse normal B cells with myeloma cells, or produced from Epstein-Barr virus-immortalized B cell clones, have demonstrated that NAbs are highly polyreactive. A single monoclonal NAb is capable of binding more than three apparently structurally unrelated self and/or non-self antigens (Dighiero et al., 1983; Prabhakar et al., 1984; Seigneurin et al., 1988). At least 20% of all immunoglobulins in mouse or human normal sera have been shown to be autoreactive based on immunoabsorption experiments using a panel of self-antigens, including actin, tubulin, histone, myosin, keratin, DNA, myoglobin, cytochrome c,

collagen, myelin basic protein, spectrin, albumin, transferrin, IgG, thyroglobulin, cholesterol, and phosphatidic acid (Avrameas et al., 1988; Shoenfeld et al., 1987; Martini., et al., 1989). Thus, polyreactivity and autoreactivity are two prominent features of NAb.

NAbs form a dense idiotype-like network in the peripheral antibody repertoire through V region-dependent interactions (Dietrich et al., 1992; Avrameas and Ternynck, 1993). This interaction between two immunoglobulin molecules, called 'connectivity', can occur in IgG-IgM, IgG-IgG or IgM-IgM forms (Avrameas and Ternynck, 1993). Human F(ab')₂ IgG NAb eluted from the same F(ab')₂-coupled Sepharose columns exhibited a higher reactivity against a panel of autoantigens and some commonly encountered microbial antigens than those antibodies in the effluent of the columns and those unchromatographed material (Dietrich et al., 1992). However, there was no difference in reaction to vaccinal antigens and to distant foreign antigens between connected and non-connected IgG (Dietrich et al., 1992). These results indicate that connective NAb is more autoreactive. In mice, natural IgM antibodies also showed a high degree of idiotypic connectivity (Holmberg et al., 1984; Kearney et al., 1990). Thus, connectivity is a fundamental feature of the NAb repertoire. Beyond the NAb repertoire, connectivity may also exists between NAb and other self molecules, such as members of the immunoglobulin superfamily (reviewed in Avrameas and Ternynck, 1993), T cell receptors and other immune factors (discussed below). Therefore, dynamic, multiple and continuous interactions between NAb and a diverse spectrum of self structures represents a complicated physiological autoimmune phenomenon. Alterations of the normal patterns

of connectivity in the circulating antibody repertoires including both IgG and IgM has been recently observed in patients with systemic lupus erythematosus, a typical autoantibody-mediated autoimmune disease (Ayoub et al., 1997).

2. Production of NAb

NAb appears to be produced by surface IgM⁺, IgD[±], CD23⁻, CD11⁺ and CD5[±] B1 lymphocytes, a subset of B cells different from conventional B cells (B2) which produce hyperimmune antibodies (Tarlinton, 1994). However, B2 cells have been also found to produce NAb (Reap et al., 1993).

Analysing the V region sequences of monoclonal IgM NAb derived from 'natural' hybridomas of newborn mice has revealed that NAb are encoded by germline gene segments (Calsson et al., 1991). This has also been observed in studies using Igs derived from adult B cell hybridomas or immortalized B cell lines (Baccala et al., 1989; Chen et al., 1991; Martin et al., 1992). The generation of autoreactive B cells that produce NAb has been proposed as a result of positive selection in early stages of B cell ontogeny (reviewed in Stollar et al., 1997). The antigens involved in this selection process are thought to include both endogenous and exogenous origins. Endogenous components include self antigens and idiotypic interactions (Portnoi et al., 1986; Forsgren, et al., 1991), while exogenous antigens are environmental antigens mainly existing in food and air. Antigen-free mice, fed with an ultrafiltered, chemically defined low molecular weight diet, and germ-free mice raised in a sterile environment and given a sterilized diet, produced comparable levels of serum IgM, but IgG and IgA levels were only 5%-10%

of those mice maintained under specific pathogen-free conditions (Bos et al., 1989; Haury et al., 1997). Interestingly, the serum IgG levels were correlated with foreign antigen load, with the highest in specific pathogen-free mice > germ-free mice > antigen-free mice (Haury et al., 1997). When tested using an immunoblotting analysis which employed a variety of homologous tissue extracts and purified IgM, a similar pattern of IgM reactivity was noted in these three groups (Haury et al., 1997). From this study, it was concluded that the production of most natural IgM antibodies is independent of external stimuli, probably bacterial antigens in the diet (Haury et al., 1997). Since in immunoblotting studies, every protein band detected by natural IgM can also be detected by natural IgG (Lacroix-Desmazes et al., 1995), the reduced natural IgG production in germ-free and antigen-free mice obviously resulted from a lack of stimuli for Ig class switch or for proliferation of the IgG-producing natural B cell clones. The external antigen-independent natural IgM production was further supported by studies on a pig model, in which the possibility that maternal immunoglobulin may select the fetal NAb repertoire was completely eliminated because maternal immunoglobulins are unable to transfer into the fetal circulation due to the special six-layered structure of the pig placenta (Cukrowska et al., 1996).

Recently, T cell activity has been demonstrated to influence NAb reactivities (Malanchere et al., 1995). In this study, euthymic and athymic mice were found to share essentially all NAb reactivities against syngeneic extracts of liver and muscle. When IgG was standardized to the same concentration, however, nude sera exhibited higher values of reactivity in all detectable bands. Reconstitution of athymic mice with splenic T cells

resulted in a decrease or disappearance of serum IgM reactivities towards certain bands and an increase in serum IgG1 and IgG2a concentrations. This study reinforces the hypothesis that there is a connectivity between the T cell repertoire and the autoantibody repertoire (Coutinho, 1989), which mutually regulate each other and control the size and quality of both systems. A recent B cell knockout model also supports this idea in that at least the numbers of CD4⁺ and CD8⁺ T cells in spleens of the B cell-deficient mice were significantly lower than those in B cell normal congenic controls (Asano and Ahmed, 1996).

3. Binding properties

Analysis of the structure of NAb has revealed that the variable (V) regions of most NAb contain a particularly high number of positively charged amino acids, especially arginine (Baccala et al., 1989; Conger et al., 1992), which can bind preferentially with structures having amino acids bearing negative charges (Gonzalez-Quintal et al., 1990). In contrast, a minor population of NAb, such as those reacting with bromelain-treated red blood cells (RBC), have neutral or an excess of negative charges in their V regions (Reininger et al., 1987; Chen et al., 1991; Conger et al., 1992) and preferentially recognize positively charged molecules (Serban et al., 1981; Cox and Hardy, 1985). Furthermore, compared to induced antibodies, the V regions of NAb have relatively higher numbers of tyrosine and serine, which bear side chain hydroxyl groups (Baccala et al., 1989; Conger et al., 1992). Thus, the antigen binding sites of NAb are hydrophilic. These hydroxyl amino acids may confer on NAb an advantageous binding to various epitopes via ionic bonds and hydrogen bridges (Baccala et al., 1989; Conger

et al., 1992). Most recently, the molecular basis of the cross-reactivity, or polyreactivity, of NAb has been elucidated by Tchernychev et al. (1997), who using a phage display library determined the epitopes recognized by human monoclonal NAb against the 55 KDa extracellular domain of the human receptor for TNF- α and a lectin from garlic. The interesting finding in this study is that NAb recognizes exposed protein epitopes that are rich in proline. Since proline is commonly present at solvent-exposed sites, such as loops, turns, helix and random coils, in most protein antigens, the polyreactivity of NAb may be due to the presence of proline-containing conformation-dependent "public" epitopes in different target antigens including both self structures and pathogenic bacteria and viruses (Tchernychev et al. 1997). Thus, the broad specificity and cross-reactivity of NAb make it play an important role in both anti-infection responses and autoimmune regulation (see below).

While hyperimmune antibodies have been selected through affinity maturation for high affinity to individual epitopes, NAb binds to an individual antigen in general with a low affinity or intrinsic affinity. However, due to its multiple binding interactions, the binding may be of high avidity or functional affinity (Ternynck and Avrameas, 1986; Adib-Conquy et al., 1993), which for IgG and IgM can be 10^3 and 10^6 respectively higher than their affinities (Hornick and Karush, 1972). By using the surface plasmon resonance technique to determine binding avidities, Diaw et al (1997) analysed five monoclonal IgM NAb against dissimilar autoantigens including cytoskeletal antigens and DNA. They found that most of these NAb expressed genes in a close germiline configuration and that the binding kinetic constants of all five NAb were

indistinguishable from those observed for immune antibodies (Diaw et al., 1997). Therefore, depending on the the local concentration of NAb and the antigen, NAb can bind strongly, or not, to the antigen and may play regulatory roles.

It has long been noted that NAb may preferentially react with carbohydrate determinants. Carbohydrate-reactive NAb fractionated from normal mouse serum by glycoprotein fetuin- or thyroglobulin-coupled Sepharose chromatography could bind and agglutinate erythrocytes of various species. This group of NAb was also able to bind with cells from mouse heart, kidney, thymus and spleen. The binding of these NAb fractions to mouse splenocytes was partially inhibited by the presence of some saccharides such as sialic acid, D-galactose, N-acetyl-D-glucosamine and D-mannose (Sela et al., 1975). In humans, approximately 1% of circulating IgG NAb have a narrow specificity to the carbohydrate epitope Gal- α 1-3Gal β 1-4GlcNAc-R (termed the α -galactosyl epitope) (Galili et al., 1984). However, humans generally do not express this epitope or express it at a very low level compared with non-primate mammals, which express large amounts of α -galactosyl epitopes but produce little anti-Gal NAb (Galili, 1993). Anti-band 3 IgG NAb has been well demonstrated to initiate antibody-dependent phagocytic removal of senescent red blood cells from the circulation (Lutz et al., 1987). Recently, the epitope on band 3 proteins for anti-band 3 binding has been reported as poly-N-acetyllactosaminyl saccharide chains (Beppu et al., 1996). In addition to the carbohydrate determinants, protein parts of molecules are also essential for NAb recognition because pronase treatment of the T cell lymphomas markedly reduced NAb binding capacities (Chow et al., 1992). This suggests that certain protein segments either directly compose

the epitope or build up a structure to support the epitope for NAb binding.

4. Biological functions

(1). Physiological role

Removal of the metabolic and catabolic waste from the circulation of the organism, and/or depletion of modified products such as antigens released upon cell death, damage or aging, have been considered as one of the major physiological functions of NAb. NAb has been shown to preferentially bind with enzymes, such as acetyl cholinesterase (Lidar et al., 1997), 2-oxoacid dehydrogenase complexes (Rowley et al., 1992), aldolase, catalase, creatine kinase etc (Berneman et al., 1992), and cytoskeleton components, such as actin, myosin and tubulin (Berneman et al., 1992). It was shown that keratin-reactive NAb enhanced the elimination of keratin following keratinocyte death (Hinter et al., 1987). Red blood cells undergo a series of changes in their membrane structures upon aging. This at least includes an alteration in membrane carbohydrate (e.g., a loss of sialic acid) and an exposure of β - and α -galactosyl residues, both of which are directly associated with an increase in natural IgG binding on aged RBC membranes (reviewed in Gershon, 1992). Neuraminidase treatment to remove sialic acid from the surface of human young RBC increased IgG binding and phagocytosis (Kay, 1978). NAb specific to β -galactose (Alderman et al., 1980 and 1981) and α -galactose epitopes (Galili et al., 1985) have been isolated. The anti- α -Galactose (anti-Gal) NAb did not bind to human young RBC, but bound to the densest (oldest) RBC (Sorette et al., 1991). In addition, natural anti-band 3 antibodies were also found to participate in the elimination of senescent RBC (Lutz et al., 1987). The binding between NAb and senescent RBC

eventually results in either activation of the complement system leading to cell lysis, or phagocytosis by monocytes and macrophages, or both (reviewed in Gershon, 1992).

Similarly, NAb has been implicated in the elimination of senescent platelets because removal of IgG from aged platelets reduced their phagocytosis by autologous monocytes (Khansari and Fudenberg, 1983).

Recently, NAb has been found to react with nerve growth factor in circulation. Thus, NAb may serve as carriers of growth factors (Dicou and Nerriere, 1997).

(2). Anti-infection activity

NAb is able to react with bacterial antigens (Russell and Beighton, 1982; Carroll et al., 1985; Morell et al., 1989). The role of NAb in resistance against pneumococcal infections has been well documented in mice (Briles et al., 1982; Yother et al., 1982; Briles et al., 1981a and b). It was noted that mice bearing an X-linked immunodeficiency (*xid*) gene, which is associated with the lack of CD5⁺ B cells and low serum natural IgM and IgG3 antibody levels, were 1000 to 10,000 times more susceptible to lethal infection by *S. pneumoniae* than normal mice (Briles et al., 1981a; Yother et al., 1982). Passive transfer of normal serum IgG3 or anti-phosphocholine NAb successfully protected *xid*-mice from infection with *S. pneumoniae* (Briles et al., 1981b).

In humans, NAb in the serum of nonimmune individuals mediates C3 fixation to *Mycobacterium leprae* (*M. Leprae*) and C1q binding to the major surface glycolipid of *M. leprae*, phenolic glycolipid 1 (Schlesinger and Horwitz, 1994). Human natural IgM has been shown to enhance monocyte phagocytosis of *Leishmania donovani* in vitro (Navin et al., 1989). Anti-Gal NAb have protected humans from being infected by type

C retroviruses endogenous to various nonprimate species through complement-mediated inactivation of the retrovirus (Rother et al., 1995). Similarly, IgM NAb binding to an asialo-oligosaccharide, gangliotetraose, on HIV-infected cells initiated cytolysis by homologous complement (Wu et al., 1996). Children with agammaglobulinemia usually suffer from various infections and die early in life. However, the disease is diminished just by injecting normal gamma globulins every 21 days (reviewed in Dighiero, 1997). Considering the protective effect of NAb on virus infections in lower species such as rainbow trout, which is unable to make high specific and high affinity antibodies (Michel et al. 1990; Gonzalez et al., 1989), NAb may serve as a first barrier of defense.

(3). NAb in immunoregulation

Over the past decade, it has been clearly established that NAb can react with functional molecules of the immune system. This includes V regions of immunoglobulins (Rossi et al., 1989), idiotypic determinants of immunoglobulins (Sultan et al., 1987; Rossi et al., 1988; Dietrich and Kazatchkine, 1990; Ronda et al., 1994), framework and variable determinants of the β chain of the $\alpha\beta$ T cell receptor (Kruger et al., 1993; Dedeoglu et al., 1993; Marchalonis et al., 1994; Wang et al., 1994), CD4 (Hurez et al., 1994), CD5 (Vassilev et al., 1993), interleukin (IL) 1- α (Mae et al., 1991; Hansen et al., 1994), IL-8 (Reitamo et al., 1993), interferon (IFN)- γ (Caruso et al., 1990 and 1994), tumor necrosis factor (TNF)- α (Boyle et al., 1993), and Fc- γ (Rossi et al., 1988). Thus, it is not surprising that IgG in normal human serum bound to autologous phytohemagglutinin (PHA)-activated lymphocytes and inhibited autologous mixed lymphocyte reaction (MLR) (Wolf-Levin et al., 1993). Passive infusion of intravenous

immunoglobulin (IVIg), which is mostly of IgG isotype and prepared from a large pool of normal healthy individuals, has been demonstrated in patients to improve symptoms in several autoimmune diseases, such as autoimmune cytopenias (Bussel et al., 1983; MaGuire et al., 1987) and anti-factor VIII autoimmune disease (Sultan et al., 1984). This beneficial effect of IVIg has been associated with the inhibition effect of IVIg on the pathogenic antibody-producing clones (Dietrich et al., 1993) and the pathogenic T cell functions (Saoudi et al., 1993). The later mechanism was further supported by the observation that IVIg directly affects cytokine production by T cells, B cells and monocytes/macrophages (reviewed in Andersson et al., 1996). IVIg inhibited the production of IL-2, IL-3, IL-4, IL-5, IL-10, TNF- β and granulocyte-macrophage colony stimulating factor (GM-CSF) in anti-CD3 monoclonal antibody- or phorbol ester-stimulated lymphocytes in vitro (Andersson et al., 1993; Amran et al., 1994), whereas it induced a transient production of IFN- γ and IL-6 by mononuclear and natural killer (NK) cells in vivo (Ling et al., 1993). These data support an important role of NAb in immune regulation. So far, little is known about the ability of NAb to influence the T helper 1 (Th1)-T helper 2 (Th2) balance in the immune response.

The immunoregulatory role of NAb is also expressed in its potential for antigen presentation. Naive B cells bearing surface IgM NAb are potential antigen presenting cells for priming CD4⁺ T cells against protein antigens in vivo (Constant et al., 1995). In other cases, the immune complexes formed by NAb and antigens activate complement, which enhances antigen uptake by all B cells (Thornton et al., 1996).

(4). Anti-tumor activity

In 1975, it was found that sera from several murine strains had cytotoxic reactivity against a variety of syngeneic and allogeneic tumor cell lines when assayed in the presence of rabbit complement (Martin and Martin, 1975). This observation was later confirmed by Menard et al who showed that not only anti-tumor NAb from BALB/c mice lysed syngeneic fibrosarcoma cells in vitro, but the level of circulating NAb was inversely correlated with the growth of a transplanted fibrosarcoma in vivo (Menard et al., 1977). These early studies introduced an important aspect of innate immunity in the resistance against tumors.

Ample evidence has suggested a role for NAb in tumor resistance. First, there is a positive correlation between the NAb binding levels of the tumor and the sensitivity of the tumor to NAb-mediated lysis in vitro and natural resistance mechanisms in vivo. The L5178Y-F9 T cell lymphoma treated with the tumor promoting phorbol ester 12-O-tetradecanoyl-phorbol-13-acetate (TPA), produced an increased cellular heterogeneity in sensitivity to NAb and complement-dependent cytotoxicity (Chow, 1984b). Cells selected following TPA treatment of the L5178Y-F9 through complement-dependent syngeneic NAb cytolysis showed a reduced sensitivity to NAb and complement, and increased resistance to elimination in vivo (Chow and Chan, 1987). High NAb binding lines selected from TPA treated cells through fluorescence-activated cell sorting (FACS) showed an increase in sensitivity to complement-dependent NAb lysis, increased NAb binding and a reduction in the tumor frequency of threshold s.c. inocula (Tough and Chow, 1988).

Second, there is an inverse correlation between serum NAb levels and tumor resistance in mice (Chow et al., 1981; Ehlich et al., 1984; Gil et al., 1990) and rats (Itaya et al., 1982). Old mice, which have higher levels of cytotoxic anti-tumor NAb than young mice, produced lower tumor frequencies than young mice when both NK-sensitive and NK-resistant syngeneic lymphoma were injected subcutaneously (s.c.) (Chow et al., 1981). In a B cell deficient model, mice exhibiting a low serum NAb titer produced significantly higher numbers of tumors than mice with high serum NAb levels (Bennet and Chow, 1991). Passive i.v. administration of NAb in xid-bearing mice reduced the frequency and prolonged the latency of a s.c. tumor challenge (Chow, 1995). Recently, it has been shown that normal healthy humans have natural IgM antibodies that are cytotoxic for human neuroblastoma cells. Infusion of purified normal human IgM into nude rats bearing human solid neuroblastomas led to growth arrest of even large tumors (David et al., 1996).

Third, tumors with a high NAb binding capacity were eliminated or clonally inhibited *in vivo*. This is based on the studies in which the tumors retrieved from injection sites exhibited a significant decrease in NAb binding levels compared with their starting lines including the L5178Y-F9 and SL2-5 (Brown et al., 1986), the LYNAb⁺ (L5178Y-F9 TPA/NAbs⁺3) (Zhang and Chow, 1997) and the oncogenic ras-transformed 10T½ fibroblast clone I3T2.1 (Tough et al., 1995). These tumors selected *in vivo* also showed reduced sensitivities to complement-mediated NAb lysis *in vitro* and increased tumorigenicity *in vivo* as demonstrated either by their reduced rate of clearance following i.p. injection (Chow, 1984a; Brown and Chow, 1985; Brown et al., 1986), or by their

increased tumor frequency and reduced tumor latency following s.c. inoculation (Brown and Chow, 1985; Tough et al., 1995; Zhang and Chow, 1997). The metastatic capabilities of these selected tumors also increased *in vivo* (Reese and Chow, 1992). This selection *in vivo* for reduced sensitivity to natural resistance is thymus-independent since tumors from both normal and thymus-depleted, irradiated and bone marrow-reconstituted (ATxBM) mice exhibited similar decreases in sensitivities to NAb and to NK cells *in vitro* (Brown and Chow, 1985). These data strongly suggest that NAb participate in the selection of tumors *in vivo* and under the selective pressure of NAb, only those tumors with a low reactivity to NAb could survive.

Finally, injection of NK resistant, NAb-preincubated P815 lymphoma cells into syngeneic mice produced tumors with a significantly lower frequency compared with untreated tumor cells, or cells preincubated in specifically absorbed serum (Chow et al., 1981). Similarly, rat hepatoma cells expressing higher levels of α -D-galactose on the cell surfaces were less able to colonize lungs pretreated with human serum NAb which contains anti-Gal natural IgG and IgM (Kawaguchi et al., 1994). These data argue strongly that NAb-mediated natural resistance mechanisms do exist *in vivo*.

The mechanisms by which NAb acts against tumors *in vivo* are unclear. Several potential mechanisms derived from studies in NAb rejection of xenografts might also be applicable to explain NAb anti-tumor responses. These mechanisms include opsonization of tumor cells leading to phagocytosis by macrophages, complement-dependent cytotoxicity and antibody dependent cell-mediated cytotoxicity (ADCC) by NK cells or blood monocytes and macrophages (Galili, U. 1993; Good et al., 1992; Sandrin et al., 1993;

Collins, 1995). These mechanisms also have been shown to be related to anti-tumor responses mediated by specific anti-tumor antibodies (Gil et al., 1990; Herlyn et al., 1985). Expression of α -Gal epitopes on tumor cell surfaces leads to binding of anti-Gal NAb and phagocytosis of tumor cells by human macrophages (LaTemple et al., 1996). In this case, the synthesis of α -Gal epitopes on human pre-B leukemia ALL-1 cells was up-regulated by introducing the glycosylation enzyme gene α -1,3-galactosyltransferase into the cell, and a 10-fold lower concentration of anti-Gal NAb compared with the physiological level in vivo induced a dramatic enhancement in phagocytosis of the α -Gal⁺ ALL-1 cells by macrophages (LaTemple et al., 1996). This raises an interesting hypothesis that anti-Gal NAb may be useful as an adjuvant to augment autologous tumor vaccines (Galili and LaTemple, 1997).

Another possibility is that NAb may directly interfere with the growth of the tumor in vivo. This idea is based on the findings that passive infusion of NAb into syngeneic normal mice markedly reduced the number of pre-B cells in bone marrow (Sundblad et al., 1991b) and injection of IVIg into patients with autoimmune disorders inhibited pathogenic B cell clones (Dietrich et al., 1993). It was also found that IVIg could suppress thrombin-induced cytosolic Ca²⁺ movement and nitric oxide (NO) production in aortic endothelial cells from guinea pig (Schussler et al., 1996). Culture supernatants of LPS-stimulated murine normal B lymphocytes inhibited the growth of LPS-stimulated B cells at the G1 stage of the cell cycle via an IgM antibody (Uher et al., 1992). Tumor-reactive human monoclonal natural IgM antibodies not only inhibited the in vitro growth of human colon carcinoma cell lines and induced complement-mediated cell lysis, but

were able to induce MHC class I molecule expression on the tumor cells (Bohn et al., 1994). These observations raises the possibility that NAb regulates cells through interaction with certain targets localized on the cell surface for controlling cell growth and function. Therefore, the direct biological effects of NAb on tumor cells may provide an important mechanism for NAb acting in vivo against neoplasia.

In summary, the multireactive nature and quantitatively high expression of NAb argue that NAb must be considered a regulator in both physiological and pathological situations. Its high avidity binding with cell surface structures makes it an ideal regulator for controlling cell functions through signaling.

(B) Protein Kinase C

1. Isoforms and Structure

Protein kinase C (PKC) is a multigene family consisting of at least eleven distinct lipid-dependent protein-serine/threonine kinases. PKC is thought to play an important role in signal transduction triggered by a variety of ligand receptor systems, including growth factors, hormones and neurotransmitters. All isoforms have similar structural and enzymatic properties but exhibit different modes of tissue distribution, developmental expression, activation and kinetic properties (Nishizuka, 1988). All cells express more than one isoform (Nishizuka, 1988). The isoforms can be divided into three distinct groups: (1) Ca^{2+} -dependent conventional PKCs (cPKCs: including isoforms α , $\beta 1$, $\beta 2$ and γ), (2) Ca^{2+} -independent novel PKCs (nPKCs: including isoforms ϵ , δ , $\eta(\text{L})$, θ and μ), (3) phorbol ester-independent atypical PKCs (aPKCs: including ζ and λ). The first

two groups can be activated by phorbol esters, whereas the third group is not (reviewed in Newton, 1995).

The primary structure of all PKC isoforms is composed of a single polypeptide chain containing a regulatory domain and a catalytic domain. Sequence comparison among mammalian species has led to the identification of four highly conserved regions (C1-C4) and five variable regions (V1-V5) (reviewed by Azzi et al., 1992). At the N-terminal part of the enzyme where the regulatory domain is located, the C1 region is immediately preceded by an autoinhibitory pseudosubstrate sequence, removal of which from the kinase core is associated with the activation of PKC (Orr and Newton, 1994). The C2 section seems to be the Ca^{2+} binding site of cPKCs, because deletion of the C2 region of PKC- β confers to the kinase activity, independent of Ca^{2+} (Kaibuchi et al., 1989). The C-terminal half of the polypeptide contains the catalytic domain (C3-V5), which has the ATP-binding site and the substrate-recognition site.

The cPKC isoforms possess all four constant (C1-C4) and five variable (V1-V5) regions (Azzi et al., 1992). The nPKC and aPKC enzymes do not require Ca^{2+} and lack the C2 region (Azzi et al., 1992; Newton, 1995). The molecular weight of the PKC family ranges from 77 to 115 KDa. PKC- μ is the largest reported member of the family at 115 KDa (Johannes et al., 1994).

Almost all PKC isoforms are encoded by independent genes (reviewed in Huppi et al., 1994) except PKC- β 1 and - β 2 which are derived from a single RNA transcript by alternative splicing (Coussens et al., 1987). These two isoforms are different only in 3 amino acids at their C-terminus.

2. Activation and Downregulation

In the classic pathway of PKC activation, ligands binding to cell surface receptors results in activation of phosphoinositide-specific phospholipase C (PI-PLC), which catalyses phosphatidylinositol 4,5-bisphosphate (PIP₂) and generates two intracellular second messengers: 1) inositol 1,4,5-triphosphate (IP₃), which mobilizes intracellular Ca²⁺ stores (reviewed in Berridge, 1987) and 2) diacylglycerol (DAG), a physiological activator of cPKCs and nPKCs (reviewed in Lee and Severson, 1994; Exton, 1996). In addition to PI turnover, there are two other sources for DAG: 1) hydrolysis of phosphatidylcholine and 2) hydrolysis of phosphatidic acid (reviewed in Nishizuka, 1992; Lee and Severson, 1994). In these two cases, there is no generation of IP₃ and no rise in intracellular Ca²⁺. Thus, the PKC pathway can be stimulated independently of changes in intracellular Ca²⁺ concentration.

Acidic phospholipids, such as phosphatidylserine (PS), function as essential cofactors of PKC activation. Of all the naturally occurring phospholipids tested, PS is the most effective cofactor in supporting PKC activity (Lee and Bell, 1986). However, the cPKCs require Ca²⁺ as well for full enzymatic activity. Calcium and acidic phospholipids cause PKC to undergo a conformational change exposing a binding site for PS, a normal component of the inner leaflet of the plasma membrane (Bell and Burns, 1991). The cooperation of calcium, PS and DAG results in a conformational change in the PKC molecule, which causes the pseudosubstrate region to be displaced from the active site of the enzyme, rendering the PKC catalytically active (Exton, 1996). Studies on the PS dependence of PKC autophosphorylation and substrate phosphorylation showed that

autophosphorylation, a process which confers PKC sensitivity to stimuli, is favoured at intermediate PS concentrations while substrate phosphorylation dominates at higher PS concentrations. In contrast to the modulation exerted by PS, DAG activates PKC equally towards substrate phosphorylation and autophosphorylation (Newton and Koshland, 1990).

Like DAG, phorbol esters can activate all the PKC isoforms except the α PKCs by binding to the regulatory domain, which induces the unfolding of the enzyme and exposes the catalytic sites (reviewed in Newton, 1995).

On activation *in vivo* by calcium and DAG or phorbol ester, PKC's membrane affinity is dramatically increased (Newton, 1995) and most PKCs translocate from the cytosolic location in resting cells to a membrane-associated site (Kraft and Anderson, 1983). Studies in neutrophils have shown that the distribution of PKC between cytosol and membrane is a dynamic equilibrium controlled by levels of free calcium (Phillips et al., 1989). Calcium may regulate the distribution as well as the activation of PKC. Furthermore, Ca^{2+} -induced associations are reversible (Reviewed in Rasmussen et al., 1995). More physiological activation of PKC by stimuli that generate DAG typically leads to only partial translocation, suggesting that these physiological signals may activate only a subset of the PKC isoforms. This is much different from stimulation by phorbol esters, which is the strongest activator of PKC detected to date. It has been recently demonstrated that some cells have a significant amount of activable PKCs in their native membranes. Growth factors such as the epidermal growth factor (EGF), the fibroblast growth factor (FGF) and IL-2 stimulate PKC activity in target cells not by inducing the

translocation of cytosolic enzyme to membranes, but by activating the pre-existing pool of membrane PKCs (Chakravarthy et al., 1994).

Phorbol ester-induced PKC translocation is a two-step process (Bazzi and Nelsestuen, 1989; Kazanietz et al., 1992). The first step is to form the reversible PKC-membrane complex. This step seems to be dependent on the presence of low concentrations of Ca^{2+} for the cPKCs and can be reversed on Ca^{2+} chelation. However, this step might be also independent of Ca^{2+} (Rasmussen et al., 1995). In the second step, PKC irreversibly integrates into the membrane and is constitutively activated. The activity of membrane-inserted PKC is not influenced by Ca^{+2} or phorbol esters (Bazzi and Nelsestuen, 1989). Whereas phorbol esters function largely by forming the irreversible PKC-membrane complex, DAG activates PKC largely in a reversible complex. In addition, since phorbol esters are much more potent than DAG and only slowly metabolized in cells (Bazzi and Nelsestuen, 1989), TPA induces marked and prolonged activation of PKC while DAG-stimulated PKC activation and translocation is transient and short-lived (Drust and Martin, 1985). Not all isoforms are translocated to the plasma membrane following TPA stimulation. For instance, in NIH 3T3 fibroblasts, after TPA treatment, the overproduced PKC- α , and - ϵ concentrate at cell membrane edges, while PKC- β 2 associates with actin-rich cytoskeleton and PKC- γ accumulates in the Golgi apparatus (Goodnight et al., 1995). This data is also consistent with the hypothesis that different isoforms may have distinct functions through targeting each specific substrate (Goodnight et al., 1995).

Activation of PKC results in the eventual proteolytic degradation or downregulation

of the enzyme. The hydrolytic cleavage of PKC by the calcium-dependent proteases calpain I and II occurs at one or two specific sites in the V3 hinge (Kishimoto et al., 1989) and yields two PKC fragments: a 36 KDa regulatory domain and a 45-49 KDa catalytic domain. The later sometimes is called PKM, which possesses 50% of the original enzyme activity for PKC- β , 100% for PKC- α and 65% for PKC- γ (Azzi et al., 1992). PKM is also Ca^{2+} - and the lipid-cofactor-independent (Azzi et al., 1992). Blockade of calpain activities in erythrocytes and erythroleukemia cells has been found to inhibit PKC functions (Ai and Cohen, 1993; Melloni et al., 1987). However, it remains unclear whether the generation of PKM in other cell types is also an essential step for PKC function. Moreover, PKC isoforms may have differential proteolytic downregulation because of the difference in their cellular type, subcellular localization and structural conformation (Kiley et al., 1991).

In addition to the modulation of PKC activity by second messengers which stimulate the membrane association of PKC and resulting pseudosubstrate exposure, PKC activity is also controlled by phosphorylation which regulates the active site and subcellular distribution of the enzyme (Keranen., et al., 1995).

3. Substrates

Proteins bearing the sequences of serine (S)/threonines (T)-X-lysine (K)/arginine (R); K/R-X-S/T; K/R-X-X-S/T; K/R-X-S/T-X-S/T-X-K/R; and K/R-X-X-S/T-X-K/R are potent targets of PKC (X can be any amino acid) (Pearson and Kemp, 1991). Although many proteins can be phosphorylated in vitro by PKC isoforms, the direct in vivo phosphorylation by PKC is observed in only a few molecules. Some of the more

important physiological substrates are discussed below.

(1) MARCKS

MARCKS, *myristoylated alanine-rich C kinase substrate*, an 80-87 KDa protein, has a very high alanine content and a very basic 25-amino-acid domain that represents the site of PKC phosphorylation. MARCKS is predominantly located at the plasma membrane of quiescent fibroblasts. Stimulation of PKC by phorbol ester treatment resulted in a rapid phosphorylation of MARCKS (Isacke et al., 1986; Rodriguez-Pena and Rozengurt, 1986) and translocation from the plasma membrane to Lamp-1-positive lysosomes (Allen and Aderem, 1995). Dephosphorylation of MARCKS increases the Ca^{2+} -dependent affinity ($K_d=2-5$ nM) for calmodulin, whereas phosphorylation of MARCKS reduces its affinity for calmodulin about 200-fold (McIlroy et al., 1991). Overexpression of MARCKS in rat 1 fibroblasts reduces the free concentration of calmodulin in these cells (Herget et al., 1994). Therefore, the phosphorylation state of MARCKS controlled by PKC and serine/threonine phosphatases may provide other mechanisms for regulation of intracellular Ca^{2+} levels (Blackshear, 1993).

It has been demonstrated in vitro that dephosphorylated MARCKS binds to and cross-links actin better than phosphorylated forms (Hartwig et al, 1992). This result indicates that MARCKS may serve as a mediator for PKC-controlled cell motility, secretion, membrane trafficking and mitogenesis (reviewed by Aderem, 1995). MARCKS knock-out mice display abnormal brain development and all pups died either before birth or within a few hours of birth, suggesting a role for MARCKS in normal brain development and postnatal survival (Stumpo et al., 1995). Most recently, MARCKS has

been postulated to be a novel growth suppressor in melanocytes based on the fact that MARCKS mRNA and protein are downregulated significantly in the murine B16 melanoma cells compared with syngeneic normal melanocytes (Brooks et al., 1996). Transfection of B16 cells with MARCKS cDNA produced clones exhibiting reduced proliferative capacity and decreased anchorage-independent growth compared with control cells (Brooks et al., 1996).

(2) Cytoskeletal Proteins

Phosphorylation of cytoskeletal proteins by PKC, for example, vinculin, lamin B and tau, has been reported (Werth et al., 1983; Cooper et al., 1989). Phosphorylation of lamin B by purified activated PKC- β 2 leads to solubilization of the isolated nuclear envelope protein (Hocevar et al., 1993). PKC has been found to colocalize with microtubules in pyramidal neurons (Kose et al., 1990). Phosphorylation of the microtubule-associated tau proteins by PKC has been associated with a reduced capacity of tau to promote tubulin assembly (Correas et al., 1992). PKC- β 2, but not PKC- β 1, has been found to bind to actin following stimulation by phorbol esters (Blobe et al., 1996). This interaction between PKC- β 2 and actin markedly enhanced autophosphorylation of PKC- β 2 and altered its substrate specificity (Blobe et al., 1996). In differentiated HL-60 cells, PKC- δ has been demonstrated to associate with vimentin intermediate filaments in an active (autophosphorylated) state and that vimentin itself was also phosphorylated (Owen, 1996). In intact nerve endings, PKC- ϵ physically binds to filamentous actin in an active state. The actin binding region of PKC- ϵ has been localized to its regulatory domain (Prekeris et al., 1996). Moreover, IL-2 also induces activation and translocation

of PKC- ζ to actin cytoskeleton in T lymphocytes (Gomez et al., 1995). Taken together, these results suggest that PKC plays an important part in the maintenance of cell morphology and function.

(3) Cell Surface Molecules

PKC activation by phorbol esters results in downregulation for several cell surface molecules, such as the major histocompatibility class I antigen (Peyron and Fehlmann, 1988), CD3, CD5 (Alberola-Ila et al., 1993), CD4 (Petersen et al., 1992), gp90^{MEL-14} (Jung and Dailey, 1990), and receptors for C5a (Rubin et al., 1991), TNF α (Galeotti et al., 1993), EGF (Davis and Czech, 1984), transferrin (Davis et al., 1986), IL-2 (Onishi et al., 1992) and platelet activating factor (Zhou et al., 1994). However, it is not clear yet for most of these molecules whether PKC modulates these molecules by direct phosphorylation or an indirect mechanism. Hunter et al. (1984) and Downward et al. (1985) reported that PKC phosphorylates the EGF receptor on ser 654, causing its internalization and hence, downregulating the receptor. However, an EGF receptor mutation (ser 654 to alanine) failed to influence downregulation (Morrison et al., 1993). After PKC phosphorylation, the ability of the insulin receptor to phosphorylate tyrosines on phosphatidylinositol 3 (PI3) kinase is reduced (Chin et al., 1994). Phosphorylation of the acetylcholine receptor by PKC results in an increased rate of desensitization (Hopefield et al., 1988). The *drosophila* photoreceptor (Hardie et al., 1993) and the Na⁺/H⁺ transporter (Panet and Atlan, 1990) have also been found to be phosphorylated by PKC under physiological conditions. PKC phosphorylated the insulin receptor β -subunit on threonine 1348, serines 1305 and 1306 both in vitro and in vivo (Chin et al.,

1993; Ahn et al., 1993). More recently, receptor-like protein tyrosine phosphatase α (RPTP α) and adhesion molecule integrin alpha 6A subunit have been shown to be substrates for PKC (Tracy et al., 1995; den Hertog et al., 1995; Gimond et al., 1995).

(4) Intracellular Signal Transducers

Raf

Raf protein serine/threonine kinases are pivotal molecules in signal transduction pathways and are essential for growth and development in worms, flies, frogs and mammals (reviewed in Williams and Roberts, 1994). PKC- α directly phosphorylates ser 499 and ser 259 of raf-1, both in vitro and in vivo (Kolch et al., 1993). Other researchers have reported that phosphorylation occurred at ser 497 and ser 619 of raf-1 (Carroll and May, 1994). Since phosphorylation at these sites occurs prior to stimulation of raf-1 activity (Isumi et al., 1991), it indicates that phosphorylation at these sites may not be sufficient for activation of raf-1 (Macdonald et al., 1993). The full activation of raf-1 appears to require a ras-controlled phosphorylation step (reviewed in Burgering and Bos, 1995).

p53

The p53 tumor suppressor protein is a potent transcription factor, whose activation leads to cell growth arrest at the G1/S and G2/M boundary or the induction of apoptosis (reviewed by Donehower and Bradley, 1993; Levine, 1997). p53 is phosphorylated at several amino- and carboxy-terminal sites in vivo and by a number of different protein kinases in vitro (reviewed by Meek, 1994). PKC- α , β I and β II can phosphorylate p53 in vitro (Baudier et al., 1992), which results in activation of the sequence-specific DNA

binding function of p53 (Delphin and Baudier, 1994; Hupp and Lane, 1994; Takenaka et al., 1995). The proposed major site of phosphorylation by PKC is serine 378 in human p53 (Takenaka et al., 1995) and serine 370 and threonine 377 in murine p53 (Milne et al., 1996). However, mutations at residues between 370 and 372 did not induce loss of any of the in vivo phosphopeptides. Thus, direct phosphorylation of p53 by PKC in vivo is still an open question. Milne et al have shown that TPA-dependent stimulation of p53 phosphorylation occurs (at least in mouse cells) through phosphorylation of p53 by the mitogen-activated protein kinase (MAPK) pathway (Milne et al., 1994 and 1996).

4. Involvement of PKC in Tumorigenesis

(1) PKC Isoform Overexpression and Tumor Induction

Overexpression of the exogenous $\beta 1$ isoform of PKC in R6 rat embryo fibroblasts (Housey et al., 1988), C3H 10T $\frac{1}{2}$ murine embryo fibroblasts (Krauss et al., 1989) and PKC- γ in NIH 3T3 murine fibroblasts (Persons et al., 1988) revealed subtle changes in morphology, and cells would grow in soft agar, but only in the presence of TPA. PKC- γ overexpressing cells sporadically formed tumors in nude mice, whereas PKC- $\beta 1$ -overproducing R6 cells were only weakly tumorigenic (Housey et al., 1988) and PKC- $\beta 1$ -overexpressing 10T $\frac{1}{2}$ cells were non-tumorigenic in nude mice. Overexpression of PKC- δ seems to inhibit cellular growth and to block cell cycle at G2/M (Watanabe et al., 1992; Mischak et al., 1993), while overexpression of PKC- ϵ induced transformation and tumorigenesis in two lines of fibroblasts, mouse NIH 3T3 and R6 (Mischak et al., 1993; Cacace et al., 1993) as well as one line of rat colonic epithelial cells (Perletti et al., 1996), indicating that PKC- ϵ might be an oncogene. In contrast, overexpression of PKC-

α in Swiss 3T3 cells did not display a transformed morphology nor were they capable of growth in soft agar (Eldar et al., 1990). Moreover, overexpression of PKC- ζ in NIH 3T3 cells did not induce transformation or tumorigenicity (Montaner et al., 1995). These data suggest that alterations of some of the PKC isoforms may play a role in malignant processes.

(2) PKC activity and Specific isoform Expression in Tumors

PKC activity is altered in certain malignancies. Elevated PKC activity has been found in breast cancer (O'Brian et al., 1989) and adenomatous pituitaries (Alvaro et al., 1992). The metastatic potential of certain tumors correlated with PKC activity. The more aggressive leukemic cells contained higher PKC activity than less aggressive ones (Aflalo et al., 1992). After the fifth sequential orthotopic transplantation passage of the human colorectal cancer cell line SW620, total PKC activity was increased in metastatic cells (Kuranami et al., 1995). Moreover, PKC- α , - δ , - η expression increased with serial passages, while PKC- β was lost. Cells from a highly metastatic subpopulation of the amelanotic melanoma cell line, B16a, exhibited higher levels of membrane bound PKC than a less metastatic subpopulation of cells (Liu et al., 1992). A similar finding was made by Raptis et al. (1993) that a clone of mouse NIH 3T3 fibroblasts had a high membrane-associated PKC activity and was as tumorigenic as polyoma-transformed cells, although this clone is still anchorage-dependent. By contrast, the activity of the membrane-bound PKC was significantly decreased in human liver cancer tissues compared with that of the adjacent normal tissues; while the PKC activity in the cytosolic fraction was not significantly different (Chang et al., 1996). PKC activity has been also

found to be reduced in colon carcinomas (Guillem et al., 1987; Kopp et al., 1991; Sakanoue et al., 1991; Levy et al., 1993; Attar et al., 1996). These alterations of PKC activity in different tumors are not due to point mutations in PKC genes because so far no evidence has indicated this possibility, but rather resulted from abnormal regulations induced by other oncogenic factors (see below). Therefore, it is expected that tumors with different cellular contexts may exhibit distinct alterations in PKC activity.

There is evidence showing that PKC- β expression may exert a negative regulation for growth of certain tumors. For example, overexpression of PKC- β 1 in colorectal cancer cell lines (HT-29) decreased their tumorigenicity (Choi, 1990). PKC- β mRNAs were decreased in 30 of 39 human colon tumors (Levy et al., 1993). Downregulation of the PKC- β gene occurs frequently during the process of transformation of melanocytes because PKC- β was expressed in melanocytes, but was undetectable by Northern analysis in 10 of 11 melanoma cell strains (Powell et al., 1993). However, it is not the case in other tumors. The expression of PKC- β was observed in the invasive but not the noninvasive gastric cancer cells (Schwartz et al., 1993). PKC- β was specifically elevated in thyroid cancer tissues compared to the normal thyroid gland (Hagiwara et al., 1990). Syngeneic rats that developed rhabdomyosarcoma tumors demonstrated a decrease in PKC- α and - ϵ but an increase in PKC- β (Hanania et al., 1992). These conflicting results indicate that the function of distinct isoforms relies on their cell types, and malignancy is a combinatorial result.

(3) Role of PKC in Transformation by Oncogenes

Although PKC is not a protooncogene product, it can substitute for or synergize

with authentic oncoproteins to promote transformation. It has been known that many of the oncoproteins that act at the early steps of the signal transduction cascade, such as ras, src, erbB2, sis and abl are able to increase cellular DAG, the endogenous activator of PKC (Wolfman and Macara, 1987; Diaz-Laviada et al., 1990; Chiarugi et al., 1989). In studies by Diaz-Laviada et al., (1990), src- and ras-transformed NIH 3T3 cells had elevated levels of DAG, but no downregulation of PKC, detected by immunoblotting. Instead, they found a "permanent" translocation of PKC to the plasma membrane using immunofluorescence. In an inducible ras expression model, PKC was, indeed, initially activated by p21^{ras} but prolonged p21^{ras} expression led to PKC downregulation (Haliotis et al., 1988). Ras-induced partial downregulation of PKC was confirmed by several other laboratories in other fibroblast systems (Huang et al., 1988; Weyman et al., 1988; Pulverino et al., 1990; Fu et al., 1991). The partial activation and downregulation of PKC in ras transformants appears to be a prerequisite for ras transformation, because ras-microinjected cells depleted of PKC by phorbol ester treatment failed to respond to mitogenic stimulation unless PKC was comicroinjected into the cell (Lacal et al., 1987). In other circumstances, oncogene products were able to alter PKC isoform expression. Transformation of rat embryo fibroblast and liver epithelial cells by ras lead to an increase in PKC- α and - δ and a decrease in PKC- ϵ (Borner et al., 1990, 1992a). The tumorigenic progression induced by oncogenic ras or the py-MT/pp60 c-src complex in Caco-2 cells is associated with upregulation of PKC- α gene transcription and expression as well as with constitutive PKC activation (Delage et al., 1993).

(C) Ras Oncogene and Signal Transduction

1. Mammalian ras family

Ras proteins play critical roles in the control of cell growth and differentiation (reviewed in Lowy and Willumsen, 1993). The ras family consists of three functional genes, H-ras, K-ras and N-ras in the mammalian genome (Lowy and Willumsen, 1993). Ras proteins locate on the inner surface of the plasma membrane where they transmit signals from tyrosine kinase receptors and some receptors coupled to heterotrimeric G proteins to a downstream cascade of serine/threonine kinases, which then activate nuclear factors and control gene expression and protein synthesis (Lowy and Willumsen, 1993). The H-ras, K-ras and N-ras proteins are 188-189 amino acids long, with the first 86 residues at the N-terminus being 100% identical and the next 78 residues being 79% identical. However, their last 25 residues at the C-terminus are divergent. The C-terminal part of the ras protein mediates its association with the inner face of the plasma membrane (Cox and Der, 1992). Mutation of this part of the ras protein resulted in defective cytosolic distribution and transformation (Willumsen et al., 1984).

The mRNA expression levels of the ras family are different in different mouse tissues. For example H-ras is predominantly expressed in skin and skeletal muscle, K-ras is chiefly expressed in gut and thymus, and N-ras is highest in testis and thymus (Leon et al., 1987). Thus, it is concluded that at least one of the three ras genes is expressed in all cell types (Leon et al., 1987).

2. Activating mutation and tumorigenesis

Physiologically, ras activity is controlled by its binding to GTP and GDP. Only its

GTP-bound form is biologically active. It becomes inactive when it is converted to the GDP-bound form by its intrinsic GTPase activity (Lowy and Willumsen, 1993). This conversion process is delicately and precisely regulated by a few distinct GTPase activating proteins (GAPs) (Lowy and Willumsen, 1993).

Mutations of the p21 ras protein, commonly found in codon 12, 13 or 61, result in a persistent activation of ras protein by reducing its intrinsic GTPase activity and/or increasing the intrinsic nucleotide exchange rate, which renders the ras protein transforming (Lowy and Willumsen, 1993). The activating mutations of ras oncogenes are found in nearly one-third of all human cancers (reviewed by Waldmann and Rabes, 1996) as well as in experimental tumors induced by numerous carcinogens (Balmain and Brown, 1988; Barbacid, 1987). It also has been observed that mutations of a particular ras gene predominate in tumors of specific tissue types. For example K-ras mutations are frequently found in lung, pancreas and colorectal carcinoma. N-ras mutations are reported in leukemia and lymphoma, and H-ras mutations are detected in certain types of oral cancer, thyroid and skin cancers (reviewed by Cerutti et al., 1994). In melanoma, the frequency of ras mutation was found to be 5% to 35% and N-ras mutation is significantly associated with melanoma progression (Herlyn and Satyamoorthy, 1996). In addition, expression of an activated ras oncogene is sufficient to induce transformation of numerous established rodent cell lines (Barbacid, 1987) and immortalized human cells (Amastad et al., 1988).

3. The ras signaling network

Studies in *Drosophila* and *Caenorhabditis elegans* have shown that ras plays a

critical role in cellular differentiation (Satoh et al., 1992). Blocking ras function by microinjection of neutralizing p21ras antibodies into mammalian cells abrogated the DNA synthesis induced by receptor tyrosine kinases and most non-nuclear oncoproteins (Satoh et al., 1992). These results established an important role normally played by ras in transducing mitogenic and developmental signals initiated by cell-surface receptors into the cytoplasm and nucleus (Satoh et al., 1992).

It is now clear that ras signaling occurs in at least two situations. 1) ras mediates signals initiated by receptor tyrosine kinases (RTK), such as the receptors for EGF, platelet-derived growth factor (PDGF), insulin and macrophage-colony stimulating factor (M-CSF); 2) ras mediates signals initiated by cell surface receptors which lack intrinsic tyrosine kinase activity but can activate intracellular tyrosine kinases such as src, abl and neu (Maruta and Burgess, 1994). In both situations, the phosphorylated intracellular domain of RTK or src provides docking-sites for tyrosine kinase substrates, proteins containing the src Homology 2 (SH2) domain, including the growth factor receptor binding protein 2 (Grb2) and the SH2 domain-bearing collagen-like protein, Shc (Rozakis-Adcock et al., 1992). The association of Grb2 and Shc is achieved by domain interactions through their SH2 and the src Homology 3 (SH3) domains. The SH3 domain of Grb2 interacts with son of sevenless (Sos) in both stimulated and unstimulated cells. Thus, it is thought that the Grb2-Sos complex needs to be translocated from the cytosol to the plasma membrane where the complex eventually mediates the activation of ras proteins (Aronheim et al., 1994). Nature is not so simple, however, in addition to the scheme depicted here for ras activation, there are other alternative mechanisms to activate

ras proteins such as through p120 GAP and NF1 GAP (reviewed in Pronk and Bos, 1994).

The downstream effectors of ras protein include raf-1, phosphatidyl inositol 3-OH kinase and p120 GAP (reviewed by de Vries et al., 1996). An increasing amount of evidence has established the raf-1-MAPK/extracellular signal-regulated protein kinase (ERK) cascade as an important pathway in mitogenic signal transduction (Daum et al., 1994; Burgering and Bos, 1995). It is known that Ca^{2+} and PKC direct this pathway since activation of the raf-1-ERK2 cascade by TPA occurs independently of ras activation (Burgering et al., 1993). However, ras also has been shown to activate raf-1 both in vitro and in vivo (Burgering and Bos, 1995). Ras binding of raf-1 is largely GTP dependent and requires the effector region of ras and the regulatory region of raf-1 (Warne et al., 1993; Burgering et al., 1995). There is yet no direct in vitro reconstitution of ras-GTP/raf-1 activation (Macdonald et al., 1993). Co-expression of ras and raf-1 in Sf9 cells results in a relatively weak activation of raf-1 (Williams et al., 1992). Strikingly, although co-expression of PKC- α and raf-1 in Sf9 cells increased autophosphorylation activity of raf-1, the downstream MAPK kinase (MEK) activity was not increased (Macdonald et al., 1993). Thus, it appears that either PKC or ras alone is not sufficient to activate MEK. Therefore, it is likely that ras and PKC act together in vivo to activate raf-1 fully (Burgering and Bos, 1995). Moreover, other proteins (e.g., 14-3-3) may also be involved in other steps required to fully activate raf-1 (Li et al., 1995).

PART II. OBJECTIVES

Correlated studies support a role for polyclonal serum NAb acting as a mediator of natural resistance against tumors in mice. However, little is known about their mechanisms of action or about the phenotype of susceptible cells. The aim of this study was to examine the contribution of the major signaling molecule PKC, which participates in normal cell activation, in the regulation of the expression of NAb binding structures, and to assess the role of NAb in regulation of cell function and survival both *in vitro* and *in vivo*. This has been approached by investigating four different objectives. First, to investigate the regulation of the expression of NAb binding structures by a critical signal transduction molecule PKC and to test the hypothesis that NAb may control activated cells *in vivo* and thus contribute to homeostasis of the organism. It has been found that short term treatment with tumor promoter TPA up to 2 hours induced an initial decrease in NAb binding by murine L5178Y-F9 lymphomas while longer term TPA treatment for 2 days produced an increase (Sandstrom and Chow, 1994). It was also demonstrated that oncogenic ras overexpression in murine fibroblasts resulted in a heterogeneous increase in NAb binding (Tough and Chow, 1991). Since ras-transformation is associated with an increase in production of diacylglycerol, an endogenous activator of PKC, PKC may play an important role in regulation of NAb binding structures in both cell systems. Considering that NAb inhibits growth and cytokine production of mitogen-activated lymphocytes *in vitro* (Wolf-Levin et al., 1993; Andersson et al., 1993; Amran et al., 1994; Uher et al., 1992), NAb thus may contribute to regulation of activated cells in

vivo. To more-directly address this hypothesis, a PKC- β 1-overproducing 10T $\frac{1}{2}$ fibroblast clone PKC-4, which lacks a complete transformation and thus could be regarded as a constitutively active line, was employed to examine PKC regulation of NAb binding structures in vitro and NAb regulation of activated PKC-4 cells in vivo by assessing the in vivo elimination of [131 I]-dUrd-labeled PKC-4 cells.

Second, to test the prediction that NAb binding with cell surface structures may initiate intracellular signaling events. This hypothesis is based on the emerging evidence that NAb could bind with activated immune cells and suppress their secretion of cytokines. NAb was also found to inhibit NO production and intracellular Ca $^{2+}$ movement in thrombin-treated endothelial cells (Schussler et al., 1996). This evidence leads to the hypothesis that NAb reacting with cell surface structures may introduce inhibitory signals into the cells resulting in their growth arrest. To examine the NAb binding-initiated intracellular signaling events including the changes in PKC expression, tyrosine phosphorylation and DNA synthesis, the ras- and PKC- β 1-overproducing 10T $\frac{1}{2}$ fibroblast models were studied with purified NAb and a temperature increase approach.

Third, if some cell surface molecules could mediate NAb-triggered signaling, identification of the nature of these cell surface structures would be critical for understanding the biological functions of NAb. Prior studies by others who employed the Western blotting technique have demonstrated some reactivities of NAb with a variety of intracellular self antigens (Berneman et al., 1992). However, little is known about the nature of the cell surface molecules in fibroblasts that can be recognized or influenced by NAb. To characterize the NAb reactive cell surface structures, which may be key

molecules that mediate NAb-initiated signaling, immunoblotting and immunoprecipitation approaches were employed. Based on the preliminary findings in the experiments, a few well defined molecules including CD44, the receptor-like protein tyrosine phosphatase α (RPTP α) and gelatinase B were further analysed for the influence of NAb on them and for their NAb binding potentials.

Finally, although passive NAb has been demonstrated to provide a beneficial anti-tumor effect in B cell-deficient CBA/N mice (Chow, 1995), the role of passive NAb in normal mice is still uncertain. To test whether passive NAb could also reduce tumorigenicity and metastasis in normal mice, the passive NAb transfer model was investigated with the C3H and DBA/2 normal mouse strains challenged with syngeneic tumors.

CHAPTER 2

**PROTEIN KINASE C EXPRESSION IN C3H 10T½ FIBROBLASTS
ASSOCIATED INCREASED NATURAL ANTIBODY ACQUISITION WITH
SURVEILLANCE OF PRENEOPLASIA AND HOMEOSTASIS OF THE
ORGANISM**

ABSTRACT

Extensive evidence supports a role for natural antibody (NAb) acting against small tumor foci *in vivo*. Ras-transformation of murine C3H 10T½ fibroblasts, which partially activated and downregulated endogenous PKC- α , increased their serum NAb binding consistent with the requirements for natural immune surveillance. PKC-4, a rat PKC- β 1-overexpressing 10T½ clone, with an 11-fold increase in PKC activity and an activated, partially transformed phenotype, was more susceptible to v-Ha-ras transformation and acquired 80% more NAb than the parental cells assayed by flow cytometry. H7 and E-64d blockade of the PKC-dependent signal transduction pathway and phorbol ester depletion of PKC reduced NAb binding. PKC- β 1 expression and NAb binding exhibited a similar temporal recovery from TPA treatment in PKC-4 cells. Thus, the expression of NAb binding structures appears to be elevated by the constitutive increases in the basal activation of PKC in both the ras-transformation and the PKC- β 1-preneoplasia models. This, coupled with the corresponding decreases in expression of membrane PKC- α and NAb binding in confluent 10T½ cells raises the possibility that in general, cells activated through PKC are NAb sensitive. In accord with their increased reactivity with NAb, the PKC-4 was more susceptible to natural defence mechanisms *in vivo*, assayed as an increased rate of elimination of [¹³¹I]dUrd-labelled cells injected subcutaneously into syngeneic C3H mice. Together the data extend the support for a role for NAb in immune surveillance, to resistance against preneoplastic cells and argue for NAb contributing to homeostasis of the organism.

INTRODUCTION

Naturally occurring antibodies have been found in the circulation of normal unimmunized individuals of many vertebrate species and all tumors examined to date react with them. Evidence suggests that NAb participates in a first line of defence against the growth of small tumor foci (Greenberg et al., 1983). The threshold s.c. syngeneic tumor inoculum model of incipient neoplasia has consistently revealed an inverse relationship between tumorigenicity in vivo and the serum NAb binding capacity of the tumor injected or the anti-tumor NAb levels of the recipient animals, including B cell-deficient *xid*-bearing CBA/N mice (Chow et al., 1981; Chow and Bennet, 1989). Murine lymphomas preincubated with serum NAb prior to their s.c. injection into syngeneic mice produced a lower tumor frequency than untreated cells or cells treated with specifically preabsorbed serum (Chow et al., 1981). Passive i.v. administration of NAb in *xid*-bearing mice reduced the frequency and latency of a s.c. tumor challenge (Chow, 1995). Recently, passive human natural IgM was shown to inhibit neuroblastoma growth in a nude rat model (David et al., 1996). Furthermore, oncogenic ras transformation of the C3H/HeN mouse embryo fibroblast line 10T½ resulted in a marked and heterogenous increase in acquisition of NAb from syngeneic whole serum (Tough and Chow, 1991). This demonstrated an NAb susceptible phase of tumor development consistent with the concept of immune surveillance which requires that cells undergoing the neoplastic process be more sensitive to the immune system.

Considering the association of ras transformation with increased production of diacylglycerol an endogenous activator of PKC (Wolfman and Macara, 1987), oncogenic

ras augmentation of NAb binding also provided evidence for the regulation of NAb binding structures via PKC. Treatment of L5178Y-F9, a murine T-lymphoma cell line, with the tumor promoter 12-O-tetradecanoylphorbol-13-acetate (TPA) produced a rapid decrease in NAb binding capacity followed by an increase which was blocked by an inhibitor of the specific TPA receptor, PKC. This further implicated PKC in the regulation of NAb binding sites (Sandstrom and Chow, 1994).

PKC, which represents a large family of serine/threonine kinases, mediates signals triggered through the external stimulation of cells by various ligands including hormones, neurotransmitters and growth factors or by cross-linking of cell surface molecules (Nishizuka, 1986; Vogel et al., 1993). Overproduction of some PKC isoforms in certain cell types has been associated with growth abnormalities as well as transformation (Housey et al., 1988; Cacace et al., 1993). Alterations of both PKC content and PKC activity have been frequently detected in many tumor tissue types (reviewed in Basu, 1993). These data suggest a pivotal role for PKC in proliferation, differentiation and tumorigenesis (Goodnight et al., 1994).

Thus, PKC regulates the expression of cell surface molecules and has linked cellular activation with the neoplastic process. In this study, a PKC- β 1-overexpressing variant of 10T $\frac{1}{2}$ with a partially transformed phenotype (Krauss et al., 1989), was employed to more-directly examine PKC regulation of NAb binding structures on activated cells in the absence of complete transformation and to compare this with regulation by oncogenic ras.

MATERIALS AND METHODS

Mice and sera

C3H/HeN mice were obtained from the University of Manitoba vivarium (Winnipeg, Manitoba). Whole serum NAb was obtained through bleeding per axilla normal adult C3H/HeN mice anesthetized with ether and allowing the blood to clot at 4°C.

Cells

I3T2.1 was cloned following transfection of C3H 10T½ cells with a raszip 6 vector which was derived from SVX by the insertion of the v-Ha-ras gene into the BamH₁ site (Tough and Chow, 1991). 10T½-PKC-4 (PKC-4) and 10T½-MV7-5 (MV7-5) were produced by transfection of C3H 10T½ cells with a pMV7 plasmid containing the full-length PKC-β1 cDNA and the empty plasmid, respectively (Krauss et al., 1989). I3T2.1 cells were cultured in D-MEM/F12 medium (Gibco, Grand Island, NY) supplemented with 10% fetal bovine serum (FBS) (Gibco). PKC-4 and MV7-5 cells were grown in D-MEM with 10% FBS in contrast with 10% bovine calf serum (BCS) used by previous investigators (Krauss et al., 1989). 10T½ cells were maintained in D-MEM (Gibco) or D-MEM/F12 with 10% FBS. For all the experiments except those indicated, cells within 30 passages were set at the same concentration in 100-mm tissue culture dishes (Corning, Corning, NY), grown for the same period and released with 0.05% trypsin-EDTA (Gibco) for 3-5 minutes. Trypsinization does not change the results (Chow, unpublished observation).

In vitro drug treatment

TPA and E-64d (Sigma, St Louis, MO) were dissolved in dimethyl sulfoxide (DMSO,

Fisher, Fair Lawn, NJ) at a concentration of 100 $\mu\text{g/ml}$ and 15 mM, respectively, and stored at -20°C . H7 and HA1004 (Seikagaku America, St. Petersburg, FL and Sigma) were dissolved in distilled water at 10 mM concentrations and stored at 4°C in the dark. H7 is a potent inhibitor of PKC as well as of cAMP-dependent protein kinase (PKA) (PKC $K_i=3 \mu\text{M}$, PKA $K_i=6 \mu\text{M}$), while HA1004 inhibits PKA much more efficiently (PKC $K_i=40 \mu\text{M}$, PKA $K_i=2.3 \mu\text{M}$) (Hidaka et al., 1984; Kawamoto and Hidaka, 1984). For long-term treatment, drugs were added into cultures for various times as indicated.

Fluorescence-detected NAb binding

NAb binding was determined by flow cytometry using an indirect immunofluorescence technique and expressed as mean channel fluorescence (MCF) as reported previously (Tough and Chow, 1991). Briefly, aliquots of 3×10^5 cells were washed in HEPES buffered DMEM or RPMI 1640 (Gibco) containing 2.5-5% FBS and 0.1% azide. Cell pellets were resuspended in 100 μl whole or growth medium-diluted C3H/HeN serum NAb versus medium for controls and incubated at 4°C for 1 h. The antibody-coated cells were then washed and exposed for 20 min in the dark at 4°C to 100 μl of FITC-labelled goat anti-mouse IgG (Whittaker Bioproducts, Canada and Sigma) and FITC-goat anti-mouse IgM (Jackson ImmunoResearch Laboratories, PA and Sigma), diluted 1:10 and 1:20, respectively, in the wash solution. The cells were washed and fixed by incubation for 5 min at 4°C in 200 μl of 1% paraformaldehyde in PBS (pH 7.4). Samples were analyzed at 4°C for linear fluorescence at 488 nm using a Coulter Epics V Multi-parameter Sensor System (Coulter Electronics, Inc., Hialeah, FL). Data were collected on 5,000 viable

cells determined by forward and side light scatter and MCF was calculated over the entire 256 channel range by the analysis program included in the instrument's operating system. MCF was reported after subtraction of the MCF for control samples.

Preparation of cell membrane and cytosolic fractions

Approximately $1.5 \sim 2.0 \times 10^7$ of cells were detached from dishes with a rubber policeman, washed with ice-cold phosphate buffer containing 0.8% NaCl, 0.02% KCl (PBS) and 0.5 mM phenylmethylsulfonyl fluoride (PMSF) (Sigma), pH 7.4 at 4°C, and resuspended in ice-cold 50 mM Tris-HCl, pH 7.5, 10 mM benzamidine, 2 µg/ml leupeptin, 50 µg/ml PMSF, 5 µM aprotinin, 10 µg/ml soybean trypsin inhibitor, 10 µg/ml N- α -p-tosyl-L-lysine chloromethyl ketone hydrochloride and 5 µg/ml N-tosyl-L-phenylalanine chloromethyl ketone (designated as buffer A). Then the cells were sonicated at 10% power using a Microsonic Cell Disruptor, Model XL2005 (Mandel Scientific Company Ltd., ON). An equal volume of the buffer A containing in addition, 10 mM EDTA, 20 mM EGTA and 0.6% (w/v) β -mercaptoethanol (designated as buffer B), was added to each cell sample. The mixture was centrifuged at 17,000 g for 1 h at 4°C on a microcentrifuge (Biofuge A-1302, Germany). The supernatant represents the cytosolic fraction. The pellet was resuspended in 200 µl of buffer B containing 1% Triton X-100, sonicated at 20% power and extracted at 4°C for 30-60 min. After centrifugation at 17,000 g for 30 min, the supernatant was used as membrane fractions. In some experiments, whole cell lysate was prepared by extraction of cells with buffer B containing 1% Triton X-100. Protein concentrations were quantified using a Bio-Rad DC protein assay kit according to the instructions (Bio-Rad Laboratories, Hercules, CA).

Sodium dodecyl sulfate-polyacrylamide gel electrophoresis (SDS-PAGE)

Three volumes of protein samples were mixed with 1 volume of 4x gel sample buffer containing 0.4 M Tris-HCl, pH 6.8, 8% SDS, 40% (w/v) glycerol, 0.4% bromophenol blue and 6% dithiothreitol. The samples were boiled in a water bath for 5 min. SDS-PAGE was produced with Protein II xi or Mini-protein II systems (Bio-Rad). Matched aliquots of 5 ~ 80 μ l containing 10-100 μ g of proteins were loaded on an 8% or 10% SDS-polyacrylamide separating gel with a 5% polyacrylamide stacking gel. The volume of samples applied was constant or nearly constant in a given run. The high range SDS-PAGE standards or biotinylated standards (Bio-Rad) employed in every electrophoresis experiment included myosin (200 KDa), β -galactosidase (116.3 KDa), phosphorylase B (97.4 KDa), serum albumin (66.2 KDa) and ovalbumin (45 KDa). The electrophoresis was carried out at 120 v in a Tris-glycine buffer consisting of 25 mM Tris, 0.2 M glycine and 0.1% SDS. The run was terminated when the blue line reached the bottom of the gel.

Western blotting analysis

The separated proteins on the gel were electrophoretically transferred onto a nitrocellulose membrane (Bio-Rad) in a transfer buffer containing 25 mM Tris, 0.2 M glycine and 20% (v/v) methanol. The transfer was performed at 30 v overnight at 4°C. The nitrocellulose membrane (blot) was stained with 0.2% ponceau S in 3% trichloroacetic acid to monitor protein loading and transfer. After destaining with distilled water, the blot was blocked with 10% bovine serum albumin (BSA) in 50 mM Tris, pH 7.5, containing 200 mM NaCl and 0.05% v/v Tween 20 (TBST) for 1 h and

subsequently incubated for 1 h in TBST containing a 1:1000 dilution of rabbit polyclonal antibodies against the α or β PKC isoforms (Gibco). Since the plasma membrane preparations from all cell types studied including fibroblasts contain non-ionic detergent soluble actin (Mesher et al., 1981; Apgar et al., 1985; Gruenstein et al., 1975), an affinity-purified polyclonal anti-actin antibody (Sigma) was included in some experiments as an internal control to confirm an equal amount of protein loading. After three 10-min washings, blots were incubated in horseradish peroxidase-conjugated goat anti-rabbit IgG (Gibco) in TBST for 3 h and washed extensively. Blots were developed with an enhanced chemiluminescence (ECL) western blotting detection kit (Amersham, Arlington Heights, IL). In some experiments, the protein bands were probed with alkaline phosphatase-conjugated anti-rabbit IgG antibodies and subsequently visualized by using an alkaline phosphatase-substrate kit (Vector Laboratories, Inc., Burlingame, CA). Protein densities were measured in a linear range with an MCID/M4 imaging system (Imaging Research, St. Catharines, Canada).

ras infection of PKC-4 vs 10T $\frac{1}{2}$ and colony formation

Cells were infected with the v-Ha-ras and neo^r gene bearing raszip 6 vector as previously described (Tough and Chow, 1991) using a low multiplicity of infection (MOI) of 4.7×10^{-4} to test the ras transformation susceptibility of the cells. Following incubation with virus and 8 μ g/ml of polybrene for 24 h, the cells were grown in DMEM medium with 10% FBS for 10 days. Cell foci were counted after methylene blue staining. In other experiments, cells were first incubated with and without virus and polybrene for 24 h, then trypsinized and washed once with fresh medium. Cell pellets were

resuspended in 6 ml of 0.3% agar-Noble (Difco Laboratories, Detroit, MI) in DMEM containing 15% FBS and 2 ml of cells were overlaid above 5 ml of 0.5% agar in the same medium in 60 mm petri dishes. The cells were overlaid every week with fresh DMEM containing 15% FBS (Krauss et al., 1989). After 7 or 19 days, colonies greater than 0.2 mm were counted under an inverted microscope. Colonies were randomly isolated and cultured in DMEM containing 10% FBS.

Tumorigenicity assays

Aliquots of 4×10^3 and 2×10^6 cells in final volumes of 100 and 170 μ l, respectively, were injected s.c. into syngeneic adult C3H mice and tumor development at the site of injection was monitored by assessing the two dimensional size of the tumor nodule for at least 30 days. The largest diameter and the diameter perpendicular to it were measured by calipers and multiplied.

$[^{131}\text{I}]$ deoxyuridine ($[^{131}\text{I}]$ dUrd) labelling and in vivo natural resistance assay

Cell labelling with $[^{131}\text{I}]$ dUrd was performed as described previously (Chow et al., 1983). Briefly, aliquots of 1.1×10^6 cells were set up in DMEM medium containing 10% FBS for 24 h before adding $[^{131}\text{I}]$ dUrd at a final concentration of 0.3 μ Ci/ml. The $[^{131}\text{I}]$ dUrd incorporation was allowed for 6 h at 37°C in a humidified incubator with 5% CO₂. Then the cells were harvested by trypsinization and washed three times with Hanks balanced salt solution (HBSS) at room temperature. Aliquots of 9×10^5 cells in 0.1 ml of HBSS were injected s.c. into 4 mice for each cell line. The mice were whole-body counted in a Beckman 8,000 gamma counter (Irvine, CA) at time 0, at 16 h and thereafter at intervals of 24 h for a total of 3 days. The amount of radioactive label

remaining in the mice at each time point was expressed as a percentage of the whole-body counts at time 0. All the mice in the label-clearance experiments were maintained on drinking water supplemented with 1% KI to minimize uptake of released iodine. This rapid elimination assay was previously demonstrated to be a measure of tumor sensitivity to thymus-independent natural resistance in that similar rates of tumor clearance were observed in normal and thymus-deficient animals (Carlson et al., 1980).

Statistical Analysis

The paired Student *t* test (P_{cd}) and the independent Student *t* test (P_{ij}) were used to assess the significance of the differences observed in NAb binding, colony formation and label-clearance experiments. $P > 0.05$ was not considered significant.

RESULTS

NAb binding and PKC expression of PKC-4, I3T2.1 and 10T½

Initial experiments completed within 4 weeks on early passage cells (up to 10 passages) grown in 10% FBS showed that the syngeneic serum NAb binding to PKC-4 cells was approximately 50% higher than the control-drug resistant 10T½ variant MV7-5 (Table 2.1, Expt. 1). Early passage cells transferred to growth in 10% BCS demonstrated the same relative NAb binding with PKC-4 acquiring more than twice the NAb of 10T½ (Table 2.1, footnote d). Since the NAb binding of 10T½ cells was not lower than MV7-5, the 10T½ was subsequently used as a control for both the v-Ha-ras and PKC-β1 expressing variants. Repeated analysis using both subconfluent and confluent cultures showed that the PKC-4 (up to 18 passages) bound at least 80% more NAb than the 10T½

Table 2.1. NAb binding to I3T2.1, PKC-4 and parental 10T½ cells.

Expt # ^a	Mean NAb binding (MCF) ± SE				
	10T½	I3T2.1	MV7-5	PKC-4	P _{td} ^b
1 (5)	54.9±4.3	-	46.5±6.6	68.2±11.5 ^c	<0.05
2 (8)	43.1±5.8	69.1±7.5	-	-	<0.01
3 (6)	52.1±8.6	66.3±10.1	-	-	<0.01
4 (9)	48.0±5.5	-	-	91.8±16.8	<0.01
5 (6)	57.5±8.6	-	-	103.6±16.7	<0.05
6 (4)	52.6±3.9	-	-	81.9±3.0	<0.01
	37.5±2.4 ^d	-	-	94.0±10.9 ^d	<0.02

^a The number of assays is in parentheses. Experiments 1,2,5 and 6 were assayed using confluent cultures, and Experiments 3 and 4 were assayed using subconfluent cultures.

^b Compared with 10T½ unless indicated otherwise.

^c Compared with MV7-5.

^d Early passage cells were grown for 6-30 days in 10% BCS.

(Table 2.1) and this was associated with the marked overexpression of the exogenous PKC- β 1 at 77 KDa (refer to Fig 2.3A and Table 2.3 footnote a) as previously reported (Krauss et al., 1989). In comparison, I3T2.1, a high NAb binding clone of ras transformed 10T $\frac{1}{2}$, bound 27% and 60% more NAb than the parental cells when assayed using subconfluent and confluent cultures, respectively (Table 2.1).

Since 10T $\frac{1}{2}$, but not I3T2.1 and PKC-4, exhibited contact inhibition upon reaching confluence, NAb binding was also assessed in parallel on subconfluent vs confluent cultures for each cell line. Different binding patterns emerged. More NAb was bound by subconfluent than confluent 10T $\frac{1}{2}$ cells, while there was no difference in NAb acquisition by subconfluent vs confluent I3T2.1 cells (Table 2.2). Confluent PKC-4 cells tended to bind more NAb than did the subconfluent PKC-4 cells (Table 2.2). It has been shown that PKC- α is the predominant isoform of PKC expressed in 10T $\frac{1}{2}$ cells (Weyman et al., 1988). Immunoblotting analysis of the endogenous PKC- α production revealed that subconfluent 10T $\frac{1}{2}$, I3T2.1 and PKC-4 all expressed more membrane PKC- α than their confluent counterparts (Table 2.3). The cytosolic fractions of 10T $\frac{1}{2}$ and PKC-4 lines exhibited no differences for subconfluent versus confluent cells and only a minimal percentage increase in PKC- α for confluent I3T2.1 cells. In general, PKC- α levels detected in the cytosolic compartments tended to be slightly lower in I3T2.1 and PKC-4 cells compared with 10T $\frac{1}{2}$ but were at least 50% less in the membrane fractions of the I3T2.1 and PKC-4, respectively, when assayed on subconfluent or confluent cells (Fig 2.1 and Table 2.3). PKC- β 1 expression levels were not different in subconfluent versus confluent PKC-4 cells (Table 2.3).

Table 2.2. NAb binding of subconfluent vs confluent 10T½ variants

Expt# ^a	Cells	Mean NAb binding (MCF) ± SE		
		Subconfluence	Confluence	P _{td}
1 (5)	10T½	55.0±4.2	41.3±5.0	<0.05
2 (3)	I3T2.1	56.1±3.6	53.8±4.8	NS
3 (4)	PKC-4	75.7±11.7	96.8±16.8	NS

^a The number of assays is in parenthesis.

NS, not significant.

Table 2.3. PKC- α and PKC- β 1 expression in membrane and cytosolic fractions of 10T $\frac{1}{2}$ variants

Expt# ^a	PKC isoforms	Cells	Membrane fraction		Cytosolic fraction	
			Subconfluence	Confluence	Subconfluence	Confluence
1 (4)	PKC- α	10T $\frac{1}{2}$	1.0	0.76 \pm 0.04 ^b	1.0	1.01 \pm 0.08
		I3T2.1	0.40 \pm 0.05 ^b	0.25 \pm 0.05 ^{c,d}	0.86 \pm 0.11	1.07 \pm 0.2
2 (3)	PKC- α	10T $\frac{1}{2}$	1.0	0.75 \pm 0.05	1.0	0.96 \pm 0.07
		PKC-4	0.50 \pm 0.11 ^b	0.33 \pm 0.09 ^c	0.82 \pm 0.18	0.81 \pm 0.19
3 (2)	PKC- β 1	PKC-4	1.0	1.18 \pm 0.13	1.0	1.23 \pm 0.30

^a PKC- α and - β 1 were detected by immunoblotting and analysed by densitometry. PKC-4 cells expressed PKC- β 1 at 77 KDa, while there was no detectable PKC- β 1 expression in 10T $\frac{1}{2}$ and I3T2.1 cells. The results, expressed as mean \pm SE, were arbitrary units relative to subconfluent 10T $\frac{1}{2}$ as 1.0 for Expts 1 and 2 and subconfluent PKC-4 as 1.0 for Expt 3. The number of assays is shown in parenthesis.

^b $P_{td} < 0.05$, compared with subconfluent 10T $\frac{1}{2}$.

^c $P_{td} < 0.05$, compared with confluent 10T $\frac{1}{2}$.

^d $P_{td} < 0.01$, compared with subconfluent I3T2.1.

Fig 2.1. PKC- α expression in membrane fractions of subconfluent 10T $\frac{1}{2}$ variants. Aliquots of 10 μ g membrane proteins of subconfluent 10T $\frac{1}{2}$, I3T2.1 and PKC-4 were assessed by immunoblotting with anti-PKC- α antibody. The result is one of three independent experiments which produced similar observations. The densitometry analysis was summarized in Table 2.3.



Colony formation, tumorigenicity and ras infection of PKC-4, I3T2.1 and 10T½ cells

Previous reports of PKC-4 cells grown in media containing BCS described a partially transformed phenotype in that they exhibited disorganized growth morphology and loss of contact inhibition, but were unable to form colonies in soft agar and were not tumorigenic in nude mice (Krauss et al., 1989). In the present study, PKC-4 cells were cultured in 10% FBS rather than 10% BCS. In FBS, PKC-4 tended to pile up after reaching confluence similar to the cells grown in BCS (Krauss et al., 1989). However, with growth for 12 days after reaching confluence, the cell clusters appeared like foci, 1.5 to 4 mm in diameter when stained with methylene blue. During 7 days of culture in 0.3% soft agar containing 15% FBS, 5% of PKC-4 cells formed small colonies (0.2 to 0.5 mm in diameter) compared with 55% of I3T2.1 cells (Table 2.4, Expt 1). 10T½ cells could not form colonies either on plastic or in soft agar even after culture for one month (data not shown). PKC-4 cells grown in FBS for 4 weeks and re-established in 10% BCS for 19 days also produced a small number of colonies in soft agar (Table 2.4, Expt 4). The low percentage of colony forming PKC-4 cells is consistent with the presence of a small proportion of cells which have undergone an oncogenic change.

High dose subcutaneous inocula of 2×10^6 PKC-4 cells were able to develop small tumor nodules of 4 mm in diameter at the s.c. injection site in 5/5 syngeneic C3H mice early on (Table 2.5, Expt 1). However, complete regression of tumors had occurred in 4/5 mice 29 days after the injection and persisted throughout the 45 observation days. PKC-4 cells which were re-cultured in 10% BCS for one month exhibited a similar pattern of tumor growth and high regression in 4/4 mice (Table 2.5, Expt 1). In contrast,

Table 2.4. Colony formation by 10T½ vs PKC-4 cells with and without ras infection.

Expt #	Cells	Mean number of colonies \pm SE		
		Virus	0 μ l	20 μ l
1 ^a	PKC-4		<u>47.3\pm9.4</u> 959.2 \pm 116.9	NA
	I3T2.1		<u>113.7\pm10.4</u> 206.0 \pm 18.5	NA
2 ^b	10T½		0	44.5 \pm 27.5
	PKC-4		106.0 \pm 5.5	199.5 \pm 5.5
3 ^c	10T½		0	0.4 \pm 0.1
	PKC-4		123.0 \pm 5.5	277.0 \pm 13.0
4 ^d	PKC-4		<u>28.0\pm2.0</u> 929.3 \pm 77.9	NA

(Table 2.4 footnote)

^a 3.3×10^4 PKC-4 and 1.7×10^4 I3T2.1 cells were cultured in triplicate in 0.3% agar in DMEM containing 15% FBS in 60 mm petri dishes. Colonies and all other seeded cell sites (1-5 cells) were counted per cm^2 (mean \pm SE) at day 7. Colony formation is shown as the number of colonies divided by the cell sites seeded per cm^2 . Thus, the colony forming efficiency was 4.9% and 55.2% for PKC-4 and I3T2.1, respectively.

^b 2×10^5 cells were infected with 20 μl of ras retrovirus with a MOI of 4.7×10^{-4} and grown in standard tissue culture medium (10% FBS) for 12 days in 100 mm petri dishes. Foci (1.5 to 4 mm in diameter) were stained with methylene blue and counted per whole plate. Results are from two independent experiments.

^c 2×10^5 cells were seeded in a 100-mm dish and infected with 20 μl of ras retrovirus with a MOI of 4.7×10^{-4} for 2 days. Then the cells were replated in three 60-mm dishes in 0.3% agar in DMEM containing 15% FBS and cultured for 19 days. Colonies (0.2 to 0.5 mm in diameter) were counted per cm^2 (mean \pm SE).

^d 3.3×10^4 PKC-4 cells, which were pre-cultured in BCS for 16 days, were transferred in triplicate to 0.3% agar plates containing 15% BCS in 60 mm petri dishes for another 19 days. Colonies and all other seeded cell sites were counted per cm^2 as outlined in Expt 1. The colony forming efficiency was 3.0%.
NA, not assayed.

Table 2.5. Tumorigenicity of 10T½, PKC-4 and ras-infected variants.

Expt#	Cells	Number of cells injected (s.c.)	Tumor frequency	Regression frequency ^a	Mean tumor size (cm ²) ± SE
			15 days	29 to 45 days	29 days
1	10T½	2x10 ⁶	0/2	0/0	NA
	PKC-4	2x10 ⁶	5/5	4/5 ^c	NA
	PKC-4 ^b	2x10 ⁶	4/4	4/4 ^d	NA
2	I3T2.1	4x10 ³	5/6 ^f	0/5 ^e	NA
	PKC-4	4x10 ³	0/6 ^f	0/0 ^e	NA
3	PKC-4 (5 subclones)	2x10 ⁶	5/5	1/5 ^c	1.0 ± 0.3 ^g
	10T½-ras (4 subclones)	2x10 ⁶	4/4	1/4 ^c	4.6 ± 1.4
	PKC-4-ras (5 subclones)	2x10 ⁶	5/5	4/5 ^c	0.4 ± 0.3 ^h

^a All regressing tumors had completely disappeared except for 1 of 4 regressing tumors for the PKC-4-ras clones in experiment 3.

^b PKC-4 cells had been recultured in 10% BCS for one month before injection.

^c Twenty nine days, ^d 35 days, ^e 45 days and ^f 31 days after injection, respectively.

^g P < 0.05 compared with 10T½-ras subclones.

^h P < 0.03 compared with 10T½-ras subclones.

NA, not assayed.

while 5/5 of the PKC-4 subclones isolated after 19 days growth in soft agar were similarly tumorigenic at 2×10^6 cells in the single mouse tested for each, only 1/5 subclones regressed (Table 2.5, Expt 3). This supported the idea that a small subpopulation of PKC-4 cells were tumorigenic and these had been isolated through cloning in soft agar. Furthermore, subcutaneous injection of 4×10^3 cells, a threshold inoculum for I3T2.1 which should not produce a tumor in every mouse, resulted in tumor outgrowth beginning after 20 days in I3T2.1 inoculated mice. By day 45, 5 of 6 mice challenged with I3T2.1 exhibited large tumors and none of 6 mice given 4×10^3 PKC-4 cells had tumors (Table 2.5, Expt 2). Together these data confirm the idea that a transforming genetic alteration is expressed in only a small proportion of PKC-4 cells. Similar to our previous reports (Tough and Chow, 1991), s.c. inoculation of 2×10^6 10T $\frac{1}{2}$ cells did not grow out in the two mice tested (Table 2.5, Expt 1).

Previously, PKC- β 1 introduction and overproduction in rat embryo fibroblasts was associated with increased cellular susceptibility to ras-induced transformation (Hsiao et al., 1989). However, PKC-4 cells were shown to be more resistant to transformation by γ -irradiation and the same group indicated that preliminary observations suggested that PKC-4 cells were also more resistant to transformation by v-Ha-ras oncogene or benzo[α]pyrene diolepoxide (Hei et al., 1994). In the present study, retroviral introduction of v-Ha-ras into PKC- β 1 overexpressing PKC-4 cells yielded at least twice as many additional colonies as similar infection of the parental 10T $\frac{1}{2}$ assayed in standard tissue culture (Table 2.4, Expt 2) and via growth in agar (Table 2.4, Expt 3). The discrepancy between these two studies is probably due to the use of FBS which is more

supportive of cell growth than BCS, and factors in the FBS which can enhance both spontaneous and ras-induced transformation in PKC-4 cells. In fact, the presence of factors in FBS but not BCS was considered to enhance oncogenic ras-induced transformation of 10T½ and rat 6 fibroblasts (Egan et al., 1989; Hsiao et al., 1987). The data from this study suggest that the bulk of the PKC-4, the 90-95% which can not form colonies in agar were more easily transformed by ras and thus preneoplastic.

Assessment of the tumor forming capacity of the agar-isolated clones showed that the 4 ras-transformed 10T½ clones tested at 2×10^6 cells in one mouse each were more aggressively tumorigenic than the similarly generated ras-transfected PKC-4 clones and the PKC-4 subclones. They exhibited a low regression rate and produced statistically larger tumors at the injection site 29 days after s.c. inoculation compared to the ras-transfected PKC-4 clones and the PKC-4 subclones (Table 2.5, Expt 3). In contrast, the ras-transfected PKC-4 clones exhibited a higher regression frequency (4/5) compared with that of the ras-transfected 10T½ clones (1/4) and the PKC-4 subclones (1/5) (Table 2.5, Expt 3), although there was no significant difference in their growth properties in vitro (data not shown). Together, this suggested that the few cells in PKC-4 capable of forming tumors were highly malignant, while ras transformation of the bulk of PKC-4 cells which were not able to form a colony, produced tumor cells which were less malignant than ras transformed 10T½ cells. This is consistent with the observation that PKC-β1 inhibited the in vivo growth of human colon cancer lines in which either a normal or a mutated c-K-ras oncogene was expressed (Goldstein et al., 1995). These data argue that PKC-β1 overexpression may increase the susceptibility of ras-transformed cells

to natural resistance and/or adaptive immune defence in vivo.

Sensitivity of PKC-4 to natural resistance in vivo

Within 24 h after s.c. cell inoculation, whole body gamma counting revealed that [¹³¹I]dUrd-labelled, high NAb binding PKC-4 cells were eliminated significantly faster from syngeneic C3H mice than 10T½ cells (Table 2.6). The ratio of remaining PKC-4 vs 10T½ cells decreased over the 3 days of the assay. Furthermore, compared to 10T½, PKC-4 cells exhibit a greater growth capacity in vitro such that PKC-4 could grow in low serum conditions and yield high densities (Krauss et al., 1989). Considering the growth advantage of PKC-4, their more rapid in vivo elimination compared with 10T½ is therefore very meaningful.

NAb binding of H7 treated cells

After treatment for 1 day with 25 µM H7, 10T½, I3T2.1 and PKC-4 cells appeared more dendritic and less flat and this persisted for the three days of treatment compared with no change in the growth morphology of cells treated with the PKA inhibitor, HA1004. H7 decreased NAb binding of all cell lines in a dose-dependent (data not shown) and time-dependent manner (day 2 shown in Table 2.7). HA1004 did not show any effect on NAb binding, further implicating PKC activity in the upregulation of NAb binding sites.

NAb binding of E-64d treated cells

Activation of PKC is followed by neutral protease, calpain-mediated proteolytic degradation of the enzyme to produce PKM, the activated, Ca²⁺- and phospholipid-independent catalytic fragment of PKC (Savart et al., 1992). In erythrocytes and

Table 2.6. Elimination of ^{131}I -dUrd-labelled PKC-4 vs 10T $\frac{1}{2}$ cells in vivo

Expt # ^a	Cells	Mean percentage retained radioactivity \pm SE			
		0 h	16 h	40 h	64 h
1	10T $\frac{1}{2}$	100	86.8 \pm 5.7	56.0 \pm 5.2	33.3 \pm 2.8
	PKC-4	100	84.5 \pm 5.3	41.4 \pm 2.7 ^b	23.1 \pm 1.7 ^c
2	10T $\frac{1}{2}$	100	96.2 \pm 2.0	73.3 \pm 3.5	48.5 \pm 3.0
	PKC-4	100	88.0 \pm 1.3 ^c	52.2 \pm 3.9 ^c	33.9 \pm 3.8 ^c

^a Adult male C3H mice, 9-11 weeks old and 7-9 weeks old were employed in experiments 1 and 2 respectively with 4 in each group. Aliquots of 9×10^5 ^{131}I -dUrd-labelled cells were injected s.c. and whole body retained radioactivity assayed over 3 days was expressed as a percentage of cpm at time 0 immediately after the injection.

^b $P_{ti} < 0.05$ compared with 10T $\frac{1}{2}$.

^c $P_{ti} < 0.02$ compared with 10T $\frac{1}{2}$.

Table 2.7. NAb binding of cells treated with PKC inhibitors or TPA for 2 days.

Cells ^a	Mean NAb binding (MCF) \pm SE			
	Control	Drugs		% decrease
10T $\frac{1}{2}$ (4)	37.1 \pm 4.2	H7	31.5 \pm 2.0	15.0
(6)	35.7 \pm 2.6	HA1004	36.7 \pm 4.7	-2.8
(6)	47.3 \pm 6.5	TPA	36.3 \pm 3.8 ^b	23.3
I3T2.1 (4)	50.1 \pm 10.5	H7	35.2 \pm 7.2 ^b	29.7
(2)	55.1 \pm 23.1	HA1004	56.4 \pm 26.3	-2.4
(3)	40.2 \pm 5.7	TPA	28.6 \pm 4.2 ^b	28.9
PKC-4 (6)	56.5 \pm 4.9	H7	45.0 \pm 4.0 ^b	20.4
(2)	61.9 \pm 11.2	HA1004	60.4 \pm 12.5	2.4
(6)	54.1 \pm 3.9	TPA	48.8 \pm 4.2	9.8
(4)	70.8 \pm 6.3	E64-d	56.8 \pm 8.3 ^b	19.8
(4)	70.8 \pm 6.3	DMSO	68.9 \pm 10.0	2.7

^a Cells were treated with TPA (100 ng/ml), H7 (25 μ M), HA1004 (25 μ M), E64-d (30 μ M), or DMSO (0.2%) for two days. The number of experiments is shown in parentheses.

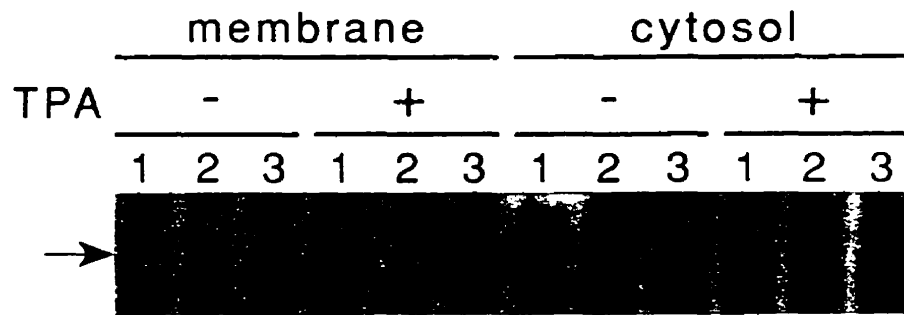
^b $P_{id} < 0.05$.

erythroleukemia cells, the generation of PKM is a key step in the function of PKC (Ai and Cohen, 1993; Melloni et al., 1987). E-64 blocks calpain mediated degradation of PKC to PKM, and 20 μ M efficiently inhibited TPA-induced PKC cleavage and the function of PKC (Ai and Cohen, 1993). After two days treatment of PKC-4, 30 μ M of E-64d a permeable derivative of E-64, significantly reduced NAb binding by 20% while comparative concentrations of DMSO did not show any effect on NAb binding (Table 2.7). This result extends the support for PKC upregulation of NAb binding in PKC-4 cells.

NAb binding and PKC expression by TPA treated cells

TPA is a tumor promoter and a strong PKC activator. Prolonged TPA treatment is shown to deplete conventional PKCs including PKC- α , β and γ (reviewed in Goodnight et al., 1994). TPA treatment for 24 h was shown to efficiently deplete PKC- α in v-Ha-ras transformed NIH 3T3 cells (Diaz-Laviada et al., 1990) and PKC- β 1-overproducing rat embryo fibroblasts (Borner et al., 1992b). With longer ½-3 day exposures to 100 ng/ml TPA, 10T½ cells lost their flat appearance and PKC-4 cells became much rougher than their untreated or DMSO treated controls. The transformed morphology of I3T2.1 did not change noticeably in culture with TPA. TPA reduced NAb binding and the downregulation persisted over the 3 observation days for 10T½ and I3T2.1 (day 2 shown in Table 2.7). However, NAb binding in PKC-4 cells showed a 30% decrease at 12 hours with a mean MCF \pm SE of 31.5 ± 3.8 which was significantly lower than untreated cells at 44.4 ± 7.0 with $P_{td} < 0.02$. This was followed by a recovery of NAb binding after TPA treatment for one day assayed at 38.9 ± 7.0 and a return to control levels on days

Fig 2.2. PKC- α expression in 10T $\frac{1}{2}$ variants treated with TPA. 10T $\frac{1}{2}$ (lane 1), I3T2.1 (lane 2) and PKC-4 (lane 3) were treated with (+) and without (-) 100 ng/ml TPA for 2 days. An aliquot of 20 μ g membrane and 100 μ g cytosolic proteins of each cell line was assessed. Arrow indicates PKC- α .



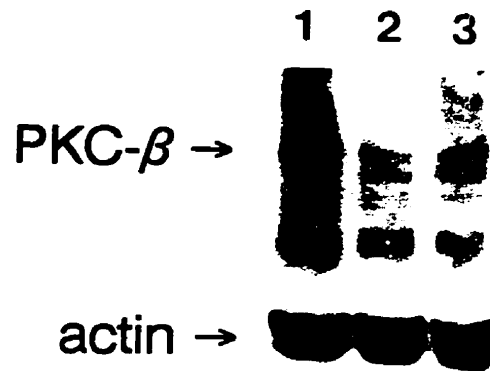
3 and 4 at 49.0 ± 14.7 and 44.4 ± 1.9 respectively. Analysis of PKC expression by immunoblotting 2 days after TPA treatment showed that PKC- α was completely absent from the cytoplasmic and membrane compartments in all three cell types (Fig 2.2) but a trace amount of PKC- $\beta 1$ still existed in PKC-4 (Fig 2.3). After TPA treatment of PKC-4 for four days, the ratio of PKC- $\beta 1$ expression relative to the DMSO control returned to nearly 50% of the control (Fig 2.3 A and B). The result was identical to that detected with both the ECL and the alkaline phosphatase-substrate systems (data for the later were not shown). The resistance of PKC- $\beta 1$ in PKC-4 to TPA treatment is consistent with a similar finding in PKC- $\beta 1$ -overexpressing rat embryo fibroblasts (Borner et al., 1992b). Thus, the rapid recovery of NAb binding in PKC-4 was accompanied by a reappearance in PKC- $\beta 1$ expression, further substantiating the role of PKC in the upregulation of NAb binding structures.

DISCUSSION

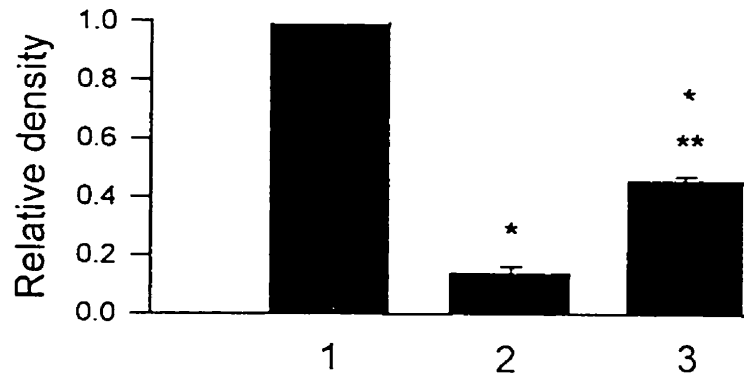
In PKC-4, the marked overexpression of PKC- $\beta 1$ and consequently very high basal level of PKC enzyme activity is likely responsible for the significant increase in expression of NAb binding structures compared to the parental 10T $\frac{1}{2}$. This is supported by the evidence that H7 and E-64d inhibitors of PKC reduced the NAb binding by PKC-4 and that changes in NAb binding by TPA-treated PKC-4 cells exhibited a temporal relationship with the disappearance and reappearance of the PKC- $\beta 1$ protein. In keeping with this thinking, the elevated NAb binding of I3T2.1 relative to the parental 10T $\frac{1}{2}$ is likely dependent upon the constitutive PKC activation which has been associated with

Fig 2.3. PKC- β 1 expression in PKC-4 cells treated with TPA. A) PKC-4 cells were treated with 100 ng/ml TPA for 2 (lane 2) and 4 (lane 3) days, or with 0.2% DMSO for 4 days (lane 1). PKC- β 1 was detected by immunoblotting with whole cell lysate extracted from cells with 1% Triton X-100. The result represents three independent experiments with similar observations which were summarized in B). B) Densitometry analysis of three independent experiments. Data were arbitrary units (mean \pm SE) relative to DMSO controls as 1.0. Statistical analysis was performed on original densities without conversion. * $P_{td} < 0.02$ compared with lane 1. ** $P_{td} < 0.01$ compared with lane 2.

A)



B)



oncogenic ras expression. Murine fibroblasts transformed by an activated ras oncogene exhibited elevated levels of diacylglycerol an endogenous activator of PKC, followed by activation and partial downregulation of the PKC (Wolfman and Macara, 1987; Chiarugi et al., 1989; Haliotis et al., 1988). The basal level of phosphorylation of a membrane-associated 80-KDa substrate of PKC also increased in ras-transformed fibroblasts suggesting high endogenous PKC activity in the ras transformants (Wolfman and Macara, 1987). Moreover, this ras-induced PKC activation process appears essential for ras transformation since ras-microinjected cells depleted of PKC by phorbol ester treatment did not respond to mitogenic stimulation unless PKC was comicroinjected into the cell (Lacal et al., 1987). In the present study, the greater tendency for H7 inhibition of NAb binding in I3T2.1 > PKC-4 > 10T½ cells (Table 2.7), further suggests the dependence on PKC for the increases in NAb binding associated with ras-transformation and PKC-β1 overexpression. Moreover, the observation that proliferating subconfluent 10T½ cells bound more NAb and expressed more PKC-α in their membrane fractions than resting confluent cells coupled with the evidence that PKC activity was higher in membranes of subconfluent versus confluent 10T½ cells (Miloszevska et al., 1986), also supports the idea that PKC regulates NAb binding structures in a relatively normal albeit immortalized fibroblast line. This growth status-dependent NAb acquisition was regulated differently in the 10T½ variants constitutively producing ras or PKC-β1 proteins with no decrease in NAb binding observed at confluence corresponding with their lack of sensitivity to contact inhibition. Taken together, these data argue strongly for the dependence of NAb binding on PKC expression and activation, suggesting that cells undergoing activation via

the PKC pathway may be particularly susceptible to NAb-mediated regulation. This is supported by the ability of NAb to reduce the cycling of I3T2.1 cells in culture (see Chapter 3). Thus, the intriguing possibility is raised that NAb regulates the behaviour of normal activated cells undergoing proliferation, differentiation or programmed cell death.

Previous investigators have described the *in vitro* binding of a monoclonal human natural IgM antibody to human tumor cells and to normal CD3⁺ T cells polyclonally stimulated by phytohemagglutinin (PHA), with a subsequent reduction in the proliferation of the tumor cells only (Bohn et al., 1994). In addition, IgG in normal human serum bound to autologous PHA-activated T lymphocytes but not to non-activated CD3⁺ T cells (Wolf-Levin et al., 1993). The increased expression of CD45RA, a transient early marker for T cell activation (Deans et al., 1992), on L5178Y-F9 T lymphoma cells repeatedly treated with TPA and selected through flow cytometry for high NAb binding (Zhang and Chow, 1997) also supports increased reactivity of NAb with activated T cells. Thus, the idea that NAb regulates cellular activation provides one theoretical basis for the beneficial effects of intravenous immunoglobulin against autoimmune and inflammatory diseases (Leung et al., 1987; Schwartz, 1990) and for NAb homeostasis of the organism (Avrameas, 1991). In particular, NAb control of cellular activation would clearly contribute to autoregulation of the immune system.

Multistage carcinogenesis is considered to involve the sequential acquisition of a variety of genetic mutations which endows a cell with increasingly altered growth characteristics and at last converts a normal cell to a fully malignant tumor cell. Overexpression of PKC- β 1 in PKC-4 cells grown in FBS was associated with an *in vitro*

growth advantage and an increased susceptibility to spontaneous and ras oncogene transformation. Considering the key role for PKC in signaling for cellular activation, this argues that PKC-4 expresses an activated cell phenotype which links the epigenetic changes that occur upon stimulation of normal cells with the genetic changes in preneoplastic cells exhibiting few alterations in DNA and only limited growth autonomy. Overproduction of PKC- β 1 in PKC-4 cells was also associated with a significant increase in NAb binding capacity similar to the transformation of 10T $\frac{1}{2}$ cells by oncogenic ras (Tough and Chow, 1991). The faster clearance of the high NAb binding PKC-4 cells compared with the low NAb binding non-tumorigenic parental 10T $\frac{1}{2}$ cells in a rapid in vivo elimination assay of natural resistance demonstrated the augmented sensitivity of the PKC- β 1 overexpressing cells to host-mediated natural defence. These results provide the first evidence suggesting NAb controls activated cells in vivo and supporting an NAb susceptible phase of preneoplasia consistent with the concept of immune surveillance. The extension of NAb-mediated surveillance to preneoplastic states moves the first line of immunological defense against tumor development closer to the initial events in this multistep process.

In summary, the data demonstrate that overexpression of PKC- β 1 in 10T $\frac{1}{2}$ cells, like oncogenic ras transformation, resulted in an increase in NAb binding capacity. Thus, the constitutive increase in the basal activation of PKC in both ras transformed and PKC- β 1 overexpressing 10T $\frac{1}{2}$ cells upregulated NAb binding, identifying PKC, an integral signaling molecule of normal cellular activation, as a key regulator of NAb binding structures. The correlating decreases in NAb acquisition and PKC- α expression when

10T½ cells reach confluence and the correspondence of high NAb binding and increased rapid elimination of the PKC-4 in vivo argued for NAb contributing to the regulation of activated cells in vivo and thus to homeostasis of the organism. Furthermore, the increased neoplastic potential of the PKC-4 extended the support for NAb mediated resistance against tumor development to surveillance of preneoplasia.

CHAPTER 3

NATURAL ANTIBODY BINDING-INDUCED INTRACELLULAR SIGNALING

EVENTS IN C3H 10T½ FIBROBLASTS

ABSTRACT

The cell surface binding ability of NAb makes it potentially an ideal regulator in controlling cell functions through signaling. Flow cytometry has revealed that both 10T½ and the ras-overexpressing I3T2.1 cells bound significantly less NAb at 37°C versus 4°C. However, the PKC-β1-overproducing PKC-4 exhibited a slight increase in acquisition of NAb at 37°C. A marked loss of cell surface NAb was also observed in the all three lines after raising the temperature from 4°C to 37°C, and this was partially inhibited by H7, a PKC inhibitor, but not by HA1004, a PKA inhibitor. This suggested that PKC is involved in an NAb binding-initiated downregulation of NAb bound on the cell surface. Immunoblotting analysis revealed an increase of 20% for PKC-β1 and 80% for PKC-α in the membrane fractions of the PKC-4 treated with purified NAb at 4°C followed by a raise in temperature to 37°C for 30 min compared with NAb-treated cells kept at 4°C. Moreover, the tyrosine phosphorylation level of a membrane-associated 60-KDa protein (p60) detected with a monoclonal anti-phosphotyrosine antibody was markedly reduced by NAb coating and raising the temperature, and this was concordant with the marked release of membrane receptor-like protein tyrosine phosphatase α (RPTPα) into the cell supernatant. Furthermore, cocultivation of I3T2.1 with purified NAb resulted in growth inhibition assessed as a decrease in total cell numbers and an increase in cell numbers in G0/G1 phase in the cell cycle. All together, these data argue that the interaction of NAb with cell surface structures initiated an intracellular response including rapid PKC-dependent signaling events, the release of membrane molecules and bound NAb, a reduction in phosphotyrosine levels of p60 and over time the suppression

of cell proliferation, which may contribute to a basic biological mechanism for NAb controlling activated cells in both physiological and pathological conditions.

INTRODUCTION

NAb is characterized by low affinity but high avidity binding to a variety of self and nonself antigens (Avrameas and Ternynck, 1993). Their high reactivity with tumors suggests that NAb plays an important role in a first line of defense against the growth of small tumor foci (Greenberg et al., 1983). It has been demonstrated that transformation of the murine fibroblast C3H/HeN line 10T $\frac{1}{2}$ induced by co-introduction of the v-H-ras oncogene and the neomycin resistance (*neo^r*) gene followed by G418 selection resulted in a marked and heterogenous increase in syngeneic whole serum NAb binding and natural killer (NK) cell sensitivity (Tough and Chow, 1991). These results demonstrated an NAb susceptible phase of tumor development and regulation of NAb binding structures by signal transduction molecules.

Protein kinase C (PKC), which represents a large family of serine/threonine kinases, participates in one of the major cell signal transduction pathways. It is activated by the external stimulation of cells by various ligands including hormones, neurotransmitter and growth factors (Nishizuka, 1986) or by cross-linking cell surface molecules, such as T cell receptor/CD3 complexes (Hausz et al., 1993; Buday et al., 1994), and membrane immunoglobulins (Mittelstadt et al., 1993; Vogel et al., 1993). In addition, PKC activation by tumor-promoting phorbol esters phosphorylates a number of cell surface molecules. This results in rapid downregulation for the major histocompatibility class I

antigen (Peyron and Fehlmann, 1988), CD3, CD5 (Alberola-Ila et al., 1993), CD4 (Petersen et al., 1992), gp90^{MEL-14} (Jung and Dailey, 1990) and receptors for C5a (Rubin et al., 1991), TNF- α (Galeotti et al., 1993), EGF (Davis and Czech, 1984), transferrin (Davis et al., 1986), IL-2 (Onish et al., 1992) and platelet activating factor (PAF) (Zhou et al., 1994). In contrast, expression of some molecules is upregulated by TPA treatment, for example, CD2 (Alberola-Ila et al., 1993) and the intercellular adhesion molecule-1 (ICAM-1) (Bouillon and Audette, 1993). In addition, PKC also phosphorylates a variety of downstream signaling molecules such as I-kB (Ghosh and Baltimore, 1990) and raf-1 (Kolch et al., 1993), which eventually regulate transcription factors and alter gene expression. Overproduction of introduced rat PKC- β 1 in 10T $\frac{1}{2}$ cells resulted in partial transformation as well as an increase in the ability to acquire NAb, and the later was directly associated with an increased susceptibility to elimination by natural surveillance mechanisms in vivo (see Chapter 2). Thus, PKC is not only an intracellular signaling molecule that mediates signals triggered by external stimuli, but also actively regulates the expression of cell surface receptors and NAb binding structures.

Phosphorylation of tyrosine residues of intracellular proteins is another important part of signal transduction. The level of phosphotyrosines is regulated by two groups of enzymes, the protein tyrosine kinases (PTKs), which are responsible for phosphorylating the tyrosines, and the protein tyrosine phosphatases (PTPs), which dephosphorylate the tyrosines leading to either stimulation or inactivation of the protein. Several reports have shown the ability of PTPs to counteract the effect of oncogenic PTKs (reviewed in Cool and Fisher, 1993). Some PTPs have an extracellular domain, a transmembrane segment

and two intracellular catalytic domains. This group of PTPs is defined as the receptor-like PTPs (RPTPs) (reviewed in Charbonneau and Tonks, 1992). So far, however, the mechanisms for regulation of these RPTPs activities have been not well elucidated. There is evidence suggesting that treatment of CV-1 kidney cells with phorbol esters stimulated PTP activities in membranes of the cells (Brautigan and Pinault, 1991). It has been demonstrated that RPTP α , a ubiquitous RPTP, is a substrate of PKC (Tracy et al., 1995; den Hertog et al., 1995) and its activity seems to be increased following PKC phosphorylation (den Hertog et al., 1995). TPA treatment of RPTP α -overexpressing cells also induced RPTP α translocation to membranes (Tracy et al., 1995). Thus, activation of RPTPs may represent part of PKC signaling.

Several mechanisms have been proposed for NAb surveillance of neoplasia, such as opsonization of tumor cells leading to phagocytosis by macrophages, complement-dependent cytotoxicity and ADCC by NK cells, blood monocytes and macrophages (reviewed in Miller et al., 1989). Recently, it has been found that a tumor-reactive monoclonal human natural IgM antibody not only inhibited the growth of human colon carcinoma cell lines and induced complement-mediated cell lysis *in vitro*, but induced MHC class I molecule expression on the same tumors (Bohn et al., 1994). The latter observation is of particular interest, because it implies that NAb may regulate cell growth and function by altering signaling events. This hypothesis is supported by the notions that human IVIg selectively suppressed the thrombin-induced intracellular Ca²⁺ increase and nitric oxide release in aortic endothelial cells from guinea pigs (Schussler et al., 1996).

Previously, Chow and colleagues have shown that the temperature of the incubation

with syngeneic serum NAb could greatly affect NAb binding levels of the L5178Y-F9 T cell (Chow et al., 1992). In this lymphoma system, it was found that cells bound less NAb when assayed at 37°C compared with that at 4°C. Cells pre-coated with NAb at 4°C then warmed to 37°C lost most of their surface NAb (Chow et al., 1992). These data imply that under physiological conditions, NAb reacting with cell surface structures may influence certain intracellular biological events which in turn downregulate NAb binding levels.

In order to determine the signaling potential of NAb, the 10T½ murine fibroblast model including ras- and PKC-β1-overproducing systems was employed. Intracellular signaling events, including alterations in PKC expression and protein tyrosine phosphorylation, were analysed. Since NAb was shown to bind CD45 a lymphocyte marker belonging to the RPTP subfamily (Zhang and Chow, unpublished data), RPTPα a CD45-like RPTP was investigated for its potential involvement in NAb-initiated signaling. Effects on cell cycling were also assessed as a consequence of NAb signaling.

MATERIALS AND METHODS

Cell culture

The cell lines and culture conditions were the same as described in Chapter 2.

Fluorescence-detected NAb binding

Aliquots of 3×10^5 cells were washed with HEPES buffered F12 medium containing 1% FBS (1% FBS/F12). Cells were pretreated with H7 at 25 μM for 20 to 60 min at 37°C prior to the 1-h incubation with 100 μl C3H serum NAb diluted to 1:3 to 1:5, or wash

medium at 4°C or 37°C in the presence or not of H7. For the temperature shift assay, a 1-h incubation of cells in NAb at 4°C with and without H7 or HA1004 at 25 μ M was followed by a further incubation at 37°C or at 4°C for 20 min. The cells were then washed with 1% FBS/F12 at 4°C. The subsequent incubation with the second FITC-conjugated antibodies was performed at 4°C as described in Chapter 2.

For short-term TPA treatment, 3×10^5 cells were incubated in 10% FBS/medium containing 100 ng/ml of TPA and 0.2% (v/v) DMSO for different periods of time from 5 to 120 min at 37°C. In some experiments, aliquots of 3×10^5 PKC-4 cells were pre-incubated with H7 or HA1004 at 25 μ M, or E-64d at 30 μ M for 30 min at 37°C, followed by the addition of TPA at 100 ng/ml for 1 h at 37°C. Control cells were treated with either drug alone or 0.2% DMSO. To stop the reaction, cold wash medium was added to the cell mixture which was then centrifuged at 4°C. Cells were then incubated with serum NAb at 4°C for 1 h and subsequently exposed to the second FITC-conjugated anti-mouse antibodies as described in Chapter 2.

Purification of IgG and IgM from normal C3H mouse serum

The IgG fraction of mouse serum was purified by a modification of the method described by Adib et al (1990). Briefly, a 6 ml aliquot of pooled C3H mouse serum was ultracentrifuged for 1 h at 10,000 g at 4°C. Lipoproteins were removed from the top. The serum was then precipitated with a final concentration of 50% saturated ammonium sulfate for 6 h at 4°C. The precipitate was obtained by centrifugation at 3,000 g for 30 min at 4°C and redissolved in PBS. After dialysis against PBS and centrifugation, the precipitated and redissolved serum was mixed with an equal volume of the starting buffer

containing 1.5 M glycine and 3 M NaCl at pH 8.9 and passed through a 6x1.5 cm column of protein A-Sepharose (Sigma) which was previously equilibrated with the starting buffer. After extensive washing, the column was eluted with 0.1 M acetate, 0.15 M NaCl buffer at pH 3.0. The IgM-containing effluents and IgG-containing eluates were neutralized with 1 M H₃PO₄ and 1 M Tris, respectively, and dialyzed against PBS. The IgM-containing fractions were reprecipitated with 50% saturated ammonium sulfate and purified by filtration through an HR-S-300 column (Sigma, 60x2.5 cm), which was equilibrated with PBS. The first peak of eluted fractions with the highest concentrations of proteins contained IgM detected by immunoblotting and was used as purified IgM in the subsequent studies. Both IgG and IgM fractions were dialyzed against PBS and concentrated by centrifugation with Centricon 30 filters with a molecular weight cut-off at 30 KDa (Amicon, Inc., Beverly, MA). The concentrations of IgG and IgM were determined either by a Bio-Rad DC protein assay kit or by E(1%)=13.5 for IgG and E(1%)=12.0 for IgM at 280 nm. The purity of IgG and IgM was assessed on 6-8% SDS-polyacrylamide gels followed by silver or Coomassie Brilliant blue staining. Under non-reducing conditions, the purified IgG migrated as one predominant band around 150 KDa and IgM as one dominant band on the top of the gel above 200 KDa. Under reducing conditions, IgG NAb exhibited two dominant bands around 47-55 and 25 KDa, whereas IgM showed a few bands around 170-180, 160, 75-80 and 66 KDa. Immunoblotting with antibodies against mouse IgG whole molecule and IgM μ chain confirmed the dominance of IgG and IgM heavy chains around 47-55 and 75-80 KDa, respectively. The cell binding activities of the purified NAb fractions were determined

by flow cytometry using the appropriate FITC-conjugated second antibodies.

To prepare IgG and IgM depleted serum, ammonium sulfate-precipitated C3H serum was consecutively passed through a protein A-Sepharose column and an anti-mouse IgM-Sepharose column, which were previously equilibrated in PBS. The anti-mouse IgM-Sepharose was produced by chemically linking purified rabbit anti-mouse IgM antibodies (IgG class) to CNBr-activated Sepharose beads (Amersham). The effluents with the highest protein concentrations were collected, concentrated and used as IgG and IgM depleted C3H serum in experiments as indicated. In some experiments, NAb was depleted from ammonium sulfate precipitated C3H serum by adsorption with protein A coupled to cross-linked bis-acrylamide/azlactone copolymer 3M Emphaze™ beads (Pierce, Rockford, IL) and anti-mouse IgM-3M Emphaze™ beads to rule out the possibility of depleting dextran binding molecules as might occur with Sepharose-supported columns. Based on the FACS analysis, approximately 5~15% NAb still existed in these IgG and IgM depleted preparations.

For preparation of cell-absorbed NAb, a two ml aliquot of purified IgG plus IgM at final concentrations of 0.8 mg/ml of IgG and 0.25 mg/ml of IgM was incubated with 2×10^7 PKC-4 cells at 4°C for 1 h. After centrifugation, the supernatant was used as cell-absorbed NAb.

NAb and TPA treatment for Western blotting analysis

Aliquots of 5×10^6 cells were washed with ice-cold PBS and incubated for 1 h at 4°C with 1 ml of purified C3H IgG plus IgM at a final concentration of 0.8 mg/ml for IgG and 0.25 mg/ml for IgM, or 1 ml of 1.1 mg/ml IgG and IgM depleted C3H serum, cell-

absorbed NAb, an anti-H2^k monoclonal antibody (MAb), or wash medium containing 0-5% FBS and 1% HEPES in F12/DMEM. The anti-H2^k MAb, HB20 (mouse IgG2a), was prepared from culture supernatant of the hybridoma HB20 (American Type Culture Collection, Rockville, Maryland) by precipitation with 50% saturated ammonium sulfate. After one wash with cold PBS, the cells were resuspended in 400 μ l of PBS and incubated at either 4°C or 37°C for different periods of time from 15 to 45 min to assess NAb induction of early signaling events. For TPA treatment, 5×10^6 cells were incubated with 100 or 200 ng/ml of TPA at 37°C for different periods of time as indicated.

Preparation of membrane and cytosolic fractions

See Chapter 2.

SDS-PAGE

See chapter 2.

Western blotting analysis

For detection of PKC- α and PKC- β 1, the same method was used as described in Chapter 2. Some blots were stripped with stripping buffer containing 100 mM 2-mercaptoethanol, 2% SDS, 62.5 mM Tris-HCl, pH 6.7, at 50°C for 1 h and re probed with a monoclonal antibody against phosphotyrosine (clone 4G10, Upstate Biochemical, Inc., Lake Placid, NY) and HRP-conjugated goat anti-mouse IgG (Sigma). Since stimulation of PKC with TPA does not affect the solubility of membrane actin (Dwyer-Nield et al., 1996), an anti-actin antibody (Sigma) was employed in some experiments as an internal control to confirm an equal amount of protein loading. The densitometry analysis of the blots was outlined in Chapter 2. The densities of the protein bands were

normalized by actin when it was available and reported as arbitrary units (relative densities) as indicated.

Shedding of RPTP α

I3T2.1 cells were pre-treated with 100 ng/ml TPA and 0.2% DMSO or equivalent amounts of solvent DMSO for 24 h. Then, 10^7 cells were incubated for 1 h at 4°C with 0.8 ml F12 medium containing 1% FBS, or 0.8 ml of purified C3H IgG plus IgM at final concentrations of 0.33 and 0.8 mg/ml, respectively, or the same IgG plus IgM preparation preabsorbed by 1×10^7 I3T2.1 cells once or twice. After washing once with cold PBS, the cells were resuspended in 250 μ l cold PBS and then incubated at 37°C for 8 min. The supernatant was obtained by a 5,000 g centrifugation for 5 min at 4°C. A 60 μ l aliquot of each supernate was mixed with 20 μ l of 4x gel sample buffer containing 8% SDS, 40% (w/v) glycerol, 0.1 M Tris, 0.1 M dithiothreitol and 0.04% bromophenol blue at pH 6.8. The RPTP α in the supernatant was resolved by SDS-PAGE and detected by immunoblotting as described above with an anti-RPTP α anti-serum against the intracellular segment of the molecule (provided by Dr. J. Sap, Department of Pharmacology, New York university Medical Center, New York).

Cell cycle analysis by flow cytometry

Aliquots of 2×10^5 I3T2.1 cells were seeded in 60 mm petri dishes for a 1-day exposure to F12 medium with 0.5, 5 or 10% FBS. Then the medium was replaced with 3 or 4 ml of fresh medium with the same concentration of FBS with and without purified C3H NAb at a final concentration of 0.25 mg/ml of IgG and 0.1 ~ 0.25 mg/ml of IgM, or 0.35 mg/ml of IgG and IgM depleted C3H serum, or an equivalent volume of IgM-

depleted IgM fraction (designated as IgM^{lo}) or PBS. IgM^{lo} was prepared by preabsorption of purified IgM with anti-mouse IgM-3M Emphaze™ beads. After 1 or 2 days, the cells were harvested by pipetting with PBS containing 0.1% EDTA or by trypsinization and fixed with 95% ethanol overnight at 4°C. The cells were then treated overnight at 4°C with a PBS solution at pH 7.3, containing 1% BSA, 10 µg/ml of propidium iodide (Sigma) and 250 µg/ml of RNase A (Life Technologies, Inc., Gaithersburg, MD). Cellular DNA was analysed by flow cytometry by measuring the integral red fluorescence (propidium iodide-DNA) above 630 nm. Cell debris and aggregates were excluded electronically. The diploid cells containing 2N DNA were always set up with the main peak marking G0/G1 DNA content at channel 80.

Statistical analysis

The statistical significance of differences in MCF of NAb binding, PKC- α and - β 1 expression, protein tyrosine phosphorylation and cell numbers in the cell cycle compartments were assessed using the *t*-dependent (P_{td}) and *t*-independent (P_{ti}) Student *t* test. P values >0.05 were considered not significant.

RESULTS

NAb binding to cells at 4°C versus 37°C and 4°C shifted to 37°C

It was shown that the L5178Y-F9 lymphoma bound more syngeneic serum NAb when assayed at 4°C compared with the same cells at 37°C (Chow et al., 1992). In order to investigate the mechanism(s) contributing to this temperature sensitivity of NAb binding to tumor cells, two approaches were employed with two fibroblast models,

specifically cell lines bearing a ras oncogene and a PKC- β 1 signaling molecule gene. The first approach was to directly compare NAb binding levels at two different temperature conditions, 4°C versus 37°C. Unlike I3T2.1 and PKC-4 cells, 10T½ cells incubated in medium or serum NAb for 1 h at 37°C always formed aggregates. NAb binding to 10T½ and I3T2.1 cells was more than 40% less when assayed at 37°C compared with 4°C (Table 3.1), similar to the L5178Y-F9 T lymphoma (Chow et al., 1992). H7, a PKC inhibitor, tended to increase NAb binding in I3T2.1 cells when H7 was added to cells 20 to 60 min prior to incubation with NAb in the presence of H7 for another 60 min at 37°C. Interestingly, PKC-4 cells exhibited a slightly higher NAb binding at 37°C compared with that at 4°C and H7 even slightly increased NAb binding a little further at 37°C. The second approach was based on the speculation that if 4°C was a condition which optimized the stability of NAb binding to cell surface structures by reducing membrane fluidity and/or minimized membrane enzyme activities that may mediate the instability of NAb binding at 37°C, raising the temperature from 4°C to 37°C for 20 min should produce alterations which for both cases would lead to a reduction in NAb binding levels. As expected, a significant loss of precoated NAb was detected after the temperature was raised. Such losses were observed in all three cell lines studied, amounting to approximately 68% for 10T½, 73% for I3T2.1 and 46% for PKC-4 (Table 3.2). Moreover, the reductions in pre-coated NAb in 10T½ and PKC-4 cells were partially inhibited by H7, but not by HA1004, a PKA inhibitor (Table 3.2). Thus, the data from both approaches suggest that NAb binding with 10T½ and I3T2.1 cells under physiological conditions likely stimulated PKC which in turn downregulated NAb

Table 3.1. NAb binding at 4°C vs 37°C

Expt# ^a	Cells	Mean NAb binding (MCF) \pm SE			
		4°C	37°C	37°C + H7	% decrease 37°C vs 4°C
1 (7)	10T $\frac{1}{2}$	54.5 \pm 5.6	30.8 \pm 1.6 ^b	-	43.5
2 (5)	I3T2.1	66.6 \pm 11.3	37.1 \pm 14.1 ^b	45.0 \pm 12.6 ^c	44.3
3 (6)	PKC-4	124.9 \pm 19.5	140.6 \pm 20.4 ^c	-	-12.6
4 (3)	PKC-4	160.8 \pm 8.1	181.5 \pm 6.9	193.7 \pm 6.2 ^d	-12.9

^a NAb binding was performed either at 4°C or at 37°C with and without H7 (25 μ M). The number of assays is in parenthesis.

^b 10T $\frac{1}{2}$ cells tended to form clumps at 37°C. Although pipeting cells could segregate some clumps before FACS analysis, the data may only represent single cells of the total cell population. $P_{td} < 0.01$, compared with cells incubated at 4°C.

^c $P_{td} < 0.02$

^d $P_{td} \leq 0.05$, compared with cells incubated at 37°C.

^e NS.

Table 3.2. NAb binding at 4°C vs 4°C shifted to 37°C with and without H7 treatment

Exp# ^a	Cells	Mean NAb binding (MCF) \pm SE				
		4°C→4°C	4°C→37°C	4°C→37°C +H7	4°C→37°C +HA1004	% decrease 4°C → 37°C
1 (5)	10T½	74.5 \pm 8.6	23.9 \pm 4.7 ^b	30.0 \pm 5.6 ^c	24.4 \pm 5.1	67.9
2 (5)	I3T2.1	64.2 \pm 14.1	17.3 \pm 4.3 ^d	18.4 \pm 4.9	16.5 \pm 3.3	73.1
3 (5)	PKC-4	70.9 \pm 8.1	38.2 \pm 4.0 ^d			46.1
4 (3)	PKC-4	78.4 \pm 11.4	38.4 \pm 5.8	47.4 \pm 8.7 ^c	40.5 \pm 6.5	51.0

^a Cells were incubated with serum NAb \pm H7 or HA1004 (25 μ M) at 4°C for 1 h, then the temperature of the incubation was increased to 37°C for 20 min versus incubation in NAb at 4°C for 1 h and 20 min. The incubation with FITC-conjugated anti-mouse immunoglobulin second antibodies was subsequently performed at 4°C. The number of assays is in parenthesis.

^b $P_{td} < 0.01$ compared with 4°C control.

^c $P_{td} < 0.05$ compared with 4°C plus the shift to 37°C for HA1004-treated controls.

^d $P_{td} < 0.02$ compared with 4°C control.

binding, while PKC-4 cells seemed to be more resistant to this NAb-induced reduction in NAb binding, probably due to the very high PKC activities expressed in this line.

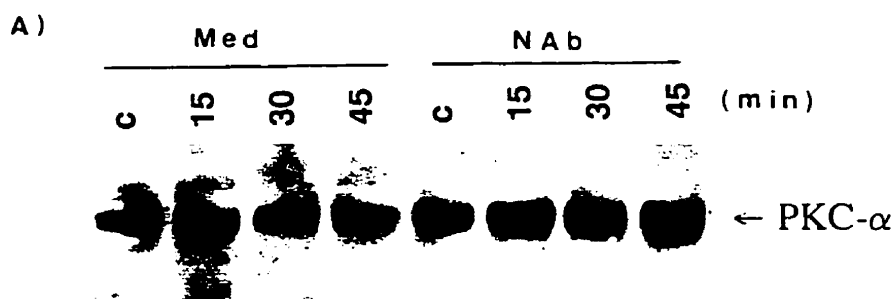
PKC expression in cells treated with NAb at 4°C versus 37°C and 4°C shifted to 37°C

In order to determine if PKC is involved in the NAb-initiated downregulation of NAb binding to tumor cells, the kinetic expression of PKC was investigated in cytosolic and membrane fractions following exposure of cells to NAb at 4°C and a rise in temperature to 37°C. Immunoblotting with anti-PKC- α and - β antibodies revealed that a temperature shift from 4°C to 37°C for PKC-4 cells preincubated with purified NAb induced an increase in the membrane PKC- α and - β (Fig 3.1, 3.2 and Table 3.3). Thirty min after the temperature was raised to 37°C, the increase in membrane PKC amounted to 20% for PKC- β 1 and 80% for PKC- α above the levels of NAb-treated cells maintained at 4°C (Table 3.3). Interestingly, NAb-treated PKC-4 cells at 4°C also exhibited a slight increase in membrane PKC- β 1 and PKC- α compared with medium-treated control cells. Preabsorption of purified NAb fractions with PKC-4 cells eliminated the increase in membrane PKC (Fig 3.3 and Table 3.3). Similar treatment of PKC-4 cells with either growth medium supplemented with 0-5% FBS, or anti-H2^k MAb HB20, or IgG and IgM depleted C3H serum induced either no change or a slight decrease in membrane PKC- α and - β 1 (Fig 3.1, 3.2, 3.3 and Table 3.3). Moreover, the same treatment of 10T $\frac{1}{2}$ and I3T2.1 cells with purified NAb also induced an increase in membrane PKC- α (Fig 3.4 and Fig 3.5). Changes in expression levels of PKC in cytosolic fractions were not consistently observed.

Fig 3.1. Expression of PKC- α in membrane fractions of PKC-4 cells treated with purified NAb. (A) PKC-4 cells were treated with culture medium free of FBS (Med) or purified NAb (NAb). C denotes a 1-h incubation at 4°C followed by a 45-min incubation at 4°C and 15, 30 and 45 indicate a 1-h incubation at 4°C followed by a 37°C incubation for 15, 30 and 45 min, respectively. This result was typical of three independent experiments summarized in Table 3.3.

(B) Relative densities of (A) expressed as arbitrary units relative to the medium control at 4°C as 1.0.

A)



B)

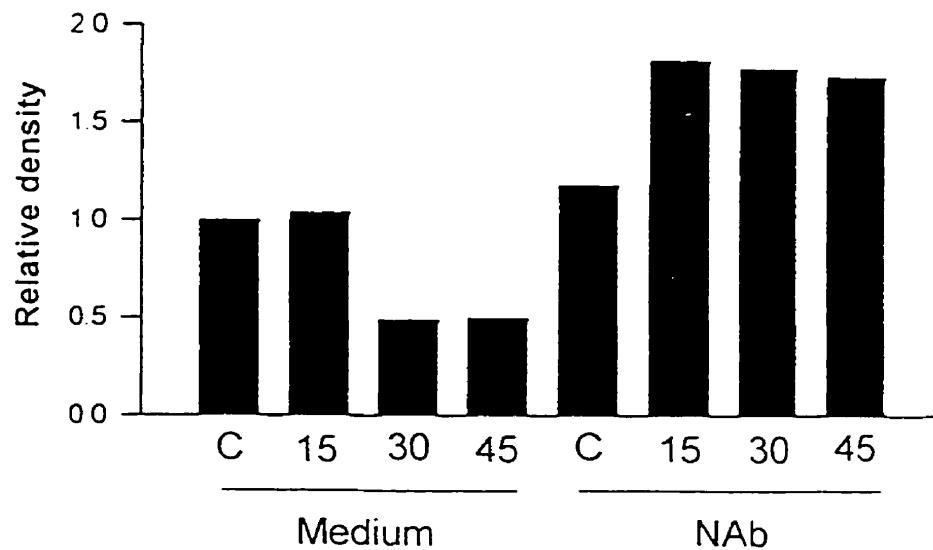
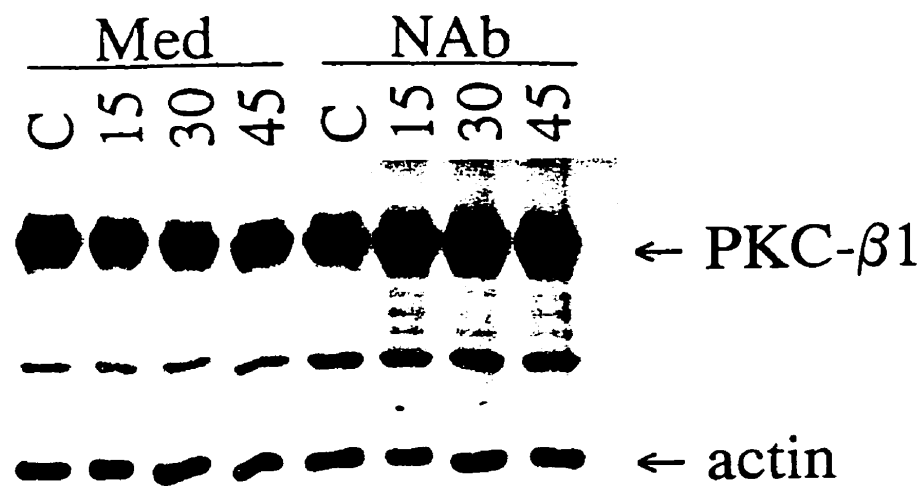


Fig 3.2. Expression of PKC- β 1 in membrane fractions of PKC-4 cells treated with purified NAb. (A) PKC-4 cells were treated with culture medium free of FBS (Med) or purified NAb (NAb). C denotes a 1-h incubation at 4°C followed by a 45-min incubation at 4°C and 15, 30 and 45 indicate a 1-h incubation at 4°C followed by a 37°C incubation for 15, 30 and 45 min, respectively. This result was typical of four independent experiments summarized in Table 3.3.

(B) Relative densities of (A) normalized by actin and expressed as arbitrary units relative to the medium control at 4°C as 1.0.

A)



B)

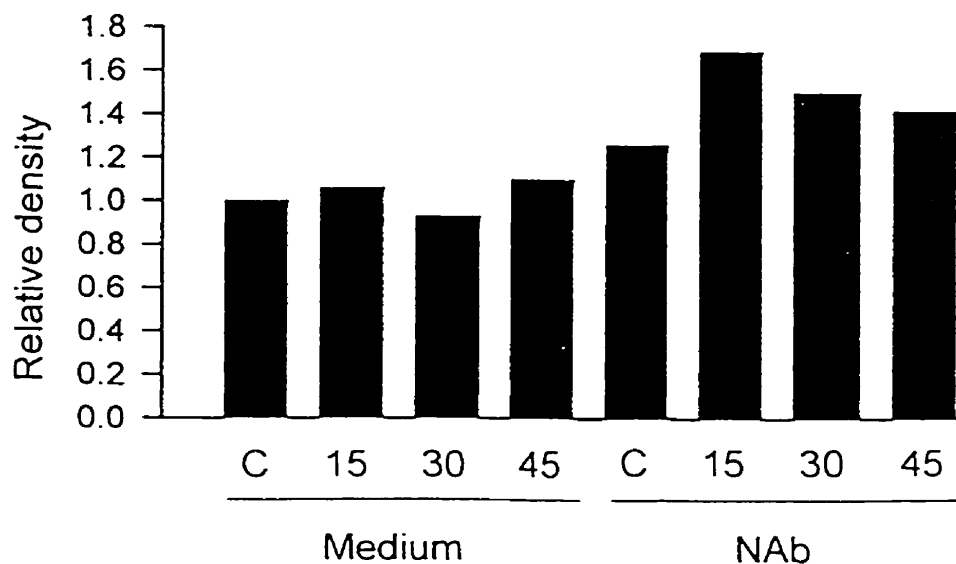


Table 3.3. Membrane PKC- α and PKC- β expression in PKC-4 cells treated with purified NAb, pre-absorbed NAb or anti-H2^k MAb HB20

Expt# ^a	PKC isoform	Treatment	Relative densities (mean \pm SE)	
			4°C \rightarrow 4°C 30 to 45 min	4°C \rightarrow 37°C 30 min
1 (4)	PKC- β 1	medium	1.0	0.97 \pm 0.06
		NAb	1.20 \pm 0.09	1.41 \pm 0.11 ^b
2 (3)	PKC- α	medium	1.0	0.81 \pm 0.14
		NAb	1.06 \pm 0.15	1.95 \pm 0.41 ^b
3 (3)	PKC- β 1	medium	1.0	0.89 \pm 0.02
		As NAb	0.89 \pm 0.02	0.72 \pm 0.15 ^c
4 (3)	PKC- β 1	medium	1.0	0.94 \pm 0.07
		HB20	0.99 \pm 0.07	0.83 \pm 0.12 ^c

^a PKC-4 cells were incubated with medium containing 0-5% FBS, purified NAb, purified NAb pre-absorbed by PKC-4 cells (As NAb) or anti-H2^k MAb HB20 for 1 h at 4°C followed by one wash with PBS at 4°C. The cells were then incubated in PBS either at 4°C for 30-45 min or at 37°C for 30 min. Membrane preparations were resolved in 8% gels and the blots were detected by the anti-PKC- α and - β antibodies. Band densities were expressed as arbitrary units relative to control cells treated with medium at 4°C as 1.0. The statistical analysis was performed after conversion. The number of assays is in parenthesis.

^b $P_{td} < 0.05$ compared with medium-treated controls with a raise in temperature to 37°C for 30 min.

^c NS.

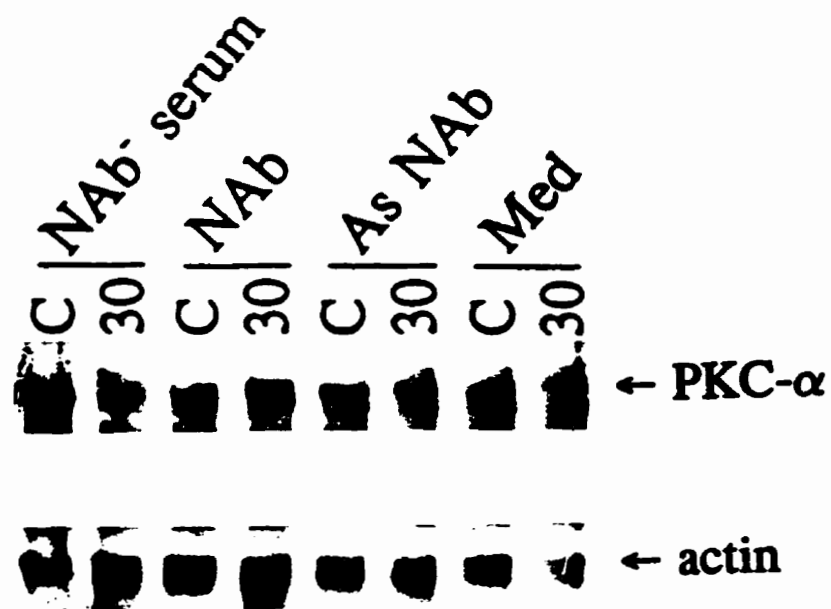
Fig 3.3. Expression of PKC- α in membrane fractions of PKC-4 cells treated with purified NAb, pre-absorbed NAb and IgG and IgM depleted syngeneic serum.

(A) PKC-4 cells were treated with IgG and IgM depleted C3H serum (NAb⁻), purified NAb (NAb), NAb preabsorbed by PKC-4 cells (As NAb), or culture medium containing 1% FBS (Med). The NAb⁻ C3H serum was prepared by passing ammonium sulfate precipitated C3H serum through 3M EmphazeTM plastic beads supported protein A and anti-mouse IgM columns. C denotes a 1-h incubation at 4°C followed by a 30-min incubation at 4°C and 30 indicates a 1-h incubation at 4°C followed by a 30-min incubation at 37°C. This result was typical of three independent experiments summarized in Table 3.3. The NAb⁻ serum similarly prepared by adsorption with Sepharose supported protein A and anti-mouse IgM columns yielded similar observations in immunoblotting with anti-PKC- β antibodies. Two actin bands were detected in this experiment. These two forms of actin were assumed to be γ (upper band) and β (lower band) isoforms of actin which have slightly different molecular weights (DeNofrio et al., 1989; Otey et al., 1986; Hooek et al., 1991). Due to the poor development of the lower form of actin in the first lane on the left and the last lane on the right, only the upper band of actin was measured throughout all lanes for controlling the protein loading.

(B) Relative densities of (A) normalized by actin and expressed as arbitrary units relative to the NAb⁻ serum control at 4°C as 1.0.

Fig 3.3

A)



B)

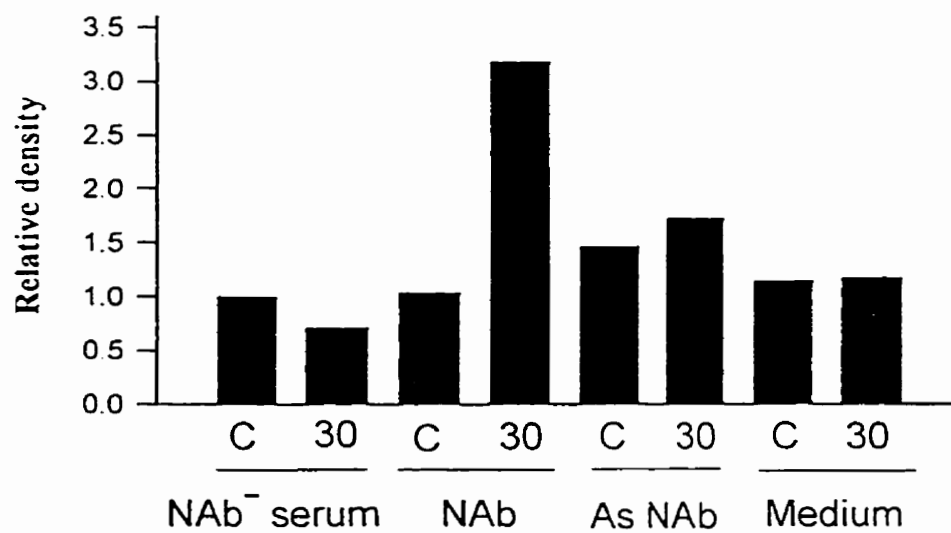
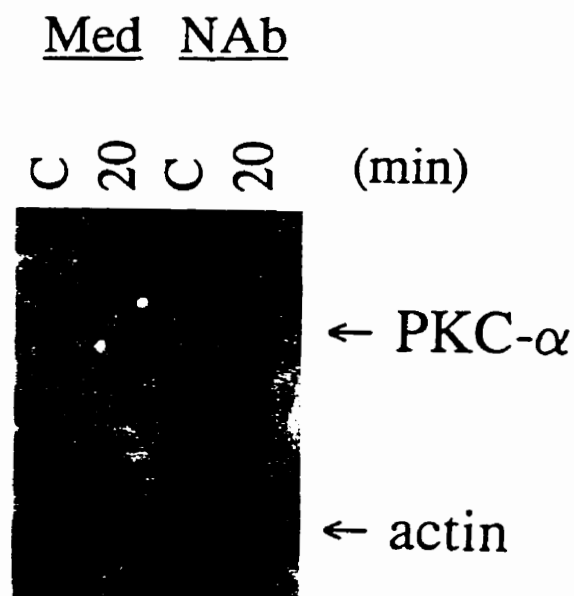


Fig 3.4. Expression of PKC- α in membrane fractions of 10T $\frac{1}{2}$ cells treated with purified NAb. (A) 10T $\frac{1}{2}$ cells were treated with F12 medium containing 5% FBS (Med) or purified NAb (NAb). C denotes a 1-h incubation at 4°C followed by a 20-min incubation at 4°C and 20 indicates a 1-h incubation at 4°C followed by a 20-min incubation at 37°C. The result confirmed two previous experiments in which whole serum and the raise in temperature were studied. (B) Relative densities of (A) normalized by actin and expressed as arbitrary units relative to the medium control at 4°C as 1.0.

A)



B)

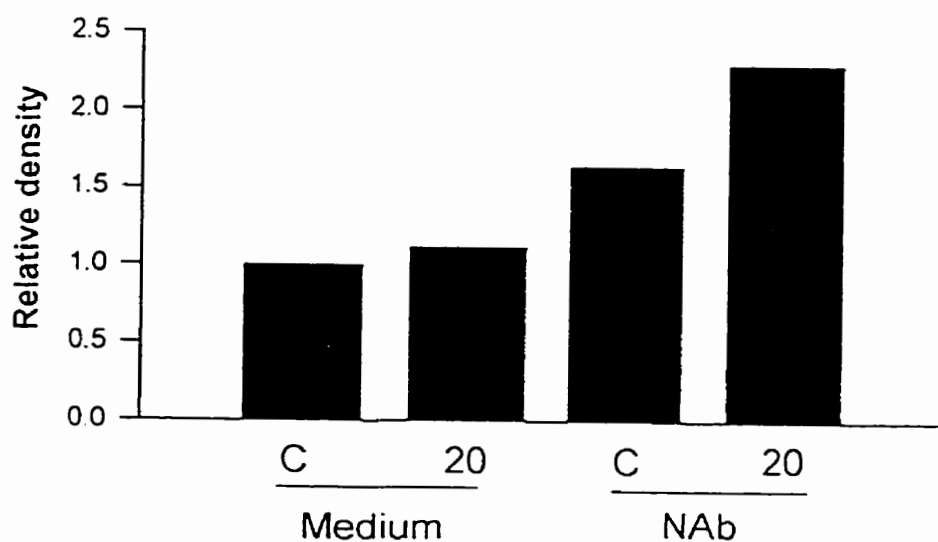
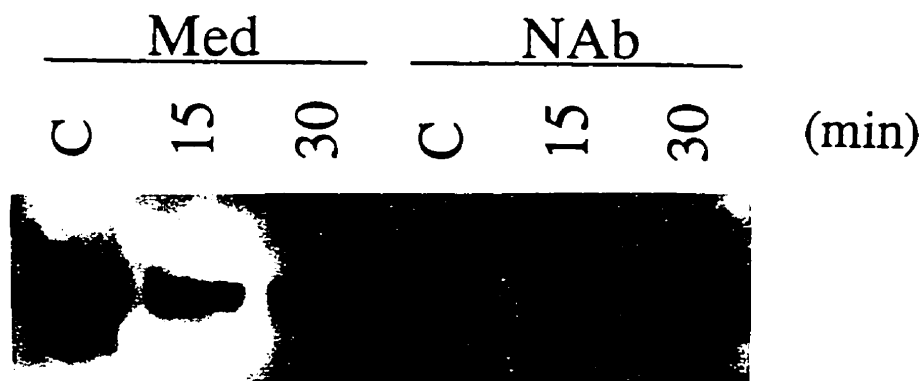


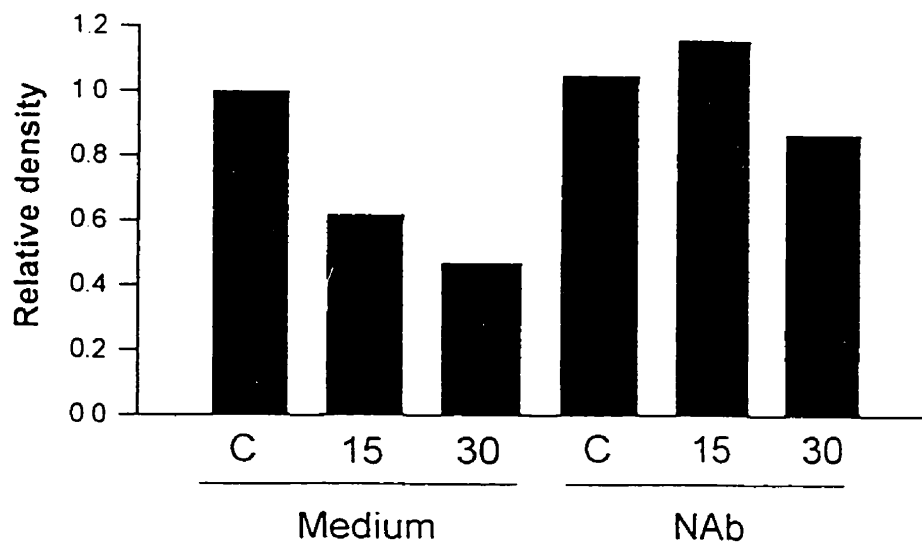
Fig 3.5. Expression of PKC- α in membrane fractions of I3T2.1 cells treated with purified NAb. (A) I3T2.1 cells were treated with culture medium free of FBS (Med) or purified NAb (NAb). C denotes a 1-h incubation at 4°C followed by a 30-min incubation at 4°C and 15 and 30 indicate a 1-h incubation at 4°C followed by a 37°C incubation for 15 and 30 min, respectively. This result confirmed one previous experiment in which whole serum NAb was used.

(B) Relative densities of (A) expressed as arbitrary units relative to the medium control at 4°C as 1.0.

A)



B)



Detection of protein tyrosine phosphorylation in PKC-4 cells treated with NAb at 4°C versus 4°C shifted to 37°C

Since protein tyrosine phosphorylation is an important biological event in signaling, the alterations in phosphorylation of tyrosine residues of intracellular proteins were examined by immunoblotting using a MAb (4G10) specific to the phosphotyrosyl residues. Following the increase in the temperature from 4°C to 37°C, a time-dependent decrease in the reactivity of a membrane associated 60-KDa protein (p60) with 4G10 was detected in PKC-4 cells treated with either growth medium supplemented with 0-1% FBS, or purified NAb (Fig 3.6 and Fig 3.7, Table 3.4), or purified NAb pre-absorbed by PKC-4 cells (Fig 3.7). However, PKC-4 cells treated with purified NAb exhibited a more profound reduction in 4G10 binding suggesting that NAb augmented the process of the loss of phosphotyrosine epitopes from p60 associated with the rise in temperature (Fig 3.6 and Fig 3.7, Table 3.4). Interestingly, the NAb-coated cells kept at 4°C for 45 min also exhibited a considerable level of reduction in phosphotyrosine of p60 in two independent experiments (one typical experiment is shown in Fig 3.6) and a slight reduction in the third experiment in which the NAb-coated cells were maintained at 4°C for 30 min (Fig 3.7 and Table 3.4). In addition, the anti-phosphotyrosine reactivity in cytosolic fractions exhibited no change.

PKC expression and NAb binding of cells treated with TPA

It was previously shown that short-term TPA treatment of L5178Y-F9 cells at 37°C induced a decrease in their NAb binding ability (Sandstrom and Chow, 1994). In this study, two min after adding TPA at 37°C, extensive translocation to the membrane

Fig 3.6. p60 tyrosine dephosphorylation in PKC-4 treated with purified NAb. (A) PKC-4 cells were treated with purified NAb (NAb) or culture medium free of FBS (Med). The membrane fractions were assessed with the anti-phosphotyrosine MAb 4G10. C denotes a 1-h incubation followed by a 45-min incubation at 4°C and 15, 30 and 45 indicate a 1-h incubation at 4°C followed by a 37°C incubation for 15, 30 and 45 min, respectively. This result was typical of three independent experiments (Table 3.4). (B) Relative densities of (A) expressed as arbitrary units relative to the medium control at 4°C as 1.0.

A)

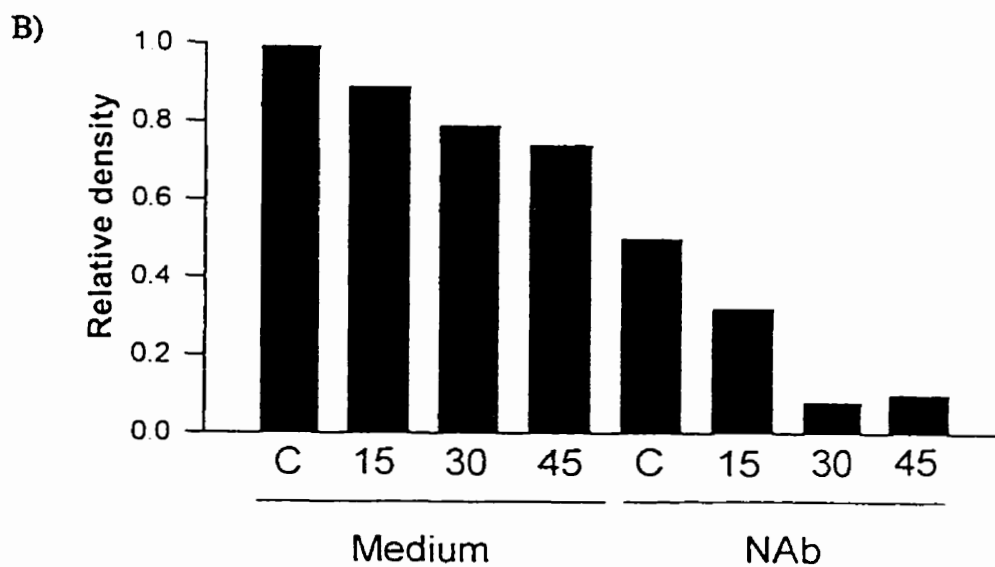
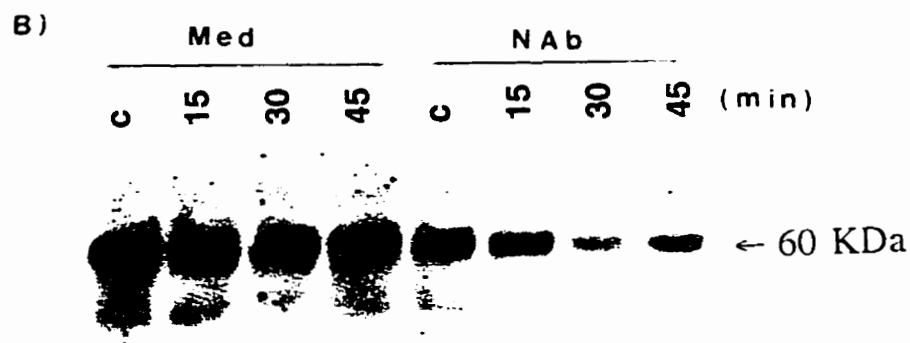
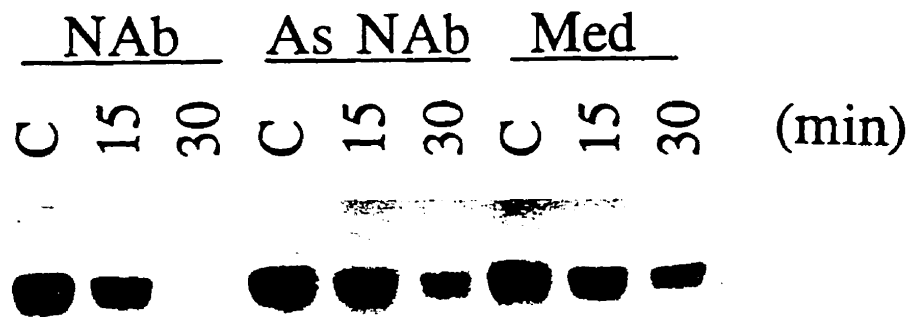


Fig 3.7. p60 tyrosine dephosphorylation in PKC-4 treated with purified NAb and pre-absorbed NAb. (A) PKC-4 cells were treated with purified NAb, NAb preabsorbed by PKC-4 cells (As NAb), or culture medium containing 1% FBS (Med). C denotes a 1-h incubation followed by a 30-min incubation at 4°C and 15 and 30 indicate a 1-h incubation at 4°C followed by a 37°C incubation for 15 and 30 min, respectively. This result was typical of three independent experiments summarized in Table 3.4.

(B) Relative densities of (A) normalized by actin and expressed as arbitrary units relative to the medium control at 4°C as 1.0.

A)



B)

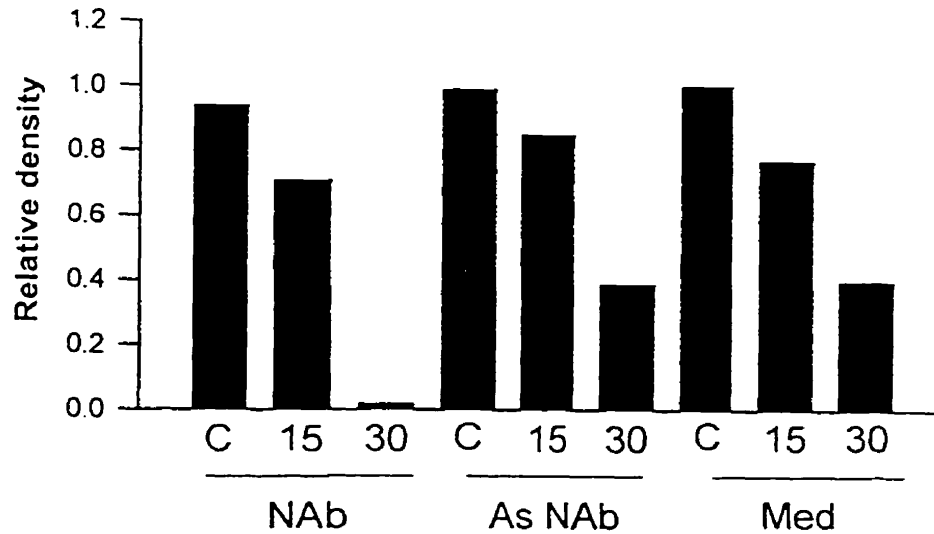


Table 3.4. p60 tyrosine dephosphorylation in PKC-4 cells treated with purified NAb

Treatment ^a	Relative densities (mean±SE)		
	4°C → 4°C 30-45 min	4°C → 37°C 15 min	4°C → 37°C 30 min
medium	1.0	0.78±0.06	0.48±0.16
NAb	0.61±0.17	0.55±0.12	0.11±0.06 ^b

^a PKC-4 cells were incubated with medium containing 0-1% FBS or purified NAb for 1 h at 4°C followed by one washing with PBS at 4°C. The cells were then incubated in PBS either at 4°C for 30 to 45 min or at 37°C for 15 or 30 min. Cell membrane fractions were resolved in 8% gels and detected by the monoclonal anti-phosphotyrosine antibody 4G10. The densities of p60 were measured by densitometry and presented in arbitrary units relative to medium treatment at 4°C as 1.0. The statistical analysis was performed after conversion.

^b $P_{ti} < 0.05$ compared with NAb-treated controls kept at 4°C.

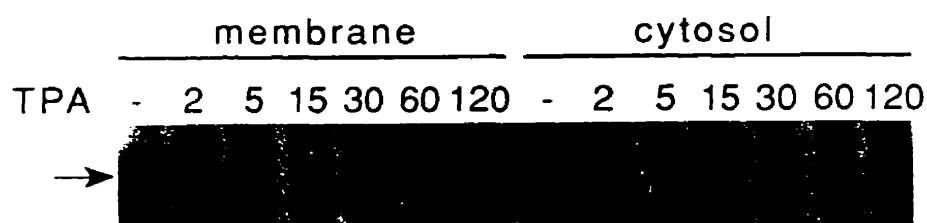
fraction was seen for PKC- α in 10T $\frac{1}{2}$ cells (Fig 3.8A) and for PKC- β 1 in PKC-4 cells (Fig 3.8B). Thirty min later, both PKC- β and PKC- α had gradually decreased from both membrane and cytosolic fractions (Fig 3.8 A and B), evidence of a downregulation process similar to other cell lines examined (Regazzi et al., 1986). A corresponding rapid decrease in the ability to acquire NAb was found in all three cell lines within 1 h of TPA treatment (Table 3.5). Solvent concentrations of DMSO did not exhibit an effect on NAb binding (Table 3.5). Moreover, E-64d and H7, but not HA1004, partially blocked the downregulation of the NAb binding potential of TPA treated PKC-4 cells (Table 3.6). The data suggested that the NAb-induced PKC activation and downregulation of NAb binding could be simulated by the PKC activator TPA.

Detection of RPTP α in supernatant from cells preincubated with NAb followed by a raise in the temperature from 4°C to 37°C

NAb has been found to bind CD45, a lymphocyte surface RPTP (Zhang and Chow, unpublished data), indicating that NAb binding to CD45 may influence its function. To examine the potential functioning of RPTP α , the CD45-like ubiquitous RPTP, in NAb-initiated signaling, RPTP α was assessed in supernatant from NAb-coated cells following a rise in the temperature from 4°C to 37°C. As can be seen in Fig 3.9, NAb significantly induced more release of RPTP α as well as many other non-specifically detected background molecules from the cell surface (Fig 3.9, lane 2) compared with 1% FBS/medium-treated control (Fig 3.9, lane 1). Pre-absorption of NAb by I3T2.1 cells markedly reduced the release of RPTP α and other non-specific cell surface molecules (Fig 3.9, lanes 4 and 5). Moreover, TPA treatment of I3T2.1 cells for 1 day slightly

Fig 3.8. PKC expression in response to TPA treatment. Anti-PKC- α and anti-PKC- β were used to detect changes in PKC- α expression in 10T $\frac{1}{2}$ cells (A) and PKC- β 1 in PKC-4 cells (B) after exposure to 200 ng/ml of TPA for 2, 5, 15, 30, 60 and 120 min versus untreated controls (-). Both membrane and cytosolic proteins were analyzed. The pointers indicate PKC- α (A) and PKC- β 1 (B), respectively. The band below PKC- α and - β 1 is due to nonspecific binding of avidin-HRP which was incubated with the blot to visualize the molecular weight standards. Cells treated with 100 ng/ml of TPA showed identical results.

A)



B)

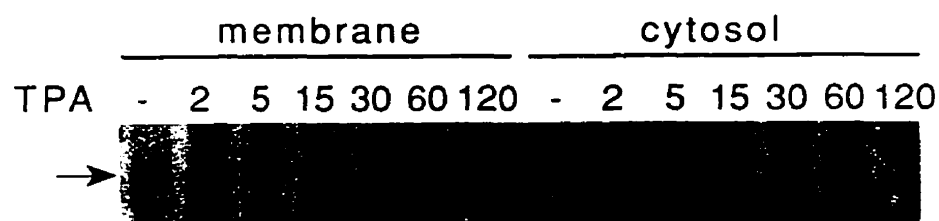


Table 3.5. NAb binding of cells after short-term TPA treatment

Exp# ^a	Cells	Mean NAb binding (MCF) \pm SE		
		Control	TPA	DMSO
1 (3)	10T½	66.8 \pm 3.0	56.9 \pm 2.2 ^b	-
2 (4)	I3T2.1	58.6 \pm 10.3	41.1 \pm 6.7 ^c	-
3 (4)	PKC-4	71.7 \pm 21.2	53.8 \pm 16.5 ^c	-
4 (2)	PKC-4	58.0 \pm 4.0	-	58.9 \pm 5.4

^a Cells were treated with medium, 100 ng/ml TPA in culture medium containing 0.2% DMSO, or medium with 0.2% DMSO for 60 min prior to assessment of NAb binding. The number of assays is in parentheses.

^b $P_{ii} < 0.05$

^c $P_{id} < 0.05$

Table 3.6. NAb binding of PKC-4 cells treated briefly with TPA in the presence of H7, H1004 or E-64d

Exp # ^a	Mean NAb binding (MCF) \pm SE					
	Control	TPA	H7	H7 + TPA	HA1004	HA1004 + TPA
1 (6)	80.6 \pm 11.7	66.7 \pm 12.1 ^b	79.4 \pm 10.2	73.2 \pm 12.0 ^c	75.9 \pm 9.3	65.9 \pm 10.5
	Control	TPA	E-64d	E-64d + TPA		
2 (5)	85.4 \pm 11.0	66.3 \pm 12.9 ^b	81.5 \pm 11.0	74.9 \pm 14.1 ^d		

^a Cells were pretreated with H7 (25 μ M), HA1004 (25 μ M) or E-64d (30 μ M) for 30 min at 37°C, then TPA (100 ng/ml) was added for 60 min, or the cells were treated with medium, H7, HA1004 or E-64d alone for 90 min all at 37°C. NAb binding was assayed at 4°C. The number of assays is in parentheses.

^b $P_{td} < 0.02$ compared with untreated controls.

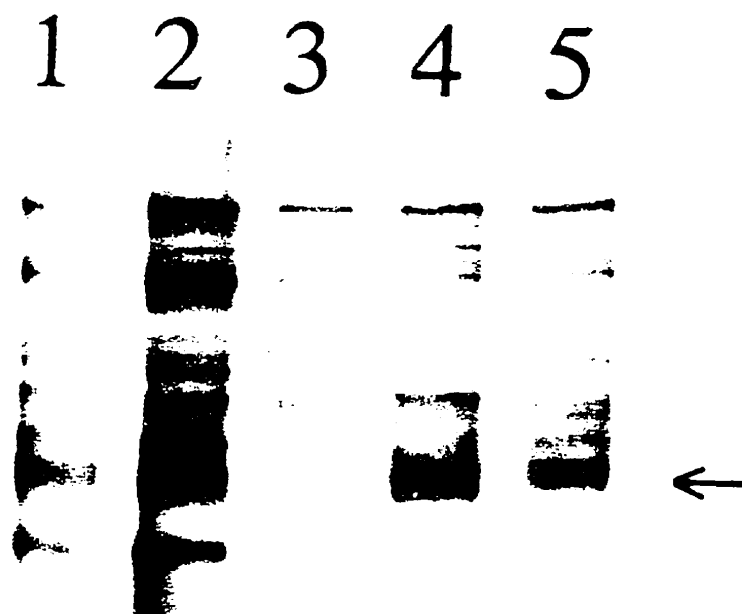
^c $P_{td} < 0.05$ compared with TPA treatment.

^d $P_{td} < 0.02$ compared with TPA treatment.

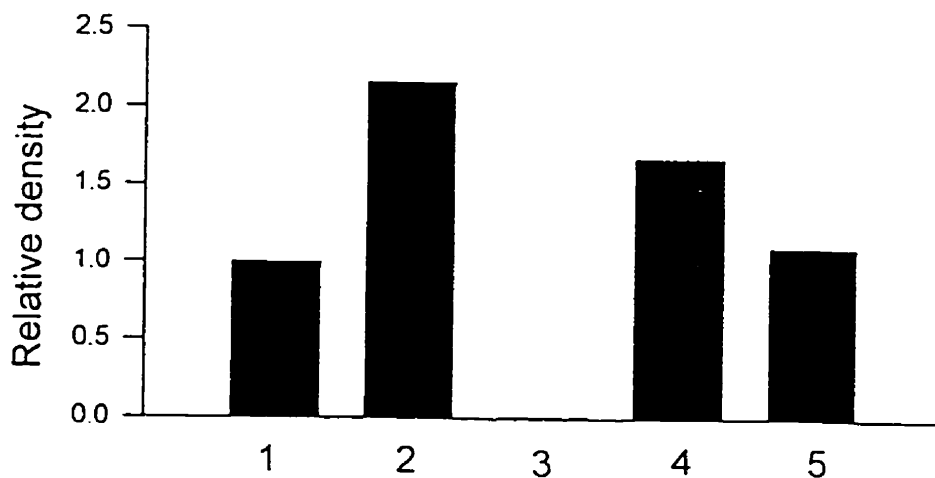
Fig 3.9. Shedding of RPTP- α induced by NAb. (A) I3T2.1 cells were preincubated with culture medium containing 1% FBS (lane 1), purified NAb (lanes 2 and 3), purified NAb preabsorbed by 10^7 I3T2.1 cells once (lane 4) and twice (lane 5). After one wash, a supernatant was prepared from the cells by raising the temperature from 4°C to 37°C. Lane 3 shows the supernatant produced from the same number of I3T2.1 cells which were pretreated with 100 ng/ml of TPA for one day. An equal volume of each supernatant was assessed by SDS-PAGE and immunoblotting with an anti-serum against RPTP α . The arrow indicates the 130-KDa RPTP- α . This result confirmed two previous experiments in which whole serum NAb was used.

(B) Relative densities of (A) expressed as arbitrary units relative to lane 1 as 1.0.

A)



B)



reduced NAb binding levels with a mean MCF \pm SE of 30.9 ± 6.9 versus untreated cells at 40.2 ± 5.7 with $P_{\text{adj}} > 0.1$ ($n=3$). This pretreatment with TPA completely abolished NAb-induced shedding of RPTP α and other non-specifically detected molecules (Fig 3.9, lane 3), even though the membrane RPTP α level at 0.79 ± 0.19 was reduced by only 21% following TPA treatment versus 1.0 for DMSO treated controls.

Cell cycle analysis following NAb treatment

In order to investigate the biological consequence of the NAb-initiated signaling in 10T $\frac{1}{2}$ variants, purified NAb was added to the tissue culture and DNA synthesis was assessed by analyzing the cell cycle by flow cytometry. Since PKC stimulation is often associated with cell activation, a growth stimulatory effect of NAb was initially expected when purified NAb was added to starved I3T2.1 cells. Surprisingly, the purified IgG (0.25 mg/ml) plus IgM NAb (0.1 ~ 0.25 mg/ml) significantly arrested 11% more cells at the G0/G1 phase of the cell cycle during a 3-day assay (Table 3.7, Expt 1). The growth inhibitory activity of NAb was mainly present in IgM fractions whereas IgG itself at 0.25 mg/ml had no effect (Table 7, Expts 2 and 3). The IgG and IgM depleted C3H serum prepared by protein A- and anti-mouse IgM-Sepharose adsorption seemingly promoted cell growth as assessed by a slight increase in cell numbers in S phase and a decrease in the G0/G1 stage (Table 3.7, Expt 4). Moreover, preliminary experiments performed with 10T $\frac{1}{2}$ and PKC-4 cells also showed some inhibitory effect of the purified IgM or IgG plus IgM NAb on cell cycling (Table 3.7, Expts 5 and 6).

To further test whether NAb can also inhibit cell growth under normal culture conditions, the effect of serum factors was first examined on cell growth. I3T2.1 cells

Table 3.7. NAb inhibition of cell growth in low serum culture

Expt # ^a	Cells	Treatment	% of cell numbers in cell cycle (mean ±SE)		
			G0/G1	S	G2/M
1 (3)	I3T2.1	PBS	53.0±2.6	25±1.0	22.3±1.7
		IgG+IgM	59.3±2.4 ^b	17±2.1 ^c	23.7±1.2
2 (2)	I3T2.1	PBS	55.0±3.0	24.0±0.0	21.5±2.5
		IgM	59.5±2.5	18.0±2.0	23.0±1.0
3 (2)	I3T2.1	PBS	50.0±2.0	27.5±1.5	22.5±0.5
		IgG	47.5±3.5	31.5±8.5	20.5±5.5
4 (2)	I3T2.1	PBS	55.0±3.0	22.0±2.0	26.0±7.0
		NAb ⁻ serum	51.0±1.0	24.5±0.5	24.0±2.0
5 (1)	10T½	PBS	71	13	16
		IgM	74	11	15
6 (2)	PKC-4	PBS	57.5±2.5	20.5±0.5	22.0±3.0
		IgG+IgM	60.0±0.0	17.5±1.5	23.0±1.0
(1)	PKC-4	PBS	55	20	25
		IgM	57	14	29

^a Cells were cultured in F12 medium with 0.5% FBS for one day and then the medium was replaced by fresh medium with 0.5% FBS for another 2 days in the presence of purified C3H NAb at a final concentration of 0.25 mg/ml of IgG and 0.1-0.25 mg/ml of IgM, or 0.35 mg/ml of the IgG and IgM depleted C3H serum (NAb⁻ serum), or an equal volume of PBS. Cells distributed in the cell cycle were analysed by flow cytometry and the number of assays is in parenthesis.

^b P_{td} < 0.05, compared with PBS treated cells.

^c P_{ti} < 0.05, compared with PBS treated cells.

maintained in 0.5% FBS medium changed their appearance from a transformed to a more flat non-transformed morphology, while cells grown in either 5% or 10% FBS medium exhibited a fully transformed morphology. Addition of NAb into these cultures did not significantly influence the shape of cells. Compared with cells in 10% FBS medium, the total cell numbers was slightly reduced when I3T2.1 cells were cultured in 0.5% or 5% FBS medium for a period of 2 days, whereas the total cell number in 0.5% FBS medium was greatly decreased over a total of 3 days (Table 3.8, Expt 1). Treatment of I3T2.1 cells with purified IgM at 0.1 mg/ml for 1 day decreased the total cell numbers by 33% and 24% for cultures supplemented with 5% and 10% FBS, respectively (Table 3.8, Expts 2, 3). Preadsorption of IgM from the purified IgM NAb with anti-mouse IgM-3M Emphaze™ plastic beads reduced IgM binding levels by 85% based on the FACS analysis and decreased the protein concentration by 53% determined by measuring the optical density of proteins at 280 nm. This IgM-depleted IgM fraction (IgM^{lo}) produced similar cell numbers compared with PBS controls (Table 3.8, Expt 2).

Flow cytometry analysis of the cell cycle revealed a subtle increase in cell numbers at G0/G1 phase along with the decrease in concentrations of FBS in culture from 10 to 5, 0.5 and 0%, during a 2-day assay (Table 3.9, Expt 1). Extending the growth of I3T2.1 cells in 0.5% FBS medium for 3 days markedly prolonged the cell doubling time but the cells were still able to pass through the G0/G1 phase without synchronization at this stage. IgM NAb significantly increased the G0/G1 population and reduced the G2/M population in cultures with 5% FBS medium while the IgM^{lo} fraction induced a similar pattern of distribution of cells in the cell cycle compared with PBS controls (Table 3.9,

Table 3.8. Influence of FBS and NAb on growth of I3T2.1 cells

Expt# ^a	FBS (%)	Treatment	Cell numbers (mean \pm SE) ($\times 10^5$)	
			1 + 1 day	1 + 2 days
1 (2)	0	-	1.67 \pm 0.27	NA
	0.5	-	9.55 \pm 0.35	11.20 \pm 0.80
	5	-	9.90 \pm 0.40	22.63 \pm 1.38
	10	-	12.45 \pm 0.45	28.88 \pm 0.13
2 (3)	5	PBS	10.87 \pm 0.98	NA
		IgM	7.27 \pm 1.45 ^c	NA
		IgM ^{lo}	11.8 \pm 0.06	NA
3 (3)	10	PBS	12.97 \pm 1.42	NA
		IgM	9.83 \pm 0.50 ^d	NA

^a Independent cultures of I3T2.1 cells were grown in F12 medium with different concentrations of FBS for 1 day and then the medium was replaced by fresh medium supplemented with the same concentrations of FBS for another 1 (1+1) or 2 (1+2) days in the presence or not of purified IgM at a final concentration of 0.1 mg/ml or an equivalent amount of 0.1 ml of IgM-depleted IgM fractions (IgM^{lo}) or PBS. The cells were harvested by trypsinization and the total cell numbers were counted. The number of independent samples assayed is given in parenthesis.

^b $P_{ti} < 0.02$ compared with PBS or IgM^{lo} treated cells.

^c $P_{ti} < 0.05$ compared with IgM^{lo} treated cells.

^d NS.

NA, not assayed.

Table 3.9. Influence of FBS and NAb on cell cycling of I3T2.1 cells

Expt# ^a	FBS (%)	Treatment	% of cell numbers in cell cycle (mean \pm SE)					
			1 + 1 day			1 + 2 days		
			G0/G1	S	G2/M	G0/G1	S	G2/M
1 (2)	0	-	65.3 \pm 0.3	21.3 \pm 1.2	13.0 \pm 1.2	NA	NA	NA
	0.5	-	56.0 \pm 1.0	26.0 \pm 3.0	18.0 \pm 4.0	53.0 \pm 3.0	18.0 \pm 5.0	29.5 \pm 7.5
	5	-	53.5 \pm 2.0	20.5 \pm 1.5	26.0 \pm 1.0	58.0 \pm 2.0	15.5 \pm 1.5	26.5 \pm 0.5
	10	-	51.5 \pm 2.5	26.0 \pm 0.0	23.0 \pm 2.0	53.5 \pm 0.5	16.5 \pm 0.5	30.0 \pm 2.0
2 (3)	5	PBS	50.0 \pm 1.7	18.3 \pm 2.3	32.0 \pm 3.6	NA	NA	NA
		IgM	56.3 \pm 1.2 ^b	20.0 \pm 1.5	24.0 \pm 1.0 ^c	NA	NA	NA
		IgM ^{lo}	50.3 \pm 1.3	19.3 \pm 0.9	29.7 \pm 0.9	NA	NA	NA
3 (3)	10	PBS	50.0 \pm 1.2	25.0 \pm 4.0	24.7 \pm 3.0	NA	NA	NA
		IgM	53.7 \pm 0.9	19.0 \pm 0.0	27.3 \pm 0.9	NA	NA	NA

^a Independent cultures of I3T2.1 cells were grown in F12 medium with different concentrations of FBS for 1 day and then the medium was replaced by fresh medium supplemented with the same concentrations of FBS for another 1 (1+1) or 2 (1+2) days in the presence or not of purified IgM (final 0.1 mg/ml) or an equivalent amount (0.1 ml) of IgM-depleted IgM fractions (IgM^{lo}) or PBS. The cells were harvested by trypsinization and the cell cycle was analysed by flow cytometry. The number of independent samples assayed is given in parenthesis.

^b P_{ii} < 0.05 compared with PBS or IgM^{lo} treated cells.

^c P_{ii} < 0.02 compared with IgM^{lo} treated cells.

NA, not assayed.

Expt 2). The ability of IgM NAb to synchronize cells in G0/G1 was reduced in cultures containing 10% FBS (Table 3.9, Expt 3).

DISCUSSION

The cell surface binding capacity of NAb makes it an ideal regulator for control of cell functions through signaling potentials. It has been demonstrated that the interaction of growth factors with their cell surface receptors activates several intracellular pathways that ultimately lead to DNA replication and cell division (reviewed in Cantley et al., 1991). Some transducer enzymes that interact with these surface receptors include phosphoinositide-specific phospholipase C (PI-PLC), ras GTPase-activating protein (GAP) and type II phosphoinositide kinase (PI3K) (Ullrich and Schlessinger, 1990; Cantley et al., 1991). Hydrolysis of phosphatidylinositol 4,5-bisphosphate (PIP₂) by PI-PLC yields two second messengers: 1) inositol 1,4,5-triphosphate (IP₃), which mobilizes intracellular Ca²⁺ stores and increases cytosolic Ca²⁺ concentrations (Berridge, 1987) and 2) diacylglycerol (DAG), a physiological activator of PKC (reviewed in Lee and Severson, 1994; Exton, 1996). PKC not only phosphorylates membrane receptors and regulates their functions, but also phosphorylates raf-1 kinase and stimulates the mitogen-activated protein kinase (MAP) cascade (reviewed in Williams and Roberts, 1994). These observations support an important role for PKC in the signal transduction pathways.

The present study was initiated to characterize signaling events following syngeneic NAb interaction with cell surface structures. The initial experiments revealed that both parental 10T^{1/2} and its ras-overexpressing variant I3T2.1 bound less syngeneic NAb when

assayed at 37°C compared with 4°C, similar to a previous report describing the T lymphoma model (Chow et al., 1992). Unexpectedly, NAb binding levels in PKC-4 cells was slightly increased at 37°C compared with 4°C. One interpretation for the stable and slight increase in NAb binding in PKC-4 cells at 37°C is that this cell line has 11-fold more PKC activity than the parental 10T½, which confers upon the cells more resistance to the NAb binding-initiated downregulation mechanism(s). This possibility was supported by the notion that PKC-4 cells were more resistant to TPA-induced downregulation of both PKC-β1 expression and NAb binding (Chapter 2). Since pretreatment of the I3T2.1 and PKC-4 with H7 slightly increased NAb binding at 37°C, it is likely that the NAb interaction with cell surface molecules resulted in a PKC-mediated mechanism which tended to reduce NAb binding on the cell surface. This hypothesis was further supported by using the temperature shift model to accentuate the physiological process. When the temperature was raised from 4°C to 37°C for 20 min, all 10T½ variants exhibited a marked reduction in their precoated NAb, and this decrease in NAb binding was partially blocked by H7, but not by HA1004. The 46% reduction in NAb binding in PKC-4 cells detected following a raise in the temperature from 4°C to 37°C compared with the 70% decrease in the bound NAb in the 10T½ and I3T2.1 suggests again that PKC-4 cells were more resistant to NAb binding-initiated downregulation of precoated NAb. When comparing the significance of H7 inhibition in the downregulation of precoated NAb in these three cell lines, it was noted that the reduction in NAb binding in I3T2.1 cells obviously was not so significantly prevented by H7 as in the 10T½ and PKC-4. This discrepancy between these cells is probably due

to their differences in basal levels of DAG. H-ras overexpression in NIH 3T3 cells induced a 2-4 fold increase in DAG levels compared with the parental line (Matyas and Fishman, 1989; Carnero et al., 1994), whereas PKC- β 1 overproduction in the R6-PKC3, a rat embryo fibroblast line bearing an introduced PKC- β 1 gene and possessing 50 fold higher PKC activity than parental R6 cells, decreased basal DAG levels by nearly 50% compared with parental cells (Pai et al., 1991). Since the partial PKC- α activation and downregulation in H-ras-transformed 10T $\frac{1}{2}$ cells was inferred from a similar increase in DAG production (Weyman et al., 1987) and R6-PKC3 and PKC-4 do have many similarities in their partially transformed phenotype and responses to TPA treatment (Housey et al., 1988; Krauss et al., 1989), it is highly possible that I3T2.1 cells have higher basal levels of DAG than PKC-4 and 10T $\frac{1}{2}$ cells. If so, a constitutively higher level of DAG production in the I3T2.1 may persistently stimulate the membrane molecules to a late stage of activation, or a state of 'ready to be downregulated', which is less dependent on PKC stimulation and thus more resistant to H7 inhibition.

In accord with the involvement of PKC in the NAb-initiated reduction in precoated NAb loss from the cell surface, immunoblotting analysis clearly revealed that purified NAb stimulated PKC translocation to the membrane fractions following a rise in the temperature from 4°C to 37°C. In contrast, controls, including cells incubated with the IgG and IgM depleted C3H serum, purified NAb preabsorbed by PKC-4 cells, an anti-H2^k monoclonal antibody HB20, and 0-5% FBS in PBS or culture medium, tended to induce some reduction in membrane PKC following a rise in temperature to 37°C. The downregulation of membrane PKC in these control cells was possibly due to a

temperature-dependent initiation of metabolic events, which likely relied on activated PKC. Since there was a lack of any powerful external stimulators in these cases, the membrane PKC was just consumed with little recruitment from the cytosol. In contrast, extensive binding of NAb on the cell surface efficiently triggered PKC translocation from the cytosol to membrane fractions, which also tended to occur even at 4°C (Table 3.3). This would not only compensate for the downregulation of native membrane PKC, but would accumulate to build up an increase in PKC proteins. Therefore, the observed 20% increase for PKC- β 1 and 80% increase for PKC- α in membrane fractions from NAb-coated cells was likely an underestimation of PKC activation by NAb at 37°C. The higher ratio of PKC- α translocating to the membrane fractions than PKC- β 1 is not likely due to a different selective redistribution of these two isoforms because TPA treatment of both PKC- α - and PKC- β 1-overproducing NIH 3T3 cells induced both isoforms to translocate to the cell membrane edges detected by fluorescence staining (Goodnight et al., 1995). Even considering the fact that NAb already induced a considerable level of increase in membrane PKC- β 1 before the raise in the temperature to 37°C, the ratio of the increase for PKC- β 1 was still less than that for PKC- α . This suggests that NAb binding may affect PKC- α and PKC- β 1 differentially. As a result of the NAb interaction with cell surface receptors, PKC- α -mediated biological events could be proportionally more increased than PKC- β 1-mediated events. Thus, the balance between PKC- α - and PKC- β 1-controlled events could be shifted after NAb binding at 4°C and the raise in the temperature to 37°C. It has been noted that these two isoforms exhibit different biological functions in that PKC- β 1 overexpression in R6 fibroblasts provoked enhanced

growth and partial transformation while PKC- α overexpression in the same cell led to a marked inhibition of cellular growth (Housey et al., 1988; Borner et al., 1991 and 1995). Since NAb-induced growth inhibition in I3T2.1 cells was associated with activation of PKC- α (Fig 3.5) and in I3T2.1 cells, PKC- α is predominantly expressed while there is no expression of PKC- β 1 at all, the proportionally higher PKC- α activation following NAb binding may also be associated with the introduction of negative growth signals for the PKC-4.

During the temperature increase procedure, the NAb binding likely builds up maximally at 4°C when the activity of the cells is reduced by energy deprivation and a decrease in membrane fluidity. Upon exposure to 37°C, the NAb-induced mechanisms would start up vigorously with PKC translocating to the membrane. This may reflect the physiological situation at the very beginning of PKC activation following NAb binding with cells. Thus, it is conceivable that under physiological conditions, continuous interaction of NAb with cell surface structures could stimulate PKC activation which in turn results in a reduction in NAb binding and changes in downstream biological events.

NAb-initiated alterations in both PKC expression and NAb binding were successfully simulated by TPA with TPA accentuating the stimulation of PKC translocation and downregulating NAb binding levels. It has been noted that physiological factors are always very mild when they stimulate PKC, which differs from TPA, the strongest stimulator of PKC found so far. For example, the native membrane PKC activity was found to increase about 1.5-fold after growth factor stimulation of erythrocytes but there was no detectable translocation of cytosolic PKC to membranes (Chakvarthy et al.,

1994). In the present study, a reduction of PKC protein in cytosolic fractions of cells treated with purified NAb was not consistently observed. This may be due to the high proportion of cellular PKC in the cytosol. The cytosolic pool of PKC in 10T½ cells possesses nearly 90% of the total detectable cellular PKC activity (Weyman et al., 1987), and even in PKC-4 cells, which have an 11-fold increase in PKC activity compared with the parental line, at least 70% of the PKC activity exists in the cytosol (Rotenberg et al., 1990). Thus, a small amount of PKC movement away from the cytosolic compartment may be difficult to detect with the immunoblotting method.

PTPs are intrinsic antagonists of protein tyrosine kinases (PTKs) and control the levels of tyrosine phosphorylation required for cell growth and differentiation by dephosphorylating phosphotyrosyl residues of proteins (reviewed in Tonks, 1996). It has been found that NAb could bind to CD45, an abundant RPTP of lymphocytes (Zhang and Chow, unpublished data). Thus, NAb may influence CD45 functions by direct binding with this molecule. RPTP α is a ubiquitous RPTP and is expressed on 10T½ variants (Chapter 4). In this study, RPTP α was found to be preferentially released to the supernatant from cells incubated with purified NAb using the same temperature shift procedure, while control medium with 0-1% FBS, or purified NAb preabsorbed with cells, yielded far less RPTP α in the supernatant. Pretreatment of cells with TPA to deplete PKC abolished the NAb-induced shedding of RPTP α and other unknown molecules. Since long-term TPA treatment of I3T2.1 only resulted in a 23% reduction in NAb binding and a 21% decrease in membrane RPTP α , the complete elimination of RPTP α shedding in TPA treated, PKC- α depleted I3T2.1 cells is likely due to the

depletion of the PKC-mediated mechanism in these cells rather than due just to the reduction in the capacity to bind NAb and the decrease in RPTP α expression. However, whether the 23% of the NAb binding sites which are lost from I3T2.1 cells following TPA treatment are key structures for NAb signaling is presently not known. Considering the fact that activation of PKC could enhance RPTP α activities (den Hertog et al., 1995), the interaction of NAb with cell surface structures may directly or indirectly influence the functions of RPTP α . Moreover, brief treatment with TPA for 1 h in A431, 293 and HeLa cells has been found to induce proteolytic cleavage and internalization of two receptor-like PTPs, LAR and RPTP δ (Aicher et al., 1997). In the present study, proteolysis of RPTP α was not likely induced because the intact molecule was detected in the supernatant with anti-RPTP α antibody which recognizes the cytoplasmic part of this molecule (Daum et al., 1994). Whether there was any internalization of RPTP α in addition to its shedding following NAb binding and a rise in the temperature is currently not clear.

Immunoblotting with a monoclonal anti-phosphotyrosine antibody 4G10 detected a time-dependent reduction in the reactivity of 4G10 with p60, a 60-KDa membrane-associated molecule. In this case, NAb likely enhanced the process of the loss of phosphotyrosine epitopes from p60. It is presently unclear about the mechanism of this loss of 4G10 binding to p60. This may be resulted either from an increase in PTP activity or a reduction in PTK activity which is responsible for maintaining the normal phosphotyrosine levels of p60. Alternatively, other unknown proteolytic process may be also able to eliminate 4G10 epitope from p60. So far, the nature of p60 is also unknown.

There are a few membrane-associated molecules around 60 KDa such as cytoskeletal proteins vimentin and peripherin and signaling molecules of the src family including src and fyn. Moreover, it also remains to be determined whether RPTP α is responsible for the decrease in 4G10 binding to p60. It is interesting to note that a considerable level of reduction in phosphotyrosine levels of p60 was even observed at 4°C in NAb treated PKC-4 cells. This is concordant with the slight PKC translocation at 4°C in NAb treated PKC-4 cells. Therefore, the activities of these intracellular signaling enzymes were not completely suppressed by the low temperature. Our previous observation that the pattern of bound NAb changed from speckled to patched over time at 4°C (Chow, unpublished observation) further supports this conclusion.

It is well known that many cell surface receptors including the growth factor receptors require cross-linking for triggering intracellular signal transduction. It is presumed that even though NAb is a relatively low affinity antibody, its multireactivity and high connectivity features would make NAb bind with cell surface structures through multiple ways. For instance, NAb could cross-link two different close membrane molecules having similar epitopes. The anti-Ig activity-possessing NAb would further cross-link close NAb, eventually building up a massive cross-linking or even a multilayer binding on the cell surface. As mentioned above, NAb patching on the cell surface occurs at 4°C. This suggests that cross-linking of membrane molecules through NAb does occur and this may be a key step for NAb initiation of signal transduction. Following signal transduction, many cell surface receptors exhibit shedding or internalization a process known as receptor desensitization which intends to avoid

overstimulation by the ligands. Consistent with this view, a variety of cell surface molecules including RPTP α and the bound NAb were released to the supernatant following the rise in temperature from 4°C to 37°C (also see Chapter 4). This indicates that the release of cell surface molecules and bound NAb was part of the NAb-initiated cellular response.

NAb showed a growth inhibitory effect when cocultivated with I3T2.1 cells. It was likely that IgM NAb was more efficient in the inhibition of cell growth than IgG NAb when used at a similar concentration. Purified IgM alone suppressed cell growth in both 0.5% and 5% serum cultures likely through arresting cells at G0/G1 stage in the cell cycle. Interestingly, in the presence of 10% FBS the effect of NAb inhibition on cell growth was diminished compared with the 5% FBS-containing culture, a condition which by itself did not significantly slow cell doubling. An excess of growth factors in 10% FBS may have partially reversed the inhibitory effect of IgM NAb or extra bovine serum proteins may have complexed with IgM NAb and reduced the cell surface binding of IgM NAb. Preadsorption of the purified IgM with anti-mouse IgM-coupled polymerized acrylamide beads abolished the growth inhibitory activity of IgM indicating that other macromolecules copurified with IgM from the gel filtration column likely did not account for the growth suppressive activity in the purified IgM fractions. Moreover, preliminary experiments in 0.5% FBS showed that purified IgG and IgM also tended to inhibit growth of 10T½ and PKC-4 cells, but the degree of inhibition in PKC-4 cells was likely lower than that in I3T2.1 cells. This may be due to the difference in their cellular contexts which could render them more or less susceptible to the NAb-mediated

suppression mechanism. This growth suppressive effect of NAb on I3T2.1 cells supports a previous report that natural IgM antibodies secreted by LPS-stimulated normal mouse splenic B cells prevented ^3H -thymidine incorporation of LPS-activated fresh B cells and blocked the growth of these cells in G0 and G1 stages in the cell cycle during a 2-day assay (Uher et al., 1992). The similarity between these two studies suggests that NAb may control activated cells through a mechanism which inhibits cell proliferation. This reinforces the idea that NAb may preferentially react with activated cells and contributes to the homeostasis of the organism (Chapter 2).

The mechanism(s) of growth suppression induced by NAb are presently not clear. The emerging evidence has suggested that PKC could function to inhibit the cell cycle at mid to late G1 stage depending on the cell type and the timing of PKC activation during the cell cycle (reviewed in Livneh and Fishman, 1997). The molecular mechanism of this cell cycle inhibition by PKC has been associated with a blockage in the normal phosphorylation of the tumor suppressor retinoblastoma Rb protein (Zhou et al., 1993), a pivotal regulator positioned at a critical point in the first two thirds of the G1 phase of the cell cycle (Weinberg, 1995). However, due to the complexity of the NAb binding features on the cell surface, it could be more than one mechanism responsible for the final growth inhibition. It has been noted that 20 min after infusion of IVIg into patients, the plasma IFN- γ and IL-6 levels increased and shortly after returned to normal levels (Ling et al., 1993). This indicates a transient activation of monocytes/macrophages and NK cells (Ling et al., 1993). Since the long-term effect of IVIg in vivo has been frequently documented to be immunosuppressive (see Chapter 1), it is possible that NAb

reaction with these immune cells *in vivo* may induce an early transient activation followed by a later inhibition for their growth. However, it also remains unknown about the mechanism of NAb-induced growth suppression in immune cells. In addition to growth suppression, NAb binding to target cells *in vivo* may induce necrosis of the cells by activating the complement system and may also induce apoptosis through NK cell- and macrophage-mediated killing mechanisms. However, it is currently unknown whether NAb alone can initiate any apoptosis of the target cells.

In summary, NAb binding to fibroblasts resulted in activation of the signaling molecule PKC as assessed by an increase in membrane PKC proteins based on the temperature increase model. PKC activation following NAb binding was partially responsible for the downregulation of the cell surface NAb bound at 37°C or at 4°C and shifted to 37°C, because this reduction could be partially prevented by H7. The PKC stimulating effect of NAb was successfully simulated by TPA with TPA accentuating PKC translocation and downregulating NAb binding levels. In addition, the NAb interaction with cell surface structures induced the release of RPTP α and other cell surface molecules into the cell supernatant and a reduction of reactivity of 4G10 with a 60-KDa membrane-associated molecule. Moreover, NAb inhibited growth of I3T2.1 cells as assessed by a reduction in total cell numbers and an increase in cell numbers in the G0/G1 phase of the cell cycle. All the data suggested that NAb reacting with cell surface structures efficiently initiated an intracellular response including rapid PKC-dependent signaling events, the release of cell surface molecules and NAb, a reduction in phosphotyrosine levels of p60, and, over time, the suppression of cell growth, which may

provide a basic biological mechanism for NAb control of activated cells under certain physiological and pathological conditions.

CHAPTER 4

**NATURAL ANTIBODY INTERACTION WITH CELL SURFACE MOLECULES
EXPRESSED ON v-Ha-ras- AND PKC- β 1-OVEREXPRESSING 10T $\frac{1}{2}$
FIBROBLASTS AND L5178Y-F9 LYMPHOMAS**

ABSTRACT

NAb has been demonstrated to regulate cell functions possibly through binding with cell surface molecules. Western blotting analysis of membrane extracts from the parental 10T½, v-Ha-ras-overexpressing I3T2.1 and PKC-β1-overproducing PKC-4 cells revealed that NAb eluted from viable cells or purified from normal syngeneic serum recognized at least 20 cell surface molecules in each line ranging from 220 to 20 KDa under reducing conditions. Purified NAb immunoblotting of cell surface molecules purified from biotinylated 10T½ variants with avidin-coupled agarose also detected a set about 20 molecules in each line. Both I3T2.1 and PKC-4 cells exhibited a more intense NAb staining at 200, 170, 160, 110, 90, 80, 70 and 66 KDa compared with the parental 10T½. Moreover, upon raising the temperature from 4°C to 37°C, both pre-coated NAb and many membrane molecules were released to the supernatant. Immunoblotting of the supernatant with purified NAb produced a molecular profile similar to that detected with purified biotinylated membrane molecules. Anti-mouse IgG and IgM antibody-coupled agarose precipitation of the supernatant obtained from NAb-coated cells following a rise in temperature to 37°C yielded a 90-KDa molecule (p90). Altogether, these data suggest that NAb could react with a variety of cell surface molecules, which may be key structures for NAb signaling and regulation of cell functions. Investigation of candidate membrane molecules as potential NAb targets including CD44 and gelatinase B, which have similar molecular weights to the precipitated p90, and RPTPα, which has been shown to be involved in the NAb-initiated signaling, did not yield a definitive answer. However, correlations between NAb binding and CD44 expression suggested that NAb

may bind CD44.

INTRODUCTION

NAb has been shown to resist against tumors both in vivo and in vitro (see Chapter 1). A monoclonal tumor reactive natural IgM inhibited the growth of human colon carcinomas in vitro and induced expression of MHC class I antigens on the same tumor (Bohn et al., 1994). As already discussed in Chapter 3, NAb binding with cell surface structures directly initiated PKC-dependent signaling events and inhibited cell growth in ras-overexpressing 10T½ fibroblasts. In addition, NAb suppressed growth of mitogen-stimulated lymphocytes in vitro (see Chapter 1). These observations reveal an important aspect of the biological roles for NAb in controlling tumor cells and activated normal cells through signaling potentials.

However, so far little is known about the cell surface structures through which NAb regulates the cell functions. Limited studies in immune cells have demonstrated an interaction between NAb and the framework and variable determinants of the β chain of the $\alpha\beta$ T cell receptor (Cruger et al., 1993; Dedeoglu et al., 1993; Marchalonis et al., 1994), MHC class I and class II antigens (Berneman et al., 1992), CD3 (Berneman et al., 1992), CD4 (Berneman et al., 1992; Hurez et al., 1994), CD5 (Vassilev et al., 1993) and CD8 (Berneman et al., 1992). The NAb targets expressed on fibroblasts are largely unknown.

Western blotting, or immunoblotting, has been used frequently for determining the molecular nature of NAb reactive antigens regarding their molecular weight and

composition. With this method, Berneman et al (1992) have demonstrated that at least 220 protein constituents from mouse tissue extracts reacted with purified syngeneic NAb. In this study, immunoprecipitation of iodinated cell surface molecules with IgG NAb yielded molecules which migrated in SDS-polyacrylamide gels to the same position as MHC class I and class II antigens immunoprecipitated by specific monoclonal anti-MHC class I and class II antibodies (Berneman et al., 1992). Western blotting has also been used for isolation of sperm (Auer et al., 1995) and neuron (Moore et al., 1994) surface autoantigens with autoantibodies from patients and autoimmune animals.

Previous studies have demonstrated a positive correlation between NAb binding and CD45 expression in the L5178Y-F9 murine T lymphoma model including the high NAb binding variant of the L5178Y-F9, LYNAb⁺, which was selected in vitro through TPA stimulation and FACS and a low NAb binding variant of LYNAb⁺, X2SC, which was selected in vivo by passaging LYNAb⁺ cells twice in syngeneic DBA/2 mice (Zhang and Chow, 1997). This has led to identification of CD45 as a NAb target through approaches including ELISA and a blocking assay (Zhang and Chow, unpublished data). In the 10T½ fibroblast model, both ras-transformed and PKC-β1-overproducing variants exhibited an increase in NAb binding (Chapter 2), while introduction of myc oncogene into ras-overexpressing I3T2.1 cells decreased NAb binding levels (Tough and Chow, unpublished data). Thus, both cell systems are ideal models for examining the relationship between NAb binding and expression of cell surface molecules.

In order to elucidate the binding features of NAb with the cell surface structures that may be involved in the NAb-initiated signaling, this study was attempted to characterize

NAb reactive cell surface structures by using immunoprecipitation and Western blotting methods. Corresponding to the protein bands detected by NAb in primary immunoblotting experiments, a few cell surface proteins with well defined molecular characteristics including CD44 and gelatinases B were further analyzed as candidate targets of NAb. Since the receptor-like protein tyrosine phosphatase α (RPTP α) has been shown to be involved in the NAb-initiated signaling in 10T $\frac{1}{2}$ fibroblasts (Chapter 3), and NAb has been found to bind with CD45 (Zhang and Chow, unpublished data), a RPTP α -like glycoprotein, the potential reaction between NAb and RPTP α was also investigated in this study.

MATERIALS AND METHODS

Mice and sera

DBA/2 mice were from the University of Manitoba vivarium. Serum was prepared the same way as described in Chapter 2. C3H mice and serum were the same as used in Chapter 2.

Cell culture

10T $\frac{1}{2}$ and its ras- and PKC- β 1-overexpressing variants were maintained in F12 and DMEM as described in Chapter 2. The murine T cell lymphoma L5178Y-F9 and its derivative LYNAb⁺ and X2SC were cultured in Fisher's medium (FM) (Life Technologies, Grand Island, NY) supplemented with 10% FBS. The LYNAb⁺, previously named L5178Y-F9 TPA/NAb⁺3, was a high NAb binding subpopulation selected for three cycles from TPA-stimulated L5178Y-F9 through fluorescence-activated

cell sorting (FACS) (Tough and Chow, 1988). The X2SC was a population recovered from LYNAb⁺ twice-selected through growth in vivo (Zhang and Chow, 1997).

In vivo selection

An aliquot of 1×10^4 I3T2.1 cells was injected s.c. into each of 5 syngeneic adult C3H mice. Thirty five days after injection, tumors were removed from the injection site and minced to release tumor cells. After washing with F12 medium, tumor cells were plated in petri dishes in F12 medium supplemented with 10% FBS plus 400 $\mu\text{g/ml}$ of G418 (Life Technologies) to eliminate normal fibroblast contamination from tumor tissues. G418 was also added to one plate of I3T2.1 which was continuously maintained in vitro as a control. Medium was replaced every three days with fresh medium containing G418. Cells were replated at 1×10^5 per 100-mm dish when the culture reached high densities. After nine days growth with G418, tumor cells were returned to normal culture conditions and tested for NAb binding and CD44 expression at the same time.

Retroviral myc oncogene infection

I3T2.1 cells were infected with SVX, a recombinant retrovirus bearing the neo^r gene, and VM virus, which carries the myc oncogene in the form of the p110 gag-myc fusion gene from pv-myc (Land et al., 1983), and the neo^r marker. The infection was performed as described in Chapter 2 by using a multiplicity of infection (MOI) at 1.7 and 3.5 for VM virus, 0.08 and 0.15 for SVX, in the presence of 8 $\mu\text{g/ml}$ of polybrene. After incubation with virus for 2 days, cells were replated to expand the cell numbers and then frozen down in liquid N₂. NAb binding tests were performed on early passage cells which were not frozen. For CD44 studies, frozen cells were recovered and CD44

expression levels were determined by flow cytometry.

Neuraminidase treatment

Aliquots of 2×10^6 cells were washed with PBS and resuspended in 200 μ l neuraminidase (4 U/ml) (Sigma Chemical Co., St. Louis, MO) in Hank's balanced salt solution (HBSS) (Life Technologies) containing NaOH at 0.5 mM. The cells were incubated at 37°C with 5% CO₂ for 50 min with occasional shaking. For controls, the cells were treated the same way with only 200 μ l of HBSS/NaOH.

Fluorescence-detected NAb binding

The method was as described in Chapter 2.

Fluorescence-detected CD44 expression

10T $\frac{1}{2}$ variants were harvested by trypsinization as outlined in Chapter 2. Aliquots of 3×10^5 cells were washed with PBS containing 1% FBS and 0.02% azide and incubated with 100 μ l of 10 μ g/ml monoclonal anti-CD44 antibodies for 1 h at 4°C. Two monoclonal antibodies (MAbs) to murine CD44, KM114 (rat IgG1) and IM7 (rat IgG2b) (PharMingen, San Diego, CA), were used in this study. Although both MAbs are able to detect all CD44 isoforms, KM114 recognizes a different CD44 epitope from that detected by IM7 (Zheng et al., 1995). After two washes with 1% FBS in PBS at 4°C, the cells were incubated with FITC-conjugated goat anti-rat IgG antibodies (Organon Teknika Corp., West Chester, PA) for 20 min at 4°C. Cells were then washed and analyzed by flow cytometry as described in Chapter 2. An unrelated MAb, 14.8 (rat IgG 2b), specific for CD45, was included as an isotype control. Background binding was determined in cells incubated with only the FITC-conjugated anti-rat IgG antibody and

deducted when calculating the specific value of anti-CD44 MAb binding.

L5178Y-F9 cells were analysed the same way with biotin-labelled KM114 and IM7 (PharMingen) at a final concentration of 1 $\mu\text{g}/\text{ml}$. After washing, cells were then incubated with phycoerythrin (PE)-conjugated streptavidin (Jackson ImmunoResearch Laboratories, Mississauga, Ontario) for 20 min at 4°C and analyzed by flow cytometry.

Preparation of cell membrane-specific NAb

Serum NAb was adsorbed onto 10T $\frac{1}{2}$ variants and subsequently eluted from the cell surface. Briefly, 2×10^7 to 4×10^7 cells of each of the 10T $\frac{1}{2}$, I3T2.1 and PKC-4 lines were incubated with 600 μl of C3H serum diluted 1:1 in PBS for 1 h at 4°C. After two washes with PBS at 4°C, at least 92% of the cells were still able to exclude trypan blue. The cells were pelleted and resuspended in 1 ml of 0.1 M glycine-HCl buffer at pH 2.8 with shaking for 10 min at 4°C. After a 3-min centrifugation at 5,000 g, the supernatant was neutralized with 1 M Tris and centrifuged once to remove precipitates. The eluted NAb was dialysed against PBS overnight at 4°C and stored at 4°C.

Purification of IgG and IgM NAb from normal C3H and DBA/2 serum

IgG and IgM NAb were purified through protein A-coupled and anti-mouse IgM antibody-coupled Sepharose columns, respectively, as outlined in Chapter 3. In some experiments, IgG and IgM NAb were purified through 3M-EmphazeTM plastic bead-supported protein A and -anti-mouse IgM columns (see Chapter 3).

Preparation of cell membrane antigens

Cell membrane fractions were prepared by sonication of $1.2 \sim 2.1 \times 10^7$ cells and ultracentrifugation as described in Chapter 2. Membrane pellets were extracted for 1 h

at 4°C with RIPA buffer consisting of 20 mM Tris, pH 7.6, 2 mM EDTA, 0.15 M NaCl, 10 mM KCl, 1% NP-40, 0.1% SDS, 1% sodium deoxycholate, 5 µg/ml leupeptin and 5 µg/ml aprotinin (Peng and Cartwright, 1995). After a 5-min centrifugation at 17,000 g, the protein concentration of the supernatant was measured using a Bio-Rad protein detection kit as described in Chapter 2. This preparation was used as crude membrane proteins in immunoblotting analysis.

An alternative preparation of cell membrane antigens was made through purification of biotinylated cell surface structures with avidin-coupled agarose (Sigma). The biotinylation procedure of Hausmann et al (1992) was employed in this study. Briefly, 10^7 /ml cells were incubated with N-hydroxysuccinimidobiotin (NHS-biotin) (Sigma) at 50 µg/ml in PBS for 25 min at room temperature and then washed with PBS. Membrane fractions were extracted as described above. A total of 400 µg of membrane proteins in 300 µl RIPA buffer was incubated for 2 h at 4°C with 100 µl avidin-agarose (1:1, v/v), or plain Sepharose (agarose, polymerized galactose) as a control prepared by blocking the CNBr-activated Sepharose (Sigma) with glycine. The agarose beads were washed 4 times with 1:1 diluted RIPA buffer and once with PBS at 4°C. The antigens were eluted by incubation with 70 µl of 2x gel sample buffer containing 4% SDS, 0.2 M Tris, 20% glycerol, 0.02% bromophenol blue, 3% dithiothreitol, at pH 6.8, and boiling for 10 min. This preparation was used as purified membrane proteins.

Preparation of released cell surface antigens from the supernatant of cells incubated at 4°C with and without NAb and raised to 37°C

Cells were surface labeled with NHS-biotin as mentioned above. An aliquot of 10^7

labeled cells was incubated at 4°C for 1 h with 350 μ l of purified NAb containing a final concentration of 0.5 mg/ml of IgG and 0.6 mg/ml of IgM, or 350 μ l of 0.5% BSA in PBS. In some experiments, cells were not biotinylated and were incubated the same way with 600 μ l of 1:1 diluted C3H serum NAb, or culture medium containing 1% FBS, or NAb-depleted C3H serum, which was prepared by adsorption of whole C3H serum with an excess of protein A- and anti-mouse IgM antibody-coupled Sepharose. After one wash with cold PBS at 4°C, the cells were resuspended in 300 μ l of PBS and incubated at 37°C for 8 to 10 min. The supernatant was obtained by a 5-min centrifugation at 1000 g and was used for immunoprecipitation and immunoblotting.

Immunoprecipitation

For CD44 immunoprecipitation, the membrane proteins from biotinylated 10T $\frac{1}{2}$ variants were prepared as described above. The biotinylated L5178Y-F9 variants were extracted with the lysis buffer containing 20 mM Tris, pH 8.0, 0.85% LiCl, 1 mM EDTA, 0.5 mM aprotinin and 1% Triton X-100. Aliquots of 400 μ g of membrane proteins from 10T $\frac{1}{2}$ and 600 μ g of cellular proteins from L5178Y-F9 variants were incubated with 10 to 15 μ g of IM7 and KM114 overnight at 4°C. The mixture was then incubated with 40 μ l of goat anti-rat IgG antibody-coupled agarose for 2 h at 4°C. Agarose pellets were washed twice with high salt buffer containing 0.6 M NaCl, 0.0125 M KPO $_4$, 0.02% NaN $_3$, at pH 7.4, twice with detergent buffer containing 0.05% NP-40, 0.1% SDS, 0.3 M NaCl, 10 mM Tris, pH 8.6, and once with PBS (Camp et al., 1991).

For RPTP α immunoprecipitation, 10T $\frac{1}{2}$ variants were extracted with the lysis buffer mentioned above. Aliquots of 825 or 1825 μ g of whole cell extracts were

incubated with 10 or 12 μ l of rabbit anti-RPTP α anti-serum (obtained from Dr. J. Sap, Department of Pharmacology, New York University Medical Center, New York) overnight at 4°C. In another experiment, isolated membrane proteins from 5×10^6 of 10T $\frac{1}{2}$ variants were precipitated with 10 μ l anti-RPTP α anti-serum. Immune complexes were recovered by a 2-h incubation with protein A-coupled Sepharose at 4°C. The precipitates were washed three times with the lysis buffer and once with PBS at 4°C.

For precipitation of released cell surface molecules, the cell supernatant was prepared from cells treated with serum NAb, NAb-depleted serum or 3% FBS in growth medium at 4°C followed by a raise in temperature to 37°C. Aliquots of 250 μ l supernatant were precipitated with 75 μ l of goat anti-mouse IgG and IgM antibody-coupled agarose (Caltag Laboratories, So. San Francisco, CA) for 2 h at 4°C. The precipitates were washed once with PBS. In some experiments, the same supernatant from NAb-coated cells was precipitated with plain Sepharose as another control.

Immune complexes were then eluted by boiling in 2x gel sample buffer as mentioned above.

SDS-PAGE

The method was described in Chapter 2. Reducing conditions were used unless otherwise indicated.

Immunoblotting

Following electrophoresis, proteins were transferred onto nitrocellulose membranes (Bio-Rad Laboratories, Hercules, CA) at 30 volts overnight at 4°C in a renaturing buffer containing 10 mM NaHCO₃, 3 mM Na₂CO₃, 20% v/v methanol, at pH 9.9

(Dunn, 1986). The membrane was blocked with 10% BSA in TBST wash buffer for 1 h at room temperature as described in Chapter 2. The purified natural IgG and IgM were diluted in TBST at 20 $\mu\text{g/ml}$ of IgG and 90 $\mu\text{g/ml}$ of IgM. The IgG and IgM NAb were used together unless otherwise indicated. The eluted NAb was used without dilution but complemented by Tween-20 to a final concentration of 0.05%. The membranes were allowed to react with NAb in plastic bags at 4°C overnight. After three 10-min washes with TBST, the nitrocellulose sheets were incubated with 1:1000 diluted alkaline phosphatase-conjugated antibodies to mouse IgG (Sigma) and IgM (Dimension Laboratories Inc., Mississauga, Ontario) for 1 h at room temperature. Following three washes, the proteins were made visible by a substrate reaction described in Chapter 2.

For detection of biotinylated CD44, the proteins were transferred onto nitrocellulose membranes in the Tris-glycine buffer as outlined in Chapter 2. The blots were probed with avidin-HRP, followed by the ECL developing procedure as described in Chapter 2.

Gelatin zymography

Zymography was performed as described by Hibbs et al (1985). Briefly, equal amounts of membrane proteins from 10T $\frac{1}{2}$, I3T2.1 and PKC-4 cells were resolved on 8% SDS-polyacrylamide gels containing 1 mg/ml of gelatin (Fisher Scientific Ltd., Nepean, ON) under non-reducing conditions. After electrophoresis, the gels were washed twice with 2.5% (v/v) Triton X-100 for 2 h at room temperature to remove the SDS, and three times with distilled water for 5 min to remove the Triton X-100. The gels were then incubated in 50 mM Tris-HCl, 0.2 mM NaCl, 20 mM CaCl₂, at pH 7.4 and 37°C for 24–48 h and stained with 0.5% (w/v) Coomassie Brilliant Blue R-250 in 45% (v/v)

methanol and 10% (v/v) acetic acid for 2 h. After destaining in the same solution without dye, gelatinase activity became visible as a clear band in a blue background.

In separate experiments, aliquots of 300 μ l (0.5 mg/ml) of the membrane fractions from PKC-4 were incubated at 4°C for 1 h with 200 μ l (v/v) of gelatin-coupled agarose (Sigma), or 200 μ l (v/v) of plain Sepharose equilibrated with 50 mM Tris-HCl, 150 mM NaCl, 5 mM CaCl₂, 0.02% Tween-20, at pH 7.6 (Collier et al., 1988). After incubation, the agarose was washed 4 times with the equilibration buffer containing 200 mM NaCl. Then the beads were eluted with 50 μ l of 1:1 diluted 4x non-reducing gel sample buffer containing 8% SDS, 0.4 M Tris, 40% (w/v) glycerol, 0.4% bromophenol blue, at pH 6.8. The supernatant and the eluted materials were assessed under non-reducing conditions as before.

Statistical analysis

The paired student *t* test (P_{td}) and the independent student *t* test (t_i) were used to assess the significance of the differences observed in NAb and MAb binding and in RPTP α expression. $P > 0.05$ was not considered significant.

RESULTS

SDS-PAGE fractionation and immunoblotting analysis of membrane molecules

To determine the molecular features of NAb reactive cell surface structures, crude plasma membrane preparations were resolved on SDS gels and transferred onto nitrocellulose membranes under renaturing conditions. NAb immunoblotting detected at least 20 protein bands ranging from 220 to 20 KDa in each of the 10T½, I3T2.1 and

PKC-4 (Fig 4.1, lanes 3 to 6). *ras*- and PKC- β 1-overexpressing cells exhibited a different immunoblot profile from parental 10T $\frac{1}{2}$ both quantitatively and qualitatively, mainly in proteins around 150 and 160-170 KDa (Fig 4.1, lanes 4, 5 and 6). 10T $\frac{1}{2}$ cells had a stronger staining by NAb in these two regions compared with I3T2.1 and PKC-4 (Fig 4.1). Since crude membrane preparations were contaminated by cytoskeletal molecules assayed by the detection of actin (see Chapter 3, Fig 3.2 and Fig 3.4), membrane molecules were subsequently purified through a biotin-avidin precipitation procedure. Cell surface molecules were first labeled with biotin and then extracted from membrane pellets with an SDS-containing RIPA lysis buffer to break inter-molecular associations. The biotinylated cell surface molecules were specifically precipitated with avidin-coupled agarose. The eluted molecules from avidin-agarose were free of actin for all three cell lines in one experiment and contained only a trace amount of actin for 10T $\frac{1}{2}$ and PKC-4 in a second experiment (data not shown). Probing the purified membrane molecules which were free of actin with purified NAb revealed that in 10T $\frac{1}{2}$ cells, some proteins around 160-170, 150, 90 and 45-50 KDa were reduced to nearly background levels (Fig 4.2). I3T2.1 and PKC-4 cells also showed a quantitative reduction in molecular masses at 90 and 45-50 KDa (Fig 4.2). Compared with the 10T $\frac{1}{2}$, the intensities of some protein bands around 200, 170, 160, 110, 90, 80, 70 and 66 KDa were higher in both I3T2.1 and PKC-4 cells (Fig 4.2). This was consistent with the high NAb binding phenotypes of I3T2.1 and PKC-4.

In addition, both the eluted NAb and the affinity purified NAb (IgG + IgM) were found equally effective for immunoblotting. When used separately, IgG and IgM NAb

Fig 4.1. Immunoblotting of cell surface molecules from 10T $\frac{1}{2}$ variants with eluted NAb. Crude membrane extracts from 10T $\frac{1}{2}$ (lane 4), I3T2.1 (lane 5) and PKC-4 (lane 6), and supernatant from biotinylated I3T2.1 cells preincubated with 0.5% BSA in PBS (lane 1) or purified NAb (lane 2) followed by a raise in temperature from 4°C to 37°C, were resolved on 8% gels. Lane 3 is a membrane extraction from non-treated biotinylated I3T2.1 cells. NAb H chains in lane 2 were around 80 (μ chain) and 50 (γ chain) KDa. Molecular mass markers as described in Chapter 2 are indicated on the left. The result represents one of two identical experiments with similar observations.

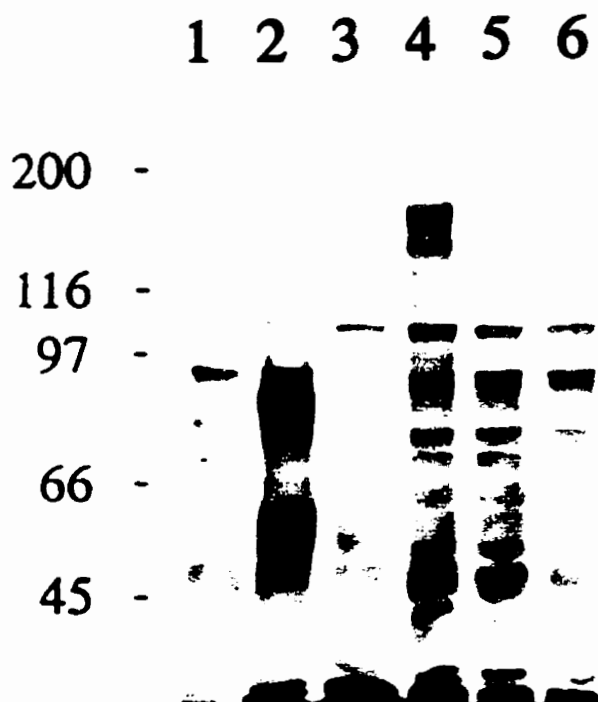
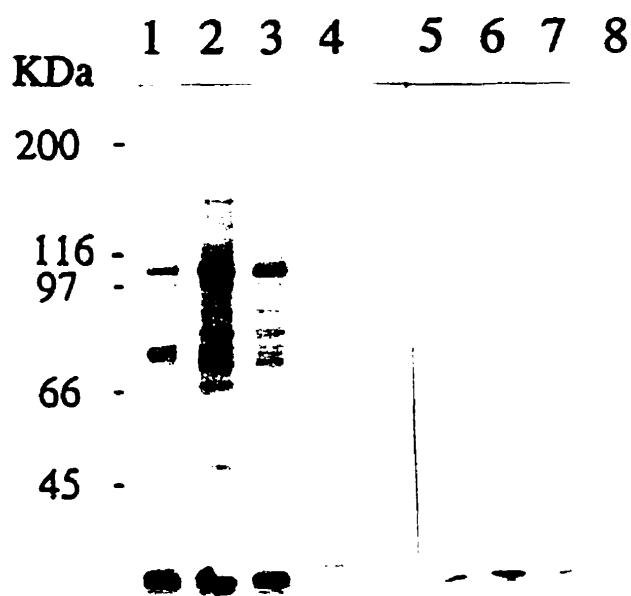


Fig 4.2. Immunoblotting of purified biotinylated membrane molecules with purified NAb (IgG + IgM). 10T $\frac{1}{2}$ (lanes 1, 4, 5 and 8), I3T2.1 (lanes 2 and 6) and PKC-4 (lanes 3 and 7) were surface labeled with NHS-biotin. Labeled molecules were precipitated from membrane fractions with avidin-coupled agarose (lanes 1, 2, 3, 5, 6 and 7), or plain Sepharose (lanes 4 and 8), and resolved on 8% gels. After transfer to nitrocellulose membrane, the proteins were detected with purified NAb followed by a second alkaline phosphatase-conjugated anti-mouse IgG and IgM antibody (lanes 1 to 4) or with only the second antibody (lanes 5 to 8). Molecular mass markers are indicated on the left. The result represents one of two identical experiments with similar observations.



exhibited a different capacity for probing some protein molecules (Fig 4.3). For instance, natural IgM reacted more intensively with molecules around 220, 200, 150-160, 90, 80 and 66 KDa which were only weakly detected by using an even higher concentration of IgG NAb (Fig 4.3). To simulate a physiological condition, a combination of purified IgG and IgM NAb was employed subsequently in most experiments.

Shedding of cell surface structures

It was previously shown that NAb binding at 4°C was decreased when assayed after a temperature shift to 37°C (see Chapter 3). In order to determine the fate of the cell surface molecules and the bound NAb, the cells were biotinylated and the molecules in the supernatant obtained from NAb-coated cells raised to 37°C, were fractionated on SDS-PAGE. 10T½, I3T2.1 and PKC-4 all released a variety of their surface molecules ranging in molecular mass from at least 220 to 20 KDa when separated under reducing conditions regardless of cell pre-treatment with either PBS, culture medium, or purified NAb (Fig 4.4. 10T½ and PKC-4 data not shown). Both PBS and NAb resulted in shedding of cell surface molecules with a similar molecular profile, but purified NAb always induced a more intensive release than PBS containing 0.5% BSA and culture medium containing 1% FBS (Fig 4.4) (Data for culture medium were not shown). Moreover, the molecular pattern of the supernatant was much different from that of untreated membrane lysate. Some molecules in the supernatant can be recognized from their native membrane counterparts based on their migration in SDS gels, while certain proteins seemed to be unique in NAb and PBS supernatant, such as the 70- and 50-KDa bands (Fig 4.4). Not all membrane proteins were released into the supernatant upon NAb

Fig 4.3. Immunoblotting of the PKC-4 membrane proteins with purified IgM or IgG NAb. PKC-4 membrane fractions (all lanes) were resolved on 8% gels and detected with either purified IgM at a final concentration of 40 μ g/ml (lanes 1 and 2) or IgG at a final concentration of 220 μ g/ml (lanes 3 and 4). The subsequent incubation was performed with AP-conjugated goat anti-mouse IgG for IgG NAb (lanes 3 and 4) and rabbit anti-mouse μ chain for IgM NAb (lanes 1 and 2). Each lane contained an equal amount of proteins. The result was repeated once with similar observations.

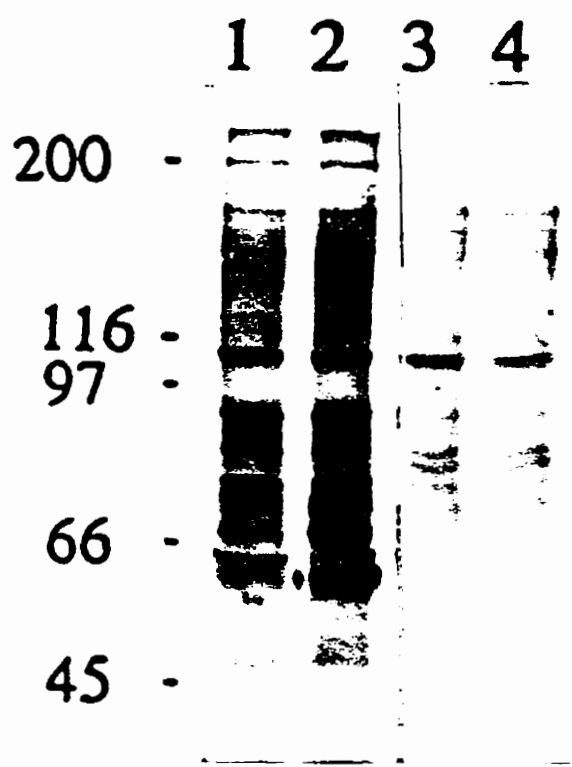
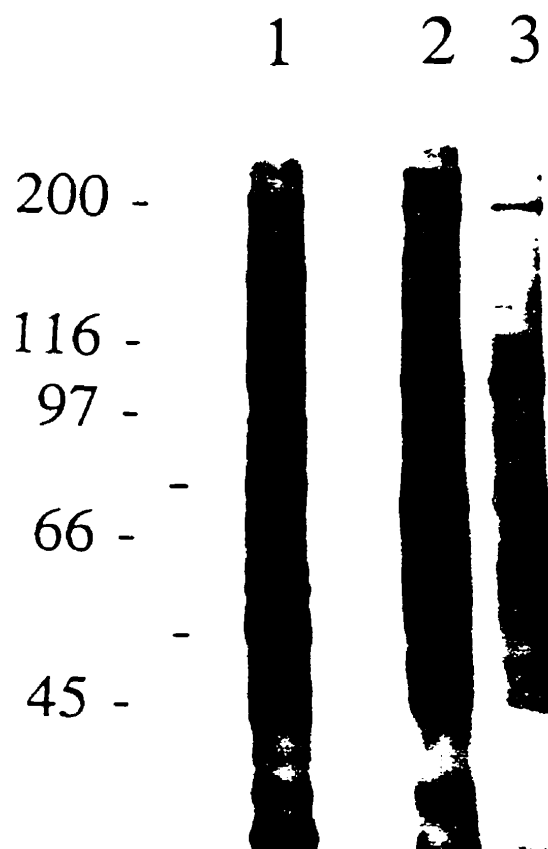


Fig 4.4. Shedding of cell surface structures. I3T2.1 cells were surface labeled with NHS-biotin and incubated with purified NAb (lane 2) or 0.5% BSA in PBS (lane 3) at 4°C, followed by a rise in temperature to 37°C. The supernatant (lanes 2 and 3) and the membrane fraction from untreated cells (lane 1) were resolved on 8% gels and transferred onto the nitrocellulose membrane. The blot was probed with HRP-conjugated avidin and developed with the ECL system. Molecular mass markers are indicated on the left. This result confirmed previous experiments with C3H whole serum NAb.



incubation and a rise in temperature, because native membrane lysate contained more biotinylated protein bands than NAb supernatant (Fig 4.4, lane 1 vs lane 2).

NAb immunoblotting of molecules in cell supernatant

Purified NAb detected at least 20 protein bands in supernatant produced from cells incubated with PBS or serum NAb followed by raising the temperature from 4°C to 37°C (Fig 4.5). In both I3T2.1 and PKC-4 cells, the 110 and 90 KDa protein bands detected by NAb were the predominant molecules under both reducing and non-reducing conditions (Fig 4.5 and Fig 4.1). Mouse Ig heavy chains were also detected in the supernatant of NAb-coated cells under reducing conditions (Fig 4.1 and Fig 4.5), indicating that both NAb and the cell surface antigens came off the cell surface during the temperature shift procedure. Furthermore, although PBS, culture medium and NAb all induced a similar immunoblot profile, NAb was uniformly the strongest inducer throughout the studies.

Anti-mouse Ig precipitation of molecules from supernatant of NAb-coated cells raised to 37°C

The supernatant, prepared from cells incubated with culture medium, NAb-depleted C3H serum or whole serum NAb followed by a rise in temperature from 4°C to 37°C, were precipitated with goat anti-mouse IgG and IgM antibody-coupled agarose. A 90-KDa molecule (p90) was precipitated reproducibly from the supernatant of NAb-coated cells and detected by purified NAb through immunoblotting analysis (Fig 4.6). However, precipitation from supernatant of cells treated with NAb-depleted C3H serum or culture medium did not yield a 90-KDa molecule. Plain Sepharose itself was also unable to

Fig 4.5. Immunoblotting of released cell surface molecules with purified NAb. Cell supernatant was prepared by a temperature shift procedure from PKC-4 (lanes 1 and 2) and I3T2.1 (lanes 3 and 4) cells preincubated with 1% FBS in PBS (lane 1), 1:1 diluted C3H serum (lane 2), natural IgG + IgM antibodies purified through 3M-EmphazeTM plastic bead-supported protein A and anti-mouse IgM columns (lanes 3 and 4). An equal volume of the supernatant was resolved on 8% gels under reducing (lanes 1, 2 and 3) and non-reducing (lane 4) conditions. Lanes 1 and 2 versus lanes 3 and 4 were from two different gels. Molecular mass markers are indicated on the left. NAb H chains in lane 2 were around 80 (μ chain) and 50 (γ chain) KDa. The small amount of immunoglobulin subunits detected in lane 3 was due to the smaller amount of purified NAb (final concentration of 0.33 mg/ml for both natural IgG and IgM antibodies) used in the cell incubation. This experiment represented one of three independent experiments with similar results.

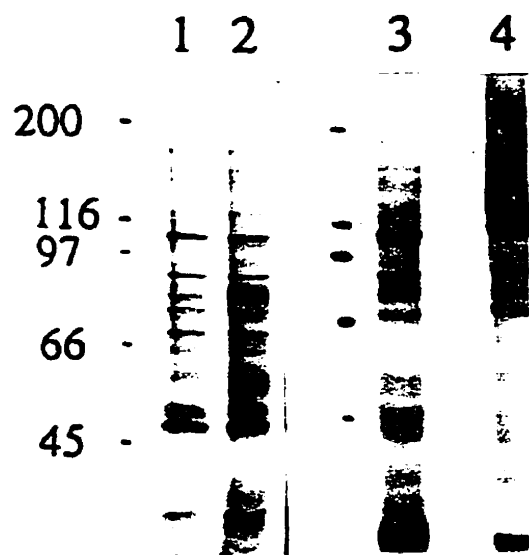


Fig 4.6. Immunoprecipitation and immunoblotting of a 90-KDa molecule with purified NAb. Supernatant was prepared by the temperature shift procedure from I3T2.1 cells preincubated at 4°C with 1% FBS in F12 medium (lane 1), 1:1 diluted C3H serum (lane 2) and 1:1 diluted C3H serum depleted of IgG and IgM NAb by preadsorption of the serum with an excess of protein A- and anti-mouse IgM antibody-coupled Sepharose (lane 3). An equal volume of the supernatant obtained at 37°C was precipitated with goat anti-mouse IgG and IgM antibody-coupled Sepharose. The precipitates were resolved on 8% gels and the isolated molecules were detected by NAb immunoblotting. From the top to the bottom, the arrows on the right indicate the 90-KDa molecule, NAb μ chains (80 KDa) and probably cross reactive goat IgG γ chains (50 KDa), respectively. Molecular mass markers are indicated on the left. This result was repeated three times with I3T2.1 cells and three times with PKC-4 cells with similar observations.



precipitate this molecule (Data not shown). The precipitation of p90 was reproducible from supernatant of cells coated with IgG plus IgM NAb purified through 3M Emphaze™ plastic beads-supported protein A and anti-mouse IgM chromatography (data not shown).

Analysis of RPTP α expression and NAb immunoblotting

CD45 has been found to be recognized by NAb assayed by ELISA and a cell surface blocking analysis by flow cytometry (Zhang and Chow, unpublished data). Since RPTP α , a CD45-like transmembrane PTP, was involved in NAb-initiated signaling in 10T $\frac{1}{2}$ fibroblasts (Chapter 3), this study investigated the relative expression of RPTP α related to NAb binding and whether NAb could bind RPTP α by immunoblotting analysis.

RPTP α was examined by immunoblotting, and quantified by densitometry analysis. RPTP α was expressed as a 130-KDa molecule mainly in the membrane fractions in 10T $\frac{1}{2}$ variants (Fig 4.7). The level of its surface expression in confluent 10T $\frac{1}{2}$ cells was increased, while slightly but not significantly decreased in confluent I3T2.1 and PKC-4 compared with their subconfluent counterparts (Table 4.1). The cytosolic production of RPTP α in 10T $\frac{1}{2}$ cells was also increased after the cells reached confluence, but was reduced in confluent I3T2.1 cells. Compared with 10T $\frac{1}{2}$, membrane RPTP α expression in PKC-4 cells was dramatically downregulated by more than 50% independent of growth states (Fig 4.7 and Table 4.1). Immunoprecipitation of RPTP α from confluent cells showed a significantly lower level of production in I3T2.1 and PKC-4 than in 10T $\frac{1}{2}$ (Fig 4.8 and Table 4.2).

To show a direct interaction of NAb with RPTP α in immunoblotting, RPTP α was

Fig 4.7. RPTP α expression in 10T $\frac{1}{2}$ variants. Membrane (m) and cytosolic (c) fractions of subconfluent (lane 1) and confluent (lane 2) 10T $\frac{1}{2}$ variants were resolved on 10% gels. The blot was detected with a rabbit anti-RPTP α anti-serum. A indicates the position of RPTP α as a 130-KDa molecule. B shows the immature RPTP α at 110 KDa which lacks the N-linked carbohydrates whereas C represents the precursor of RPTP α at ~90 KDa (Daum et al., 1994; Tracy et al., 1995). The origin of the lower molecular weight bands below C was presumed to be non-specific. The densities of RPTP α were summarized in Table 4.1.

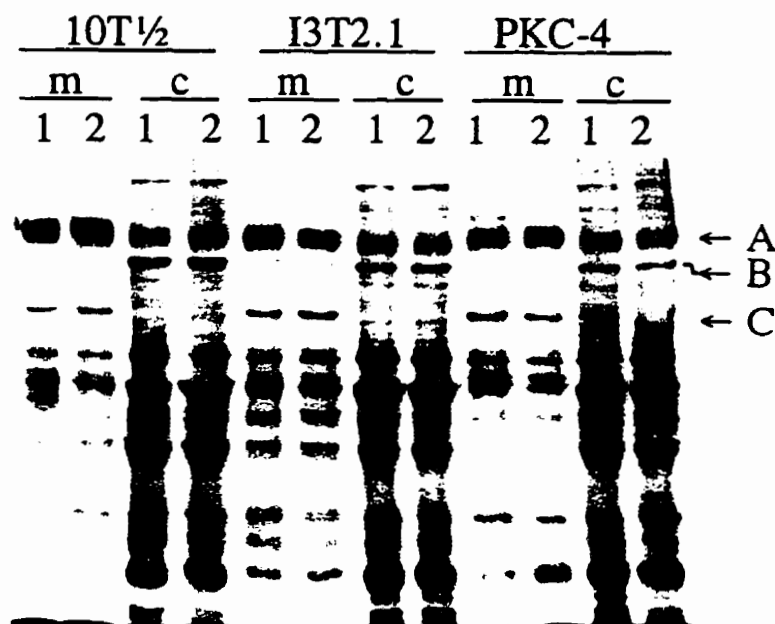


Table 4.1. RPTP α expression in cellular compartments of subconfluent and confluent cells

Expt# ^a	Cells	Membrane fractions		Cytosolic fractions	
		Subconfluence	Confluence	Subconfluence	Confluence
1 (5)	10T $\frac{1}{2}$	1.0	1.42 \pm 0.14 ^b	1.0	1.83 \pm 0.28 ^c
	13T2.1	1.09 \pm 0.04	0.97 \pm 0.15 ^d	1.20 \pm 0.08	1.01 \pm 0.15 ^{e,f}
2 (4)	10T $\frac{1}{2}$	1.0	1.38 \pm 0.18 ^b	1.0	2.04 \pm 0.20 ^c
	PKC-4	0.47 \pm 0.06 ^b	0.38 \pm 0.08 ^d	1.05 \pm 0.27	1.03 \pm 0.27

^a RPTP α expression was detected by immunoblotting and analysed by densitometry. The number of assays is in parenthesis. The levels of RPTP α detected are reported in arbitrary units (mean \pm SE), with 10T $\frac{1}{2}$ membrane and cytosol expression of RPTP α each designated as 1.0. The paired Student *t* test was performed on the original densities without conversion.

^b $P_{td} < 0.05$ compared with subconfluent 10T $\frac{1}{2}$ membrane expression.

^c $P_{td} < 0.05$ compared with subconfluent 10T $\frac{1}{2}$ cytosolic expression.

^d $P_{td} < 0.05$ compared with confluent 10T $\frac{1}{2}$ membrane expression.

^e $P_{td} < 0.05$ compared with confluent 10T $\frac{1}{2}$ cytosolic expression.

^f $P_{td} < 0.05$ compared with subconfluent 13T2.1 cytosolic expression.

Fig 4.8. Immunoprecipitation of RPTP α from 10T $\frac{1}{2}$ variants. Confluent 10T $\frac{1}{2}$ (lane 2), I3T2.1 (lane 3) and PKC-4 (lane 4) cells were extracted with lysis buffer containing 1% Triton X-100. The whole cell lysate was immunoprecipitated with the anti-RPTP α anti-serum. The immunoprecipitates versus 10T $\frac{1}{2}$ membrane proteins (lane 1) were resolved on 8% gels and the isolated proteins were detected with the same anti-RPTP α antibody. The upper arrow indicates RPTP α and the lower arrow indicates the rabbit immunoglobulin H chains. The densities of RPTP α were summarized in Table 4.2.



Table 4.2. RPTP α immunoprecipitation from confluent cells

Expt# ^a	Mean ratio of RPTP α expression \pm SE		
	10T $\frac{1}{2}$	I3T2.1	PKC-4
1 (2)	1.0	0.58 \pm 0.01	0.44 \pm 0.03
2 (1)	1.0	0.44	0.18
3 (3)	1.0	0.54 \pm 0.05 ^b	0.35 \pm 0.09 ^b

^a The number of assays is in parenthesis. The level of RPTP α expression was shown in arbitrary units relative to 10T $\frac{1}{2}$ as 1.0. In Expt 1, RPTP α was precipitated from 825 or 1825 μ g of whole cell lysate. In Expt 2, RPTP α was precipitated from cell membrane fractions from 5×10^6 cells per cell line. Expt 3 was a summary of Expt 1 and Expt 2. The statistical analysis was performed on original densities of RPTP α without conversion.

^b $P_{td} < 0.05$ compared with 10T $\frac{1}{2}$ cells.

purified from 10T½ membrane fractions through the standard immunoprecipitation procedure and resolved by SDS-PAGE under reducing conditions. After transfer to nitrocellulose membrane, the purified RPTP α could not be detected by purified NAb even though NAb clearly reacted with other membrane molecules loaded beside the RPTP α (data not shown). This observation was reproducible in three independent experiments.

Analysis of CD44 expression and NAb immunoblotting

In order to identify the NAb reactive 90-KDa membrane molecule, cell surface molecules with similar molecular weight were considered for investigation. CD44 is just one with a molecular mass around 85-90 KDa. Due to its well defined molecular characteristics and its importance in cell-cell, cell-matrix adhesion and tumor metastasis (reviewed in Sy et al., 1996), the possibility that NAb may bind CD44 and influence CD44-mediated tumor progression in vivo was examined.

CD44 in the L5178Y-F9 lymphoma system

CD44 expression

The high NAb binding subpopulation, LYNAb⁺, selected from TPA-treated L5178Y-F9 through FACS, had a slightly higher level of CD44 expression than the parental L5178Y-F9 line when assayed repeatedly by flow cytometry using anti-CD44 MAbs (Table 4.3, Expts 2 and 4). Immunoprecipitation of biotinylated cell surface molecules with anti-CD44 monoclonal antibodies showed that L5178Y-F9 cells expressed a heterogenous molecule around 97 KDa, while LYNAb⁺ cells produced a more heterogenous array around 85-97 KDa (Fig 4.9). The lower molecular weight bands

Table 4.3. CD44 expression in L5178Y-F9 variants

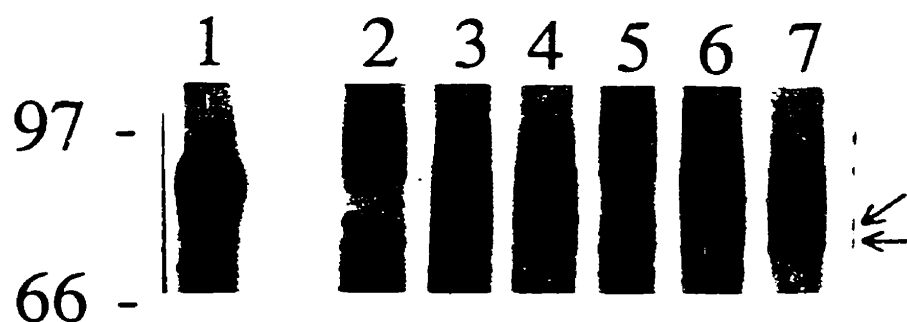
Expt# ^a	Antibody	Mean binding (MCF) \pm SE		
		L5178Y-F9	LYNAb ⁺	X2SC
1 (2)	NAb	57.5 \pm 13.7	66.4 \pm 16.9	45.9 \pm 6.6
2 (3)	IM7	85.1 \pm 9.9	94.0 \pm 7.1	44.5 \pm 1.7 ^b
3 (3)	KM114	67.3 \pm 2.3	63.5 \pm 3.2	33.9 \pm 1.0 ^b
4 (11)	KM114	53.3 \pm 4.6	60.2 \pm 4.4 ^c	-

^a CD44 expression levels were analysed by flow cytometry. The number of assays is in parenthesis.

^b $P_{td} < 0.02$ compared with LYNAb⁺.

^c $P_{td} < 0.05$ compared with L5178Y-F9.

Fig 4.9. Immunoprecipitation of CD44 from I3T2.1 and L5178Y-F9 variants. The I3T2.1 (lane 1), L5178Y-F9 (lanes 2 and 5), LYNA^b (lanes 3 and 6) and X2SC (lanes 4 and 7) were surface biotinylated. The whole cell lysate was precipitated with KM114 (lane 1 to lane 4) and IM7 (lane 5 to lane 7). The precipitates were resolved on 8% gels. After transfer onto the nitrocellulose membrane, the blot was probed with HRP-conjugated avidin and developed with the ECL system. Molecular mass markers are indicated on the left. The arrows indicate non-specific precipitation. This experiment was repeated once for all three L5178Y-F9 cell lines with similar results.



below CD44 (Fig 4.9) were non-specifically precipitated molecules since they also appeared with the anti-rat IgG-Sepharose in the absence of IM7 and KM114 MAbs. Moreover, it seemed that immunoprecipitation revealed a more profound increase in CD44 expression in LYNAb⁺ cells at protein levels (comparing Fig 4.9 and Table 4.3).

CD44 expression and NAb binding of tumors grown in vivo

LYNAb⁺ cells were selected twice through growth in vivo and the final tumor (designated X2SC) was recovered in vitro (Zhang and Chow, 1997). As previously reported (Zhang and Chow, 1997), NAb binding to these tumor cells was decreased compared with the starting line (Table 4.3, Expt 1). Interestingly, CD44 expression in these tumors was reduced to approximately 50% of that in the starting line LYNAb⁺ assayed by flow cytometry using anti-CD44 MAbs (Table 4.3, Expts 2 and 3). Immunoprecipitation with both anti-CD44 MAbs also revealed a significant reduction in the 85-97 KDa CD44 proteins in the X2SC compared with the LYNAb⁺ (Fig 4.9).

Binding of anti-CD44 MAb and NAb to neuraminidase treated cells

As previously demonstrated (Zhang and Chow, 1997), the NAb binding capacity of neuraminidase-treated L5178Y-F9 cells was always significantly increased compared with untreated controls. The level of KM114 binding in L5178Y-F9 cells was increased more than 2-fold following neuraminidase treatment, while IM7 binding was only slightly increased (Table 4.4). LYNAb⁺ cells treated with neuraminidase in one single experiment also showed a marked increase in the binding of KM114 monoclonal antibodies (Table 4.4).

Table 4.4. Anti-CD44 MAb binding in L5178Y-F9 and LYNAb⁺ cells treated with neuraminidase

Expt# ^a	Cells	MAb	Mean binding (MCF) \pm SE		% increase
			Control	Neuraminidase	
1 (2)	L5178Y-F9	IM7	187.8 \pm 12.4	214.7 \pm 0.4	14.3
2 (3)	L5178Y-F9	KM114	27.7 \pm 3.6	89.8 \pm 2.5 ^b	224.2
3 (1)	LYNAb ⁺	KM114	37.8	77.0	103.7

^a The number of assays is in parenthesis.

^b $P_{td} < 0.01$ compared with controls.

CD44 in the fibroblast system

CD44 expression in 10T½ and variants

Immunoprecipitation of biotinylated cell membrane fractions with IM7 and KM114 MAbs showed that all 10T½ variants expressed a heterogenous CD44 at 85-90 KDa (Fig 4.9, lane 1 and Fig 4.10). Compared with the parental 10T½, I3T2.1 and PKC-4 cells expressed more CD44 (Fig 4.10). Flow cytometry analysis also revealed an increased surface expression of CD44 for both I3T2.1 and PKC-4 cells compared with the 10T½ (Table 4.5).

CD44 expression and NAb binding in ras-transformed cells after myc oncogene introduction

A myc oncogene was introduced into I3T2.1 cells through a retroviral infection procedure. Cells infected with myc-bearing VM virus, but not the control SVX, exhibited an overproduction of the gag-myc fusion oncoprotein at 110 KDa assayed by immunoblotting, and a consistent reduction in NAb binding (Chow and Tough, unpublished data). Flow cytometry analysis using IM7 MAbs showed that CD44 expression in the myc-bearing I3T2.1 was also significantly decreased compared with the control SVX-infected cells and the parental I3T2.1 (Table 4.6).

Binding of CD44 MAb and NAb to Neuraminidase treated cells

As demonstrated by Tough et al (1995), neuraminidase treatment reproducibly increased NAb binding levels by at least 30% in I3T2.1 cells compared with untreated controls (data not shown). In contrast, the binding of two anti-CD44 MAbs, KM114 and IM7, especially KM114, to I3T2.1 cells was significantly reduced upon neuraminidase

Fig 4.10. Immunoprecipitation of CD44 from 10T $\frac{1}{2}$ variants. 10T $\frac{1}{2}$ (lanes 1 and 2), I3T2.1 (lanes 3 and 4) and PKC-4 (lanes 5 and 6) were biotinylated. The membrane fractions were extracted and precipitated with IM7 (lanes 1, 3 and 5) or 14.8 isoform control MAb (lanes 2, 4 and 6). The precipitates were resolved on 8% gels. After transfer onto the nitrocellulose membrane, the blot was probed with HRP-conjugated avidin and developed with the ECL system. Molecular mass markers are indicated on the left. CD44 immunoprecipitation in I3T2.1 was repeated three times with similar results.

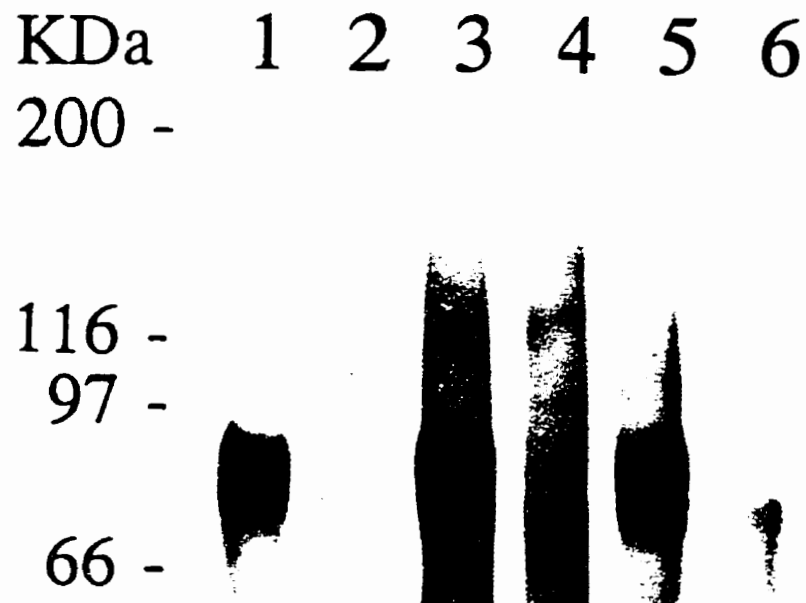


Table 4.5. CD44 expression in 10T½ variants

Cells ^a	Mean MAb binding (MCF) ± SE	% increase	P _{td}
10T½	96.0 ± 4.2		
I3T2.1	133.7 ± 11.1	39.3	<0.05
PKC-4	138.4 ± 9.8	44.2	<0.05

^a The levels of CD44 expression were determined by flow cytometry with IM7 monoclonal antibody. The result represents three independent tests (mean ± SE). An isotype control MAb 14.8 did not show any binding to these cells (data not shown).

Table 4.6. CD44 expression on parental and the v-myc/neo^r-infected I3T2.1 cells

Cells ^a	Mean IM7 MAb binding (MCF) \pm SE	P _{td}
10T $\frac{1}{2}$	51.9 \pm 4.1	
I3T2.1	64.2 \pm 6.2	<0.05 ^b
I3T2.1+v-myc/neo ^r -1	45.0 \pm 3.2	<0.01 ^c
I3T2.1+v-myc/neo ^r -2	49.6 \pm 3.9	<0.01 ^d
I3T2.1+neo ^r -1	66.5 \pm 4.1	NS
I3T2.1+neo ^r -2	65.0 \pm 5.8	NS

^a Infection of I3T2.1 cells with v-myc or SVX yielded two populations for each, designated as I3T2.1+v-myc/neo^r-1 and -2 and I3T2.1+neo^r-1 and -2, respectively, where 2 represents a higher MOI than 1. The expression levels of CD44 were detected with anti-CD44 MAb IM7. The results came from three independent experiments.

^b Compared with 10T $\frac{1}{2}$.

^c Compared with I3T2.1+neo^r-1 cells. P_{td}<0.05 compared with I3T2.1.

^d Compared with I3T2.1+neo^r-2 cells.

NS, not significant

treatment (Table 4.7).

CD44 expression and NAb binding of tumors grown in vivo

Injection of 1×10^4 I3T2.1 cells subcutaneously into 5 syngeneic C3H mice yielded two tumors in 2 out of 5 mice at 35 days after tumor inocula. Tumor cells were recovered in vitro and cultured with G418 for 9 days. Thereafter, cells were maintained in conventional medium until testing. Similar to previous observations (Tough et al., 1995), these two I3T2.1 variants exhibited small and transient reductions in NAb binding. CD44 expression assayed by flow cytometry was only very slightly lower than the G418-cultured control cells when assayed 2 days after the 9-day culture with G418 (Table 4.8). However, when tested 4 days after the 9-day culture with G418, both NAb and anti-CD44 MAb binding to these two tumors were increased compared with the parental line (Table 4.8).

Immunoblotting analysis of CD44 with NAb

CD44 was immunoprecipitated from I3T2.1 and LYNAb⁺ membrane fractions with a standard protocol and assessed by immunoblotting with purified NAb. In both cell systems, purified NAb did not show any reactivity with purified CD44 under reducing conditions even though on the same blot the biotinylated CD44 from I3T2.1 showed up at 85-90 KDa and NAb stained other membrane molecules positively (data not shown). This observation was reproducible in two other repeats for the I3T2.1 and one repeat for the LYNAb⁺.

Analysis of gelatinase expression

To identify the NAb reactive p90 described above, type IV collagenases with

Table 4.7. Anti-CD44 MAb binding to I3T2.1 cells treated with neuraminidase

Expt# ^a	MAb	Mean MAb binding (MCF) \pm SE		% decrease
		Control	Neuraminidase	
1 (3)	IM7	124.6 \pm 5.4	102.8 \pm 2.6 ^b	17.5
2 (4)	KM114	78.3 \pm 4.0	52.0 \pm 1.6 ^b	33.6

^a The number of assays is in parenthesis.

^b $P_{td} < 0.05$ compared with controls.

Table 4.8. NAb and anti-CD44 MAb binding to I3T2.1 and in vivo selected variants

Expt# ^a	Cells	Mean Ab binding (MCF)	
		NAb	IM7
1	I3T2.1	68.0	82.3
	I3T2.1-G418	62.0	86.8
	I3T-1	52.9	84.3
	I3T-2	57.1	82.9
2	I3T2.1	57.9	83.8
	I3T2.1-G418	52.8	81.3
	I3T-1	77.8	91.2
	I3T-2	70.1	93.7

^a Tumors recovered from I3T2.1 injection sites, designated as I3T-1 and -2, were maintained in vitro with G418 for 9 days and out of G418 thereafter. G418 was also added to some I3T2.1 cells for 9 days as a control, which was designated as I3T2.1-G418. Expt 1 and 2 were performed on days 2 and 4 respectively after 9 days culture with G418.

molecular weights of 92 KDa (gelatinase B) and 72 KDa (gelatinase A) were also examined. Both enzymes are secreted by a variety of cell types as pro-enzymes and activated extracellularly, but they also physiologically associate with cell surface structures and play a role in cell remodelling, migration and tumor metastasis (Mazzieri et al., 1997; Patridge et al., 1997).

Gelatin zymography has been shown to be a specific assay for analyzing the enzyme activity of gelatinase A and B (reviewed in Parsons et al., 1997). During the electrophoresis and subsequent experimental procedure, all forms of the gelatinases including the inactive pro-enzymes are activated (Cao et al., 1995). All 10T½ variants showed gelatinase activities in their membrane extracts predominantly at 72 and 62 KDa, which represent the mouse pro-gelatinase A and gelatinase A, respectively (Fig 4.11). Compared with 10T½ and I3T2.1, PKC-4 cells exhibited a significantly higher level of gelatinase activities at 110 and 92 KDa, which represent the mouse pro-gelatinase B and gelatinase B, respectively (Fig 4.11). A reduction of gelatinase A activities in I3T2.1 cells was also found comparing with 10T½ (Fig 4.11 B). Gelatin-agarose completely removed the gelatinase activities from the membrane fractions of PKC-4 assayed by zymography (Fig 4.12), but the reactivity of the 110 and 90 KDa antigens with NAb was not reduced at all when assessed with the gelatinase-depleted membrane fractions by immunoblotting (Fig 4.13). However, several molecules eluted from gelatin-agarose precipitates, but not from plain Sepharose, were able to be detected by NAb in immunoblotting (Fig 4.13).

Fig 4.11. Gelatin zymography of membrane fractions from 10T $\frac{1}{2}$ variants. (A) Equal amounts of proteins in crude membrane fractions from 10T $\frac{1}{2}$ (lane 1) and PKC-4 (lane 2) cells were resolved on 8% gels in the presence of 1 mg/ml gelatin under non-reducing conditions. The zymography was allowed to proceed for 20 h at 37°C. (B) 10T $\frac{1}{2}$ (lane 1), I3T2.1 (lane 2) and PKC-4 (lane 3) cells were assessed the same way as in (A). The zymography was allowed to proceed for 36 h at 37°C. The arrows indicate mouse pro-gelatinase B (110 KDa), gelatinase B (92 KDa), pro-gelatinase A (72 KDa) and gelatinase A (62 KDa). Molecular mass markers are indicated on the left. This experiment was repeated twice for all three lines with similar observations.

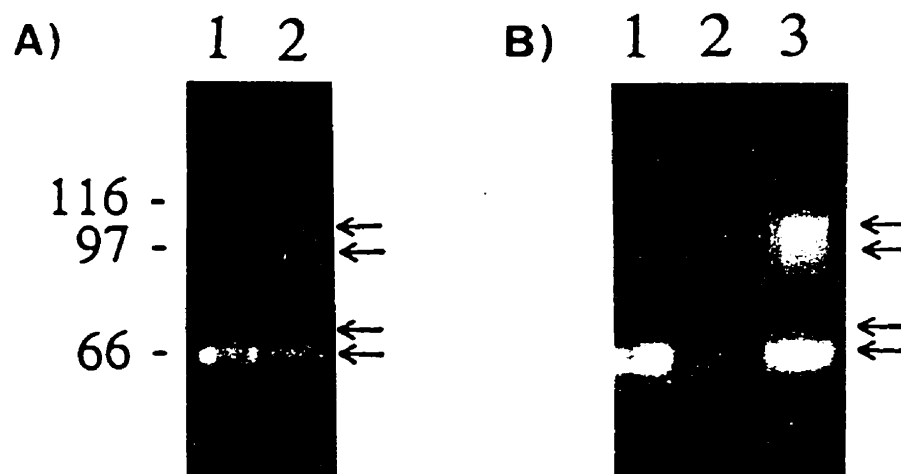


Fig 4.12. Gelatin zymography of membrane fractions from PKC-4. PKC-4 membrane fractions were absorbed by plain Sepharose and gelatin-agarose, respectively. The supernatant from plain Sepharose (lane 2), gelatin-agarose (lane 3), eluted material from plain Sepharose (lane 4) and gelatin-agarose (lane 5) versus non-treated membrane proteins (lane 1) were resolved on 8% gels under non-reducing conditions and the gelatin zymography was allowed to proceed for 20 h at 37°C. Molecular mass markers are indicated on the left. The arrows indicate mouse pro-gelatinase B (110 KDa), gelatinase B (92 KDa), pro-gelatinase A (72 KDa) and gelatinase A (62 KDa), respectively.

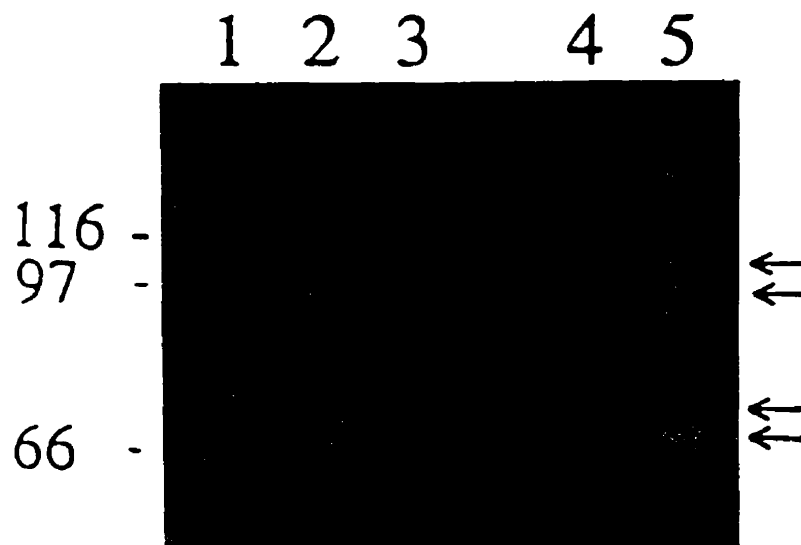
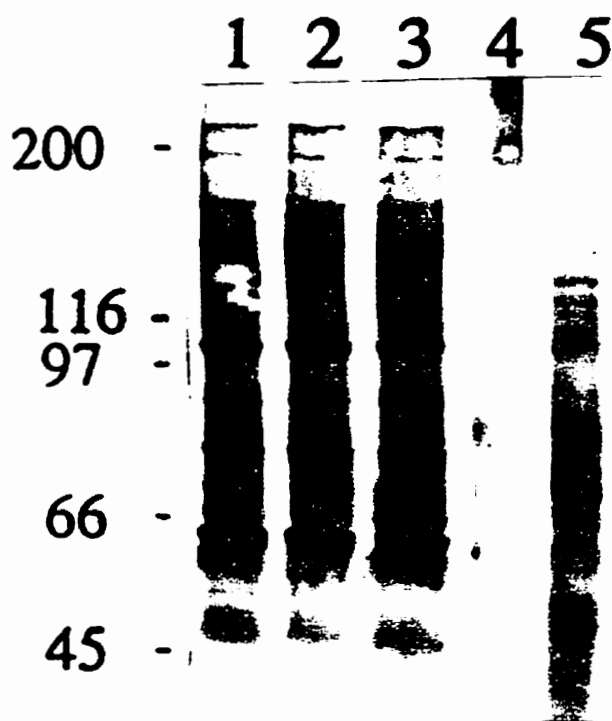


Fig 4.13. Immunoblotting of the 90-KDa molecule with purified NAb. PKC-4 membrane fractions were absorbed with plain Sepharose or gelatin-agarose. The supernatant from plain Sepharose (lane 2), gelatin-agarose (lane 3) versus non-absorbed membrane proteins (lane 1), and eluted materials from plain Sepharose (lane 4) and gelatin-agarose (lane 5) were resolved on 8% gels under non-reducing conditions. The proteins were transferred onto nitrocellulose membrane and detected with purified NAb. Molecular mass markers are indicated on the left. This experiment was repeated once with similar observations.



DISCUSSION

This study was initiated to characterize NAb reactive cell surface antigens expressed on 10T½ fibroblasts by using the Western blot technique. A renaturing condition using a bicarbonate buffer was employed for the protein transfer. This has been proven to be able to enhance autoantibody recognition of self membrane antigens (Auer et al., 1995). Immunoblotting of crude plasma membrane proteins from all three 10T½ cell lines with purified or cell surface-eluted NAb demonstrated varying reactivity of NAb to a set of at least 20 proteins with molecular weights extending from 220 to 20 KDa. Purification of the biotinylated cell surface molecules basically removed contamination by cytoskeleton components assayed by the detection of actin. In immunoblotting with these purified membrane proteins which were free of actin, purified NAb detected a different molecular profile in 10T½ variants in that the 200, 170, 160, 110, 90, 80, 70 and 66 KDa protein bands detected in I3T2.1 and PKC-4 cells were more intensely stained by NAb than those of parental 10T½. This indicates that these cell surface molecules may be preferentially upregulated by the overexpressing ras and PKC-β1, consistent with the high NAb binding phenotypes of the I3T2.1 and PKC-4. Compared with the immunoblotting using crude membrane extracts, the intensities of some protein bands at 160-170, 150 and 45-50 KDa for 10T½ and at 45-50 KDa for I3T2.1 and PKC-4 were reduced to background levels. This suggests that these bands may come from cytoskeletal or intracellular membrane parts, or both. It remains unclear why the 160-170 and the 150 KDa molecules were preferentially extracted from the 10T½ and to a lesser degree from PKC-4 while not from the I3T2.1. One possibility is that the overexpressing ras and

PKC- β 1 may alter the normal association of certain membrane surface molecules with cytoskeletal components. This is supported by the observation that I3T2.1 developed a fully transformed morphology, which exhibited a round, shuttle-like shape compared with parental 10T $\frac{1}{2}$ which was flat and had more dendrites, whereas the PKC-4 only exhibited a partially transformed morphology (also see Krauss et al., 1989). Moreover, purified IgM NAb seemed to be more efficient for immunoblotting than natural IgG, but both immunoglobulin fractions detected a similar molecular profile in the crude membrane preparations. This is consistent with a previous report that all protein bands detected by natural IgM also can be detected by natural IgG (Lacroix-Desmazes et al., 1995).

It was previously found that pre-coated NAb at 4°C was markedly reduced when the temperature of the incubation was raised to 37°C (see Chapter 3). Analysis of the supernatant prepared from the cells pre-treated with PBS containing 0.5% BSA (BSA/PBS) or NAb followed by a rise in temperature to 37°C has demonstrated that in addition to the shedding of pre-bound NAb, a variety of cell surface molecules ranged from at least 220 to 20 KDa were released to the environment. NAb immunoblotting of these released membrane molecules also showed a set of at least 20 protein bands ranging from 220 to 20 KDa for both I3T2.1 and PKC-4 cells examined. This confirmed the immunoblotting experiments with purified biotinylated cell surface molecules. In addition, the shedding of membrane molecules and bound NAb is concordant with the observation that NAb binding with cell surface structures initiated PKC-dependent signaling (Chapter 3) which in turn resulted in an intensive release of these structures. Since PKC was responsible for the downregulation of pre-coated NAb (Chapter 3), the

small level of release of membrane molecules occurring in 0.5% BSA/PBS may be due to a low level of PKC activation, which was likely associated with the temperature shift-induced intracellular biological response (Chapter 3). It is presently not known whether internalization also occurred during this study, but some cell surface molecules such as T cell receptors (Minami et al., 1987), MHC class I antigen (Gur et al., 1997) and EGF receptors (Nelson et al., 1997) do utilize internalization for recycling. In addition, it remains uncertain whether proteolytic cleavage also happened for some cell surface molecules during their shedding.

The precipitation of a 90-KDa molecule from the supernatant of NAb-coated cells with an anti-mouse Ig antibody-coupled agarose further supported the idea that NAb directly binds some surface molecules on cells under physiological conditions. However, it was currently unclear about the origin of p90. It also remains to be excluded that p90 is an Fc receptor, contaminating cytoskeletal proteins, or fetal bovine serum proteins that may normally bind with the cultured cells. The failure to precipitate more targets from supernatant of NAb-coated cells may be due to the following possibilities: (1) NAb are low affinity antibodies. The binding strength between NAb and its targets in solution may be greatly reduced, compared to the binding on a relatively solid cell surface where a high avidity binding could be built up by cross-linking different cell surface structures and cross-linking NAb molecules through anti-Ig activities. If so, the 90-KDa molecule precipitated through NAb may represent a high affinity target for NAb. Moreover, it is also possible that washing steps during the precipitation may lose the antigens bound to NAb. (2) In addition to shedding of NAb complexes, PKC was also activated during this

process (Chapter 3). It is well known that PKC can phosphorylate membrane receptors and induce conformational changes in these molecules, which has been shown for the $\alpha6\beta1$ integrin to cause a loss of binding to its ligand laminin (Hogervorst et al., 1993). Therefore, the immune complexes formed by NAb and its cell surface structures may dissociate from each other as soon as they are released into the supernatant.

An attempt to determine the NAb reactivity with known cell surface molecules was initiated in this study. NAb has been found to bind with CD45, a lymphocyte surface antigen belonging to the PTP family (Zhang and Chow, unpublished data). This family of enzymes controls the levels of tyrosine phosphorylation required for cell growth and differentiation (Charboneau and Tonks, 1992). Similar to CD45, RPTP α is another member of this family with a more ubiquitous expression. In 10T $\frac{1}{2}$, confluent cells expressed more RPTP α both in the membrane and cytosolic fractions, which is consistent with other reports that receptor-like PTPs are associated with cell density-dependent inhibition of growth in that high density cells always have an increased production of RPTPs at both PTP activity and protein levels compared with their subconfluent counterparts (Pallen and Tong, 1991; Mansbridge et al., 1992; Rijksen et al., 1993; Ostman et al., 1994; Campan et al., 1996; Gaits et al., 1995). In contrast, RPTP α expression levels were slightly lower in confluent than subconfluent I3T2.1 and PKC-4 cells, probably due to the loss of contact inhibition in these two lines. Therefore, RPTP α appears to play a negative regulatory role for cell proliferation in 10T $\frac{1}{2}$ cells. Interestingly, it was observed for the first time that PKC- $\beta1$ overexpression in PKC-4 downregulated RPTP α membrane expression more than 50% independent of growth

states (Tables 4.1 and 4.2). The RPTP α expression levels in subconfluent versus confluent 10T $\frac{1}{2}$ cells were also inversely correlated with PKC- α expression levels (compare Table 4.1 with Table 2.3). Therefore, PKC activation likely downregulates the RPTP α expression levels in 10T $\frac{1}{2}$ cells.

The level of RPTP α expression in subconfluent versus confluent 10T $\frac{1}{2}$ cells was inversely correlated with the NAb binding capacities. It was also noted that in general NAb binding was higher ranking in PKC-4 > I3T2.1 > 10T $\frac{1}{2}$ (Chapter 2), but RPTP α expression levels were higher in 10T $\frac{1}{2}$ \geq I3T2.1 > PKC-4. Immunoblotting of the purified RPTP α with NAb did not show reactivity. Thus, it still remains unclear whether NAb could directly bind with RPTP α . Since NAb enhanced shedding of this molecule during a temperature shift procedure (Chapter 3), NAb may directly or indirectly influence the function of RPTP α in this study. In future, it would be worthwhile to test this issue through other approaches such as ELISA using purified RPTP α .

The observation of the 90-KDa molecule reacting with NAb in immunoblotting assays has led to a search for potential cell surface target antigens with a similar molecular weight. Two candidate molecules, CD44 and gelatinase B, were found to be around 90 KDa and expressed on fibroblasts.

CD44, a heavily glycosylated adhesion molecule ranging from 85 to 220 KDa, expresses as a large number of isoforms (reviewed in Sy et al., 1996). 10T $\frac{1}{2}$ and its variants expressed only the standard form, a heterogenous 85-90-KDa molecule possibly due to different glycosylation patterns. Immunoprecipitation revealed that the L5178Y-F9 T cell lymphoma expressed a high molecular weight CD44 around 97 KDa, while the

LYNAb⁺ variant selected for high NAb binding produced a more heterogenous form around 85-97 KDa. It remains unclear whether the 97 KDa CD44 was due to a more intensive glycosylation of the standard form or was a different isoform of the CD44 family. The former possibility appears to be supported by the fact that LYNAb⁺ differs from L5178Y-F9 in that LYNAb⁺ was generated through stimulation of the L5178Y-F9 by TPA and subsequent selection through FACS. It has been found that TPA treatment could alter glycosylation in cell surface receptors, such as the receptor for human urokinase-type plasminogen activator in U937 cells (Behrendt et al., 1990) and fibronectin receptors in K562 cells (Symington et al., 1989). When comparing the CD44 expression levels detected with flow cytometry with those assayed by immunoprecipitation, an inconsistency between these two experimental approaches was noted. The former showed a small increase in anti-CD44 MAb surface binding in the LYNAb⁺, while the later showed a large increase in CD44 proteins in the same line compared with L5178Y-F9. The reason for causing the discrepancy is currently not clear. One possibility is that different carbohydrate compositions of CD44 in these two lines may yield a different dissociation constant for binding of anti-CD44 MAbs. This may make the anti-CD44 MAb binding reach the plateau faster in L5178Y-F9 than in LYNAb⁺ and a 1-hour incubation with MAbs at a final concentration of 1 μ g/ml may be not sufficient to reflect the actual binding capacity of the cells.

When carefully analyzing the potential epitopes for NAb and the two monoclonal anti-CD44 antibodies in both 10T $\frac{1}{2}$ and L5178Y-F9 cell models, a difference between these two systems was found. Neuraminidase treatment uniformly increased NAb binding

in both systems, suggesting that NAb preferentially binds to asialo structures on the cell surface. In contrast, the binding of IM7 and KM114 to I3T2.1 decreased following neuraminidase treatment, but increased in L5178Y-F9 system. These data indicate that although cells of both models expressed the standard form of CD44, the glycosylation patterns of CD44 were likely very different for these two cell systems. This hypothesis was further supported by the observation that 10T $\frac{1}{2}$ variants could bind fluorescence-conjugated hyaluronan (F-HA), a natural ligand of CD44, while L5178Y-F9 variants did not (data not shown). Since the F-HA binding is often increased by removing carbohydrate moieties from CD44 molecules (reviewed in Sy et al., 1996), it is highly possible that the F-HA binding sites of CD44 in the L5178Y-F9 variants were blocked by carbohydrates.

It seemed to be a positive correlation between CD44 expression and NAb binding levels in the 10T $\frac{1}{2}$ fibroblast system. Consistent with the high NAb binding phenotype of I3T2.1 and PKC-4, the CD44 surface expression levels were significantly higher in I3T2.1 and PKC-4 than in parental 10T $\frac{1}{2}$. The upregulation of CD44 expression induced by ras- and PKC- β 1-overexpression likely resulted from a similar mechanism because both PKC and ras eventually signal the transcription factor activator protein (AP-1), which regulates the expression of the CD44 genes (Hofmann et al., 1993; Lamb et al., 1997). Interestingly, myc overexpression in I3T2.1 resulted in downregulation of both NAb binding and CD44 expression. NAb binding was also similarly decreased in myc-transfected 10T $\frac{1}{2}$ populations (Chow and Tough, unpublished data). Studies by others also showed a negative effect of the myc oncogene on expression of some membrane

molecules. For example, myc overexpression downregulated MHC class I antigens in human melanoma cells (Griffioen et al., 1995) and $\alpha3\beta1$ integrins in human osteosarcoma cells (Judware and Culp, 1997). The mechanism(s) for myc downregulation of these cell surface molecules are presently unknown. I3T2.1 tumors recovered from growth in vivo exhibited a transient slight reduction in NAb binding. The subsequent increase in NAb binding in these tumor cells was associated with an increase in CD44 surface expression. The correlation between NAb binding and CD44 expression in 10T $\frac{1}{2}$ fibroblasts indicates that CD44 may be an NAb target. However, a direct interaction of NAb and purified CD44 was not observed in NAb immunoblotting under reducing conditions.

There was also likely a positive correlation between NAb binding levels and CD44 expression in the L5178Y-F9 lymphoma model. The high NAb binding L5178Y-F9 variant LYNAb⁺ expressed more CD44 on the cell surface. The in vivo selected low NAb binding LYNAb⁺ variant X2SC expressed only 50% of CD44 of the LYNAb⁺. As in the 10T $\frac{1}{2}$ model, these data also strongly suggest that NAb may bind CD44 and this binding may selectively eliminate L5178Y-F9 tumors in vivo. Strikingly, a direct interaction between NAb and purified CD44 from LYNAb⁺ cells was also not detected in NAb immunoblotting under reducing conditions. One interpretation for this study is that the observed changes in NAb binding and CD44 expression in these two cell systems just are two coincident events. An alternative possibility is that NAb may bind CD44 but with a relatively low affinity, whereas immunoblotting was just not sensitive enough to detect such a low affinity binding. In fact, problems do exist in Western blotting. One

is that the extensive wash procedure required often removes antibodies which are not firmly bound. Thus, for the low affinity NAb, this may result in a false negative blotting. Another problem is that SDS and reducing agents may destroy the important conformational epitopes on the antigens, causing a loss of NAb recognition. In future, other approaches such as using ELISA with purified CD44 are certainly essential to clarify this issue.

Another 90-KDa candidate studied for NAb recognition was the mouse 92-KDa gelatinase B (also called type IV collagenase B or matrix metalloproteinase 9). Mouse gelatinase B is secreted by a variety of cell types including fibroblasts, macrophages, T lymphocytes and neoplastic cells as a 110 KDa latent form and can be activated proteolytically to yield a 90-92 KDa form (Masure et al., 1993; Yamagata et al., 1989; Goetzl et al., 1996). The major function of gelatinases is degradation of the extracellular matrix components including type IV, V and VII collagens, fibronectin and gelatin. Thus they play important roles in angiogenesis, wound healing, tumor progression and metastasis (reviewed in Parsons et al., 1997). In the present study, all 10T½ variants possessed this gelatinase activity in their membrane extracts assayed by zymography, supporting previous reports that gelatinase B is physiologically associated with the cell membrane surface (Mazzieri et al., 1997; Patridge et al., 1997). Interestingly, PKC-4 expressed a dramatically higher level of gelatinase B activity in membrane fractions than 10T½ and I3T2.1. This is assumed to have resulted from the very high production of PKC-β1 protein and enzyme activity in PKC-4, which either upregulated the membrane association of gelatinase B or increased the production of gelatinase B, or both. In

addition to the 92-KDa gelatinase B, all three cell lines also expressed low molecular weight gelatinases around 72 and 62 KDa in their membrane fractions, which represent the mouse pro-gelatinase A and gelatinase A, respectively (Kinoh et al., 1996). Compared with parental 10T½, I3T2.1 cells had a reduced level of gelatinase A activity. It is presently unknown whether the reduction of the membrane-associated 62 KDa gelatinase A in I3T2.1 cells is due to a downregulation of unknown cell surface structures for linkage of gelatinase A or a reduction in production of this enzyme. The later possibility is not likely because much evidence suggests a role for the ras oncogene in the upregulation of gelatinase activities. For example, Ha-ras overexpression in NIH 3T3 fibroblasts enhanced gelatinases A and B mRNA expression (Xuan et al., 1995) and increased gelatinase A mRNA levels in MCF10A human mammary epithelial cells (Giunciuglio et al., 1995). Introduction of the v-Ha-ras oncogene into a non-metastatic murine epithelial tumor line OV3121 upregulated gelatinolytic activity at 72 KDa and 92 KDa and conferred a metastatic phenotype upon the cells (Yanagihara et al., 1995).

Complete removal of gelatinases from membrane fractions of the PKC-4 by adsorption with gelatin-coupled agarose did not reduce NAb recognition of proteins around 110 and 90 KDa assayed by immunoblotting. This suggested that the NAb-detected 110 and 90 KDa sharp protein bands in immunoblotting were not gelatinase B. Interestingly, several molecules eluted from gelatin-agarose precipitates were indeed detected by NAb in immunoblotting. However, the question remains whether these proteins are real gelatinases or non-specific precipitates of unknown molecules. In future, it will be worthwhile to examine these proteins in the precipitates of gelatin-agarose by

using specific monoclonal anti-gelatinase antibodies.

In summary, this first study initiated with the immunoblotting method revealed that NAb recognized at least 20 cell surface molecules with different intensities ranging from 220 to 20 KDa. The successful precipitation of the 90 KDa molecule with anti-mouse Ig antibody-coupled agarose from the membrane molecule-enriched supernatant of NAb-coated cells raised to 37°C further suggested that this cell surface antigen is a real physiological target of NAb in 10T½ fibroblasts. Studies on CD44 and gelatinase B excluded these candidates from being the 90 KDa protein band detected by NAb in immunoblotting. Although we were not able to demonstrate direct NAb binding to CD44, a positive correlation between CD44 expression and NAb binding, particularly on the LYNAb⁺ selected for high NAb binding, suggests that NAb may bind CD44. These data not only presented fresh information for understanding the biological interactions of NAb with cell surface molecules but provided clues for future identification of the cell surface NAb targets.

CHAPTER 5

**REDUCED TUMORIGENICITY AND METASTASIS OF SYNGENEIC TUMOR
INOCULA IN XID-BEARING CBA/N AND B CELL NORMAL C3H and DBA/2
MICE TREATED WITH NATURAL ANTIBODIES**

ABSTRACT

Natural antibodies have been implicated in the defence against small syngeneic tumor foci in vivo. Previous investigations with the xid-bearing B cell deficient CBA/N and (CBA/J x CBA/N)F1 models showed a beneficial effect of passive i.v. NAb in the rejection of threshold s.c. syngeneic RI-28 lymphoma inocula. Now this observation has been confirmed in the CBA/N threshold s.c. tumor model treated with either purified syngeneic natural IgG or IgM antibody. Passive i.v. administration of syngeneic whole serum NAb in B cell normal C3H and DBA/2 mice also reduced the tumorigenicity of threshold s.c. syngeneic tumor inocula of v-Ha-ras-transformed 10T½ fibroblasts and LYNAb⁺ lymphomas, respectively, assessed as an increase in tumor latencies. Moreover, pretreatment of CBA/N mice with syngeneic serum NAb or ammonium sulfate-purified serum immunoglobulin fractions enhanced in vivo elimination of [¹³¹I]-dUrd-labeled RI-28 cells injected i.v.. Whole serum NAb i.v. in C3H mice also significantly reduced the colonization of I3T2.1 in the lungs assayed with an approach using two i.v. injections of tumor cells. These data suggest that passive NAb is beneficial for both B-cell deficient and B cell normal mice to resist against syngeneic tumors injected s.c. or i.v.. These observations provide more direct evidence supporting a role for NAb in the defence against tumors in vivo.

INTRODUCTION

Accumulated evidence has established a role for NAb in the defence against tumor development *in vivo*. This has been demonstrated basically by three major observations. First, there is a positive correlation between the serum NAb binding levels of the tumor *in vitro* and the sensitivity of the tumor to natural resistance mechanisms *in vivo*. A threshold s.c. syngeneic tumor inocula model, in which the dose of the tumor cells injected produced tumors at frequencies of less than 100% in recipient mice, has been shown to be a sensitive assay for evaluating the natural anti-tumor resistance mechanisms *in vivo* (Chow, 1995). High NAb binding lines selected from TPA treated L5178Y-F9 and SL2-5 lymphomas through fluorescence-activated cell sorting (FACS) for high NAb binding showed an increase in sensitivity to complement-dependent NAb lysis, increased NAb binding and a reduction in the tumor frequency of threshold s.c. inocula in syngeneic mice (Tough and Chow, 1988). Second, there is an inverse correlation between serum anti-tumor NAb levels and tumor resistance in mice (Chow et al., 1981; Ehrlich et al., 1984; Gil et al., 1990) and rats (Itaya et al., 1982). In X chromosome-linked immune-deficient (*xid*) CBA/N mice, B1 cells and serum IgM and IgG3 were deficient (reviewed in Scher, 1982). This immune deficiency has been linked to mutations of the gene for Bruton's tyrosine kinase (BTK), a critical signaling molecule for B cell differentiation (Khan et al., 1995). These mice exhibit a defect in antibody responses to both thymus-dependent and -independent antigens, but the mice generally have normal functions of T cells and macrophages (Scher, 1982). Prior studies found that the serum levels of tumor-reactive NAb in immune defective *xid* mice were very low or

undetectable (Martin and Martin, 1975). These mice produced significantly higher numbers of tumors than their normal counterparts upon challenge with threshold syngeneic tumor cells (Chow and Bennet, 1989; Bennet and Chow, 1991). Passive i.v. administration of NAb in xid-bearing mice reduced the frequency and prolonged the latency of a s.c. tumor challenge (Chow, 1995). Recently, passive human natural IgM was also shown to inhibit neuroblastoma growth in a rat model (David et al., 1996). Third, tumors with a high NAb binding capacity were eliminated or clonally inhibited *in vivo*. This is based on the studies in which the tumors retrieved from injection sites exhibited a significant decrease in NAb binding levels compared with their starting lines including the L5178Y-F9 and SL2-5 (Brown et al., 1986), the L5178Y-F9 TPA/NAb⁺3 (Zhang and Chow, 1997) and the oncogenic ras-transformed 10T $\frac{1}{2}$ fibroblast clone I3T2.1 (Tough et al., 1995). These tumors selected *in vivo* also showed reduced sensitivities to complement-mediated NAb lysis *in vitro* and increased tumorigenicities *in vivo* as demonstrated either by their reduced rate of clearance following i.p. injection (Chow, 1984a; Brown and Chow, 1985; Brown et al., 1986), or by their increased tumor frequency and reduced tumor latency following s.c. inoculation (Brown and Chow, 1985; Tough et al., 1995; Zhang and Chow, 1997). Moreover, the metastatic capability of these *in vivo* selected tumors was found to be increased *in vivo* (Reese and Chow, 1992). This selection *in vivo* for reduced sensitivity to natural resistance is thymus-independent since tumors from both normal and thymus-depleted, irradiated and bone marrow-reconstituted (ATxBM) mice exhibited similar decreases in sensitivities to NAb and to NK cells *in vitro* (Brown and Chow, 1985).

Passive transfer of various antibody preparations has been employed by many investigators to show therapeutic effects in the treatment of tumors growing s.c. or i.p. (reviewed in Dilmon, 1984). Passive administration of syngeneic whole serum NAb or purified natural IgG plus IgM antibodies in B cell-deficient xid mice has demonstrated a clear inverse relationship between NAb levels and tumorigenicity (Chow, 1995). However, the evidence for the anti-tumor effect of passive syngeneic NAb in normal mice is still lacking. In order to directly examine the beneficial effect of NAb in anti-tumor defence in normal mice, both metastasis and tumorigenicity of syngeneic tumor inocula in DBA/2 and C3H mice were investigated with the passive NAb transfer approach. In addition, to compare the potential differences of the anti-tumor activities between different immunoglobulin classes, passive purified natural IgG and IgM antibodies were each assessed for influence on the tumorigenicity of threshold syngeneic tumor inocula in xid-bearing CBA/N inbred mice.

MATERIALS AND METHODS

Mice

Inbred male DBA/2 and C3H mice were obtained from the University of Manitoba vivarium. The xid-bearing CBA/N mice, derived from the CBA/H inbred strain (Scher, 1982), and CBA/J mice were purchased from NIH (Bethesda, MD) and maintained in the University of Manitoba. Both the CBA/J and CBA/H inbred strains are derived from the original CBA/St line. The (CBA/J x CBA/N)F1 mice were derived by crossing-bred CBA/N females with CBA/J males as previously described (Chow, 1995). For each in

vivo experiment, mice were matched for age as indicated.

Natural antibodies

Whole serum NAb was obtained by bleeding males of DBA/2, C3H and CBA/J mice and female (CBA/J x CBA/N)F1 mice per axilla as described in Chapter 2. Unlike their male littermates, the female (CBA/J x CBA/N)F1 mice have normal levels of B cells and NAb. Five ml of CBA/J and 3 ml of (CBA/J x CBA/N)F1 serum NAb were pooled together and precipitated with 50% saturated ammonium sulfate as described in Chapter 3. The precipitates were redissolved in PBS (ppt NAb) and dialyzed against PBS at 4°C. Natural IgG and IgM antibodies were purified from ppt NAb by protein A-Sepharose and HR-S-300 gel filtration chromatography, respectively, as outlined in Chapter 3. Purified IgG fractions were passed through an anti-mouse IgM coupled Sepharose column to remove contaminating IgM. The effluent was concentrated and used as purified IgG. Both purified IgG and IgM were found to be free of contamination by each other assayed by immunoblotting with anti-mouse IgG (H+L) and anti-mouse μ chain antibodies (data not shown). The concentrations of purified IgG and IgM were 0.73 and 0.38 mg/ml, respectively, determined by $E(1\%) = 1.35$ for IgG and $E(1\%) = 1.20$ for IgM at 280 nm.

Tumor cells

I3T2.1, a ras-transformed 10T $\frac{1}{2}$ clone, grew as adherent cells in petri dishes containing DMEM/F12 medium supplemented with 10% FBS as described in Chapter 2. The LYNAb⁺, derived from L5178Y-F9 cells, was cultured as suspension cells in Fisher's medium containing 10% FBS (FFBS). The RI-28, a T cell leukemia line

originating in the CBA/H strain, was maintained as suspension cells in 10% FFBS.

[¹³¹I]-dUrd elimination assay

Cell labeling with [¹³¹I]-dUrd was performed as described previously (Chow et al., 1983). Briefly, RI-28 tumor cells were labeled in vitro by incubating 1.5×10^6 cells with 1 μ Ci [¹³¹I]-dUrd at a final concentration of 0.2 μ Ci/ml in 10% FFBS for 3-4 h at 37°C. Then the cells were washed three times with HBSS at room temperature. The CBA/N male mice age-matched at 6-9 weeks were injected i.v. with 0.3 ml saline or 0.3 ml 1:1 diluted whole serum NAb, or 0.3 ml 1:1 diluted ppt NAb which had been reconstituted to its original volume. Within 2 h after injection of NAb, aliquots of 1×10^5 labeled cells were injected i.v. into each of 4 mice in each group. The mice were whole-body counted as outlined in Chapter 2 at time 0, 2, 6, 8 and 25 h. The radioactivity remaining in the mice at each time point was expressed as a percentage of the whole-body counts at time 0. Potassium iodide was added routinely to the drinking water as described in Chapter 2.

Metastasis assay

Subconfluent I3T2.1 cells were harvested by trypsinization for 1 min and washed twice in HBSS. The mice were given 3 i.v. injections of 0.3 ml of saline or syngeneic whole serum NAb, 1 each on day -2, -1 and 0. Within 2 h of the last injection of NAb, an aliquot of 100 μ l HBSS containing different numbers of cells, as indicated, was injected i.v. into each mouse. In some experiments, the tumor cells were injected twice with a 1-h interval as indicated. Twenty-two days after tumor injection, the mice were killed by anesthetization and the surface tumor foci on lungs, spleens and kidneys were

counted under a dissection microscope. The lungs were infilled with Bouin's solution containing 75% (v/v) picric acid (saturated solution), 10% (v/v) formaldehyde and 5% (v/v) acetic acid. The tumor focus showed up on the lung as a white spot against the yellow background tissues.

Tumorigenicity assay

Tumor cells maintained in tissue culture were harvested by trypsinization for 1 min for I3T2.1 and pipetting for LYNAb⁺ and RI-28. Cells were washed twice in HBSS. In some initial experiments with C3H and DBA/2 mice, 3 i.v. injections of 0.3 ml of saline or syngeneic whole serum NAb were given, 1 each on day -2, -1 and 0. In subsequent experiments, C3H and DBA/2 mice were given five i.v. injections of saline or serum NAb, 0.3 ml each on day -4, -3, -2, -1 and 0. For CBA/N mice, 3 i.v. injections of 0.3 ml of saline or purified syngeneic NAb as indicated were given, 1 each on day -2, -1 and 0. Within 2 h of the last injection of NAb, an aliquot of 100 μ l HBSS containing 1.2×10^3 of the LYNAb⁺, 5×10^3 of the I3T2.1 and 1×10^4 of the RI-28 was injected s.c. into a shaved area in the middle of the lower back of each DBA/2, C3H and CBA/N mouse, respectively. Mice were observed every 2 days until 2 weeks after the appearance of the last tumor and the first day of tumor formation was recorded .

Statistical Analysis

The independent Student *t* test (P_{ij}) was used to assess the significance of the differences observed in label-clearance, tumorigenicity and metastasis experiments. The Fisher exact test was used to evaluate the significance of the tumor frequencies in the xid tumorigenicity model. $P > 0.05$ was not considered significant.

RESULTS

s.c. tumorigenicity of RI-28 in CBA/N mice given purified natural IgG and IgM i.v.

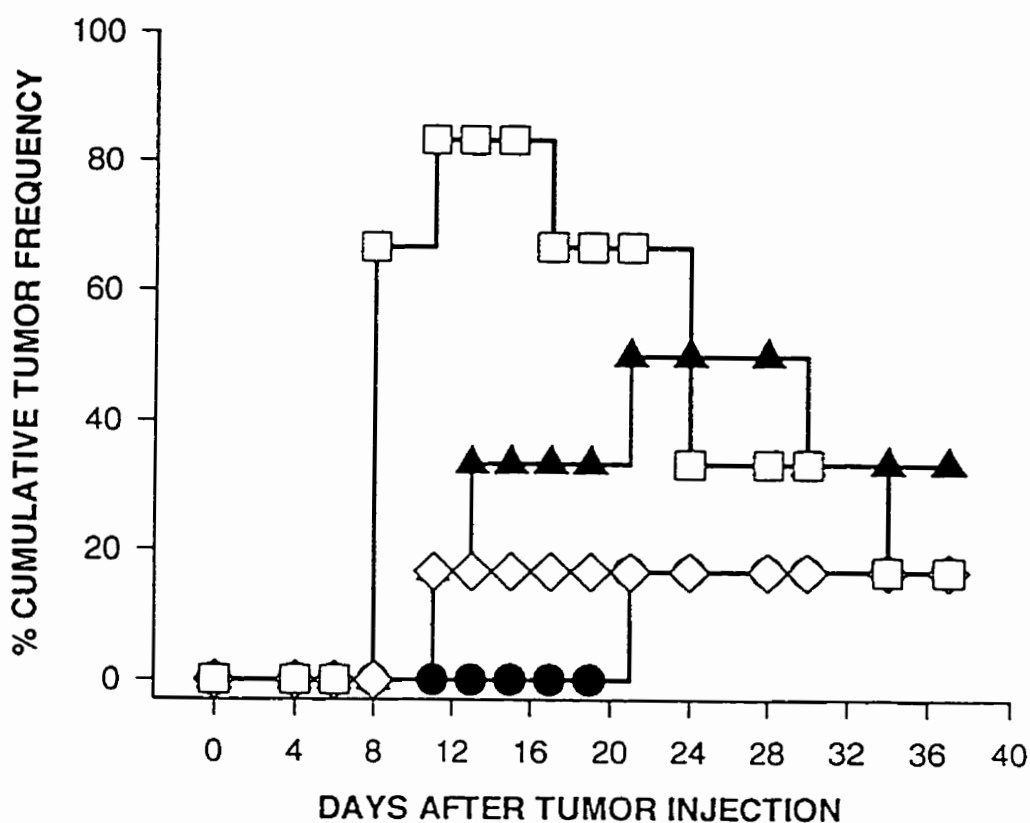
It was previously shown that injection of a combination of syngeneic IgG and IgM NAb purified through protein A and anti-mouse IgM affinity chromatographies slightly reduced the tumor frequency and prolonged the survival of (CBA/NxCBA/J)F1 male mice (Chow, 1995). In order to test whether different classes of NAb have similar anti-tumor activities in vivo, CBA/J and (CBA/JxCBA/N)F1 female whole serum NAb was purified by ammonium sulfate precipitation, followed by passing through a protein A-Sepharose column and the effluent through a HR-S-300 gel column. The threshold syngeneic s.c. tumor inocula approach was used as previously reported (Chow, 1995). Compared with ppt NAb, the RI-28 binding capacities of the purified IgG and IgM fractions reconstituted to their original volume showed a 25.8% loss in IgG activity and a 54.1% reduction in IgM NAb binding (Table 5.1). Fifteen days after the tumor inoculation, mice treated with these different NAb preparations yielded lower tumor frequencies at 33% for purified IgG NAb, 17% for purified IgM NAb ($P < 0.05$) and 0 for ppt NAb ($P < 0.01$) compared with 83% for saline treated controls (Fig 5.1). The eventual tumor latencies were also prolonged at 11 days for IgM, 15.0 ± 3.1 days for IgG, and 21 days for ppt NAb compared with 8.6 ± 0.6 days for saline-treated group (Fig 5.1). Similar to a previous report (Chow, 1995), regression of tumors was noted on day 17 after tumor inoculation for the saline-treated group and on day 30 for the purified IgG-treated group and the final tumor frequencies on day 34 were 17%, 17%, 17% and 33% in mice treated with saline, ppt NAb, IgM and IgG, respectively (Fig 5.1).

Table 5.1. RI-28 binding of IgG and IgM purified from CBA/J serum

NAb	Mean channel fluorescence (MCF)	
	FITC-conjugated anti-mouse IgG	FITC-conjugated anti-mouse IgM
ppt NAb	67.1	14.8
IgG	49.8	-
IgM	-	6.8

IgG was purified by passing ppt NAb fractions through the protein A-Sepharose-4B column. The effluent from this column were reprecipitated by ammonium sulfate and passed through the HR-S-300 column. IgG and IgM were eluted from both columns, respectively. The IgG-containing eluate was passed through a rabbit anti-mouse IgM-Sepharose-4B column to remove contaminating IgM. Both IgG and IgM were reconstituted to their original volume at concentrations of 0.73 and 0.38 mg/ml, respectively.

Fig 5.1. Cumulative tumor frequencies of RI-28 in CBA/N mice pre-treated 3 times with purified syngeneic NAb. Three i.v. injections of 0.3 ml ppt NAb (closed circle), purified IgG (closed triangle), purified IgM (open diamond) or saline (open square) were given, 1 each on day -2, -1 and 0 within 2 h prior to s.c. inoculation of 1×10^4 RI-28 cells into CBA/N male mice. There were 6 mice per group, age-matched at 9-12 weeks. The peak tumor frequencies were 17%, 50%, 17% and 83% and the tumor latencies were 21 and 15.0 \pm 3.1, 11 and 8.6 \pm 0.6 days for ppt NAb-, purified IgG-, IgM- and saline-treated groups, respectively.



s.c. tumorigenicity of LYNAb⁺ in DBA/2 mice and I3T2.1 in C3H mice given whole syngeneic serum NAb i.v.

In order to assess the anti-tumor effect of passive NAb in normal mice, the same threshold s.c. syngeneic tumor inocula model was employed in DBA/2 and C3H mice. In the initial experiments with NAb transfer, three injections of 0.3 ml of whole serum NAb from normal DBA/2 mice, given 1 each on days -2, -1 and 0 prior to syngeneic tumor s.c. challenge, produced the same tumor frequency as that in mice treated with saline (data not shown). Similarly, three injections with serum NAb in C3H mice yielded the same observation (data not shown). However, extension of the treatment to 5 injections of 0.3 ml of syngeneic serum, given 1 each on days -4, -3, -2, -1 and 0 prior to the syngeneic tumor s.c. challenge, produced an increase in tumor latency by 36% in DBA/2 ($P_i < 0.01$) (Fig 5.2) and 25% in C3H mice (Fig 5.3). The tumor frequencies were not reduced by passive NAb in DBA/2 mice (Fig 5.2) but slightly decreased in C3H mice during a period from day 17 to day 27 after tumor inocula (Fig 5.3).

i.v. RI-28 elimination in CBA/N mice given syngeneic serum NAb i.v.

It has been observed that passive human IVIg in DBA/2 mice markedly reduced the colonization of the L5178Y-F9 injected i.v. in livers (Chow, unpublished data). In order to determine the early effect of passive NAb on the injected i.v. tumor cells in vivo, RI-28 lymphoma cells were labeled with [¹³¹I]-dUrd. A single injection of 0.3 ml of 1:3 diluted CBA/J serum NAb or saline was injected i.v. into each CBA/N mouse. This was followed within 2 h by an i.v. injection of 1×10^5 [¹³¹I]-dUrd-labeled RI-28 tumor cells. A reduction in the radioactivity retained in NAb-treated mice was observed 8 h after

Fig 5.2. Cumulative tumor frequencies of LYNAb⁺ in DBA/2 mice pre-treated 5 times with syngeneic serum NAb versus saline. Five i.v. injections of 0.3 ml DBA/2 male serum NAb (closed circle) or saline (open square) were given, 1 each on day -4, -3, -2, -1 and 0 within 2 h prior to s.c. inoculation of 1.2×10^3 LYNAb⁺ cells into 9-week old DBA/2 male mice. There were 5 mice per group, and the tumor latencies were 11.4 ± 0.4 and 8.4 ± 0.7 days for serum NAb- and saline-treated groups, respectively.

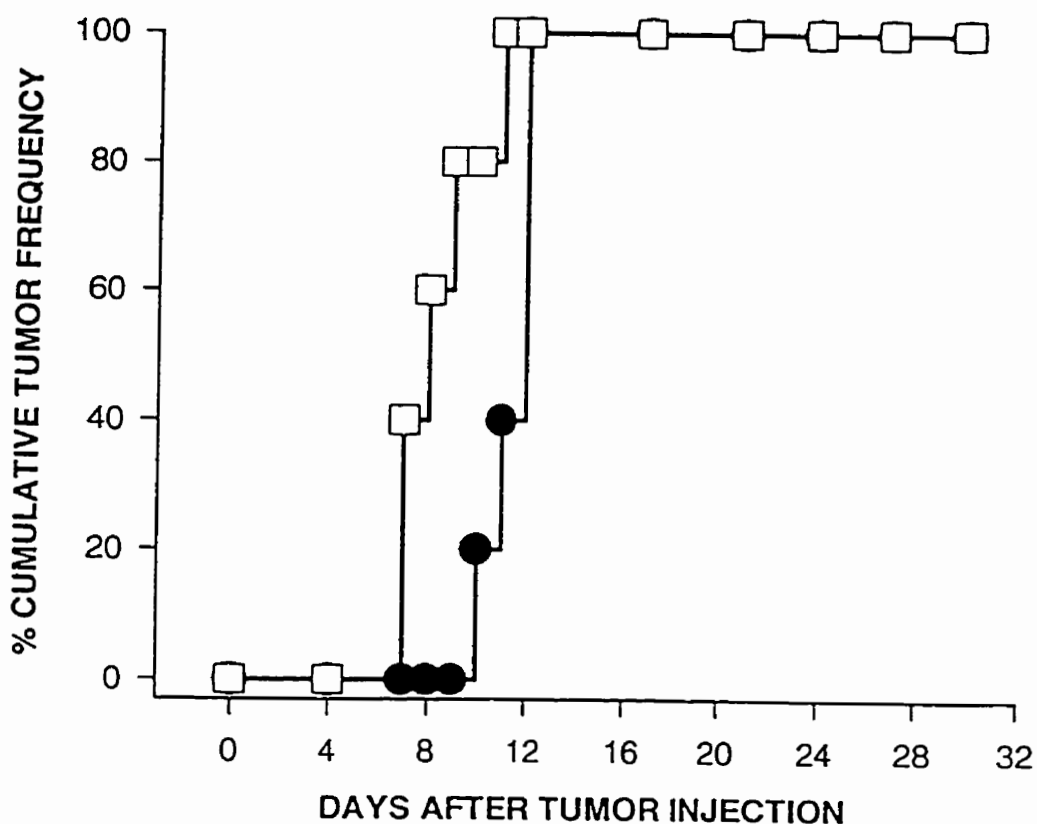
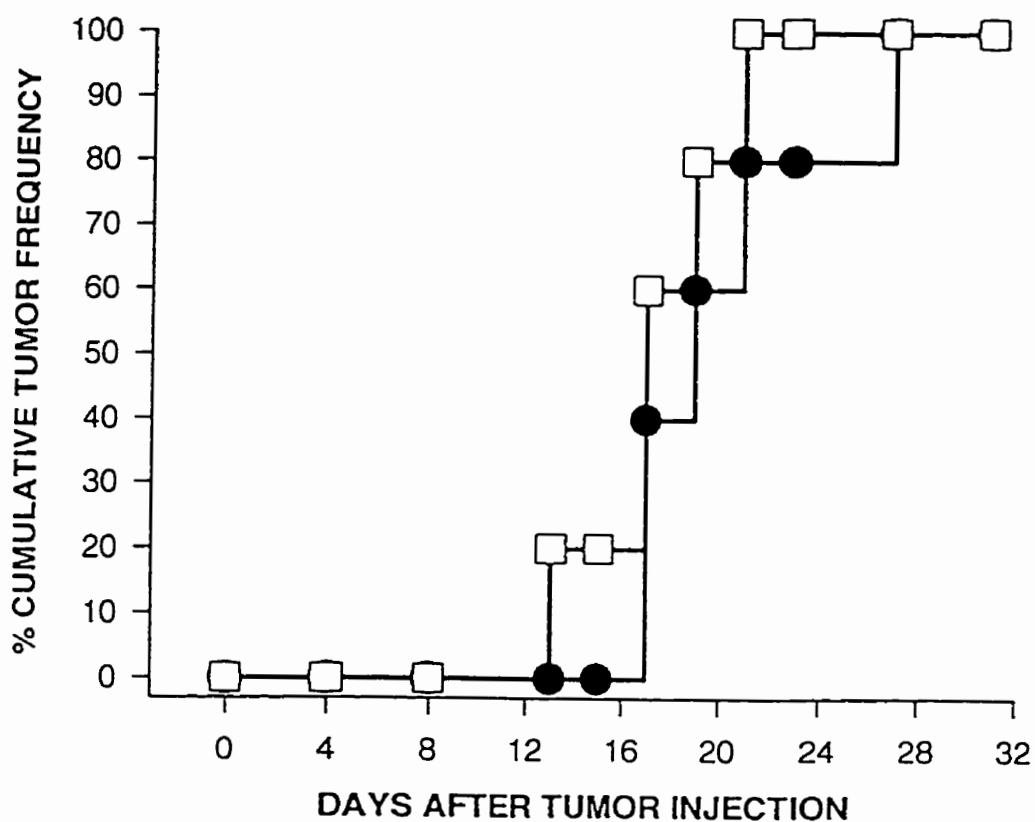


Fig 5.3. Cumulative tumor frequencies of I3T2.1 in C3H mice pre-treated 5 times with syngeneic serum NAb versus saline. Five i.v. injections of 0.3 ml DBA/2 male serum NAb (closed circle) or saline (open square) were given, 1 each on day -4, -3, -2, -1 and 0 within 2 h prior to s.c. inoculation of 5×10^3 I3T2.1 cells into 9-10-week old C3H male mice. There were 5 mice per group, and the tumor latencies were 21.8 ± 2.6 and 17.4 ± 1.3 days for serum NAb- and saline-treated groups, respectively.



tumor challenge and persisted throughout the 1 day assay (Table 5.2, Expt 1). Injection of CBA/J ppt NAb yielded similar observations (Table 5.2, Expt 2).

ras-overexpressing I3T2.1 i.v. metastasis in C3H mice given whole serum NAb i.v.

It was found previously that passive i.v. syngeneic NAb markedly reduced the colonization of i.v. injected RI-28 in the livers of (CBA/N x CBA/J)F1 male mice (Chow and Yuan, unpublished data). To evaluate whether passive syngeneic NAb could also reduce experimental metastasis in normal mice, the ras-overexpressing I3T2.1 fibroblast model was analysed. Three injections of 0.3 ml of whole serum NAb from normal C3H mice, given 1 each on days -2, -1 and 0 prior to the I3T2.1 i.v. challenge with a bolus dose of 2×10^6 cells, produced a slight decrease in tumor foci in lungs (Table 5.3, Expt 1). However, when the tumor dose was reduced to 1×10^6 and split into two i.v. injections given with a 1 h interval, the same three pre-injections of serum NAb produced a statistically significant reduction in tumor foci in lungs amounting to 62-72% with $P_{ii} < 0.01$ (Table 5.3, Expts 2 and 3).

DISCUSSION

Early studies showed that passive normal serum, plasma or whole blood in leukemic animals was able to eliminate neoplastic cells (reviewed in Kassel et al., 1977). In contrast, s.c. pre-injection of cross-reactive idiotypic bearing NAb Fab fragments obtained by papain digestion of in vivo fibrosarcoma membranes, enhanced growth of the transplanted tumor in vivo (Natori et al., 1981). In this case, however, it was not clear whether the Fab preparations were contaminated by tumor antigens which could enhance

Table 5.2. Elimination of ^{131}I -dUrd-labeled RI-28 in CBA/N mice pre-treated with NAb versus saline

Expt# ^a	Treatment	% retained radioactivity \pm SE				
		0	2 h	6 h	8 h	25 h
1	saline	100	98.7 \pm 0.8	48.2 \pm 2.4	23.2 \pm 2.4	21.9 \pm 1.0
	serum NAb	100	95.8 \pm 2.2	43.0 \pm 9.2	10.3 \pm 2.0	8.8 \pm 0.8
	P_{ii}		NS	NS	<0.001	<0.0001
2	Saline	100	88.7 \pm 3.9	46.5 \pm 5.5	18.3 \pm 1.3	17.5 \pm 1.2
	ppt NAb	100	81.0 \pm 1.7	38.2 \pm 4.3	12.9 \pm 1.7	11.7 \pm 1.3
	P_{ii}		NS	NS	<0.05	<0.02

^a CBA/N male mice age-matched at 6-9 weeks were given an i.v. injection of 0.3 ml saline or 1:3 diluted CBA/J serum NAb (Expt 1) or 0.3 ml 1:1 diluted ppt NAb which had been reconstituted to its original volume (Expt 2). Within 2 hours after the NAb injection, 1×10^5 [^{131}I]-dUrd-labeled RI-28 cells were injected i.v.. The radioactivity was immediately whole-body gamma counted and normalized as 100 at time 0. There were 4 mice in each group. The P_{ii} values represent a comparison between saline- and NAb-treated groups.

NS, not significant.

Table 5.3. Metastasis of I3T2.1 cells in C3H mice pre-treated with serum NAb

Expt#	Treatment	Number of mice	Mean surface tumor foci \pm SE	
			Lung	Liver
1 ^a	Saline	5	27.8 \pm 2.5	0
	NAb	5	21.4 \pm 7.1	0
2 ^b	Saline	5	68.4 \pm 13.5	1.6 \pm 0.9
	NAb	6	26.2 \pm 4.3 ^c	0
3 ^b	Non-treated	4	74.0 \pm 7.8	0
	Saline	4	74.3 \pm 8.9	0
	NAb	4	18.5 \pm 5.9 ^c	0

^a C3H male mice aged 9 weeks were pre-treated three times with whole syngeneic serum NAb or saline. Within 2 h after the last injection of NAb, 2×10^6 I3T2.1 cells were injected i.v.. Twenty-two days after the tumor challenge, the mice were killed and surface tumor foci were examined in lungs and livers.

^b C3H male mice aged 9 weeks were pre-treated three times with serum NAb the same way as in Expt 1. Within 2 h after the last injection of NAb, 5×10^5 I3T2.1 cells were injected i.v.. Within 1 h, a repeat injection was given with the same number of tumor cells.

^c $P_{ii} < 0.01$ compared with saline-treated controls.

tumor growth *in vivo*. Passive human anti- α -galatosyl IgG, which represents 1% of total immunoglobulins, reduced the tumor colonization in a murine model (Castronovo et al., 1987) and in a rat model (Kawaguchi et al., 1994). Human normal IgM antibodies have been found to inhibit human neuroblastoma growth in a nude rat model (David et al., 1996). In a urethane-induced carcinogenesis mouse model, mice were treated with different monoclonal NAb prior to the administration of the carcinogen urethane. Some monoclonal NAb reduced, whereas some monoclonal NAb enhanced primary tumor formation (Agassy-Cahalon et al., 1988).

It has been previously reported that injection of whole syngeneic serum NAb or a combination of purified natural IgG and IgM antibodies showed a reduction in tumorigenicity of threshold syngeneic s.c. tumor inocula in (CBA/NxCBA/J)F1 male mice (Chow, 1995). The present study with the xid-bearing CBA/N model also demonstrated that injection of either purified IgG or IgM NAb increased tumor latencies and reduced tumor frequencies. This indicates that both IgG and IgM classes of NAb have anti-tumor activities *in vivo*. Interestingly, natural IgM appeared to be slightly more effective than IgG. This may be due to the higher multivalency binding capacity of IgM than IgG and IgM could be more efficient in inducing complement-mediated lysis of the tumor cells (Herlyn et al., 1985; Ralph and Nakoinz, 1983). Alternatively, it is also possible that compared with the two valency natural IgG antibodies, the ten valency IgM NAb may induce more efficient cross-linking of cell surface molecules and thus may be more effective in inhibiting tumor growth through signaling potentials. Interestingly, subsequent regressions of RI-28 tumors were observed in both IgG NAb- and saline-

treated groups and the final tumor frequencies were almost the same for each group, similar to the previous data (Chow, 1995). The regression of RI-28 seemed to be a spontaneous process which may have resulted from an adaptive immune response or rapid growth leading to differentiation (reviewed in Prehn, 1996).

In the normal mouse model, even though the effect of passive NAb on tumorigenicity was not so profound as that in the CBA/N model, passive NAb still showed a beneficial effect in delaying tumor development assayed as an elongation of tumor latencies. The discrepancy between these two models is probably due to the limitation of NAb associated mechanism for tumor control which is already operating optimally with the endogenous levels of NAb in normal mice. In this case, the exogenous NAb may not help much to eliminate more syngeneic tumors.

Passive NAb significantly enhanced the elimination of tumor cells injected i.v. assessed as a reduction in radioactivity retained in NAb-treated CBA/N mice in a 1 day assay. This increased early elimination of the labeled RI-28 from NAb-treated mice was concordant with the later marked reduction in the number of tumor colonies on the livers in CBA/N mice (Chow and Yuan, unpublished data). In B cell normal C3H mice, passive NAb only slightly reduced the number of lung tumor foci when 2×10^6 I3T2.1 tumor cells were given i.v. in a bolus injection. The small difference between NAb- and saline-treated groups is also presumably due to the endogenous NAb. Strikingly, the NAb markedly reduced tumor colonization in the lungs when a total of 1×10^6 tumor cells was injected in two pulses, each of 5×10^5 cells. The reason for the difference between these two dose schedules is not known. One interpretation is that the first wave of tumor cells

may induce damage to the pulmonary vascular endothelium (reviewed in Ward and Weiss, 1985), resulting in activation of an NAb mediated-process such as a transient nonspecific inflammation which can take advantage of extra NAb to make the local microvascular bed more hostile to the second wave of tumor cells.

The mechanisms by which NAb acts against tumors *in vivo* have not been directly demonstrated. Studies *in vitro* with specific anti-tumor antibodies have shown that these antibodies can impact tumor cell growth by a variety of ways including opsonization leading to phagocytosis by macrophages, complement-dependent cytotoxicity, ADCC effected by NK cells and macrophages or direct action on tumor cells (reviewed in Miller et al., 1989). A monoclonal IgM antibody recognizing tumor cell surface carbohydrates has been shown to protect mice from *i.p.* or *s.c.* challenge with the tumor to which the antibody was raised (Gil et al., 1990). Pretreatment of the mice with silica to inactivate macrophages eliminated the protective effect of the antibody, indicating a macrophage-dependent mechanism for anti-tumor antibodies *in vivo*. NAb may act in a similar way to the induced antibodies because the level of anti-carbohydrate IgM NAb was also correlated with natural resistance to the same tumor (Gil et al., 1990).

It is well established that tumors which grow out *in vivo* exhibited a reduced sensitivity to natural defence mechanisms (Chow, 1984; Brown and Chow, 1985; Brown et al., 1986). In the clinic, most cancer patients are diagnosed at a relatively late stage of the disease. Therefore, it is not feasible to treat cancer patients with NAb. However, the present finding that passive NAb can reduce the metastasis of the secondary injected tumor cells provides new light for a therapeutic purpose. For instance, some colorectal

cancer patients with hepatic and pulmonary metastasises still can be treated with surgical therapies to prolong their survival (Smith et al., 1992). In this case, preadministration of human NAb (i.e., IVIg) in conjunction with a resection of their tumors may be beneficial for long-term survival. Nevertheless, further studies are essential to confirm the beneficial effect of NAb in metastatic animal models with established tumors.

In summary, the data suggest that passive NAb is beneficial for both B-cell deficient and B cell normal mice to aid in the rejection of syngeneic tumors injected s.c. or i.v.. These observations provide more direct evidence supporting a role for NAb in the defence against syngeneic tumors *in vivo*.

CHAPTER 6

DISCUSSION

Several lines of evidence suggest that NAb, an important factor of innate immunity, serves as a first line of defence against tumor development *in vivo*. Oncogenic ras transformation of murine C3H 10T½ fibroblasts increased their serum NAb binding, which has been associated with a partial activation and downregulation of PKC (Wolfman and Macara, 1987). Previous studies in the L5178Y-F9 lymphoma model demonstrated that long-term treatment with TPA, a PKC activator, resulted in an increase in NAb binding (Sandstrom and Chow, 1992). These two models strongly suggested a potential role for PKC in the regulation of NAb binding structures and link the NAb recognition with regulation by a signaling molecule PKC. Studies in signal transduction pathways have demonstrated that ligation of specific cell surface receptors results in activation of PKC, which phosphorylates a variety of intracellular molecules including membrane receptors, cytoskeletal components and downstream signal transduction molecules leading to DNA replication and changes in cell function. Stimulation of PKC with TPA results in activation of lymphocytes. Alterations of both the PKC content and PKC activity have been frequently detected in many tumor tissue types (reviewed in Basu, 1993). Moreover, a variety of oncoproteins that act at the early steps of signal transduction cascades, such as ras, src, erbB2, sis and abl, increase the production of DAG, the endogenous activator of PKC (Wolfman and Macara, 1987; Diaz-Laviada et al., 1990; Chiarugi et al., 1989; Lacal et al., 1987). The evidence not only supports a pivotal role for PKC in cell proliferation, differentiation and transformation, but indicates that PKC may be a key regulator for controlling cell susceptibility to NAb regulation mechanisms.

In this thesis, the regulatory role of PKC in NAb binding was further investigated.

In general, PKC regulates the NAb binding capacities of the cells through two different mechanisms: continuously elevated basal activation of PKC increases NAb binding levels while massive and transient activation of PKC downregulates NAb binding.

First, investigations in the PKC regulation of NAb binding function in ras- and PKC- β 1-overexpressing 10T $\frac{1}{2}$ cells revealed that persistently elevated basal activation of PKC appears to upregulate NAb binding structures on the cell surface. Blockade of this pathway by inhibition or depletion of PKC with H7, E-64d or TPA significantly reduced NAb binding levels in 10T $\frac{1}{2}$ variants. One mechanism for accounting for PKC upregulation of NAb binding structures is that continuous basal activation of PKC in both PKC-4 and I3T2.1 may stimulate certain gene regulators, such as the transcription factor AP-1 leading to activation of the CD44 promoter (Hofmann et al., 1993; Jamal et al., 1994; Lamb et al., 1997). This would increase CD44 expression on the cell surface consistent with the augmented CD44 detected on I3T2.1 and PKC-4 cells (Chapter 4). Overexpression of the ras oncogene in 10T $\frac{1}{2}$ cells increased surface expression of the receptor for hyaluronan-mediated motility (RHAMM) (Turley et al., 1993). Both I3T2.1 and PKC-4 also showed increased levels of RHAMM on their surface (Chow, unpublished data). Although it is not clear currently whether NAb can bind to CD44, a correlation between NAb binding levels and CD44 expression in both the L5178Y-F9 and the 10T $\frac{1}{2}$ systems implies that NAb may react with CD44. NAb immunoblotting with biotinylated membrane molecules purified from I3T2.1 and PKC-4 cells demonstrated an increase in densities of several protein bands ranging from 200 to 66 KDa compared with parental 10T $\frac{1}{2}$ cells (Chapter 4). Another alternative but not mutually exclusive

mechanism for the increase in NAb binding in I3T2.1 and PKC-4 is that PKC- β 1 and ras may upregulate some cytosolic glycosylation enzymes which lead to modifications of cell surface glycoproteins in 10T $\frac{1}{2}$. Accumulated evidence has suggested that transformation by ras induced an increased production of highly branched carbohydrate molecules expressed on NIH 3T3 cells (Santer et al., 1984; Collard et al., 1985) and an increased binding of the lectin peanut agglutinin in human breast epithelial cells (Rak et al., 1991). Our preliminary studies also showed that a 140-KDa membrane molecule from I3T2.1 cells bound more peanut lectin compared with that from 10T $\frac{1}{2}$ cells (data not shown). The alterations in glycosylation of cell surface molecules in PKC isoform-overexpressing cells have not been reported. However, PKC- β 1 overproduction in PKC-4 cells did result in an increase in the binding of Concanavalin A (Con A) to a 90-KDa membrane molecule assayed by Con A blotting compared with parental 10T $\frac{1}{2}$. Further analysing the relationship between this 90-KDa molecule and CD44 excluded their similarities assessed by blotting the immunoprecipitated CD44 proteins with biotinylated Con A (data not shown). TPA treatment of human erythroleukemic K562 cells for 38 h increased the heterogeneity of the fibronectin receptor by altering the N-linked glycosylation and sialylation of the molecule (Symington et al., 1989). Similarly, TPA treatment of human histiocytic lymphoma U937 cells led to alterations in glycosylation of the receptor for urokinase plasminogen activator (Behrendt et al., 1990). These observations clearly associated the glycosylation processes with the activation of the PKC pathway. Since NAb has a considerable capacity to bind with carbohydrate groups of cell surface antigens (Sela et al., 1975; Galili et al., 1984), these alterations in carbohydrate moieties

expressed on I3T2.1 and PKC-4 cells may result in recognition by NAb. Thus, cells activated through PKC, as suggested in the ras- and PKC- β 1-overexpressing models, may increase expression of certain cell surface molecules or alter glycosylation patterns of some molecules, both of which could increase NAb binding levels. This is further supported by the observation that mitogen-activated normal T lymphocytes acquired more serum NAb compared with their resting counterparts (Wolf-Levin et al., 1993).

The second mechanism for PKC regulation of NAb binding capacities in the cells is that transient and massive activation of PKC downregulates NAb binding. Short-term treatment of 10T $\frac{1}{2}$ variants (Chapter 3) and L5178Y-F9 lymphomas (Sandstrom and Chow, 1994) with TPA significantly reduced their NAb binding levels. This is consistent with observations by others that brief treatment with TPA induces downregulation of a variety of cell surface receptors such as MHC class I antigen (Peyron and Fehlmann, 1988), CD3, CD5 (Alberola-Ila et al., 1993), CD4 (Petersen et al., 1992), gp90^{MEL-14} (Jung and Dailey, 1990) and receptors for C5a (Rubin et al., 1991), TNF α (Galeotti et al., 1993), EGF (Davis and Czech, 1984), transferrin (Davis et al., 1986), IL-2 (Onish et al., 1992) and PAF (Zhou et al., 1994). The sensitivity of the expression of these membrane signaling receptors to PKC activation raises the possibility that those NAb binding sites which are also sensitive to TPA downregulation may be important signaling molecules for 10T $\frac{1}{2}$ variants. Thus, under physiological conditions, NAb reacting with signaling receptors may induce signaling events and influence cell functions.

In fact, NAb ligated with unknown cell surface signaling receptors expressed on 10T $\frac{1}{2}$ variants indeed resulted in activation of PKC assessed as a translocation of PKC

from the cytosol to membrane fractions when using a temperature shift procedure. This PKC movement was associated with the downregulation of membrane-bound NAb and the release of at least 20 plasma membrane molecules ranging from 220 to 20 KDa. H7 partially increased NAb binding levels at both 37°C and 4°C shifted to 37°C suggesting a role for PKC in the NAb interaction-initiated downregulation of NAb binding. This NAb binding-induced PKC activation and downregulation of pre-coated NAb also supports the proposal that massive and transient activation of PKC downregulates NAb binding levels. In addition, the phosphotyrosine levels of a 60-KDa membrane-associated molecule was found to be decreased after the temperature of NAb-coated cells was raised. Thus, other signaling events for controlling the protein phosphotyrosine levels obviously was induced following NAb reaction with the cells. Interestingly, RPTP α , a ubiquitous RPTP, was released into the supernatant of NAb-coated cells. It is not clear, however, whether the NAb binding-induced PKC activation and alteration of PTP or PTK activity are two linear or totally independent biological events. Nevertheless, the redistribution of PKC and corresponding downregulation of pre-bound NAb were obviously related to intracellular signal transduction. The consequence of the NAb-initiated signaling in ras-overexpressing I3T2.1 cells was growth inhibition assessed as a decrease in total cell numbers and an increase in cell numbers in G0/G1 phase in the cell cycle. This observation is consistent with studies by others showing that NAb inhibits proliferation of LPS-stimulated fresh murine B cells in vitro (Uher et al., 1992). Human IVIgG was also found to inhibit TPA/ionomycin-stimulated blast transformation and [H^3]thymidine incorporation of human blood mononuclear cells (PBMC) (Andersson et

al., 1993; Amran et al., 1994) and antigen-specific and anti-CD3-induced proliferation of PBMC (Amran et al., 1994). Similarly, IVIg has been frequently reported to suppress the proliferation of mitogen-activated purified B and T cells (Kawada and Terasaki, 1987; Van Schaik et al., 1992). Moreover, IVIg also suppresses the production of many cytokines by T cells and monocytes and IgM secretion by EBV-transformed B lymphoblastoid cells (reviewed in Mouthon et al., 1996). Thus, these data raise an intriguing possibility that NAb may control activated cells through growth inhibition potentials.

So far, most knowledge on NAb effecting activated cells was derived from studies on immune cells. Interestingly, IVIg downregulated the production of IL-2, IL-3, IL-4, IL-5, IL-10, TNF- β and GM-CSF during the initial phase of the cultures up to 48 h but not at 48-96 h (Andersson et al., 1993). This indicates that NAb recognition and regulation may be only restricted to those cells distributed in a particularly early stage of the activation process. This possibility is further supported by the notion that stimulated T cells transiently express higher levels of CD45RA, a target of NAb (Zhang and Chow, unpublished data), compared with the resting counterparts (Deans et al., 1992). Thus, only the cells with higher levels of CD45RA expression on the cell surface during a particular phase of activation would be sensitive for NAb.

Other factors may also influence the inhibitory effect of NAb on the activated cells in vivo. (1) The levels of NAb targets expressed on the 'activated' cells. Some cell markers such as CD45RA and Fc receptors are signaling receptors and can be bound with NAb. Both receptors have been shown to be upregulated during an activation

process following stimulation via TCR complexes (Deans et al., 1992; reviewed in Sandor and Lynch, 1993). Thus, NAb has a good chance to react with these elevated membrane targets and influence cell functions. (2) The sensitivity of the activated cells to NAb. IgM NAb from LPS-stimulated normal splenic B cells has been shown to inhibit the proliferation and hapten-specific IgM secretion of splenic B cells stimulated with either LPS or specific hapten antigen. However, these NAb were unable to inhibit the production of hapten-specific IgG antibodies by splenic B cells stimulated with either LPS or carrier-specific T cells in vitro (Kiss et al., 1994). Although it remains unknown about the difference in their cell surface markers expressed on IgM-secreting and IgG-secreting B cells, this observation implies that different activated cells may differ in their sensitivity to NAb regulation. (3) Other factors such as hormones or cytokines which introduce stimulating signals into the cells may counteract the inhibitory signal initiated by NAb binding. IL-2 or IL-4 were found to reverse the inhibitory effect of IVIg in both proliferation and cytokine production in phorbol ester-stimulated PBMC cultures (Amran et al., 1994). Therefore, any one of these possibilities alone or in concert with others can determine the sensitivity of the activated cells to NAb, leading to either elimination, growth inhibition or proliferation.

Although ample evidence suggests an inhibitory effect of NAb on immune cells in vitro, both inhibitory and stimulatory functions of NAb have been demonstrated in the immune system in vivo. Administration of human IVIg in autoimmune patients improves their symptoms and this was associated with the suppression of pathogenic autoantibody-producing clones (Dietrich et al., 1993) and pathogenic T cell functions (Sauodi et al.,

1993). A high dose of normal mouse IgG NAb has been shown to activate splenic B cells and CD4⁺ T cells in Balb/c mice (Sundblad et al., 1991a). In contrast, the same NAb treatment in mice resulted in a reduction in numbers of bone marrow B lineage cells, particularly the pre-B cells (Sundblad et al., 1991b). Since the Ig binding activity or connectivity is an intrinsic feature of NAb, and B cells at different stages of development may differ in their sensitivities to NAb regulation, it is not surprising that NAb plays a more complicated role in selecting the antibody repertoires by either stimulating or inhibiting the growth of certain sets of B cell clones. The interpretation for NAb stimulating CD4⁺ T cells in the later study may be due to either antigen presenting cell (APC) presentation of injected Ig fragments or serum proteins contaminating the NAb preparations or direct activation by Fc-receptor dependent multimerization (Sundblad et al., 1991a). Moreover, IVIg has been shown to transiently increase plasma IFN- γ and IL-6 levels in patients with secondary generalized epilepsy (Ling et al., 1993). This temporal cytokine production induced by IVIg seemed to be due to the transient activation of monocytes assessed by an increase in expression of surface CD64 and the high affinity Fc- γ receptor (Ling et al., 1993). Considering the ability of NAb to suppress proliferation of immune cells in vitro, it is speculated that NAb initially may induce a transient activation of the immune cells in vivo and subsequently lead to their growth inhibition through unknown mechanisms.

In addition to immune cells, NAb may also control activated somatic cells in vivo. Unfortunately, so far, evidence to support this thinking can only be obtained from studies on tumor models. It should be noted that even though tumor cells are much different

from normal activated cells, there are still some similarities between them at least in their proliferating behaviors. For a relatively normal 10T½ line, NAb binding levels were significantly higher in the proliferating population compared with the confluent resting population (Chapter 2). This indicates that normal activated somatic cells may similarly acquire more NAb. Introducing a PKC-β1 gene into 10T½ cells resulted in a disorganized growth morphology and a loss of contact inhibition (Krauss et al., 1989). Importantly, these constitutively 'activated' cells acquired 80% more serum NAb independent of their growth states (Chapter 2). The faster elimination of the high NAb binding PKC-4 in vivo provided further evidence at least for fibroblasts that cells with a few genetic changes and being 'activated' through PKC are sensitive to NAb mediated elimination mechanisms. This also reinforces the idea that NAb plays a role in suppression/elimination of early stage tumors, which are close to activated normal cells. Our threshold s.c syngeneic tumor inoculum model has been shown to model NAb regulation of the early stages of tumor development with small tumor burdens. The higher the NAb binding levels of the syngeneic tumor cells injected, the lower the tumorigenicity of the threshold s.c. tumor incula (Chow and Chan, 1987). There is also an inverse correlation between tumorigenicity and NAb levels of the recipient animals (Ehrlich et al., 1984; Gil et al., 1990; Bennet and Chow, 1991; Chow, 1995). Passive NAb in both B cell deficient (Chow, 1995; Chapter 5) and normal mice (Chapter 5) reduced the tumorigenicity of a threshold syngeneic tumor inoculum (Chapter 5). All of this evidence not only suggests a role for NAb in controlling preneoplastic and neoplastic cells in vivo, but highlights the potential regulatory role of NAb in controlling normal

somatic cells undergoing an activation process such as in wound healing or regeneration.

In the very early stages of life, such as the embryonic and fetal stages, both cell activation and cell death are extremely frequent. The production of NAb starts at the first few weeks of gestation (Cukroska et al., 1996). Studies with monoclonal NAb derived from fetal liver and cord blood B cells have shown that NAb dominates the fetal antibody repertoire (Lydyard et al., 1990; Bhat et al., 1992). Given that NAb suppresses activated cells *in vivo*, does NAb also play a role in controlling embryo and fetal activated cells *in vivo*? The answer is presently unknown due to the lack of knowledge on whether fetal NAb could bind fetal tissues and how strong the binding is. It was observed that the binding activity of NAb from adult mice could be absorbed by early stage but not by late stage syngeneic embryo tissues (Chow, unpublished observation). This suggests that the expression of autoantigens differs during the gestation period. Based on the germline origin of many NAb and their conserved specificity, one can speculate that NAb may also participate in the selection of undifferentiated fetal cells involved in both the immune system and other systems, while the significance of NAb regulation may vary with the change of antigens on self tissues.

The specificity of NAb has been shown to be mainly restricted to highly conserved autoantigens, such as DNA, histone, actin, tubulin, vimentin, topoisomerase and ribosomal P protein (reviewed in Stollar et al., 1997). Thus, NAb from one species specific to any one of these antigens also reacts with the same antigen from other species including invertebrate creatures (Stollar, 1997). Germline V_H gene segments of NAb are also conserved during evolution, as indicated by their primary structures and by the

occurrence of cross-species idiotype recognition (Stollar, 1997). The conserved nature of NAb through evolution indicates that NAb must play a fundamental role for organism survival. The anti-infection activity of NAb has been suggested to be an important function of NAb in all species from fish to humans (Dighiero, 1997). Here, the studies on the 10T½ fibroblast model, for the first time, provide evidence for NAb controlling relatively normal albeit immortalized, constitutively activated fibroblasts *in vivo*. Together with the finding that NAb could control activated immune cells, the data suggest that inhibition of activated cells is another important biological function of NAb and therefore NAb could provide basic biological mechanisms for maintaining a general homeostasis of an organism for any species.

In conclusion, 10T½ cells overexpressing an activated ras oncogene or a PKC-β1 gene increased their NAb binding capacities, identifying PKC, an integral signaling molecule of normal cellular activation, as a key regulator of NAb binding structures. This, coupled with corresponding decreases in expression of membrane PKC-α and NAb binding in resting 10T½ cells raised the possibility that in general cells activated through PKC are NAb sensitive. In addition, NAb interaction with these high NAb binding cells initiated a signal transduction mechanism including activation of PKC, shedding of cell surface molecules and the bound NAb, protein tyrosine dephosphorylation of a membrane-associated 60 KDa molecule, and over time the inhibition of DNA synthesis *in vitro*. Together with the increased *in vivo* elimination of the high NAb binding PKC-4 and the beneficial effect of passive NAb in the rejection of syngeneic tumors injected *s.c.* and *i.v.* in both the *xid*-bearing B cell deficient and B cell normal mouse models, the

data argued that NAb not only participates in immune surveillance of preneoplasia and neoplasia but also contributes to the homeostasis of the organism (Avrameas, 1991).

REFERENCES

- Aderem, A. The MARCKS family of protein kinase-C substrates. *Biochem. Soc. Trans.*, 23:587-591, 1995
- Adib-Conquy, M., Avrameas, S., and Ternynck, T. Monoclonal IgG and IgM autoantibodies obtained after polyclonal activation, show reactivities similar to those of polyclonal natural autoantibodies. *Mol. Immunol.*, 30: 119-127, 1993
- Adib, M., Ragimbeau, J., Avrameas, S., and Ternynck, T. IgG autoantibody activity in normal mouse serum is controlled by IgM. *J. Immunol.*, 145: 3807-3813, 1990
- Aflalo, E., Wolfson, M., Ofir, R., and Weinstein, Y. Elevated activities of protein kinase C and tyrosine kinase correlate to leukemic cell aggressiveness. *Int. J. Cancer*, 50:136-141, 1992
- Agassy-Cahalon, L., Yaakubowicz, M., Witz, I.P., and Smorodinsky, N.I. The immune system during the precancer period: naturally-occurring tumor reactive monoclonal antibodies and urethane carcinogenesis. *Immunol. Lett.*, 18:181-190, 1988
- Ahn, J., Donner, D.B., and Rosen, O.M. Interaction of the human insulin receptor tyrosine kinase from the baculovirus expression system with protein kinase C in a cell-free system. *J. Biol. Chem.*, 268:7571-7576, 1993
- Ai, Z., and Cohen, C.M. Phorbol 12-myristate 13-acetate-stimulated phosphorylation of erythrocyte membrane skeletal proteins is blocked by calpain inhibitors: possible role of protein kinase M. *Biochem. J.*, 296:675-683, 1993
- Aicher, B., Lerch, M.M., Muler, T., Schilling, J., and Ullrich, A. Cellular redistribution of protein tyrosine phosphatases LAR and PTP δ by inducible proteolytic processing. *J. Cell Biol.*, 138:681-696, 1997
- Alberola-Ila, J., Places, L., Fabregat, V., Vives, J., and Lozano, F. Different mechanisms regulate the monoclonal antibody-induced modulation of CD2, CD3, and CD5 in human lymphocytes. *Cell. Immunol.*, 147:247-255, 1993
- Alderman, E.M., Fudenberg, H.H., and Lovins, R.E. Binding of immunoglobulin classes to subpopulations of human red blood cells separated by density-gradient centrifugation. *Blood*, 55:817-822, 1980
- Alderman, E.M., Fudenberg, H.H., and Lovins, R.E. Isolation and characterization of an age-related antigen present on senescent human red blood cells. *Blood*, 58:341-349, 1981

Allen, L.A., and Aderem, A. Protein kinase C regulates MARCKS cycling between the plasma membrane and lysosomes in fibroblasts. *EMBO J.*, 14:1109-1120, 1995

Alvaro, V., Touraine, P., Raisman-Vozari, R., Bai-Grenier, F., Birman, P., and Joubert, D. Protein kinase C activity and expression in normal and adenomatous human pituitaries. *Int. J. Cancer*, 50: 724-730, 1992

Amran, D., Renz, H., Lack, G., Bradley, K., and Gelfand, E.W. Suppression of cytokine-dependent human T-cell proliferation by intravenous immunoglobulin. *Clin. Immunol. Immunopathol.*, 73: 180-186, 1994

Amstad, P., Reddel, R.R., Pfeifer, A., Malan Shibley, L., Mark, G.E., and Harris, C.C. Neoplastic transformation of a human bronchial epithelial cell line by a recombinant retrovirus encoding viral Harvey ras. *Mol. Carcinogen.*, 1:151-160, 1988

Andersson, U.G., Bjork, L., Skansen-Saphir, U., and Andersson, J.P. Down-regulation of cytokine production and interleukin-2 receptor expression by pooled human IgG. *Immunol.*, 79: 211-216, 1993

Andersson, J., Skansen-Saphir, U., Sparrelid, E., and Andersson, U. Intravenous immune globulin affects cytokine production in T lymphocytes and monocytes/macrophages. *Clin. Exp. Immunol.*, 104 Suppl 1:10-20, 1996

Apgar, J.R., Herrmann, S.H., Robinson, J.M., and Mescher, M.F. Triton X-100 extraction of P815 tumor cells: evidence for a plasma membrane skeleton structure. *J. Cell. Biol.*, 100:1369-1378, 1985

Aronheim, A., Engelberg, D., Li, N., al-Alawi, N., Schlessinger, J., and Karin, M. Membrane targeting of the nucleotide exchange factor Sos is sufficient for activating the Ras signaling pathway. *Cell*, 78:949-961, 1994

Asano, M.S., and Ahmed, R. CD8 T cell memory in B cell-deficient mice. *J. Exp. Med.*, 183:2165-2174, 1996

Attar, B.M., Atten, M.J., and Holian, O. MAPK activity is down-regulated in human colon adenocarcinoma: correlation with PKC activity. *Anticancer Res.*, 16:395-399, 1996

Auer, J., Pignot-Paintrand, I., and De-Almeida, M. Identification of human sperm surface glycoproteins by sperm membrane-specific autoantibodies. *Hum. Reprod.*, 10:551-557, 1995

Avrameas, S., Guilbert, B., Mahana, W., Matsiota, P., and Ternynck, T. Recognition of self and non-self constituents by polyspecific autoreceptors. *Int. Rev. Immunol.*, 3:1-15, 1988

- Avrameas, S. Natural autoantibodies: from 'Horror autotoxicus' to 'gnothi seauton'. *Immunol. Today*, 12:154-159, 1991
- Avrameas, S., and Ternynck, T. The natural autoantibodies system: between hypotheses and facts. *Mol. Immunol.*, 30: 1133-1142, 1993
- Ayouba, A., Ferreira, C., and Coutinho, A. Distinguishable patterns of connectivity in serum immunoglobulins from SLE patients and healthy individuals. *Scand. J. Immunol.*, 45:408-416, 1997
- Azzi, A., Boscoboinik, D. and Hensey, C. The protein kinase C family. *Eur. J. Biochem.*, 208:547-557, 1992
- Baccala, R., Quang, T.V., Gilbert, M., Tern ynck, T., and Avrameas, S. Two murine natural polyreactive autoantibodies are encoded by nonmutated germ-line genes. *Proc. Natl. Acad. Sci. USA.*, 86: 4624-4628, 1989
- Balmain, A., and Brown, K. Oncogene activation in chemical carcinogenesis. *Adv. Cancer Res.*, 51:147-182, 1988
- Barbacid, M. Ras genes. *Annu. Rev. Biochem.*, 56:779-827, 1987
- Barbouche, R., Forveille, M., Fischer, A., Avrameas, S., and Durandy, A. Spontaneous IgM autoantibody production in vitro by B lymphocytes of normal human neonates. *Scand. J. Immunol.*, 35:659-667, 1992
- Basu, A. The potential of protein kinase C as a target for anticancer treatment. *Pharmac. Ther.*, 59: 257-280, 1993
- Baudier, J., Delphin, C., Grunwald, D., Khochbin, S., and Lawrence, J.J. Characterization of the tumor suppressor protein p53 as a protein kinase C substrate and a S100b-binding protein. *Proc. Natl. Acad. Sci. USA.*, 89:11627-11631, 1992
- Bazzi, M.D., and Nelsestuen, G.L. Differences in the effects of phorbol esters and diacylglycerols on protein kinase C. *Biochemistry*, 28:9317-9323, 1989
- Bazzi, M.D., and Nelsestuen, G.L. Highly sequential binding of protein kinase C and related proteins to membranes. *Biochemistry*, 30:7970-7977, 1991
- Behrendt, N., Ronne, E., Ploug, M., Petri, T., Lober, D., Nielsen, L.S., Schleuning, W.D., Blasi, F., Appella, E., and Dano, K. The human receptor for urokinase plasminogen activator. NH2-terminal amino acid sequence and glycosylation variants. *J. Biol. Chem.*, 265:6453-6460, 1990

- Bell, R.M., and Burns, D.J. Lipid activation of protein kinase C. *J. Biol. Chem.*, 266:4661-4664, 1991
- Bennet, R.D., and Chow, D.A. Inverse correlation between natural antitumor antibodies and tumor susceptibility in individual xid-bearing mice. *Nat. Immun.*, 10:45-55, 1991
- Beppu, M., Ando, K., and Kikugawa, K. Poly-N-acetyllactosaminyl saccharide chains of band 3 as determinants for anti-band 3 autoantibody binding to senescent and oxidized erythrocytes. *Cell. Mol. Biol. Noisy. le. grand.*, 42:1007-1024, 1996
- Berneman, A., Ternynck, T., and Avrameas, S. Natural mouse IgG reacts with antigens including molecules involved in the immune response. *Eur. J. Immunol.*, 22:625-633, 1992
- Berridge, M.J. Inositol trisphosphate and diacylglycerol: two interacting second messengers. *Annu. Rev. Biochem.*, 56:159-193, 1987
- Bhat, N.M., Kantor, A.B., Bieber, M.M., Stall, A.M., Herzenberg, L.A., and Teng, N.N. The ontogeny and functional characteristics of human B-1 (CD5⁺ B) cells. *Int. Immunol.*, 4:243-252, 1992
- Blackshear, P.J. The MARCKS family of cellular protein kinase C substrates. *J. Biol. Chem.*, 268: 1501-1504, 1993
- Blobe, G.C., Stribling, D.S., Fabbro, D., and Hannum, Y.A. Protein kinase C β II specifically binds to and is activated by F-actin. *J. Biol. Chem.*, 271:15823-15830, 1996
- Bohn, J., Roggenbuck, D., Settmacher, U., Docke, W., Volk, H.D., Von-Baehr, R., and Jahn, S. Binding of natural human IgM auto-antibodies to human tumor cell lines and stimulated normal T lymphocytes. *Immunol. Lett.*, 39: 187-194, 1994
- Borner, C., Guadagno, S.N., Hsieh, L.L., and Weinstein, I.B. Transformation by a ras oncogene causes increased expression of protein kinase C α and decreased expression of protein kinase C ϵ . *Cell Growth & Differ.*, 1:653-660, 1990
- Borner, C., Filipuzzi, I., Weinstein, I.B., and Imber, R. Failure of wild-type or mutant form of protein kinase C α to transform fibroblasts. *Nature*, 353:78-80, 1991
- Borner, C., Guadagno, S.N., Hsiao, W.W., Fabbro, D., Barr, M., and Weinstein, I.B. Expression of four protein kinase C isoforms in rat fibroblasts. Differential alterations in ras-, src-, and fos-transformed cells. *J. Biol. Chem.*, 267:12900-12910, 1992a
- Borner, C., Guadagno, S.N., Fabbro, D., and Weinstein, I.B. Expression of four protein kinase C isoforms in rat fibroblasts. Distinct subcellular distribution and

regulation by calcium and phorbol esters. *J. Biol. Chem.*, 267:12892-12899, 1992b

Borner, C., Ueffing, M., Jaken, S., Parker, P.J., and Weinstein, I.B. Two closely related isoforms of protein kinase C produce reciprocal effects on the growth of rat fibroblasts. Possible molecular mechanisms. *J. Biol. Chem.*, 270:78-86, 1995

Bos, N.A., Kimura, H., Meeuwsen, C.G., De-visser, H., Hazenberg, M.P., Wostmann, B.S., Pleasants, J.R., Benner, R., and Marcus, D.M. Serum immunoglobulin levels and naturally occurring antibodies against carbohydrate antigens in germ-free BALB/c mice fed chemically defined ultrafiltered diet. *Eur. J. Immunol.*, 19:2335-2339, 1989

Bouillion, M., and Audette, M. Transduction of retinoic acid and γ -interferon signal for intercellular adhesion molecule-1 expression on human tumor cell lines: Evidence for the late-acting involvement of protein kinase C inactivation. *Cancer Res.*, 53:826-832, 1993

Boyden, S.V. Natural antibodies and the immune response. *Adv. Immunol.*, 5:1-28, 1965

Boyle, P., Lembach, K.J., and Wetzel, G.D. A novel monoclonal human IgM autoantibody which binds recombinant human and mouse tumor necrosis factor-alpha. *Cell. Immunol.*, 152: 556-568, 1993

Brautigan, D.L., and Pinault, F.M. Activation of membrane protein-tyrosine phosphatase involving cAMP- and Ca^{2+} /phospholipid-dependent protein kinases. *Proc. Natl. Acad. Sci. USA.*, 88:6696-6700, 1991

Briles, D.E., Nahm, M., Schroer, K., Davie, J., Baker, P., Kearney, J., and Barletta, R. Antiphosphocholine antibodies found in normal mouse serum are protective against intravenous infection with type 3 *Streptococcus pneumoniae*. *J. Exp. Med.*, 153:694-705, 1981a

Briles, D.E., Claflin, J.L., Schroer, K., and Forman, C. Mouse IgG3 antibodies are highly protective against infection with *Streptococcus pneumoniae*. *Nature*, 294:88-90, 1981b

Briles, D.E., Nahm, M., Marion, T.N., Perlmutter, R.M., and Davie, J.M. Streptococcal group A carbohydrate has properties of both a thymus-independent (TI-2) and a thymus-dependent antigen. *J. Immunol.*, 128:2032-2035, 1982

Brooks, G., Brooks, S.F., and Goss, M.W. MARCKS functions as a novel growth suppressor in cells of melanocyte origin. *Carcinogenesis*, 17:683-689, 1996

Brown, G.W., and Chow, D.A. Characterization of tumor progression from threshold tumor inocula : evidence for natural resistance. *Int. J. Cancer*, 35:385-393, 1985

Brown, G.W., Lesiuk, T.P., and Chow, D.A. Phenotypic alterations in tumors that developed from threshold subcutaneous inocula. I. Reduced binding of natural antibodies and sensitivity to hypotonic lysis. *J. Immunol.*, 136:3116-3123, 1986

Buday, L., Egan, S.E., Rodriguez-Viciana, P., Cantrell, D.A., and Downward, J. A complex of Grb2 adaptor protein, Sos exchange factor, and a 36-kDa membrane-bound tyrosine phosphoprotein is implicated in ras activation in T cells. *J. Biol. Chem.*, 269: 9019-9023, 1994

Burgering, B.M., Pronk, G.J., Van-weeren, P.C., Chardin, P., and Bos, J.L. cAMP antagonizes p21ras-directed activation of extracellular signal-regulated kinase 2 and phosphorylation of mSoS nucleotide exchange factor. *EMBO. J.*, 12:4211-4220, 1993

Burgering, B.M. and Bos, J.L. Regulation of ras-mediated signalling: more than one way to skin a cat. *Trends. Biochem. Sci.*, 20:18-22, 1995

Bussel, J.B., Kimberly, R.P., Inman, R.D., Schulman, I., Cunningham-Rundles, C., Cheung, N., Smithwick, E.M., O'Malley, J., Barandun, S., and Hilgartner, M.W. Intravenous gammaglobulin treatment of chronic idiopathic thrombocytopenic purpura. *Blood*, 62: 480-486, 1983

Cacace, A.M., Guadagno, S.N., Krauss, R.S., Fabbro, D., and Weinstein, I.B. The epsilon isoform of protein kinase C is an oncogene when overexpressed in rat fibroblasts. *Oncogene*, 8:2095-2104, 1993

Camp, R.L., Kraus, T.A., and Pure, E. Variations in the cytoskeletal interaction and posttranslational modification of the CD44 homing receptor in macrophages. *J. Cell. Biol.*, 115:1283-1292, 1991

Campan, M., Yoshizumi, M., Seidah, N.G., Lee, M.E., Bianchi, C., and Haber, E. Increased proteolytic processing of protein tyrosine phosphatase mu in confluent vascular endothelial cells: the role of PC5, a member of the subtilisin family. *Biochemistry*, 35:3797-3802, 1996

Cantley, L.C., Auger, K.R., Carpenter, C., Duckworth, B., Graziani, A., Kapeller, R., and Soltoff, S. Oncogenes and signal transduction. *Cell*, 64:281-302, 1991

Cao, J., Sato, H., Takino, T., and Seiki, M. The C-terminal region of membrane type matrix metalloproteinase is a functional transmembrane domain required for pro-gelatinase A activation. *J. Biol. Chem.*, 270:801-805, 1995

Carlson, G.A., Melnychuk, D., and Meeker, M.J. H-2 associated resistance to leukemia transplantation antigens: natural killing in vivo. *Int. J. Cancer* 25:111-115, 1980

Carlsson, L., Andersson, A., and Holmberg, D. Germ-line origin of functional idiotypic interactions: identification of two idiotypically connected, natural antibodies that are encoded by germ-line gene elements. *Eur. J. Immunol.*, 21:2285-2288, 1991

Carnero, A., Cuadrado, A., del Peso, L., and Lacal, J.C. Activation of type D phospholipase by serum stimulation and ras-induced transformation in NIH 3T3 cells. *Oncogene*, 9:1387-1395, 1994

Carroll, P., Stafford, D., Schwartz, R.S., and Stollar, B.D. Murine monoclonal anti DNA autoantibodies bind to endogenous bacteria. *J. Immunol.*, 135:1086-1090, 1985

Carroll, M.P. and May, W.S. Protein kinase C-mediated serine phosphorylation directly activates Raf-1 in murine hematopoietic cells. *J. Biol. Chem.*, 269:1249-1256, 1994

Caruso, A., Bonfanti, C., Colombrita, D., De-Francesco, M., De-Rango, C., Foresti, I., Gargiulo, F., Gonzales, R., Gribaudo, G., Landolfo, S., et al. Natural antibodies to IFN-gamma in man and their increase during viral infection. *J. Immunol.*, 144: 685-690, 1990

Caruso, A., Folghera, S., Martinelli, F., and Turano, A. Natural antibodies to interferon-gamma in humans: inhibition of the biological activity of IFN-gamma by human anti-IFN-gamma antibodies. *J. Interferon Res.*, 14: 161-164, 1994

Castronovo, V., Foidart, J.M., Vecchi, M.L., Foidart, J.B., Bracke, M., Mareel, M., and Mahieu, P. Human anti- α -galactosyl IgG reduces the lung colonization by murine MO4 cells. *Invasion Metastasis*, 7:325-345, 1987

Cerutti, P., Hussain, P., Pourzand, C., and Aguilar, F. Mutagenesis of the H-ras protooncogene and the p53 tumor suppressor gene. *Cancer Res.*, 54:1934s-1938s, 1994

Chakavarthy, B.R., Whitfield, J.F., and Durkin, J.P. Inactive membrane protein kinase Cs: a possible target for receptor signalling. *Biochem. J.*, 304:809-816, 1994

Chang, K.J., Lin, J.K., Lee, P.H., Hsieh, Y.S., Cheng, C.K., and Liu, J.Y. The altered activity of membrane-bound protein kinase C in human liver cancer. *Cancer Lett.*, 105:211-215, 1996

Charbonneau, H., and Tonks, N.K. 1002 protein phosphatases? *Annu. Rev. Cell Biol.*, 8:463-493, 1992

Chen, C., Stenzel-Poore, M.P., and Rittenberg, M.B. Natural auto- and polyreactive antibodies differing from antigen-induced antibodies in the H chain CDR3. *J. Immunol.*, 147: 2359-2367, 1991

- Chiarugi, V., Bruni, P., Pasquali, F., Magnelli, L., Basi, G., Ruggiero, M. and Farnararo, M. Synthesis of diacylglycerol de novo is responsible for permanent activation and down-regulation of protein kinase C in transformed cells. *Biochem. Biophys. Res. Commun.*, 164:816-823, 1989
- Chin, J.E., Dickens, M., Tavare, J.M., and Roth, R.A. Overexpression of protein kinase C isoenzymes α , β 1, γ , and ϵ in cells overexpressing the insulin receptor. Effects on receptor phosphorylation and signaling. *J. Biol. Chem.*, 268:6338-6347, 1993
- Chin, J.E., Liu, F., and Roth, R.A. Activation of Protein kinase C α inhibits insulin-stimulated tyrosine phosphorylation of insulin receptor substrate-1. *Mol. Endocrinol.*, 8:51-58, 1994
- Choi, P.M., Tchou-Wong, K.M., and Weinstein, I.B. Overexpression of protein kinase C in HT29 colon cancer cells causes growth inhibition and tumor suppression. *Mol. Cell. Biol.*, 10:4650-4657, 1990
- Chow, D.A., Wolosin, L.B., and Greenberg, A.H. Murine natural antitumor antibodies. II. The contribution of natural antibodies to tumor surveillance. *Int. J. Cancer*, 27:459-469, 1981
- Chow, D.A., Ray, M., and Greenberg, A.H. In vivo generation and selection of variants with altered sensitivity to natural resistance (NR): A model of tumor progression. *Int. J. Cancer* 31:99-105, 1983
- Chow, D.A. Tumor selection in vivo for reduced sensitivity to natural resistance and natural antibodies. *J. Natl. Cancer Inst.*, 72:339-346, 1984a
- Chow, D.A. Variant generation and selection: an in vivo model of tumor progression. *Int. J. Cancer*, 33:541-545, 1984b
- Chow, D.A., and Chan, J. Tumor progression in vitro: The paradoxical natural antibody and complement-selected phenotype. *Nat. Immun. Cell Growth Regul.*, 6:189-204, 1987
- Chow, D.A. and Bennet, R.D. Low natural antibody and low in vivo tumor resistance, in xid-bearing B-cell deficient mice. *J. Immunol.*, 142:3702-3707, 1989
- Chow, D.A., Yuan, X.Y., and Tough, D.F. Polyclonal natural antitumor antibody binding dynamics: preferential release of surface membrane molecules and increased metastasis. *Invasion Metastasis*, 12: 218-232, 1992
- Chow, D.A. Reduced tumorigenicity of threshold syngeneic tumor inocula in xid-bearing mice treated with natural antibodies. *Int. J. Cancer*, 60:848-853, 1995

Cobrinik, D., Dowdy, S.F., Hinds, P.W., Mittnacht, S., and Weinberg, R.A. The retinoblastoma protein and the regulation of cell cycling. *Trends. Biochem. Sci.*, 17:310-315, 1992

Collard, J.G., van Beek, W.P., Janssen, J.W.G., and Schijven, J.F. Transfection by human oncogenes: concomitant induction of tumorigenicity and tumor-associated membrane alterations. *Int. J. Cancer*, 35:207-214, 1985

Collier, I.E., Wilhelm, S.M., Eisen, A.Z., Marmer, B.L., Grant, G.A., and Seltzer, J.L. H-ras oncogene-transformed human bronchial epithelial cells (TBE-1) secrete a single metalloproteinase capable of degrading basement membrane collagen. *J. Biol. Chem.*, 263:6579-6587, 1988

Collins, B.H., Cotterell, A.H., McCurry, K.R., Alvarado, C.G., Magee, J.C., Parker, W., and Platt, J.L. Cardiac xenografts between primate species provide evidence for the importance of the alpha-galactosyl determinant in hyperacute rejection. *J. Immunol.*, 154: 5500-5510, 1995

Conger, J.D., Sage, H.J., and Corley, R.B. Correlation of antibody multireactivity with variable region primary structure among murine anti-erythrocyte autoantibodies. *Eur. J. Immunol.*, 22: 783-790, 1992

Constant, S., Schweitzer, N., West, J., Ranney, P., and Bottomly, K. B lymphocytes can be competent antigen-presenting cells for priming CD4⁺ T cells to protein antigens in vivo. *J. Immunol.*, 155: 3734-3741, 1995

Cool, D.E., and Fisher, E.H. Protein tyrosine phosphatases in cell transformation. *Sem. Cell Biol.*, 4:443-453, 1993

Cooper, D.R., Watson, J.E., Acevedo-Duncan, M., Pollet, R.J., Standaert, M.L., and Farese, R.V. Retention of specific protein kinase C isozymes following chronic phorbol ester treatment in BC3H-1 myocytes. *Biochem. Biophys. Res. Commun.*, 161:327-334, 1989

Correas, I., Diaz-Nido, J., and Avila, J. Microtubule-associated protein tau is phosphorylated by protein kinase C on its tubulin binding domain. *J. Biol. Chem.*, 267:15721-15728, 1992

Courtneidge, S.A. Protein tyrosine kinases, with emphasis on the src family. *Cancer Biol.*, 5:239-246, 1994

Coussens, L., Rhee, L., Parker, P.J., and Ullrich, A. Alternative splicing increases the diversity of the human protein kinase C family. *DNA*, 6:389-394, 1987

- Coutinho, A. Beyond clonal selection and network. *Immunol. Rev.*, 110:63-87, 1989
- Cox, K.O., and Hardy, S.J. Autoantibodies against mouse bromelain-modified RBC are specifically inhibited by a common membrane phospholipid, phosphatidylcholine. *Immunol.*, 55: 263-269, 1985
- Cox, A.D., and Der, C.J. Protein prenylation: more than just glue? *Curr. Opin. Cell Biol.*, 4:1008-1016, 1992
- Cukrowska, B., Sinkora, J., Rehakova, Z., Sinkora, M., Splichal, I., Tuckova, L., Avrameas, S., Saalmuller, A., Barot-Ciorbaru, R., and Tlaskalova-Hogenova, H. Isotype and antibody specificity of spontaneously formed immunoglobulins in pig fetuses and germ-free piglets: production by CD5⁻ B cells. *Immunol.*, 88: 611-617, 1996
- Daum, G., Eisenmann-Tappe, I., Fries, H.W., Troppmair, J., and Rapp, U.R. The ins and outs of Raf kinases. *Trends. Biochem. Sci.*, 19:474-480, 1994
- Daum, G., Regenass, S., Sap, J., Schlessinger, J., and Fisher, E.H. Multiple forms of the human tyrosine phosphatase RPTP α . Isozymes and differences in glycosylation. *J. Biol. Chem.*, 269:10524-10528, 1994
- David, K., Ollert, M.W., Juhl, H., Vollmert, C., Erttmann, R., Vogel, C.W., and Bredehorst, R. Growth arrest of solid human neuroblastoma xenografts in nude rats by natural IgM from healthy humans. *Nat. Med.*, 2:686-689, 1996
- Davis, R.J., and Czech, M.P. Tumor promoting phorbol esters mediate phosphorylation of the epidermal growth factor receptor. *J. Biol. Chem.*, 259:8545-8549, 1984
- Davis, R.J., Jonhson, G.L., Kelleher, D.J., Anderson, J.K., Mole, J.e., and Czech, M.P. Identification of serine 24 as the unique site on the transferrin receptor phosphorylated by protein kinase C. *J. Biol. Chem.*, 261:9034-9041, 1986
- de Vries, J.E., ten Kate, J., and Bosman, F.T. p21^{ras} in carcinogenesis. *Path. Res. Pract.*, 192:658-668, 1996
- Deans, J.P., Serra, H.M., Shaw, J., Shen, Y.J., Torres, R.M., and Pilarski, L.M. Transient accumulation and subsequent rapid loss of messenger RNA encoding high molecular mass CD45 isoforms after T cell activation. *J. Immunol.* 148:1898-1905, 1992
- Dedeoglu, F., Kaymaz, H., Klein, G., and Marchalonis, J.J. Light and heavy chains specifying a human IgM kappa autoantibody to a T-cell receptor V beta-antigen. *Immunol. Lett.*, 38: 223-227, 1993
- Delage, S., Chastre, E., Empeur, S., Wicek, D., Veissiere, D., Capeau, J., Gespach, C., and Cherqui, G. Increased protein kinase C alpha expression in human colonic

Caco-2 cells after insertion of human Ha-ras or polyoma virus middle T oncogenes. *Cancer Res.*, 53: 2762-2770, 1993

Delphin, C., and Baudier, J. The protein kinase C activator, phorbol ester, cooperates with the wild-type p53 species of Ras-transformed embryo fibroblasts growth arrest. *J. Biol. Chem.*, 269:29579-29587, 1994

den Hertog, J., Pals, C.E.G.M., Peppelenbosch, M.P., Tertoolen, L.G.J., de Laat, S.W., and Kruijer, W. Receptor protein-tyrosine phosphatase α activates pp60^{c-src} and is involved in neuronal differentiation. *EMBO J.*, 13:3789-3798, 1993

den-Hertog, J., Sap, J., Pals, C.E., Schlessinger, J., and Kruijer, W. Stimulation of receptor protein-tyrosine phosphatase alpha activity and phosphorylation by phorbol ester. *Cell. Growth. Differ.*, 6: 303-307, 1995

DeNofrio, D., Koock, T.C., and Herman, I.M. Functional sorting of actin isoforms in microvascular pericytes. *J. Cell Biol.*, 109:191-202, 1989

Diaw, L., Magnac, C., Pritsch, O., Buckle, M., Alzari, P.M., and Dighiero, G. Structural and affinity studies of IgM polyreactive natural autoantibodies. *J. Immunol.*, 158: 968-976, 1997

Diaz-Laviada, I., Larrodera, P., Diaz-Meco, M.T., Cornet, M.E., Guddal, P.H., Johansen, T., and Moscat, J. Evidence for a role of phosphatidylcholine-hydrolysing phospholipase C in the regulation of protein kinase C by ras and src oncogenes. *EMBO J.*, 9:3907-3912, 1990

Dicou, E., and Nerriere, V. Evidence that natural autoantibodies against the nerve growth factor (NGF) may be potential carriers of NGF. *J. Neuroimmunol.*, 75: 200-203, 1997

Dietrich, G., and Kazatchkine, M.D. Normal immunoglobulin G (IgG) for therapeutic use (intravenous Ig) contain antiidiotypic specificities against an immunodominant, disease-associated, cross-reactive idiotype of human anti-thyroglobulin autoantibodies. *J. Clin. Invest.*, 85: 620-625, 1990

Dietrich, G., Kaveri, S.V., and Kazatchkine, M.D. A V region-connected autoreactive subfraction of normal human serum immunoglobulin G. *Eur. J. Immunol.*, 22:1701-1706, 1992

Dietrich, G., Varela, F.J., Hurez, V., Bouanani, M., and Kazatchkine, M.D. Selection of the expressed B cell repertoire by infusion of normal immunoglobulin G in a patient with autoimmune thyroiditis. *Eur. J. Immunol.*, 23: 2945-1950, 1993

Dighiero, G., Lymberi, P., Mazie, J.C., Rouyre, S., Butler-Browne, G.S., Whalen, R.G., and Avrameas, S. Murine hybridomas secreting natural monoclonal antibodies reacting with self antigens. *J. Immunol.*, 131:2267-2272, 1983

Dighiero, G. Natural autoantibodies, tolerance, and autoimmunity. *Ann. N.Y. Acad. Sci.*, 815: 182-192, 1997

Dilmon, R.D. Monoclonal antibodies in the treatment of cancer. *CRC Crit. Rev. Oncol. Hematol.*, 1:357-385, 1984

Donehower, L.A., and Bradley, A. The tumor suppressor p53. *Biochim. Biophys. Acta*, 1155:181-205, 1993

Downward, J., Waterfield, M.D., and Parker, P.J. Autophosphorylation and protein kinase C phosphorylation of the epidermal growth factor receptor. Effect on tyrosine kinase activity and ligand binding affinity. *J. Biol. Chem.*, 260:14538-14546, 1985

Drust, D.S., and Martin, T.F. Protein kinase C translocates from cytosol to membrane upon hormone activation: effects of thyrotropin-releasing hormone in GH3 cells. *Biochem. Biophys. Res. Commun.*, 128:531-537, 1985

Dunn, S.D. Effects of the modification of transfer buffer composition and the renaturation of proteins in gels on the recognition of proteins on Western blots by monoclonal antibodies. *Anal. Biochem.*, 157:144-153, 1986

Dwyer-Nield, L.D., Miller, A.C.K., Neighbors, B.W., Dinsdale, D., and Malkinson, A.M. Cytoskeletal architecture in mouse lung epithelial cells is regulated by protein kinase C- α and calpain II. *Am. J. Physiol.*, 270:L526-L534, 1996

Egan, S.E., Spearman, M.A., Robert, J.J., Levy, A.B., Wright, J.A., and Greenberg, A.H. myc/ras cooperation is insufficient for metastatic transformation. (Abstract) *J. Cell. Biochem.* 13B:62, 1989

Ehrlich, R., Smorodinsky, N., Efrati, M., Yaakubowicz, M., and Witz, I.P. B16 melanoma development, NK activity cytostasis and natural antibodies in 3 and 12 month old mice. *Br. J. Cancer*, 49:769-777, 1984

Eldar, H., Zisman, Y., Ullrich, A., and Livneh, E. Overexpression of protein kinase C α -subtype in Swiss/3T3 fibroblasts causes loss of both high and low affinity receptor numbers for epidermal growth factor. *J. Biol. Chem.*, 265:13290-13296, 1990

Exton, J.H. Regulation of phosphoinositide phospholipase by hormones, neurotransmitters, and other agonists linked to G proteins. *Annu. Rev. Pharmacol. Toxicol.*, 36:481-509, 1996

Forsgren, S., Andersson, A., Hillorn, V., Soderstrom, A., and Holmberg, D. Immunoglobulin-mediated prevention of autoimmune diabetes in the non-obese diabetic (NOD) mouse. *Scand. J. Immunol.*, 34:445-451, 1991

Fu, T., Sugimoto, Y., Oki, T., Murakami, S., Okano, Y., and Nozawa, Y. Calcium oscillation associated with reduced protein kinase C activities in ras-transformed NIH3T3 cells. *FEBS Lett.*, 281:263-266, 1991

Gaits, F., Li, R.Y., Ragab, A., Ragab-Thomas, J.M., and Chap, H. Increase in receptor-like protein tyrosine phosphatase activity and expression level on density-dependent growth arrest of endothelial cells. *Biochem. J.*, 311:97-103, 1995

Galeotti, T., Boscobinik, D., and Azzi, A. Regulation of the TNF- α receptor in human osteosarcoma cells: role of microtubules and of protein kinase C. *Arch. Biochem. Biophys.*, 300:287-292, 1993

Galili, U., Rachmilewitz, E.A., Peleg, A., and Flechner, I. A unique natural human IgG antibody with anti-alpha-galactosyl specificity. *J. Exp. Med.* 160: 1519-1531, 1984

Galili, U., Flechner, I., and Rachmilewitz, E.A. A naturally occurring anti-alpha-galactosyl IgG recognizing senescent human red cells. *Prog. Clin. Biol. Res.*, 195: 263-278, 1985

Galili, U. Interaction of the natural anti-Gal antibody with alpha-galactosyl epitopes: a major obstacle for xenotransplantation in humans. *Immunol. Today*, 14: 480-482, 1993

Galili, U., and LaTemple, D.C. Natural anti-Gal antibody as a universal augments of autologous tumor vaccine immunogenicity. *Immunol. Today*, 18: 281-285, 1997

Gershon, H. Is the sequestration of aged erythrocytes mediated by natural autoantibodies?
Isr. J. Med. Sci., 28: 818-828, 1992

Ghosh, S., and Baltimore, D. Activation in vitro of NF-kappa B by phosphorylation of its inhibitor I kappa B. *Nature*, 344:678-682, 1990

Gil, J., Alvarez, R., Vinuela, J.E., Ruiz-de-Morales, J.G., Bustos, A., De-la-Concha, E.G., and Subiza, J.L. Inhibition of in vivo tumor growth by a monoclonal IgM antibody recognizing tumor cell surface carbohydrates. *Cancer Res.*, 50: 7301-5306, 1990

Gimond, C., de-Melker, A., Aumailley, M., and Sonnenberg, A. The cytoplasmic domain of alpha 6A integrin subunit is an in vitro substrate for protein kinase C. *Exp. Cell. Res.*, 216:232-235, 1995

Giunciuglio, D., Culty, M., Fassina, G., Masiello, L., Melchiori, A., Paglialunga, G., Arand, G., Ciardiello, F., Basolo, F., Thompson, E.W., et al. Invasive phenotype of MCF10A cells overexpressing c-Ha-ras and c-erbB-2 oncogenes. *Int. J. Cancer*, 63:815-822, 1995

Goetzl, E.J., Banda, M.J., and Leppert, D. Matrix metalloproteinases in immunity. *J. Immunol.*, 156:1-4, 1996

Goldstein, D.R., Cacace, A.M., and Weinstein, I.B. Overexpression of protein kinase C beta 1 in the SW480 colon cancer cell line causes growth suppression. *Carcinogenesis*, 16:1121-1126, 1995

Gomez, J., Martinez-de-Aragon, A., Bonay, P., Garcia, A., Silva, A., Fresno, M., Alvarez, F. and Rebollo, A. Physical association and functional relationship between protein kinase C zeta and the actin cytoskeleton. *Eur. J. Immunol.*, 25:2673-2678, 1995

Gonzalez, R., Matsiota, P., Torchy, C., De-Kinkelin, P., and Avrameas, S. Natural anti-TNP antibodies from rainbow trout interfere with viral infection in vitro. *Res. Immunol.*, 140: 675-684, 1989

Gonzalez-Quintial, R., Baccala, R., Alzari, P.M., Nahmias, C., Mazza, G., Fougereau, M., and Avrameas, S. Poly(Glu60Ala30Tyr10) (GAT)-induced IgG monoclonal antibodies cross-react with various self and non-self antigens through the complementarity determining regions. Comparison with IgM monoclonal polyreactive natural antibodies. *Eur. J. Immunol.*, 20: 2383-2387, 1990

Good, A.H., Cooper, D.K., Malcolm, A.J., Ippolito, R.M., Koren, E., Neethling, F.A., Ye, Y., Zuhdi, N., and Lamontagne, L.R. Identification of carbohydrate structures that bind human antiporcine antibodies: implications for discordant xenografting in humans. *Transplant Proc.*, 24:559-562, 1992

Goodnight, J., Mischak, H., and Mushinski, J.F. Selective involvement of protein kinase C isozymes in differentiation and neoplastic transformation. *Adv. Cancer Res.*, 64:159-209, 1994

Goodnight, J.A., Mischak, H.M., Kolch, W., and Mushinski, J.F. Immunocytochemical localization of eight protein kinase C isoenzymes overexpressed in NIH 3T3 fibroblasts. Isoform-specific association with microfilaments, Golgi, endoplasmic reticulum, and nuclear and cell membranes. *J. Biol. Chem.*, 270:9991-10001, 1995

Greenberg, A.H., Chow, D.A., and Wolosin, L.B. Natural antibodies: origin, genetics, specificity and role in host resistance to tumors. *Clin. Immunol. Allergy*, 3:389-420, 1983

Griffioen, M., Peltenburg, L.T., van-Oorschot, D.A., Schrier, P.I. C-myc represses

transiently transfected HLA class I promoter sequences not locus-specifically. *Immunobiology*, 193:238-247, 1995

Gruenstein, E., Rich, A., and Weihing, R.R. Actin-associated with membranes from 3T3 mouse fibroblast and HeLa cells. *J. Cell. Biol.*, 64:223-234, 1975

Guillem, J.G., O'brian, C.A., Fitzer, C.J., Forde, K.A., Logerfo, P., Treat, M., and Weinstein, I.B. Altered levels of protein kinase C and Ca²⁺-dependent protein kinases in human colon carcinomas. *Cancer Res.*, 47:2036-2039, 1987

Gur, H., Geppert, T.D., and Lipsky, P.E. Structural analysis of class I MHC molecules: the cytoplasmic domain is not required for cytoskeletal association, aggregation and internalization. *Mol. Immunol.*, 34:125-132, 1997

Hagiwara, M., Hachiya, T., Watanabe, M., Usuda, N., Iida, F., Tamai, K., and Hidaka, H. Assessment of protein kinase C isozymes by enzyme immunoassay and overexpression of type II in thyroid adenocarcinoma. *Cancer Res.*, 50:5515-5519, 1990

Haliotis, T., Trimble, W., Chow, S., Mills, G., Girard, P., Kuo, J.F., Govindji, N., and Hozumi, N. The cell biology of ras-induced transformation: Insights from studies utilizing an inducible hybrid oncogene system. *Anticancer Res.*, 8:935-946, 1988

Hanania, N., Lezenes, J.R., and Castagna, M. Tumorigenicity-associated expression of protein kinase C isoforms in rhabdomyosarcoma-derived cells. *FEBS Lett.*, 303:15-18, 1992

Hansen, M.B., Svenson, M., Abell, K., Varming, K., Nielsen, H.P., Bertelsen, A., and Bendtzen, K. Sex- and age-dependency of IgG auto-antibodies against IL-1 alpha in healthy humans. *Eur. J. Clin. Invest.*, 24: 212-218, 1994

Hardie, R.C., Peretz, A., Suss-Toby, E., Rom-Glas, A., Bishop, S.A., Selinger, Z., and Minke, B. Protein kinase C is required for light adaptation in *Drosophila* photoreceptors. *Nature*, 363:634-637, 1993

Hartwig, J.H., Thelen, M., Rosen, A., Janmey, P.A., Nairn, A.C., and Aderem, A. MARCKS is an actin filament crosslinking protein regulated by protein kinase C and calcium-calmodulin. *Nature*, 356:618-622, 1992

Haury, M., Sundblad, A., Grandien, A., Barreau, C., Coutinho, A., and Nobrega, A. The repertoire of serum IgM in normal mice is largely independent of external antigenic contact. *Eur. J. Immunol.*, 27: 1557-1563, 1997

Hausmann, S., Claus, R., and Walzel, H. Short-term culture of surface-biotinylated cells: application in non-radioactive analysis of surface protein shedding. *Immunol. Lett.*,

48:175-180, 1995

Hauss, P., Mazerolles, F., Hivroz, C., Lecomte, O., Barbat, C., and Fischer, A. GF109203X, a specific PKC inhibitor, abrogates anti-CD3 antibody-induced upregulation of CD4⁺ T cell adhesion to B cells. *Cell. Immunol.*, 150:439-446, 1993

Hei, T.K., Krauss, R.S., Liu, S.X., Hall, E.J., and Weinstein, I.B. Effects of increased expression of protein kinase C on radiation-induced cell transformation. *Carcinogenesis* 15:365-370, 1994

Herget, T., Broad, S., and Rozengurt, E. Overexpression of the myristoylated alanine-rich C-kinase substrate in Rat1 cells increases sensitivity to calmodulin antagonists. *Eur. J. Biochem.*, 225:549-556, 1994

Herlyn, D., Herlyn, M., Steplewski, Z., and Koprowski, H. Monoclonal anti-human tumor antibodies of six isotypes in cytotoxic reactions with human and murine effector cells. *Cell. Immunol.*, 92:105-114, 1985

Herlyn, M., and Satyamoorthy, K. Activated ras, yet another player in melanoma? *Am. J. Pathol.*, 149:739-744, 1996

Hibbs, M.S., Hasty, K.A., Seyer, J.M., Kang, A.H., and Mainardi, C.L. Biochemical and immunological characterization of the secreted forms of human neutrophil gelatinase. *J. Biol. Chem.*, 260:2493-2500, 1985

Hidaka, H., Inagaki, M., Kawamoto, S., and Sasaki, Y. Isoquinolinesulfonamides, novel and potent inhibitors of cyclic nucleotide dependent protein kinase and protein kinase C. *Biochemistry* 23:5036-5041, 1984

Hintner, H., Romani, N., Stanzl, U., Grubauer, G., Fritsch, P., and Lawley, T.J. Phagocytosis of keratin filament aggregates following opsonization with IgG-anti-keratin filament autoantibodies. *J. Invest. Dermatol.*, 88:176-182, 1987

Hocevar, B.A., Burns, D.J., and Fields, A.P. Identification of protein kinase C (PKC) phosphorylation sites on human lamin B. Potential role of PKC in nuclear lamina structural dynamics. *J. Biol. Chem.*, 268:7545-7552, 1993

Hofmann, M., Rudy, W., Gunthert, U., Zimmer, S.G., Zawadzki, V., Zoller, M., Lichtner, R.B., Herrlich, P., and Ponta, H. A link between ras and metastatic behavior of tumor cells: ras induces CD44 promoter activity and leads to low-level expression of metastasis-specific variants of CD44 in CREB cells. *Cancer Res.*, 53:1516-1521, 1993

Hogervorst, F., Admiraal, L.G., Niessen, C., Kuikman, I., Janssen, H., Daams, H., and Sonnenberg, A. Biochemical characterization and tissue distribution of the A and

- B variants of the integrin alpha 6 subunit. *J. Cell. Biol.*, 121:179-191, 1993
- Holmberg, D., Forsgren, S., Ivars, F., and Coutinho, A. Reactions among IgM antibodies derived from normal, neonatal mice. *Eur. J. Immunol.*, 14:435-441, 1984
- Hoock, T.C., Newcomb, P.M., and Herman, I.M. β actin and its mRNA are localized at the plasma membrane and the regions of moving cytoplasm during the cellular response to injury. *J. Cell Biol.*, 112:653-664, 1991
- Hopefield, J.F., Tank, D.W., Greengard, P., and Huganir, R.L. Functional modulation of the nicotinic acetylcholine receptor by tyrosine phosphorylation. *Nature*, 336:677-680, 1988
- Hornick, C.L., and Karush, F. Antibody affinity. III. The role of multivalence. *Immunochemistry*, 9:325-340, 1972
- Housey, G.M., Johnson, M.D., Hsiao, W.L., O'brian, C.A., Murphy, J.P., Kirschmeier, P., and Weinstein, I.B. Overproduction of protein kinase C causes disordered growth control in rat fibroblasts. *Cell*, 52:343-354, 1988
- Hsiao, W.L., Lopez, C.A., Wu, T., and Weinstein, I.B. A factor present in fetal calf serum enhances oncogene-induced transformation of rodent fibroblasts. *Mol. Cell. Biol.* 7:3380-3385, 1987
- Hsiao, W.-L.W., Housey, G.M., Johnson, M.D., and Weinstein, I.B. Cells that overproduce protein kinase C are more susceptible to transformation by an activated H-ras oncogene. *Mol. Cell. Biol.* 9:2641-2647, 1989
- Huang, M., Chida, K., Kamata, N., Nose, K., Kato, M., Homma, Y., Takenawa, T., and Kuroki, T. Enhancement of inositol phospholipid metabolism and activation of protein kinase C in ras-transformed rat fibroblasts. *J. Biol. Chem.*, 263:17975-17980, 1988
- Hunter, T., Ling, N., and Cooper, J.A. Protein kinase C phosphorylation of the EGF receptor at a threonine residue close to the cytoplasmic face of the plasma membrane. *Nature*, 311:480-483, 1984
- Hupp, T.R., and Lane, D.P. Allosteric activation of latent p53 tetramers. *Curr. Biol.*, 4:865-875, 1994
- Huppi, K., Siwarski, D., Goodnight, J., and Mischak, H. Assignment of the protein kinase C delta polypeptide gene (PRKCD) to human chromosome 3 and mouse chromosome 14. *Genomics*, 19:161-162, 1994

Hurez, V., Kaveri, S.V., Mouhoub, A., Dietrich, G., Mani, J.C., Klatzmann, D., and Kazatchkine, M.D. Anti-CD4 activity of normal human immunoglobulin G for therapeutic use. (Intravenous immunoglobulin, IVIg). *Ther. Immunol.*, 1: 269-277, 1994

Isacke, C.M., Meisenhelder, J., Brown, K.D., Gould, K.L., Gould, S.J., and Hunter, T. Early phosphorylation events following the treatment of Swiss 3T3 cells with bombesin and the mammalian bombesin-related peptide, gastrin-releasing peptide. *EMBO J.*, 5:2889-2898, 1986

Isumi, T., Tamemoto, H., Nagao, M., Kadowaki, T., Takaku, F., and Kasuga, M. Insulin and platelet-derived growth factors stimulate phosphorylation of the c-RAF product at serine and threonine residues in intact cells. *J. Biol. Chem.*, 266:7933-7939, 1991

Itaya, T., Moriuchi, T., Kodama, T., Sendo, F., and Kobayashi, H. Naturally occurring antibodies against fibrosarcoma and glioma cells in rats. *Gann*, 73:454-461, 1982

Iwata, M., Iseki, R., Sato, K., Tozawa, Y., and Ohoka, Y. Involvement of protein kinase C-epsilon in glucocorticoid-induced apoptosis in thymocytes. *Int. Immunol.*, 6:431-438, 1994

Jamal, H.H., Cano-Gauci, G.F., Buick, R.N., and Filmus, J. Activated ras and src induce CD44 overexpression in rat intestinal epithelial cells. *Oncogene*, 9:417-423, 1994

Johannes, F.J., Prestle, J., Eis, S., Oberhagemann, P., and Pfizenmaier, K. PKC μ is a novel, atypical member of the protein kinase C family. *J. Biol. Chem.*, 269:6140-6148, 1994

Judware, R., and Culp, L.A. Concomitant down-regulation of expression of integrin subunits by N-myc in human neuroblastoma cells: differential regulation of alpha2, alpha3 and beta1. *Oncogene*, 14:1341-1350, 1997

Jung, T.M., and Dailey, M.O. Rapid modulation of homing receptors (gp90^{MEL-14}) induced by activators of protein kinase C. Receptor shedding due to accelerated proteolytic cleavage at the cell surface. *J. Immunol.*, 144:3130-3136, 1990

Kaibuchi, K., Fukumoto, Y., Oku, N., Takai, Y., Arai, K., and Muramatsu, M. Molecular genetic analysis of the regulatory and catalytic domains of protein kinase C. *J. Biol. Chem.*, 264:13489-13496, 1989

Kassel, R.L., Old, L.J., Day, N.K., and Hardy, W.D.Jr. Plasma mediated leukemia cell destruction: concentration and purification of the antileukemia factor. *Proc. Soc. Exp. Bio. Med.*, 155:230-233, 1977

Kawada, K., and Terasaki, P.I. Evidence for immunosuppression by high dose gammaglobulin. *Exp. Hematol.*, 15:133-136, 1987

Kawaguchi, T., Ono, T., Wakabayashi, H., and Igarashi, S. Cell surface laminin-like substances and laminin-related carbohydrates of rat ascites hepatoma AH7974 and its variants with different lung-colonizing potential. *Clin. Exp. Metastasis*, 12:203-212, 1994

Kawamoto, S., and Hidaka, H. 1-(5-Isoquinolinesulfonyl)-2-methylpiperazine (H-7) is a selective inhibitor of protein kinase C in rabbit platelets. *Biochem. Biophys. Res. Commun.* 125:258-264, 1984

Kay, M.M.B. Role of physiological autoantibody in the removal of senescent human red cells. *J. Surpramol. Struct.*, 9:555-567, 1978

Kazanietz, M.G., Krausz, K.W., and Blumberg, P.M. Differential irreversible insertion of protein kinase C into phospholipid vesicles by phorbol esters and related activators. *J. Biol. Chem.*, 267:20878-20886, 1992

Kearney, J.F., Solvason, N., Bloem, A., and Vakil, M. Idiotypes and B cell development. *Chem. Immunol.*, 48:1-13, 1990

Keränen, L.M., Dutil, E.M., and Newton, A.C. Protein kinase C is regulated in vivo by three functionally distinct phosphorylations. *Curr. Biol.*, 5:1394-1403, 1995

Khan, W.N., Sideras, P., Rosen, F.S., and Alt, F.M. The role of Bruton's tyrosine kinase in B-cell development and function in mice and man. *Ann. N.Y. Acad. Sci.*, 764:27-38, 1995

Khansari, N., and Fudenberg, H.H. Immune elimination of aging platelets by autologous monocytes: role of membrane-specific autoantibody. *Eur. J. Immunol.*, 13: 990-994, 1983

Kiley, S.C., Parker, P.J., Fabbro, D., and Jaken, S. Differential regulation of protein kinase C isozymes by thyrotropin-releasing hormone in GH4C1 cells. *J. Biol. Chem.*, 266:23761-23768, 1991

Kinoh, H., Sato, H., Tsunozuka, Y., Takino, T., Kawashima, A., Okada, Y., and Seiki, M. MT-MMP, the cell surface activator of proMMP-2 (pro-gelatinase A), is expressed with its substrate in mouse tissue during embryogenesis. *J. Cell Sci.*, 109:953-959, 1996

Kishimoto, A., Mikawa, K., Hashimoto, K., Yasuda, I., Tanaka, S., Tominaga, M., Kuroda, T. and Nishizuka, Y. Limited proteolysis of protein kinase C subspecies by calcium-dependent neutral protease (calpain). *J. Biol. Chem.*, 264:4088-4092, 1989

- Kiss, K., Uher, F., and Gergely, J. A natural IgM antibody does inhibit polyclonal and antigen-specific IgM but not IgG B-cell responses. *Immunol. Lett.*, 39:235-241, 1994
- Kolch, W., Heidecker, G., Kochs, G., Hummel, R., Vahidi, H., Mischak, H., Finkenzeller, G., Marme, D., and Rapp, U.R. Protein kinase C α activates RAF-1 by direct phosphorylation. *Nature*, 364:249-252, 1993
- Kopp, R., Noelke, B., Sauter, G., Schildberg, F.W., Paumgartner, G., and Pfeiffer, A. Altered protein kinase C activity in biopsies of human colonic adenomas and carcinomas. *Cancer, Res.*, 51:205-210, 1991
- Kose, A., Ito, A., Saito, N., and Tanaka, C. Electron microscopic localization of gamma- and beta II-subspecies of protein kinase C in rat hippocampus. *Brain Res.*, 518:209-217, 1990
- Kraft, A.S., and Anderson, W.B. Phorbol esters increase the amount of Ca²⁺, phospholipid-dependent protein kinase associated with plasma membrane. *Nature*, 301:621-623, 1983
- Krauss, R.S., Housey, G.M., Johnson, M.D., and Weinstein, I.B. Disturbances in growth control and gene expression in a C3H/10T1/2 cell line that stably overproduces protein kinase C. *Oncogene* 4: 991-998, 1989
- Kruger, M., Rodriguez, E., Killion, C., McLaughlin-Taylor, E., and Goodenow, R. Identification and isolation of anti-T cell receptor antibodies in gammagard. In: *Intravenous IVIg: Current status of clinical applications and research topics*. Lisbon (Abstract), 1993
- Kuranami, M., Cohen, A.M., and Guillem, J.G. Analyses of protein kinase C isoform expression in a colorectal cancer liver metastasis model. *Am. J. Surg.*, 169:57-64, 1995
- Lacal, J.C., Fleming, T.P., Warren, B.S., Blumberg, P.M., and Aaronson, S.A. Involvement of functional protein kinase C in the mitogenic response to the H-ras oncogene product. *Mol. Cell. Biol.*, 7:4146-4149, 1987
- Lacroix-Desmazes, S., Mouthon, L., Coutinho, A., and Kazatchkine, M.D. Analysis of the natural human IgG antibody repertoire: life-long stability of reactivities towards self antigens contrasts with age-dependent diversification of reactivities against bacterial antigens. *Eur. J. Immunol.*, 25:2598-2604, 1995
- Lamb, R.F., Hennigan, R.F., Turnbull, K., Katsanakis, K.D., MacKenzie, E.D., Birnie, G.D., and Ozanne, B.W. AP-1-mediated invasion requires increased expression of the hyaluronan receptor CD44. *Mol. Cell Biol.*, 17:963-976, 1997

Land, H., Parada, L.F., and Weinberg, R.A. Tumorigenic conversion of primary embryo fibroblasts requires at least two cooperating oncogenes. *Nature*, 304:596-602, 1983

Landsteiner, K. *The Specificity of Serological Reactions*. Volume 27, pp357-371. Harvard University Press, Cambridge, Massachusetts. 1900

LaTemple, D.C., Henion, T.R., Anaraki, F., and Galili, U. Synthesis of alpha-galactosyl epitopes by recombinant alpha1,3galactosyl transferase for opsonization of human tumor cell vaccines by anti-galactose. *Cancer Res.*, 56: 3069-3074, 1996

La Thangue, N.B. DP and E2F proteins: components of a heterodimeric transcription factor implicated in cell cycle control. *Curr. Opin. Cell Biol.*, 6:443-450, 1994

Lee, M.H., and Bell, R.M. The lipid binding, regulatory domain of protein kinase C. A 32-KDa fragment contains the calcium- and phosphatidylserine-dependent phorbol ester binding activity. *J. Biol. Chem.*, 261:14867-14870, 1986

Lee, M.W., and Severson, D.L. Signal transduction in vascular smooth muscle: diacylglycerol second messengers and PKC action. *Am. J. Physiol.* 267:C659-C678, 1994

Leever, S.J., Paterson, H.F., and Marshall, C.J. Requirement for Ras in Raf activation is overcome by targeting Raf to the plasma membrane. *Nature*, 369:411-414, 1994

Leon, J., Guerrero, I., and Pellicer, A. Differential expression of the ras gene family in mice. *Mol. Cell. Biol.*, 7:1535-1540, 1987

Leung, D.Y., Burns, J.C., Newberger, J.W., and Geha, R.S. Reversal of lymphocyte activation in vivo in the kawasaki syndrome by intravenous gammaglobulin. *J. Clin. Invest.* 79:468-472, 1987

Levine, A.J. p53, the cellular gatekeeper for growth and division. *Cell*, 88:323-331, 1997

Levy, M.F., Pocsidio, J., Guillem, J.G., Forde, K., LoGerfo, P., and Weinstein, I.B. Decreased levels of protein kinase C enzyme activity and protein kinase C mRNA in primary colon tumors. *Dis. Colon. Rectum.*, 36:913-921, 1993

Li, S., Janosch, P., Tanji, M., Rosenfeld, G.C., Waymire, J.C., Mischak, H., Kolch, W., and Sedivy, J.M. Regulation of Raf-1 kinase activity by the 14-3-3 family of proteins. *EMBO J.*, 14:685-696, 1995

Lidar, T., Christian, A., Yakar, S., Langevitz, P., Zeilig, G., Ohry, A., Bakimer, R.,

Sorek, H., and Livneh, A. Clinically insignificant (natural) autoantibodies against acetyl cholinesterase in the sera of patients with a variety of neurologic, muscular and autoimmune diseases. *Immunol. Lett.*, 55: 79-84, 1997

Ling, Z.D., Yeoh, E., Webb, B.T., Farrell, K., Doucette, J., and Matheson, D.S. Intravenous immunoglobulin induces interferon-gamma and interleukin-6 in vivo. *J. Clin. Immunol.*, 13: 302-309, 1993

Liu, B., Renaud, C., Nelson, K.K., Chen, Y.Q., Bazaz, R., Kowynia, J., Timar, J., Diglio, C.A., and Honn, K.V. Protein kinase C inhibitor calphostin C reduces B16 amelanotic melanoma cell adhesion to endothelium and lung colonization. *Int. J. Cancer*, 52:147-152, 1992

Livneh, E., and Fishman, D.D. Linking protein kinase C to cell-cycle control. *Eur. J. Biochem.*, 248:1-9, 1997

Livneh, E., Shimon, T., Bechor, E., Doki, Y., Schieren, I., and Weinstern, I.B. Linking protein kinase C to the cell cycle: ectopic expression of PKC- η in NIH-3T3 cells alters the expression of cyclins and Cdk inhibitors and induces adipogenesis. *Oncogene*, 12:1545-1555, 1996

Lowy, D.R., and Willumsen, B.M. Function and regulation of ras. *Annu. Rev. Biochem.*, 62:851-891, 1993

Lutz, H.U. Red cell clearance (a review). *Biomed. Biochim. Acta*, 46: S65-71, 1987

Lydyard, P.M., Quartey-Papafio, R., Broker, B., Mackenzie, L., Jouquan, J., Blaschek, M.A., Steele, J., Petrou, M., Collins, P., Isenberg, D., et al. The antibody repertoire of early human B cells. I. High frequency of autoreactivity and polyreactivity. *Scand. J. Immunol.*, 31:33-43, 1990

Macdonald, S.G., Crews, C.M., Wu, L., Driller, J., Clark, R., Erikson, R.L., and McCormick, F. Reconstitution of the Raf-1-MEK-ERK signal transduction pathway in vitro. *Mol. Cell. Biol.*, 13:6615-6620, 1993

Mae, N., Liberato, D.J., Chizzonite, R., and Satoh, H. Identification of high-affinity anti-IL-1 α autoantibodies in normal human serum as an interfering substance in a sensitive enzyme-linked immunosorbent assay for IL-1 alpha. *Lymphokine Cytokine Res.*, 10: 61-68, 1991

Malanchere, E., Marcos, M.A., Nobrega, A., and Coutinho, A. Studies on the T cell dependence of natural IgM and IgG antibody repertoires in adult mice. *Eur. J. Immunol.*, 25: 1358-1365, 1995

Mansbridge, J.N., Knuchel, R., Knapp, A.M., and Sutherland, R.M. Importance of tyrosine phosphatases in the effects of cell-cell contact and microenvironments on EGF-stimulated tyrosine phosphorylation. *J. Cell. Physiol.*, 151:433-442, 1992

Marchalonis, J.J., Kaymaz, H., Schluter, S.F., and Yocum, D.E. Naturally occurring human autoantibodies to defined. *Med. Biol.*, 347: 135-145, 1994

Martin, S.E., and Martin, W.J. X chromosome-linked defect of CBA/HN mice in production of tumor reactive naturally occurring IgM antibodies. *J. Immunol.*, 115:502-507, 1975

Martini, A., Lorini, R., Zanaboni, D., Ravelli, A., and Burgio, R.G. Frequency of autoantibodies in normal children. *Am. J. Dis. Child.*, 143: 493-496, 1989

Martin, T., Duffy, S.F., Carson, D.A., and Kipps, T.J. Evidence for somatic selection of natural autoantibodies. *J. Exp. Med.* 175: 983-991, 1992

Maruta, H., and Burgess, A.W. Regulation of the Ras signalling network. *Bioessays*, 16:489-496, 1994

Masure, S., Nys, G., Fiten, P., Van-Damme, J., and Opdenakker, G. Mouse gelatinase B. cDNA cloning, regulation of expression and glycosylation in WEHI-3 macrophages and gene organisation. *Eur. J. Biochem.*, 218:129-141, 1993

Matyas, G.R., and Fishman, P.H. Lipid signaling pathways in normal and ras-transfected NIH/3T3 cells. *Cell Signal.*, 1:395-404, 1989

Mazzieri, R., Masiero, L., Zanetta, L., Monea, S., Onisto, M., Garbisa, S., and Mignatti, P. Control of type IV collagenase activity by components of urokinase-plasmin system: a regulatory mechanism with cell-bound reactants. *EMBO J.*, 16:2319-2332, 1997

McGuire, W.A., Yang, H.H., Bruno, E., Brandt, J., Briddell, R., Coates, T.D., and Hoffman, R. Treatment of antibody-mediated pure red-cell aplasia with high-dose intravenous gamma globulin. *N. Engl. J. Med.*, 317: 1004-1008, 1987

McIlroy, B.K., Walters, J.D., Blackshear, P.J., and Johnson, J.D. Phosphorylation-dependent binding of a synthetic MARCKS peptide to calmodulin. *J. Biol. Chem.*, 266:4959-4964, 1991

Meek, D.W. Post-translational modification of p53. *Semin. Cancer Biol.*, 5:203-210, 1994

Melloni, E., Pontremoli, S., Michetti, M., Sacco, O., Cakiroglu, A.G., Jackson, J.F.,

Rifkind, R.A., and Marks, P.A. Protein kinase C activity and hexamethylenebisacetamide-induced erythroleukemia cell differentiation. *Proc. Natl. Acad. Sci. USA.*, 84: 5282-5286, 1987

Menard, S., Colnaghi, H.I., and Della-Porta, G. Natural anti-tumor serum reactivity in Balb/c mice. I. Characterization and interference with tumor growth. *Int. J. Cancer*, 19:267-274, 1977

Mescher, M.F., Jose, M.J.L., Balk, S.P. Actin-containing matrix associated with the plasma membrane of murine tumor and lymphoid cells. *Nature*, 289:139-144, 1981

Michel, C., Gonzalez, R., Bonjour, E., and Avrameas, S. A concurrent increasing of natural antibodies and enhancement of resistance to furunculosis in rainbow trout. *Ann. Rech. Vet.*, 21: 211-218, 1990

Miller, V., Chow, D.A., and Greenberg, A. Natural antibodies. In: *Natural Immunity*. Ed. Nelson. pp172-217, 1989

Milne, D.M., Campbell, D.G., Caudwell, F.B., and Meek, D.W. Phosphorylation of the tumor suppressor protein p53 by mitogen-activated protein kinases. *J. Biol. Chem.*, 269:9253-9260, 1994

Milne, D.M., McKendrick, L., Jardine, L.J., Deacon, E., Lord, J.M., and Meek, D.W. Murine p53 is phosphorylated within the PAb421 epitope by protein kinase C in vivo, even after stimulation with the phorbol ester o-tetradecanoylphorbol 13-acetate. *Oncogene*, 13:205-211, 1996

Miloszewska, J., Trawicki, W., Janik, P., Moraczewski, J., Przybyszewska, M., and Szaniawska, B. Protein kinase C translocation in relation to proliferative state of C3H 10T½ cells. *FEBS Lett.*, 206:283-286, 1986

Minami, Y., Samelson, L.E., and Klausner, R.D. Internalization and cycling of the T cell antigen receptor. Role of protein kinase C. *J. Biol. Chem.*, 262:13342-13347, 1987

Mischak, H., Goodnight, J.A., Kolch, W., Martiny-Baron, G., Schaehtle, C., Kazanietz, M.G., Blumberg, P.M., Pierce, J.H., and Mushinski, J.F. Overexpression of protein kinase C-delta and -epsilon in NIH 3T3 cells induces opposite effects on growth, morphology, anchorage dependence, and tumorigenicity. *J. Biol. Chem.*, 268:6090-6096, 1993

Mittelstadt, P.R., and DeFranco, A.L. Induction of early response genes by cross-linking membrane Ig on B lymphocytes. *J. Immunol.*, 150:4822-4832, 1993

Mizumoto, K., Rothman, R.J., and Farber, J.L. Programmed cell death (apoptosis) of

- mouse fibroblasts is induced by the topoisomerase II inhibitor etoposide. *Mol. Pharmacol.*, 46:890-895, 1994
- Montaner, S., Ramos, A., Perona, R., Esteve, P., Carnero, A., and Lacal, J.C. Overexpression of PKC zeta in NIH3T3 cells does not induce cell transformation nor tumorigenicity and does not alter NF kappa B activity. *Oncogene*, 10:2213-2220, 1995
- Moore, P.M., Joshi, I., and Ghanekar, S.A. Affinity isolation of neuron-reactive antibodies in MRL/lpr mice. *J. Neurosci. Res.*, 39:140-147, 1994
- Morell, A., Vassalli, G., DeLange, G.G., Skvaril, F., Ambrosino, D.M., and Siber, G.R. Ig allotype-linked regulation of class and subclass composition of natural antibodies to group A streptococcal carbohydrate. *J. Immunol.*, 142:2495-2500, 1989
- Morrison, P., Takishima, K., and Rosner, M.R. Role of threonine residues in regulation of the epidermal growth factor receptor by protein kinase C and mitogen-activated protein kinase. *J. Biol. Chem.*, 268:15536-15543, 1993
- Mouthon, L., Kaveri, S.V., Spalter, S.H., Lacroix-Desmazes, S., Lefranc, C., Desai, R., and Kazatchkine, M.D. Mechanisms of action of intravenous immune globulin in immune-mediated diseases. *Clin. Exp. Immunol.*, 104(Suppl. 1):3-9, 1996
- Nakaigawa, N., Hirai, S., Mizuno, K., Shuin, T., Hosaka, M., and Ohno, S. Differential effects of overexpression of PKC α and PKC δ/ϵ in cellular E2F activity in late G1 phase. *Biochem. Biophys. Res. Commun.*, 222:95-100, 1996
- Natori, T., Takahashi, S., Nakagawa, H., Aizawa, M., and Itaya, T. Natural antibodies carrying a cross-reactive idiotype enhances tumor growth in the rat. *Int. J. Cancer*, 28:591-599, 1981
- Navin, T.R., Krug, E.C., and Pearson, R.D. Effect of immunoglobulin M from normal human serum on *Leishmania donovani* promastigote agglutination, complement-mediated killing and phagocytosis by human monocytes. *Infect. Immun.*, 57:1343-1346, 1989
- Nelson, J.M., and Fry, D.W. Cytoskeletal and morphological changes associated with the specific suppression of the epidermal growth factor receptor tyrosine kinase activity in A431 human epidermoid carcinoma. *Exp. Cell. Res.*, 233:383-390, 1997
- Newton, A.C., and Koshland, D.E.Jr. Phosphatidylserine affects specificity of protein kinase C substrate phosphorylation and autophosphorylation. *Biochemistry*, 29:6656-6661, 1990
- Newton, A.C. Protein kinase C: structure, function, and regulation. *J. Biol. Chem.*, 270:28495-28498, 1995

- Nishizuka, Y. Studies and perspectives of protein kinase C. *Science*, 233:305-312, 1986
- Nishizuka, Y. The molecular heterogeneity of protein kinase C and its implications for cellular regulation. *Nature*, 334:661-665, 1988
- Nishizuka, Y. Membrane phospholipid degradation and protein kinase C for cell signalling. *Neurosci. Res.*, 15: 3-5, 1992
- O'Brian, C.A., Vogel, V.G., Singletary, S.E., and Ward, N.E. Elevated protein kinase C expression in human breast tumor biopsies relative to normal breast tissue. *Cancer Res.*, 49:3215-3217, 1989
- Onishi, R., Okuma, M., and Uchiyama, T. Phorbol esters upregulate p55 and downregulate p75 expression of interleukin-2 receptors in human T cells. *Int. J. Hematol.*, 55:53-60, 1992
- Ort, J.W., and Newton, A.C. Intrapeptide regulation of protein kinase C. *J. Biol. Chem.*, 269:8383-8387, 1994
- Ostman, A., Yang, Q., and Tonks, N.K. Expression of DEP-1, a receptor-like protein-tyrosine-phosphatase, is enhanced with increasing cell density. *Proc. Natl. Acad. Sci. USA.*, 91:9680-9684, 1994
- Otey, C.A., Kalnoski, M.H., Lessard, J.L., and Bulinski, J.C. Immunolocalization of the γ isoform of nonmuscle actin in cultured cells. *J. Cell Biol.*, 102:1726-1737, 1986
- Owen, P.J., Johnson, G.D., and Lord, J.M. Protein kinase C- δ associates with vimentin intermediate filaments in differentiated HL60 cells. *Exp. Cell. Res.*, 225:366-373, 1996
- Pai, J.K., Pachter, J.A., Weinstein, I.B., and Bishop, W.R. Overexpression of protein kinase C β 1 enhances phospholipase D activity and diacylglycerol formation in phorbol ester-stimulated rat fibroblasts. *Proc. Natl. Acad. Sci. USA*, 88:598-602, 1991
- Pallen, C.J., and Tong, P.H. Elevation of membrane tyrosine phosphatase activity in density-dependent growth-arrested fibroblasts. *Proc. Natl. Acad. Sci. USA.*, 88:6996-7000, 1991
- Panet, R., and Atlan, H. Bumetanide-sensitive $\text{Na}^+/\text{K}^+/\text{Cl}^-$ transporter is stimulated by phorbol ester and different mitogens in quiescent human skin fibroblasts. *J. Cell. Physiol.*, 145:30-38, 1990
- Parsons, S.L., Watson, S.A., Brown, P.D., Collins, H.M., and Steele, R.J. Matrix metalloproteinases. *Br. J. Surg.*, 84:160-166, 1997

Partridge, C.A., Phillips, P.G., Niedbala, M.J., and Jeffery, J.J. Localization and activation of type IV collagenase/gelatinase at endothelial focal contacts. *Am. J. Physiol.*, 272:L813-L822, 1997

Pearson, R.B., and Kemp, B.E. Protein kinase phosphorylation site sequences and consensus specificity motifs: tabulations. *Methods Enzymol.*, 200:62-81, 1991

Peng, Z.Y., and Cartwright, C.A. Regulation of Src tyrosine kinase and Syp tyrosine phosphatase by their cellular association. *Oncogene*, 11:1955-1962, 1995

Perletti, G.P., Folini, M., Lin, H.C., Mischak, H., Piccinini, F., and Tashjian, A.H.Jr. Overexpression of protein kinase C epsilon is oncogenic in rat colonic epithelial cells. *Oncogene*, 12:847-854, 1996

Persons, D.A., Wilkison, W.O., Bell, R.M., and Finn, O.J. Altered growth regulation and enhanced tumorigenicity of NIH 3T3 fibroblasts transfected with protein kinase C-I cDNA. *Cell*, 52:447-458, 1988

Petersen, C.M., Christensen, E.I., Andersen, B.S., and Moller, B.K. Internalization, lysosomal degradation and new synthesis of surface membrane CD4 in phorbol ester-activated T-lymphocytes and U937 cells. *Exp. Cell Res.*, 201:160-173, 1992

Peyron, J., and Fehlmann, M. Phosphorylation of class I histocompatibility antigens in human B lymphocytes. Regulation by phorbol esters and insulin. *Biochem. J.*, 256:763-768, 1988

Phillips, W.A., Fujuki, T., Rossi, M.W., Korchak., H.M., and Johnston, R.B. Jr. Influence of calcium on the subcellular distribution of protein kinase C in human neutrophils. Extraction conditions determine partitioning of histone-phosphorylating activity and immunoreactivity between cytosol and particulate fractions. *J. Biol. Chem.*, 264:8361-8365, 1989

Polverino, A.J., Hughes, B.P., and Barritt, G.J. NIH-3T3 cells transformed with a ras oncogene exhibit a protein kinase C-mediated inhibition of agonist-stimulated Ca^{2+} inflow. *Biochem. J.*, 271:309-315, 1990

Portnoi, D., Freitas, A., Holmberg, D., Bandeira, A., and Coutinho, A. Immunocompetent autoreactive B lymphocytes are activated cycling cells in normal mice. *J. Exp. Med.*, 164: 25-35, 1986

Prabhakar, B.S., Saegusa, J., Onodera, T., and Notkins, A.L. Lymphocytes capable of making monoclonal autoantibodies that react with multiple organs are a common feature of the normal B cell repertoire. *J. Immunol.*, 133: 2815-2817, 1984

Powell, M.B., Rosenberg, R.K., Graham, M.J., Birch, M.L., Yamanishi, D.T., Buckmeier, J.A. and Meyskens, F.L.Jr. Protein kinase C β expression in melanoma cells and melanocytes: Differential expression correlates with biological responses to 12-O-tetradecanoylphorbol 13-acetate. *J. Cancer Res. Clin. Oncol.*, 119:199-206, 1993

Prehn, R.T. The paradoxical association of regression with a poor prognosis in melanoma contrasted with a good prognosis in keratoacanthoma. *Cancer Res.*, 56:937-940, 1996

Prekeris, R., Mayhew, M.W., Cooper, J.B., and Terrian, D.M. Identification and localization of an actin-binding motif that is unique to the epsilon isoform of protein kinase C and participates in the regulation of synaptic function. *J. Cell. Biol.*, 132:77-90, 1996

Pronk, G.J., and Bos, J.L. The role of p21ras in receptor tyrosine kinase signalling. *Biochim. Biophys. Acta*, 1198:131-147, 1994

Rak, J.W., Basolo, F., Elliott, J.W., Russo, J., and Miller, F.R. Cell surface glycosylation changes accompanying immortalization and transformation of normal human mammary epithelial cells. *Cancer Lett.*, 57:27-36, 1991

Ralph, P., and Nakoinz, I. Cooperation of IgG monoclonal antibodies in macrophage antibody dependent cellular cytotoxicity (ADCC) to tumor targets. *J. Leukocyte Biol.*, 35:131-139, 1984

Raptis, L., Marcellus, R.C., and Whitfield, J.F. High membrane-associated protein kinase C activity correlates to tumorigenicity but not anchorage-independence in a clone of mouse NIH 3T3 cells. *Exp. Cell. Res.*, 207:152-154, 1993

Rasmussen, H., Isales, C.M., Calle, R., Throckmorton, D., Anderson, M., Gasalla-Herraiz, J., and McCarthy, R. Diacylglycerol production, Ca^{2+} influx, and protein kinase C activation in sustained cellular responses. *Endocrine Rev.*, 16:649-681, 1995

Reap, E.A., Sobel, E.S., Cohen, P.L., and Eisenberg, R.A. Conventional B cells, not B-1 cells, are responsible for producing autoantibodies in lpr mice. *J. Exp. Med.*, 177:69-78, 1993

Reese, M.R., and Chow, D.A. Tumor progression in vivo: increased soybean agglutinin lectin binding, N-acetylgalactosamine specific lectin expression and liver metastasis potential. *Cancer Res.*, 52:5235-5243, 1992

Regazzi, R., Fabbro, D., Costa, S.D., Borner, C., and Eppenberger, U. Effects of tumor promoters on growth and on cellular redistribution of phospholipid/ Ca^{2+} -dependent protein kinase in human breast cancer cells. *Int. J. Cancer*, 37:731-737, 1986

Reininger, L., Ollier, P., Poncet, P., Kaushik, A., and Jaton, J.C. Novel V genes encode virtually identical variable regions of six murine monoclonal anti-bromelain-treated red blood cell autoantibodies. *J. Immunol.*, 138: 316-323, 1987

Reitamo, S., Remitz, A., Varga, J., Ceska, M., Effenberger, F., Jimenez, S., and Uitto, J. Demonstration of interleukin 8 and autoantibodies to interleukin 8 in the serum of patients with systemic sclerosis and related disorders. *Arch. Dermatol.*, 129: 189-193, 1993

Rijksen, G., Voller, M.C., and van-Zoelen, E.J. The role of protein tyrosine phosphatases in density-dependent growth control of normal rat kidney cells. *FEBS Lett.*, 322:83-87, 1993

Rodriguez-Pena, A., and Rozengurt, E. Phosphorylation of an acidic mol. wt. 80 000 cellular protein in a cell-free system and intact Swiss 3T3 cells: a specific marker of protein kinase C activity. *EMBO J.*, 5:77-83, 1986

Ronda, N., Haury, M., Nobrega, A., Coutinho, A., and Kazatchkine, M.D. Selectivity of recognition of variable (V) regions of autoantibodies by intravenous immunoglobulin (IVIg). *Clin. Immunol. Immunopathol.*, 70: 124-128, 1994

Rossi, F., Sultan, Y., and Kazatchkine, M.D. Anti-idiotypes against autoantibodies and alloantibodies to VIII:C (anti-haemophilic factor) are present in therapeutic polyspecific normal immunoglobulins. *Clin. Exp. Immunol.*, 74: 311-316, 1988

Rossi, F., Dietrich, G., and Kazatchkine, M.D. Anti-idiotypes against autoantibodies in normal immunoglobulins: evidence for network regulation of human autoimmune responses. *Immunol. Rev.*, 110: 135-149, 1989

Rotenberg, S.A., Krause, R.S., Borner, C.M.B. and Weinstein, I.B. Characterization of a specific form of protein kinase C overproduced by a C3H 10T1/2 cell line. *Biochem. J.*, 266: 173-178, 1990.

Rother, R.P., Fodor, W.L., Springhorn, J.P., Birks, C.W., Setter, E., Sandrin, M.S., Squinto, S.P., and Rollins, S.A. A novel mechanism of retrovirus inactivation in human serum mediated by anti-alpha-galactosyl natural antibody. *J. Exp. Med.*, 182: 1345-1355, 1995

Rowley, M.J., Maeda, T., Mackay, I.R., Loveland, B.E., McMullen, G.L., Tribbick, G., and Bernard, C.C. Differing epitope selection of experimentally-induced and natural antibodies to a disease-specific autoantigen, the E2 subunit of pyruvate dehydrogenase complex (PDC-E2). *Int. Immunol.*, 4: 1245-1253, 1992

Rowley, M.J., Buchanan, H., and Mackay, I.R. Reciprocal change with age in antibody

to extrinsic antigens. *Lancet*, 2:24-26, 1968

Rozakis-Adcock, M., McGlade, J., Mbamalu, G., Pelicci, G., Daly, R., Li, W., Batzer, A., Thomas, S., Brugge, J., Pelicci, P.G., et al. Association of the Shc and Grb2/Sem5 SH2-containing proteins is implicated in activation of the Ras pathway by tyrosine kinases. *Nature*, 360:689-692, 1992

Rubin, J., Titus, L., and Nanes, M.S. Regulation of complement 5a receptor expression in U937 cells by phorbol ester. *J. Leukocyte Biol.*, 50:502-508, 1991

Russell, R.R., and Beighton, D. Specificity of natural antibodies reactive with *Streptococcus mutans* in monkeys. *Infect. Immun.*, 35:741-744, 1982

Sakanoue, Y., Hatada, T., Kusunoki, M., Yanagi, H., Yamamura, T., and Utsunomiya, J. Protein kinase C activity as marker for colorectal cancer. *Int. J. Cancer*, 48:803-806, 1991

Sandor, M., and Lynch, R.G. Lymphocyte Fc receptors: the special case of T cells. *Immunol. Today*, 14:227-231, 1993

Sandrin, M.S., Vaughan, H.A., Dabkowski, P.L., and McKenzie, I.F. Anti-pig IgM antibodies in human serum react predominantly with Gal(alpha 1-3)Gal epitopes. *Proc. Natl. Acad. Sci. USA.*, 90:11391-11395, 1993

Sandstrom, P.A., and Chow, D.A. Phorbol ester tumor promoter regulation of natural antitumor antibody binding depends on protein kinase C and an intact microfilament system. *Nat. Immun.*, 13: 331-343, 1994

Santer, U.V., Gilbert, F., and Glick, M.C. Change in glycosylation of membrane glycoproteins after transfection of NIH 3T3 with human tumor DNA. *Cancer Res.*, 44:3730-3735, 1984

Saoudi, A., Hurez, V., de-Kozak, Y., Kuhn, J., Kaveri, S.V., Kazatchkine, M.D., Druet, P., and Bellon, B. Human immunoglobulin preparations for intravenous use prevent experimental autoimmune uveoretinitis. *Int. Immunol.*, 5: 1559-1567, 1993

Satoh, T., Nakafuku, M., and Kaziro, Y. Function of Ras as a molecular switch in signal transduction. *J. Biol. Chem.*, 267:4149-4152, 1992

Savart, M., Letard, P., Bultel, S., and Ducastaing, A. Induction of protein kinase C down-regulation by the phorbol ester TPA in a calpain/protein kinase C complex. *Int. J. Cancer* 52:399-403, 1992

Scher, I. The CBA/N mouse strain: an experimental model illustrating the influence of

the X-chromosome on immunity. *Adv. Immunol.*, 33:1-71, 1982

Schlesinger, L.S., and Horwitz, M.A. A role for natural antibody in the pathogenesis of leprosy: antibody in nonimmune serum mediates C3 fixation to the *Mycobacterium leprae* surface and hence phagocytosis by human mononuclear phagocytes. *Infect. Immun.*, 62: 280-289, 1994

Schussler, O., Lantoiné, F., Devynck, M.A., Glotz, D., and David-Duflho, M. Human immunoglobulins inhibit thrombin-induced Ca^{2+} movements and nitric oxide production in endothelial cells. *J. Biol. Chem.*, 271:26473-26476, 1996

Schwartz, G.K., Jiang, J., Kelsen, D., and Albino, A.P. Protein kinase C: a novel target for inhibiting gastric cancer cell invasion. *J. Natl. Cancer Inst.*, 85:402-407, 1993

Schwartz, S.A. Intravenous immunoglobulin (IVIg) for the therapy of autoimmune disorders. *J. Clin. Immunol.* 10:81-90, 1990

Seigneurin, J.M., Guilbert, B., Bourgeat, M.J., and Avrameas, S. Polyspecific natural antibodies and autoantibodies secreted by human lymphocytes immortalized with Epstein-Barr virus. *Blood*, 71: 581-585, 1988

Sela, B.A., Wang, J.L., and Edelman, G.M. Antibodies reactive with cell surface carbohydrates. *Proc. Natl. Acad. Sci. USA.*, 72:1127-1131, 1975

Serban, D., Pages, J.M., Bussard, A.E., and Witz, I.P. The participation of trimethylammonium in the mouse erythrocyte epitope recognized by monoclonal autoantibodies. *Immun. Lett.*, 3:315-319, 1981

Shoenfeld, Y., Segol, G., Segol, O., Neary, B., Klajman, A., Stollar, B.D., and Isenberg, D.A. Detection of antibodies to total histones and their subfractions in systemic lupus erythematosus patients and their asymptomatic relatives. *Arthritis Rheum.*, 30:169-175, 1987

Smith, J.W., Fortner, J.G., and Burt, M. Resection of hepatic and pulmonary metastases from colorectal cancer. *Surg. Oncol.*, 1:399-404, 1992

Sorette, M.P., Galili, U., and Clark, M.R. Comparison of serum anti-band 3 and anti-gal antibody binding to density separated human red blood cells. *Blood*, 77:628-636, 1991

Stollar, B.D., Lecerf, J.M., and Hirabayashi, Y. The role of autoreactivity in B cell selection. *Ann. N.Y. Acad. Sci.*, 815: 30-93, 1997

Stumpo, D.J., Bock, C.B., Tuttle, J.S., and Blackshear, P.J. MARCKS deficiency in mice leads to abnormal brain development and perinatal death. *Proc. Natl. Acad. Sci. USA.*, 92:944-948, 1995

Sultan, Y., Kazatchkine, M.D., Maisonneuve, P., and Nydegger, U.E. Anti-idiotypic suppression of autoantibodies to factor VIII (antihemophilic factor) by high-dose intravenous gammaglobulin. *Lancet*, 2: 765-768, 1984

Sultan, Y., Rossi, F., and Kazatchkine, M.D. Recovery from anti-VIII:C (antihemophilic factor) autoimmune disease is dependent on generation of anti-idiotypes against anti-VIII:C autoantibodies. *Proc. Natl. Acad. Sci. USA.*, 84:828-831, 1987

Sundblad, A., Huetz, F., Portnoi, D., and Coutinho, A. Stimulation of B and T cells by in vivo dose immunoglobulin administration in normal mice. *J. Autoimmun.*, 4:325-339, 1991a

Sundblad, A., Marcos, M., Huetz, F., Freitas, A., Heusser, C., Portnoi, D., and Coutinho, A. Normal serum immunoglobulins influence the numbers of bone marrow pre-B and B cells. *Eur. J. Immunol.*, 21:1155-1161, 1991b

Sy, M.S., Liu, D., Schiavone, R., Ma, J., Mori, H., and Guo, Y. Interactions between CD44 and hyaluronic acid: their role in tumor growth and metastasis. *Curr. Top. Microbiol. Immunol.*, 213:129-153, 1996

Symington, B.E., Symington, F.W., and Rohrschneider, L.R. Phorbol ester induces increased expression, altered glycosylation, and reduced adhesion of K562 erythroleukemia cell fibronectin receptors. *J. Biol. Chem.*, 264:13258-13266, 1989

Takenaka, I., Morin, F., Seizinger, B.R., and Kley, N. Regulation of the sequence-specific DNA binding function of p53 by protein kinase C and protein phosphatases. *J. Biol. Chem.*, 270:5405-5411, 1995

Tarlinton, D. B-cell differentiation in the bone marrow and the periphery. *Immunol. Rev.*, 137: 203-229, 1994

Tchernychev, B., Cabilly, S., and Wilchek, M. The epitopes for natural polyreactive antibodies are rich in proline. *Proc. Natl. Acad. Sci. USA.*, 94: 6335-6339, 1997

Terce, F., Brun, H., and Vance, D.E. Requirement of phosphatidylcholine for normal progression through the cell cycle in C3H/10T1/2 fibroblasts. *J. Lipid Res.*, 35:2130-2142, 1994

Ternynck, T., and Avrameas, S. Murine natural monoclonal autoantibodies: a study of their polyspecificities and their affinities. *Immunol. Rev.*, 94:99-112, 1986

Thornton, B.P., Vetvicka, V., and Ross, G.D. Function of C3 in a humoral response: iC3b/C3dg bound to an immune complex generated with natural antibody and a primary antigen promotes antigen uptake and the expression of co-stimulatory molecules by all B cells, but only stimulates immunoglobulin synthesis by antigen-specific B cells. *Clin. Exp. Immunol.*, 104: 531-537, 1996

Tonks, N.K. Protein tyrosine phosphatases and the control of cellular signaling responses. *Adv. Pharmacol.*, 36:91-119, 1996

Tough, D.F., Feng, X., and Chow, D.A. p21ras independent down-regulation of ras-induced increases in natural antibody binding during tumor progression. *Nat. Immun.*, 14: 20-34, 1995

Tough, D.F., and Chow, D.A. Natural antibody recognition of v-H-ras-induced 10T1/2 transformation. *Nat. Immun. Cell Growth Regul.*, 10:83-93, 1991

Tough, D.F., and Chow, D.A. Tumorigenicity of murine lymphomas selected through fluorescence-detected natural antibody binding. *Cancer Res.*, 48:270-275, 1988

Tracy, S., van-der-Geer, P., and Hunter, T. The receptor-like protein-tyrosine phosphatase, RPTP alpha, is phosphorylated by protein kinase C on two serines close to the inner face of the plasma membrane. *J. Biol. Chem.*, 270: 10587-10594, 1995

Tsukidate, K., Yamamoto, K., Snyder, J.W., and Farber, J.L. Microtubule antagonists activate programmed cell death (apoptosis) in cultured rat hepatocytes. *Am. J. Pathol.*, 143:918-925, 1993

Turley, E.A., Austen, L., Moore, D., and Hoare, K. Ras-transformed cells express both CD44 and RHAMM hyaluronan receptors: only RHAMM is essential for hyaluronan-promoted locomotion. *Exp. Cell. Res.*, 207:277-282, 1993

Uher, F., Alonson, M.A., Mihalik, R., Balogh, E., and Gerdely, J. Autocrine regulation of murine B lymphocyte growth by an IgM antibody. *Immunobiol.*, 185:292-302, 1992

Ullrich, A., and Schlessinger, J. Signal transduction by receptors with tyrosine kinase activity. *Cell*, 61:203-212, 1990

Van Schaik, I.N., Lundkvist, I., Vermeulen, M., and Brand A. Polyvalent immunoglobulin for intravenous use interferes with cell proliferation in vitro. *J. Clin. Immunol.*, 12:325-334, 1992

Vassilev, T., Gelin, C., Kaveri, S.V., Zilber, M.T., Bounsell, L., and Kazatchkine, M.D.

Antibodies to the CD5 molecule in normal human immunoglobulins for therapeutic use (intravenous immunoglobulins, IVIg). *Clin. Exp. Immunol.*, 92: 369-372, 1993

Vogel, L., Persin, C., and Haustein, D. Changes in the expression of Ig-associated proteins on B lymphocytes activated by anti-IgM antibodies. *Scand. J. Immunol.*, 37:277-281, 1993

Waldmann, V., and Rabes, H.M. What's new in ras genes? Physiological role of ras genes in signal transduction and significance of ras gene activation in tumorigenesis. *Pathol. Res. Pract.*, 192:883-891, 1996

Wang, E., Lake, D., Winfield, J.B., and Marchalonis, J.J. IgG autoantibodies to "switch peptide" determinants of TCR alpha/beta in human pregnancy. *Clin. Immunol. Immunopathol.*, 73: 224-228, 1994

Ward, P.M., and Weiss, L. The effects of single versus triple intravenous injections of B16 melanoma cells on the development of pulmonary tumors in mice. *Int. J. Cancer*, 36:519-521, 1985

Warne, P.H., Viciano, P.R., and Downward, J. Direct interaction of ras and the amino-terminal region of raf-1 in vitro. *Nature*, 364:352-355, 1993

Watanabe, T., Ono, Y., Taniyama, Y., Hazama, K., Igarashi, K., Ogita, K., Kikkawa, U., and Nishizuka, Y. Cell division arrest induced by phorbol ester in CHO cells overexpressing protein kinase C-delta subspecies. *Proc. Natl. Acad. Sci. USA.*, 89:10159-10163, 1992

Weinberg, R.A. The retinoblastoma protein and cell cycle control. *Cell*, 81:323-330, 1995

Werth, D.K., Niedel, J.E., and Pastan, I. Vinculin, a cytoskeletal substrate of protein kinase C. *J. Biol. Chem.*, 258:11423-11426, 1983

Weyman, C.M., Taprowsky, E.J., Wolfson, M., and Ashendel, C.L. Partial downregulation of protein kinase C in C3H 10T1/2 mouse fibroblasts transfected with human Ha-ras oncogene. *Cancer Res.*, 48:6535-6541, 1988

Williams, N.G., Roberts, T.M., and Li, P. Both p21ras and pp60v-src are required, but neither alone is sufficient, to activate the Raf-1 kinase. *Proc. Natl. Acad. Sci. USA.*, 89:2922-2926, 1992

Willumsen, B.M., Christensen, A., Hubbert, N.L., Parageorge, A.G., and Lowy, D.R. The p21 ras C-terminus is required for transformation and membrane association. *Nature*, 310:583-586, 1984

wolf-Levin, R., Azuma, T., Aoki, K., Yagami, Y., and Okada, H. Specific IgG autoantibodies are potent inhibitors of autoreactive T cell response to phytohemagglutinin-activated T cells. *J. Immunol.*, 151:5864-5877, 1993

Wolfman, A., and Macara, I.G. Elevated levels of diacylglycerol and decreased phorbol ester sensitivity in ras-transformed fibroblasts. *Nature*, 325:359-361, 1987

Wu, X., Okada, N., Iwamori, M., and Okada, H. IgM natural antibody against an asialo-oligosaccharide, gangliotetraose (Gg4), sensitizes HIV-I infected cells for cytolysis by homologous complement. *Int. Immunol.*, 8: 153-158, 1996

Xuan, J.W., Wilson, S.M., Chin, J.L., and Chambers, A.F. Metastatic NIH 3T3 x LTA cell hybrids express 72 kDa type IV collagenase. *Anticancer Res.*, 15:1227-1233, 1995

Yadin, O., Sarov, B., Naggan, L., Slor, H., and Shoenfeld, Y. Natural autoantibodies in the serum of healthy women—a five-year follow-up. *Clin. Exp. Immunol.*, 75:402-406, 1989

Yamagata, S., Tanaka, R., Ito, Y., and Shimizu, S. Gelatinases of murine metastatic tumor cells. *Biochem. Biophys. Res. Commun.*, 158:228-234, 1989

Yanagihara, K., Nii, M., Tsumuraya, M., Numoto, M., Seito, T., and Seyama, T. A radiation-induced murine ovarian granulosa cell tumor line: introduction of v-ras gene potentiates a high metastatic ability. *Jpn. J. Cancer Res.*, 86:347-356, 1995

Yother, J., Forman, C., Gray, B.M., and Briles, D.E. Protection of mice from infection with *Streptococcus pneumoniae* by antiphosphocholine antibody. *Infect. Immun.*, 36:184-188, 1982

Zhang, Z.Y., and Chow, D.A. Differential CD45 isoform expression accompanies reduced natural antibody binding in L5178Y-F9 tumor progression. *J. Immunol.*, 159: 344-350, 1997

Zheng, X.M., Wang, Y., and Pallen, C.J. Cell transformation and activation of pp60^{c-src} by overexpression of a protein tyrosine phosphatase. *Nature*, 359:336-339, 1992

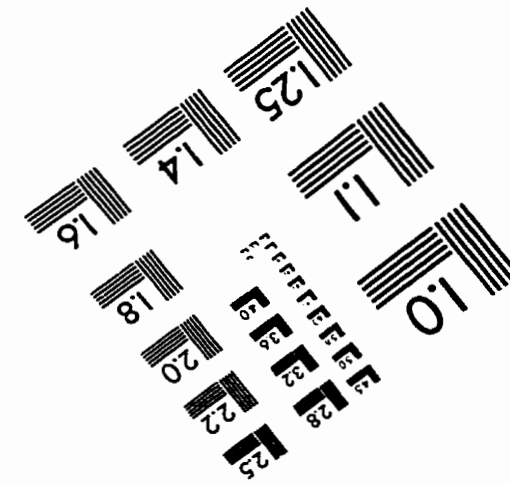
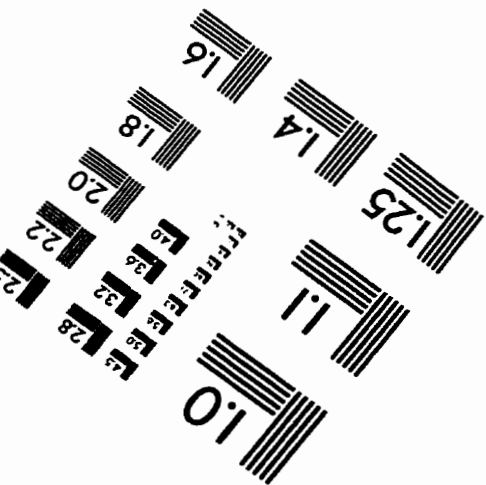
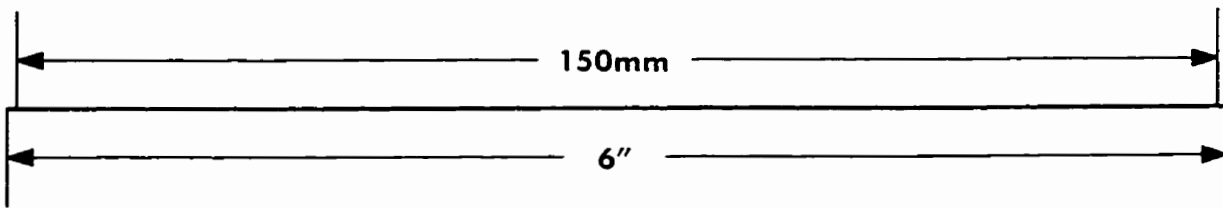
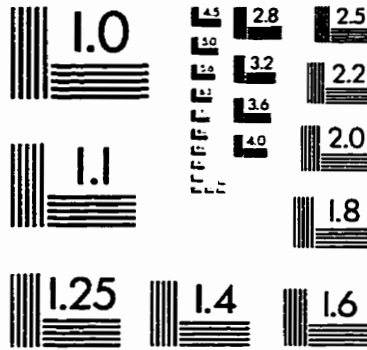
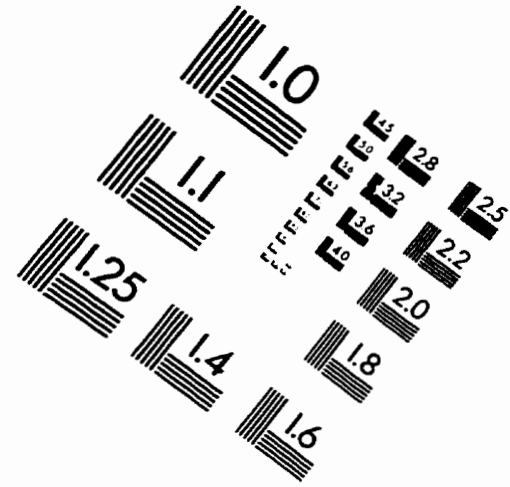
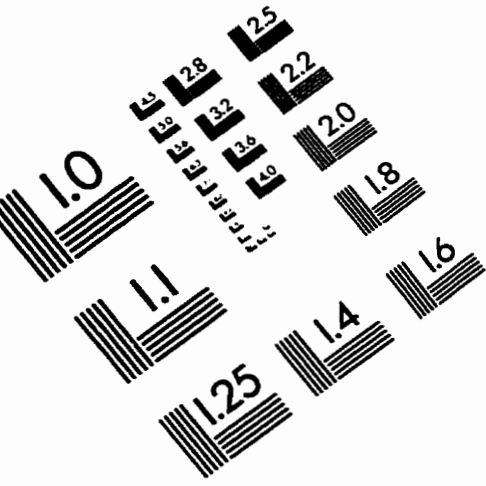
Zheng, Z., Katoh, S., He, Q., Oritani, K., Miyake, K., Lesley, J., Hyman, R., Hamik, A., Parkhouse, R.M.E., Farr, A., and Kincade, P.W. Monoclonal antibodies to CD44 and their influence on hyaluronan recognition. *J. Cell Biol.*, 130:485-495, 1995

Zhou, W., Takuwa, N., Kumada, M., and Takuwa, Y. Protein kinase C-mediated bidirectional regulation of DNA synthesis, RB protein phosphorylation, and cyclin-dependent kinases in human vascular endothelial cells. *J. Biol. Chem.*, 268:23041-23048,

1993

Zhou, W., Javors, M.A. and Olson, M.S. Impaired surface expression of PAF receptors on human neutrophils is dependent upon cell activation. *Arch. Biochem. Biophys.*, 308:439-445, 1994

IMAGE EVALUATION TEST TARGET (QA-3)



APPLIED IMAGE, Inc
1653 East Main Street
Rochester, NY 14609 USA
Phone: 716/482-0300
Fax: 716/288-5989

© 1993, Applied Image, Inc., All Rights Reserved